TOP COPY

ADAPTIVE CANCELLATION TECHNIQUES FOR NOISE REDUCTION IN ELECTROCARDIOGRAPHY

A Thesis submitted for the degree of
Doctor of Philosophy in February 1987
by A. Mukalaf B.Sc(Eng), P.G.Dip.
University of Keele

TO MY FAMILY

ACKNOWLEDGEMENTS

I should like to acknowledge my sincere appreciation and gratitude to a number of people who have contributed wholeheartedly to the completion of the research and compilation of this thesis.

My thanks go to my supervisors; Mr N. Allinson in the early stages and Dr Anthony Furness. It is to Dr Furness that I am particulary indebted, for his instructive and consistent supervision throughout the course of the project. His approach to the subject has been a constant source of encouragement and constructive criticism, not only during the period of research but also during the preparation of the manuscript.

Dr John Davis, Consultant Cardiologist, City General Hospital showed considerable interest in the project and afforded me facilities for patient data recording. Professor W. Fuller, Head of Department of Physics gave encouragement and provided valuable facilities within the Department.

I should like to thank colleagues at Keele during the period of research, especially Dr R. Winski and Mr J.D. white, who provided companionship and many hours of stimulating discussion.

For secretarial assistance throughout the project and typing of the first manuscript draft I should like to thank Mrs E. Durrant, Mrs H. Moore and Miss D. Appleby, and for typing of the finished manuscript, Mrs Ann Furness. Mr S. Cartledge is to be thanked for professional drafting of a number of diagrams.

To my family in Iraq, whom I have not seen for eight years and who encouraged me to come to Britain, I should like to dedicate this thesis.

I owe a debt of gratitude to my sister and brother-in-law, Hashim AL-KHalida for financial support during the period of research. Last, but not least, I acknowledge the support, encouragement and understanding of my wife Pauline during this time.

ABSTRACT

This thesis describes an investigation of the application of adaptive filtering techniques in electrocardiography (ECG), with particular reference to exercise testing. The main objective in this study was to observe the effectiveness of adaptive methods for noise reduction. A number of techniques, including averaging, were tested for comparison and the limitation and inadequacy of these techniques in noise reduction were used as the basis for extending the application of adaptive filtering techniques.

The theory and application of adaptive filtering relating to noise reduction in ECG has been developed, based upon the adaptive transversal filter using the Widrow-Hoff algorithm. The application of a new version of the adaptive filter, referred to the minimal time-sequence adaptive filter to enhance the ECG, was tested in order to improve cancellation with less distortion.

The coherence function was studied as the basis for selecting electrode placement for particular adaptive filtering applications. The adaptive filtering technique was found to be an appropriate method for noise reduction and can improve the signal-to-noise ratio by up to 16dB. It was also found, through the assessment of the results presented from 22 patients, that the use of adaptive filters in the exercise ECG is appropriate, after the removal of a d.c. variation.

CONTENTS

Chapter One

Introductory Considerations

Chapter Two

Characteristics of noise, interference and artifact

Chapter Three

Techniques for noise reduction

Chapter Four

Theory of adaptive filters

Chapter Five

Theory and application of time-sequence adaptive filters

Chapter Six

Applications of adaptive filters in Electrocardiography

Chapter Seven

Application of adaptive filters in Exercise Electrocardiography

Chapter Eight

Comparison of adaptive filtering techniques

Chapter Nine

Conclusions

ANNEXES

PAPER

Summary

In this study a detailed examination of adaptive filtering has been undertaken to determine the effectiveness of the technique for enhancing ECG signals with respect to noise, and its advantages over other filtering techniques.
Various filtering procedures, including signal averaging and fixed value filtering, were applied in order to reduce noise and each was observed to have particular disadvantages.

Adaptive methods were considered and developed based upon the application of adaptive filters operating under the control of Widrow-Hoff least mean square adaptive algorithm.

The theory of this filter, together with the results of application, have been presented. A large part of the practical study was concerned with the skeletal muscle noise cancellation.

Further versions of the adaptive filter were investigated in order to more effectively accommodate slow changes in the non-stationary ECG signal. Filters of this type, characterised by a smaller number of weight sets, exhibited less distortion in their performance compared to the basic adaptive filter and time sequence adaptive filters.

The study commenced using computer simulated signals. Later it was

extended to the use of real data, and applied in exercise testing. The results confirmed that a new version of adaptive filter was not particularly effective for signals such as evoked potentials when fast adaptation was required.

Experimental investigation of the ECG signal enhancement by the method of adaptive processing was performed in three stages. The first stage was concerned with the identification of noise and spatial characteristics with respect to electrode placement on the body surface. It was observed from an examination of the correlation properties of recordings obtained for various electrode placements, that the ECG signal occupies the same frequency bands in each recording and differs only in the type of noise contributed. In general as electrode separation is increased, the correlation with respect to the noise content decreases. It was observed that a minimum of 10mm separation between electrodes was necessary to effectively apply the adaptive filtering process.

The second stage of the study was concerned with the removal of the skeletal muscle activity by use of LMS adaptive filtering. Various factors that influence the performance of the adaptive filtering upon the output signal were examined. These included the convergence factor μ and the filter order N. Depending upon the statistical character of the signal and the noise, these two factors can be changed to achieve appropriate performance. A suitable value for the

applications considered were found to lie between 32-64 for the order of the filter and a value of 0.001 for the convergence factor. Different versions of adaptive filtering were applied to extract the skeletal muscle activity from the ECG signal. It was found that a minimal time sequence adaptive filter was superior in most cases over the basic LMS adaptive filter and the multi co-efficient time-sequence adaptive filters.

The third stage of this study was concerned with the important application of the adaptive filters to exercise testing. The effect of the base line variations was examined and an appropriate method developed to eliminate the influence of these variations. In order to minimize the effect of the variation, which tends to impair the performance of adaptive filters, high pass filtering prior to the adaptive filter was used. Although some distortion was observed, this was identified as being due to the overlap region between the noise and the signal.

Chapter One: Introductory Considerations

Introduction

Interest in high frequency electrocardiography as a source of clinical information, otherwise inaccessible in the band limited conventional electrocardiogram, has been apparent for well over three decades (Langner, 1952 & 1953; Langner & Geselowitz, 1962; Geselowitz et al, 1962; Langner & Lauer, 1966; Boyle et al, 1966; Flowers et al, 1969; Langner et al 1973; Sapoznikov & Weinman, 1975; Shick & Powers, 1978; Chien et al, 198 ; Kim & Tompkins, 1981). In recent years the high frequency electrocardiogram has been considered as a means of investigating surface manifest events of the specialised conduction system (Berbari et al, 1979; Vincent et al, 1980; Flowers et al, 1981; Abboud & Saded, 1982; Mehra, 1982; Berbari et al, 1983), the detection of late ventricular potentials (Simson, 1981; Simson et al, 1983; Denes et al, 1983) and cyclo-stochastic perturbations (Prasad & Gupta, 1980 & 1981).

The lack of acceptance of high frequency electrocardiography as a clinical complement to conventional electrocardiography is largely a consequence of two factors:

(i) low amplitudes for the events of interest and the attendant difficulties of separating signal from noise, and

(ii) the difficulty of confirming that events revealed within the high frequency electrocardiogram and separated from noise, are of

cardiac origin and can be designated in a meaningful way.

The more conventional methods of increasing signal-to-noise ratio such as fixed value filtering and signal averaging can provide improvements, but offer little advantage in situations where the spectral occupancy of the signal overlaps with that of the noise. Moreover, the use of signal averaging obviates the detection of beat by beat variations in the morphology of the high frequency electrocardiogram. Adaptive filtering offers the prospect of overcoming these limitations and, as a consequence of this, the basis for more confident analysis and interpretation of the fine morphological details of the surface electrocardiogram.

1.2 The surface electrocardiogram

The surface electrocardiogram represents a record of the body surface potentials arising as a result of transmembrane current and voltage variations in active cardiac muscle (Geselowitz, 1967). The measurement of potential difference at the surface of the body for a particular electrode configuration or lead can be represented by the integral solution:

$$\Phi_a = \int M(t).Z_a.dV$$

in which Φ_a is the potential difference for a lead or electrode combination.

M(t) is the current moment density or the source of current within the region of the active muscle fibres.

Z_a is a three component impedance vector characteristic of the conducting medium between the current source and the electrode sites.

dV represents an element of volume of the medium in which the currents are circulating.

The expression:

$$\Phi_a = \int M(t)\ Z_a dV$$

clearly demonstrates that surface potentials are completely determined by

(i) the factor, M(t), which relates totally to the electrical activity within the heart, and

(ii) the factor Z_a, which relates totally to the geometry and electrical characteristics of the conducting medium and electrode positioning.

In view of the dependence of surface measured potentials on the scalar product of two vectors, one of which is a lead vector, the surface ECG is lead dependent and a standardised lead system is necessary for the purpose of clinical electrocardiography. This standardised lead system specifies electrodes attached to the right arm, left arm, left foot and various chest leads V_1 to V_6, referred to a reference formed by a combination of the three limb leads as (augmented lead configurations) shown in figure 1.1a. Potential variations measured between the pairs of limb electrodes constitute the three limb leads, I, II and III.

Figure 1.1b is a normal surface recording of potential variations measured between the right arm and the left foot (lead II) during a normal cardiac cycle.

During each heart beat three principal electrical inscriptions may be identified, the P-wave, the QRS complex and the T-wave. Between the end of the P-wave the the beginning of the QRS complex, the normal ECG shows a flat baseline which is conventionally regarded as isoelectric. In actual fact it constitutes a period in which there is propagation through part of the specialised conduction system, but because of the

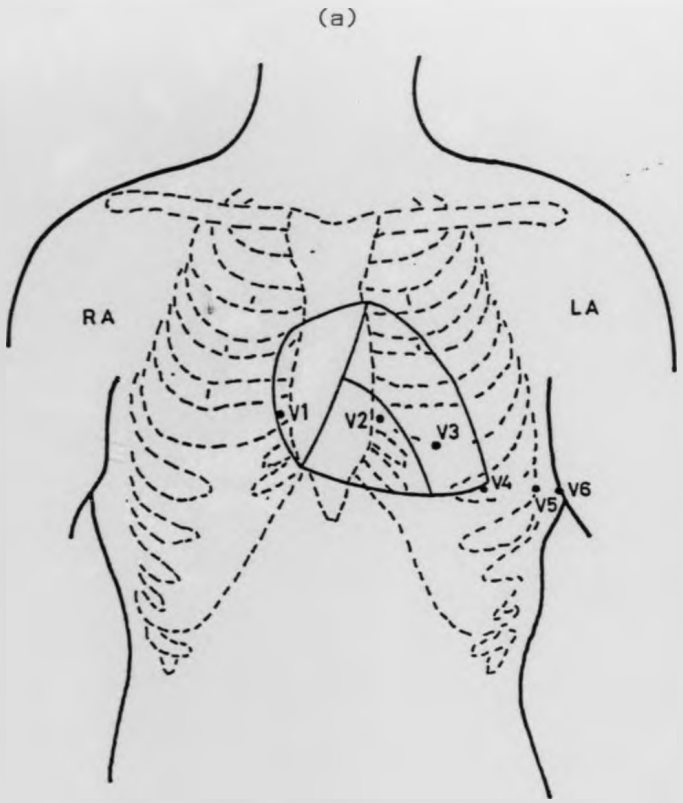

Figure 1.1(a) Standardised lead system.

Figure 1.1(b) A typical surface recording of potential.

small muscle mass involved is not obvious in the surface ECG.

The action of the cardiac cycle is triggered by the electrical impulses within specialised cells that form part of the specialised conduction system. The system includes the following features:

(i) the sinoatrial node, SA, (the natural normal 'pace-maker' of the heart)

(ii) the atrioventricular node, AV,

(iii) the bundle of His,

(iv) the bundle branches,

(v) the Purkinje fibres.

The initiation of the normal heartbeat is by the natural pacemaker of the heart, the sinoatrial node (SA). First the atrial myocardium is activated and the so-called depolarisation activity spreads throughout the atrial muscle mass, giving rise to the P-wave in the ECG and subsequent contraction of the atria. The activity then propagates into the atrioventricular node (AV) where the propagation speed is reduced and a delay occurs. This provides the mechanical advantage of allowing the ventricles to be filled with blood from the atria before they contract. After passing through the AV-node the depolarisation wave propagates along the fibres of the bundle of His, whereafter the ventricular muscle tissue (working myocardium) is activated into depolarisation via the Purkinje network of fibres.

The spreading of ventricular depolarisation results in the QRS complex and subsequent contraction of the ventricles. Sometime after depolarisation each cell within the cardiac musculature repolarises. The repolarisation of the ventricular cells starts about 200ms after depolarisation, and is manifest in the ECG as the T-wave. The repolarisation of the atria is largely masked by the large QRS complex.

Figure 1.2a shows the schematic representation of the specialised conduction system of the heart, and 1.2b is the electrocardiogram showing the inscriptions referred to above.

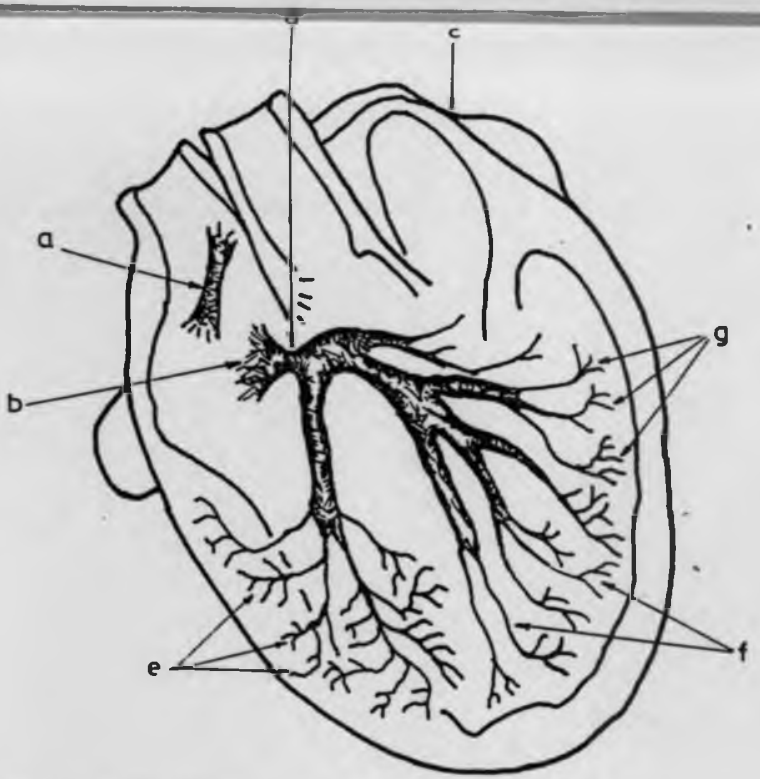

Figure 1.2(A) Schematic representation of the Specialised Conduction System.

a Sinoatrial node
b Atrioventricular node
c Remote atrial surface
d Bundle of His
e Anterior surface, right ventricle
f Apical surface
g Posterior basal area

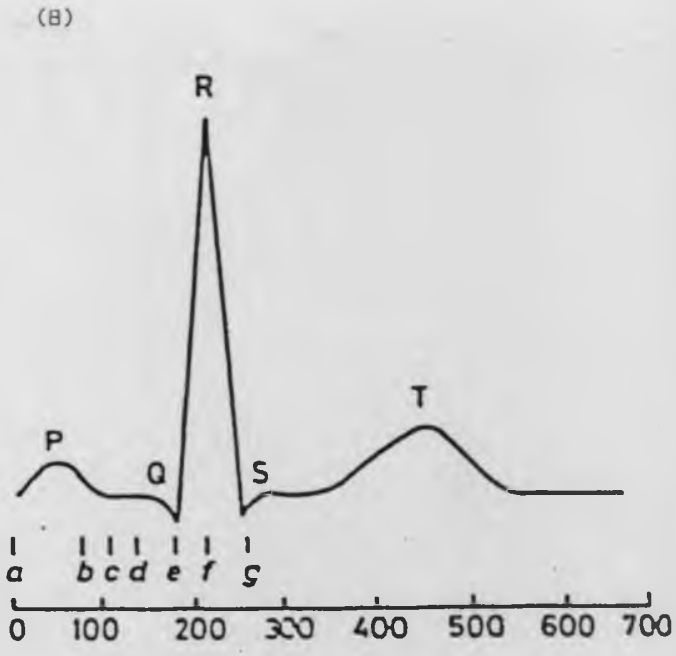

Figure 1.2(B) Electrocardiogram related to Electrical heart cycle.
(this figure adapted from a paper by Rompelman 1982)

1.3 Propagation model for signal and noise

The contamination of an ECG signal by unwanted noise can often be a problem especially in exercise ECG testing. At first sight the application of simple fixed value filtering seems to be quite sufficient for removing the noise from the ECG signal. However, overlap between the spectra of the signal of interest and that of the unwanted noise will tend to distort the signal when the filtering is applied.

Figure 1.3 shows the schematic representation of signal and noise contributing to the surface recorded ECG.

In this model, $y(t)$ is the surface recording of the signal plus noise. $x_0(t)$ and $x_1(t)$ represent the noise and signal, and $h_0(t)$ and $h_1(t)$ represent the transfer functions for signal and noise between source and surface of the body, $u_1(t)$ and $u_0(t)$ are the signal and noise components that originate from the internal resources s_1 and s_0.

$$y(t) = \sum_{i=0}^{n} x_i(t)$$

If this model were entirely representative then it would be a simple matter to separate the noise from the desired signal and possibly determine the nature of the original source of the signal. In practice, because of the distributed nature of the system and the complicated, distributed nature of the noise source, it is not

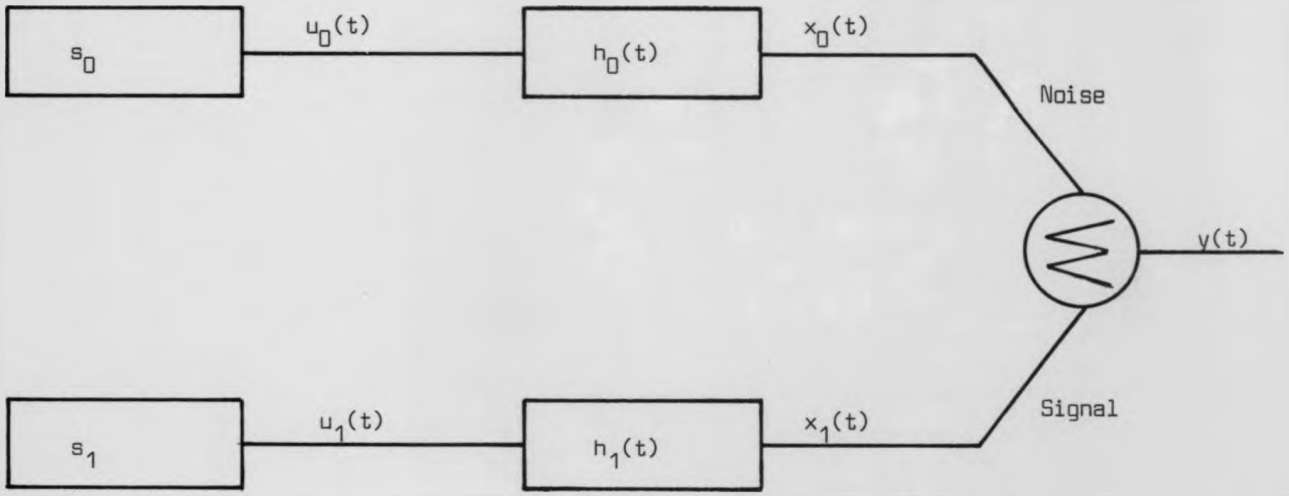

Figure 1.3 Schematic representation of signal and noise contributing to the surface ECG.

possible to make such a clear distinction.

However, this simple model is of conceptual value in so far as it indicates that the source of the signal and the source of the noise are not the same and that the tranfer characteristics between source and surface can also be considered to be different for signal and noise. Whilst in practice it is not possible to achieve filtration by simple cancellation (as suggested by the simple model), filtration by adaptive cancellation is seen as a possibility, particularly if the noise sources can be sufficiently well characterised.

1.4 Adaptive techniques in signal processing

One of the earliest techniques used for noise reduction in situations where fixed value filtering was inappropriate has been the use of coherent signal averaging. This technique gained in popularity because of the ease with which it could be implemented, and the significant improvement in signal-to-noise ratio that could be achieved. The performance of this technique depends upon the signal being repetitive and bearing a constant time relationship between itself and the averaging trigger event. Moreover, the noise must be uncorrelated with the signal. These requirements cannot always be realised in practice. In these situations other methods are required to achieve noise reduction. Adaptive cancellation is an example of such a method in which a correlated reference is conditioned to allow cancellation of the noise activity. A large part of this thesis is devoted to the investigaiton and development of the technique.

Adaptive filtering emerged as a powerful technique almost 20 years ago through the work of Widrow (1966). Many applications have subsequently been realised, including cancellation of AC interference (Widrow et al., 1975), cancellation of electrosurgical interference (Yelderman et al., 1983), separation of donor and recipient electrocardiograms obtained from heart transplant patients (Widrow et al., 1975), and enhancement of foetal electrocardiograms by cancellation of the maternal ECG (Ferrara & Widrow, 1982) as examples

of the application of adaptive filters for cancellation in electrocardiography.

In recent years, interest has been revived in wide-band, or high frequency, electrocardiograms (0.05 - 1 or 2kHz) with a view to detecting, for example, events arising from the specialised conduction system of the heart (Berbari et al., 1979; Vincent et al., 1980; Flowers et al., 1981; Abboud & sadeh, 1982; Mehra 1982; Berbari et al., 1983), late ventricular potentials (Simpson, 1981; Simpson et al., 1983; Denes et al., 1983) and cyclo-stochastic perturbations (Prasad & Gupta, 1980, 1981). In these wide-band ECG investigations, where events to be detected may be below the noise level, an efficient means of signal-to-noise enhancement is required. With these applications in mind, adaptive cancellation is now being investigated as a means of deriving noise-free, undistorted wide-band electrocardiograms.

This technique can be illustrated by reference to figure 1.4 in which two inputs are applied to the adaptive noise canceller, a primary input containing a signal s(t) plus a noise $n_0(t)$, and a reference input containing correlated noise $n_1(t)$. If the two noise sources are highly correlated a perfect cancellation of $n_0(t)$ can be achieved. The adaptive filter conditions $n_1(t)$ to match $n_0(t)$ which is then cancelled out from the primary input. Adaptive filtering also allows the cancellation of noise in a situation where the noise and signal

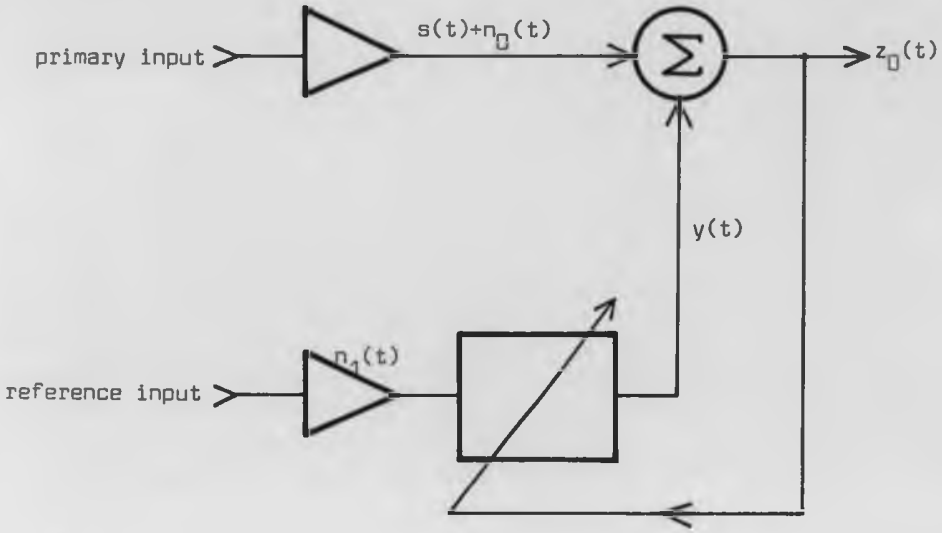

Figure 1.4 Block diagram of an adaptive noise canceller. The reference noise source $n_1(t)$ is filtered by the adaptive filter to form a best least squares estimate of the noise $n_0(t)$ in the primary signal source, yielding a best least squares estimate of the signal s(t) of the canceller output.

spectra overlap, and it is this property which makes this technique so attractive as a means of signal enhancement and worthy of further consideration in areas such as electrocardiography.

Chapter Two: Characteristics of noise, interference and artefact

2.1 Introduction

In this chapter consideration is given to the types of noise and interference that accompany the electrocardiographic signal (ECG) during recording. In deriving an ECG signal from the surface of the body, many unwanted components of noise may be encountered. Some of these components may be large in amplitude and obscure desired signals which, for some signals, can be as small as 1 - 20 μV rms. Sources of noise may be recognised within the body (bioelectric potentials), the electrode-tissue interface and within the signal acquisition and conditioning system. These sources of noise may also be considered to be of internal or external origin as illustrated in figure 2.1. Typically the components of noise include amplifier noise, tape recorder noise, lead induced noise, electrode-tissue interface effects, skeletal muscle noise and ac interference.

The acquired signal, depicted in figure 2.1 may be expressed in an equation of the form:

$$y(t) = u(t) + m(t) + n(t) \quad \ldots . 2.1$$

where $y(t)$ is the surface signal,

$u(t)$ is the signal due to the electrical activity of the cardiac musculature (ECG),

$m(t)$ the skeletal muscle noise,

and $n(t)$ the interference due to external sources

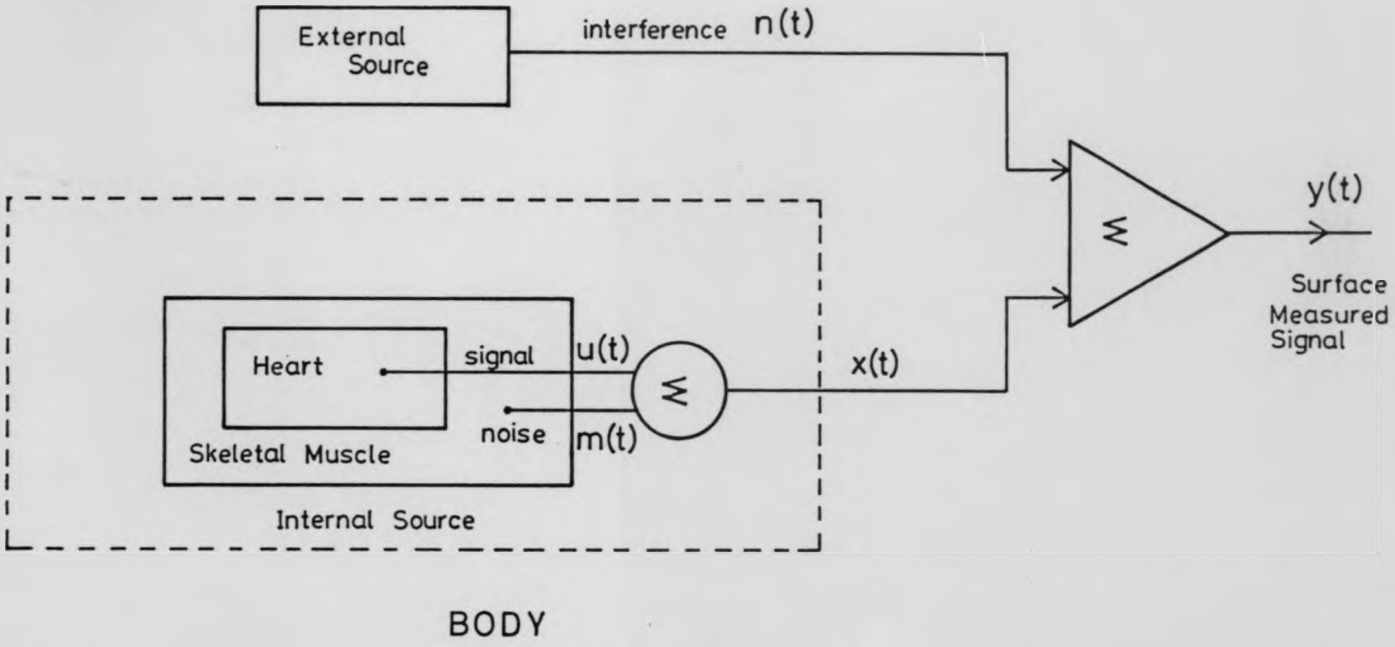

Figure 2.1 Block diagram showing the principle sources contributing to the waveforms measured from electrocardiographic leads.

In order to establish a foundation upon which an analysis of signal and noise components can be performed, a mathematical model has been prepared and its development is presented in section 2.2.

2.2 Mathematical modelling of signal and noise components of the electrocardiogram

The purpose of an accurate mathematical representation of ECG signal, muscle and noise components is to facilitate the theoretical evaluation of various methods of separating the signal from the noise. A mathematical model of the ECG signal, muscle and interference components may be considered to include internal sources ($u_i - u_n$) due to the electrical activity of the cardiac musculature which, by virtue of the volume conduction properties of the thorax, may be detected as a composite signal at the body surface. The component m(t) is the skeletal muscle activity, n(t) denotes the external sources of noise and interference, and y(t) is the surface recorded signal plus noise.

$$y(t) = u(t) + m(t) + n(t)$$

$$u(t) = \sum_{i=1}^{i=n} U_i(t)$$

where $U_i(t)$ are the individual cellular components of cardiac activity.

U(t) is to some extent a deterministic component of the surface derived signal, m(t) + n(t) are non-deterministic components.

Santopietro (1974,1977) assumed that both m(t) and n(t) have zero mean.

Thus, considering expectations:

$$E[m(t)] = E[n(t)] = 0 \quad \ldots\ldots 2.2$$

Therefore the ensemble average of equation 2.1 becomes:

$$E[y(t)] = E[u(t)] = u(t) \quad \ldots\ldots 2.3$$

The power of y(t) may be derived in the following way;

Squaring equation 2.1

$$y^2(t) = u^2(t) + m^2(t) + n^2(t) + 2u(t)m(t) + 2u(t)n(t) + 2m(t)n(t) \quad \ldots 2.4$$

Taking the ensemble average of equation 2.4

$$E[y^2(t)] = E[u^2(t)] + E[m^2(t)] + E[n^2(t)] + 2E[u(t).m(t)] + 2E[u(t).n(t)] \quad \ldots\ldots 2.5$$

Since n(t) and m(t) are independent of u(t) and with each other,

$$2E[u(t)m(t)] = 2E[m(t).n(t)] = 0$$

Equation 2.5 therefore becomes:

$$E[y^2(t) - u^2(t)] = E[m^2(t)] + E[n^2(t)] \quad \ldots\ldots 2.6$$

Santpietro (1977) suggested that as the isoelectric intervals are free of the effects of the electrical activity of the heart, therefore the noise and the interference are the predominant components within the isoelectric intervals.

$$U(t) \simeq 0$$

From equation 2.6

$$E[y^2(t)] = E[m^2(t)] + E[n^2(t)] \quad \ldots\ldots 2.7$$

And since n(t) is assumed to be stationary, the value of $E[n^2(t)]$ may be considered constant within the isoelectric intervals. The power associated with the isoelectric intervals may be considered to comprise primarily of activity associated with skeletal muscle function, particularly during exercise. When considering the mathematical model depicted in figure 2.1 the following points should be taken into account:

a) some correlated low amplitude ECG components may appear within the isoelectric interval, and

b) some activity of skeletal muscle may appear within the QRS complex.

2.3 Characteristics of noise and artifact present in the recorded ECG

In order to extend and facilitate the use of the model proposed in section 2.2, it is necessary to fully characterise the noise and artifact components, n(t) and m(t), in equation 2.1.

The source of noise and artifact considered relevant in the process of signal acquisition and conditioning are:

amplifier noise,
tape recorder noise,
lead effect,
electrode-tissue interface effect,
skeletal muscle (EMG) noise, and
ac interference.

These components of noise and interference will be discussed individually in the following sections.

2.3.1 Amplifier Noise

In situations where there is only a small input signal available, it may be impossible to distinguish the signal from the background noise and, since the signal of interest in an ECG recorded from the surface of the body is within a range of microvolts, it is then essential to amplify the signal to a level where it can effectively be subjected to further signal conditioning and processing.

The amplifier gain was chosen so that the smallest signal of interest could be detected at the output and selectively matched to the input of analogue-to-digital converter. The maximum gain that could be used was limited by the presence of the principal inscription of the ECG signal, if distortion due to amplifier saturation was to be avoided. A voltage gain of at least 70dB was found to be necessary, but it was also desirable to make the gain variable between 70-100dB. The full specification of the instrumentation amplifier used is presented in annex A.

2.3.2 Lead Considerations

The lead which constitutes the conductive pathway between the electrode and the signal acquisition circuitry may be regarded as a 'source' of noise and interference. Noise may arise in leads due to triboelectric mechanisms (Tam and Webster, 1977) and interference by virtue of electromagnetic coupling. The interference signal due to coupling is dependent upon the structure and screening of the lead, the nature of the electromagnetic source and the length of lead.

Gordon (1975) suggested that static electricity was responsible for the triboelectric noise which could affect the ECG recording from the surface of the body by:

(i) causing the ECG baseline to drift in synchrony with the motion of the lead, and,

(ii) causing high amplitude transient artifact that may result in sustained saturation.

2.3.3 Electrode-tissue Interface

It is necessary when deriving recordings of bio-electric events from the body surface to consider the influence of the electrode-skin surface. The skin consists of three principal layers, the epidermis, dermis and sub-cutaneous layer. The outermost layer, or epidermis, consists of three sub-layers two of which actively maintain an outer layer of dead material on the surface of the skin. This outermost layer of the epidermis is termed the stratum corneum. The deepest of the three sub-layers of the epidermis, the stratum germinativium is characterised by cell formation and growth. As the cells grow they are displaced outwards by newly forming cells beneath. The growing cells pass through the second of the three sub-layers, the stratum granulosum where they begin to loose their nuclear material and become dead cells.

Electrically the characteristics of the stratum corneum are distincly different from those of the living tissue that serves it. The stratum corneum may be characterised by a membrane potential. The layer may also be considered to exhbit both resistance and capacitance. Moreover, the epidermal layer in total may be considered to exhibit electrical characterisitcs that are similar to those of a parallel RC circuit. The dermis and subcutaneous layer may be considered electrically as pure resistance components.

An equivalent circuit of the skin may therefore be of the form shown in figure 2.2. It would seem apparent from the equivalent circuit

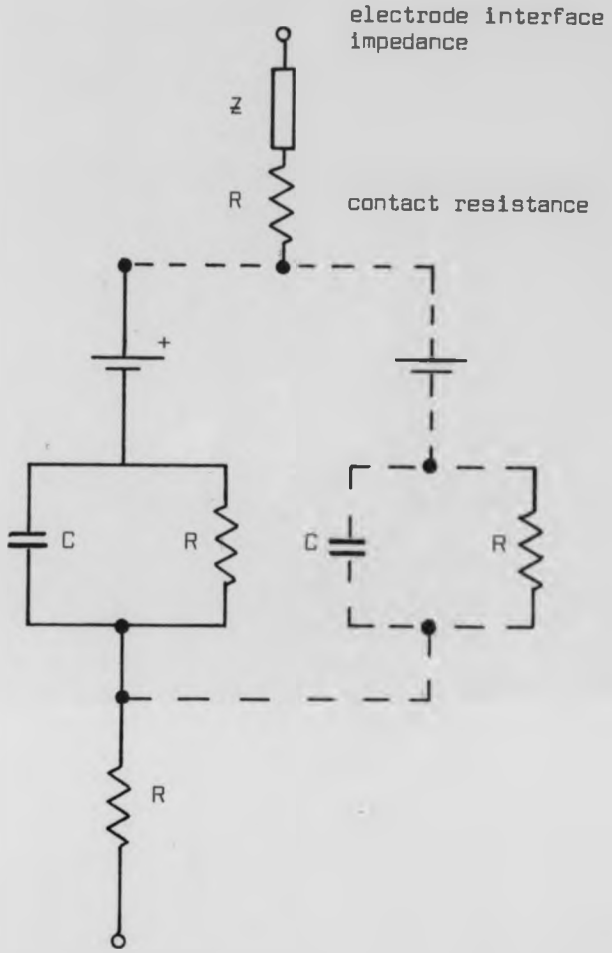

Figure 2.2 Equivalent circuit of the skin

representation of the skin that a more stable electrode-interface, suitable for recording bioelectrical events that are not of epidermal origin, may be achieved if the effect of the stratum corneum potential generator could be reduced. This may be achieved by suitable, clinically acceptable, abrasion of the stratum corneum in order to effectively bypass the potential generator and new components of this outer sublayer of dead material.

2.3.4 Skeletal muscle (EMG) noise

One of the main sources of noise in ECG's, which will be dealt with in detail in section 2.5, is the electrical activity arising from skeletal muscle function. It is a major source of interference in the high frequency ECG (Santopietro, 1974; Olivier, 1984; Sato, 1982; Jones, 1982; Miyano et al, 1980). The amount of skeletal muscle noise present in the high frequency ECG for a resting state condition can be up to 10-15dB of the random noise content. This can increase up to 20dB in the exercise ECG test. The amount of muscle noise is also dependent upon the position of the recording electrodes in relation to specific muscle masses.

In view of the problem of muscle noise in the study of the high frequency electrocardiogram, it was considered important to establish in some detail the characteristics of muscle noise in relation to conventional and non-conventional lead placements. Section 2.5 deals with the procedures, results and conclusions of a study to obtain this information.

The coherence spectrum was used as a means of characterising and comparing the muscle activity recorded from different lead positions. The coherence spectrum (coherence function) is defined as the ratio of the square of the modulus cross-spectral estimate, to the product of the spectral estimate from the two leads being considered. Coherence functions were investigated for lead positions in the frontal plane of the thorax (see section 2.5). Signals representative of these four channels are shown in figure 2.3.

The results presented in figures 2.4 - 2.6 were categorised for essentially three spectral regions:

(i) low frequency region, 100% coherence,

(ii) mid frequency region, 50% coherence,

(iii) high frequency region, 25% coherence.

It was assumed that the region in which the coherence function is under 25% is due to interference, mains and tape recorder noise which contribute to n(t) in equation 2.1. The term m(t) of equation 2.1 is likely to embrace the middle frequency region in which the coherence is 50% of the figures 2.4 - 2.6. This region could be clearly identified from the coherence function derived for the isoelectric invervals, figures 2.7 - 2.9. Components of the signal s(t) may also be encountered within this region. In the low frequency band it is quite clear that most of it is associated with the ECG signal s(t) and is highly coherent between the four channels considered. It is also clear that less coherence can be found between any pair of channels as the distance between them increases. Tables 2.1 and 2.2 summarise the relationship between the electrode placement with regard to coherence function.

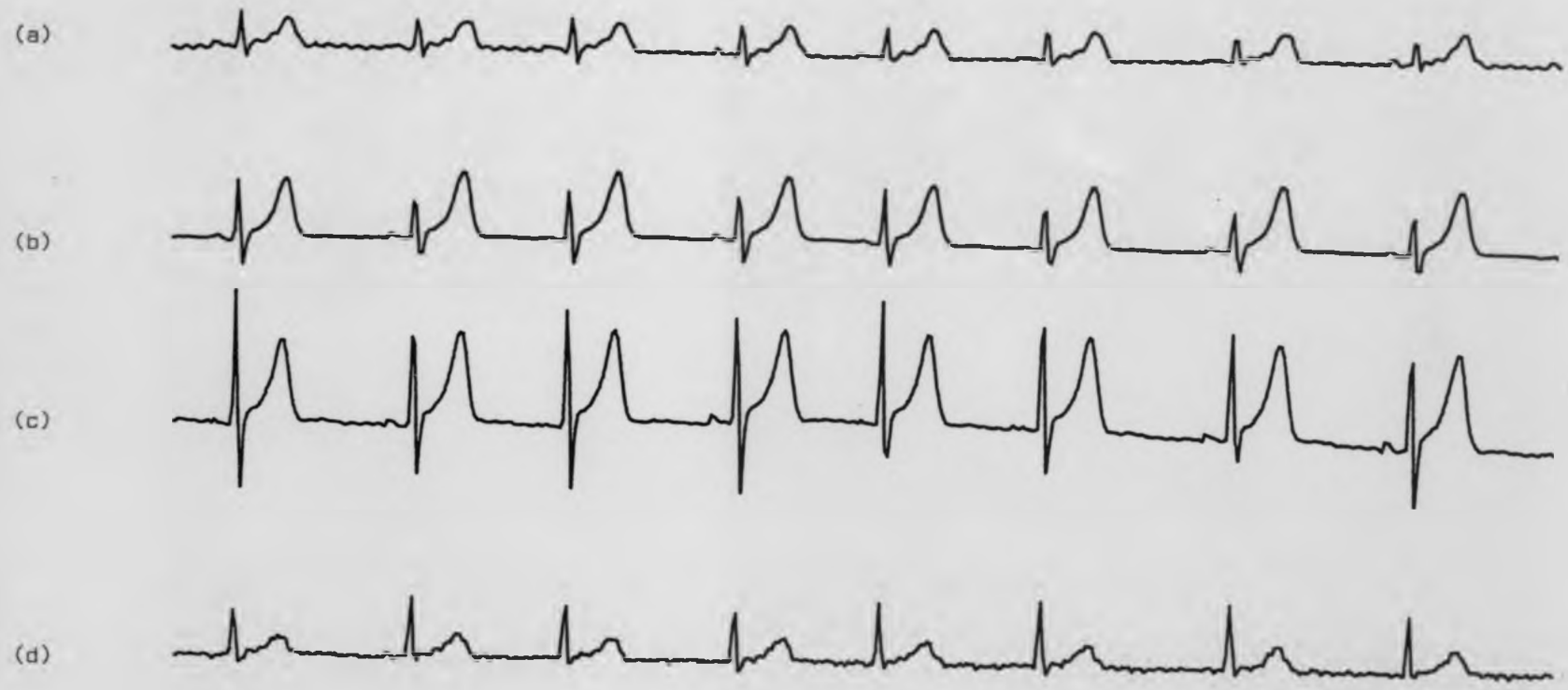

Figure 2.3 Shows the recording of four channels of ECG (10mm separation between channels)
(a) electrode placed at mid-clavicle line at the level of the 1st intercostal space.
(b) electrode placed 10mm below electrode (a).
(c) electrode placed 20mm below electrode (a).
(d) electrode placed 30mm below electrode (a).

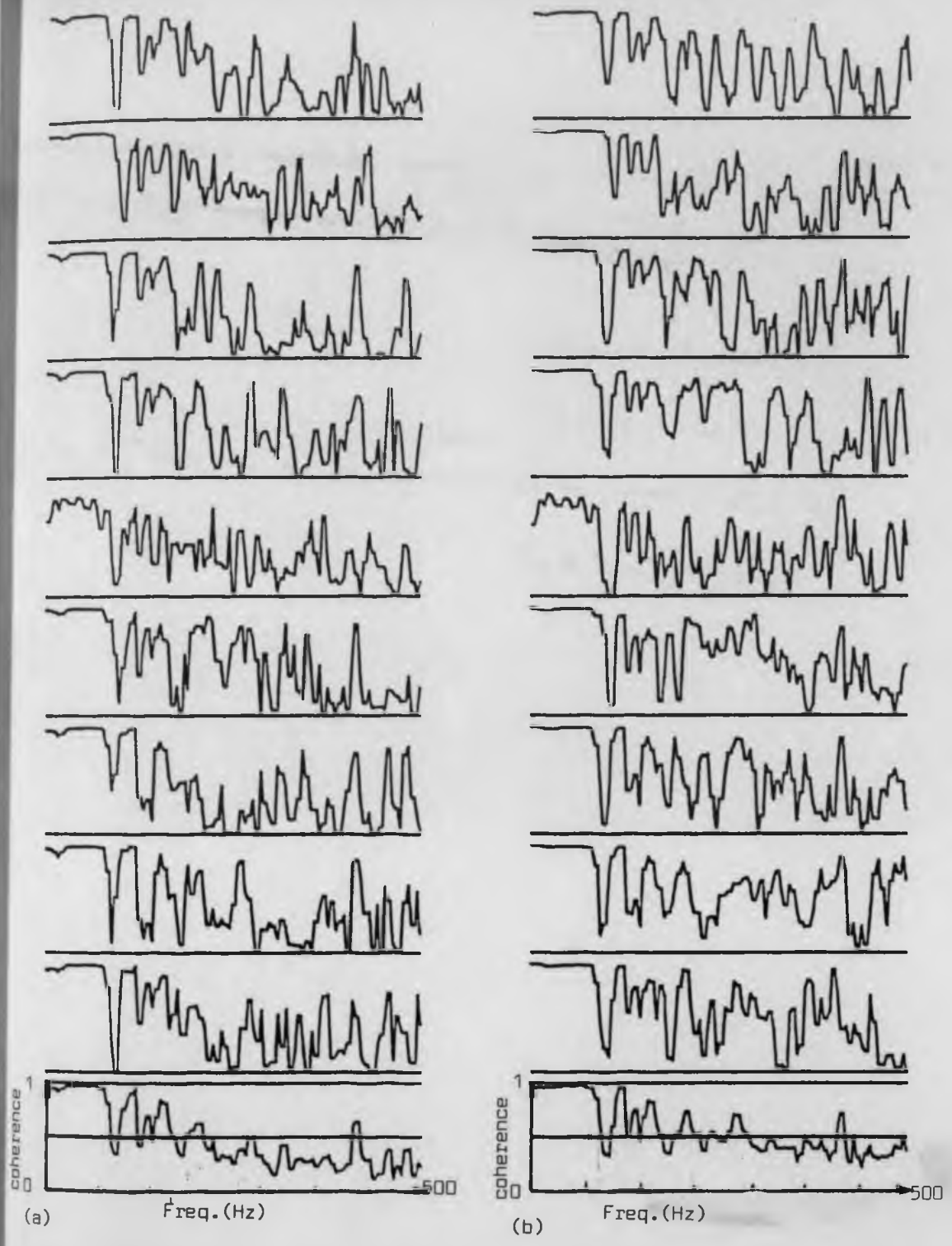

Figure 2.4 Comparison of coherence function between individual ECG cycles between;

(a) channels 1 and 2
(b) channels 1 and 3

The bottom trace is the coherence average of the individual cycles of channels 1, 2 and 3.

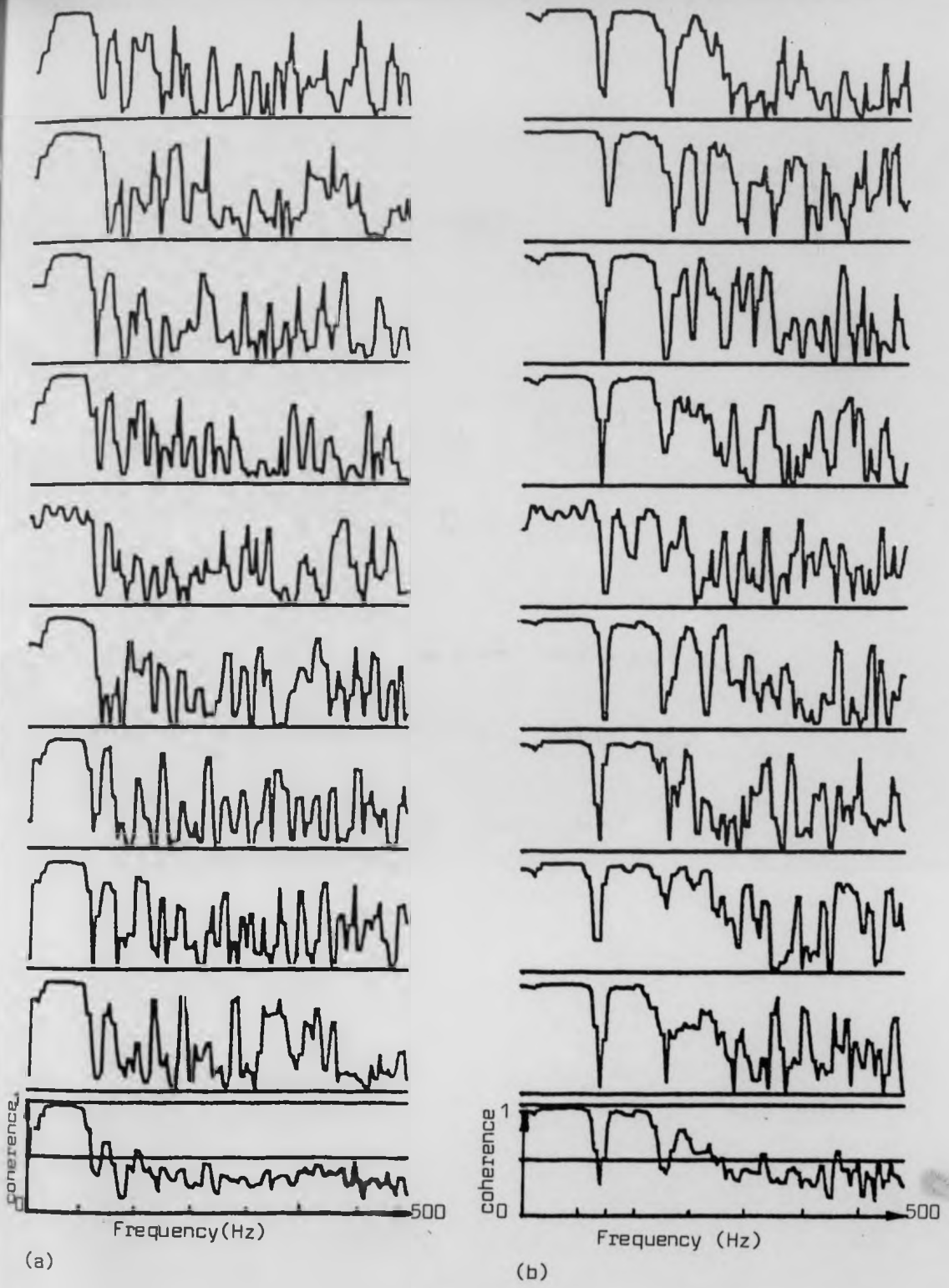

Figure 2.5 Comparison of coherence function between individual ECG cycles between;

(a) channels 1 and 4
(b) channels 2 and 3

The bottom trace is the coherence average of the individual cycles of channels 1,4 and 2,3

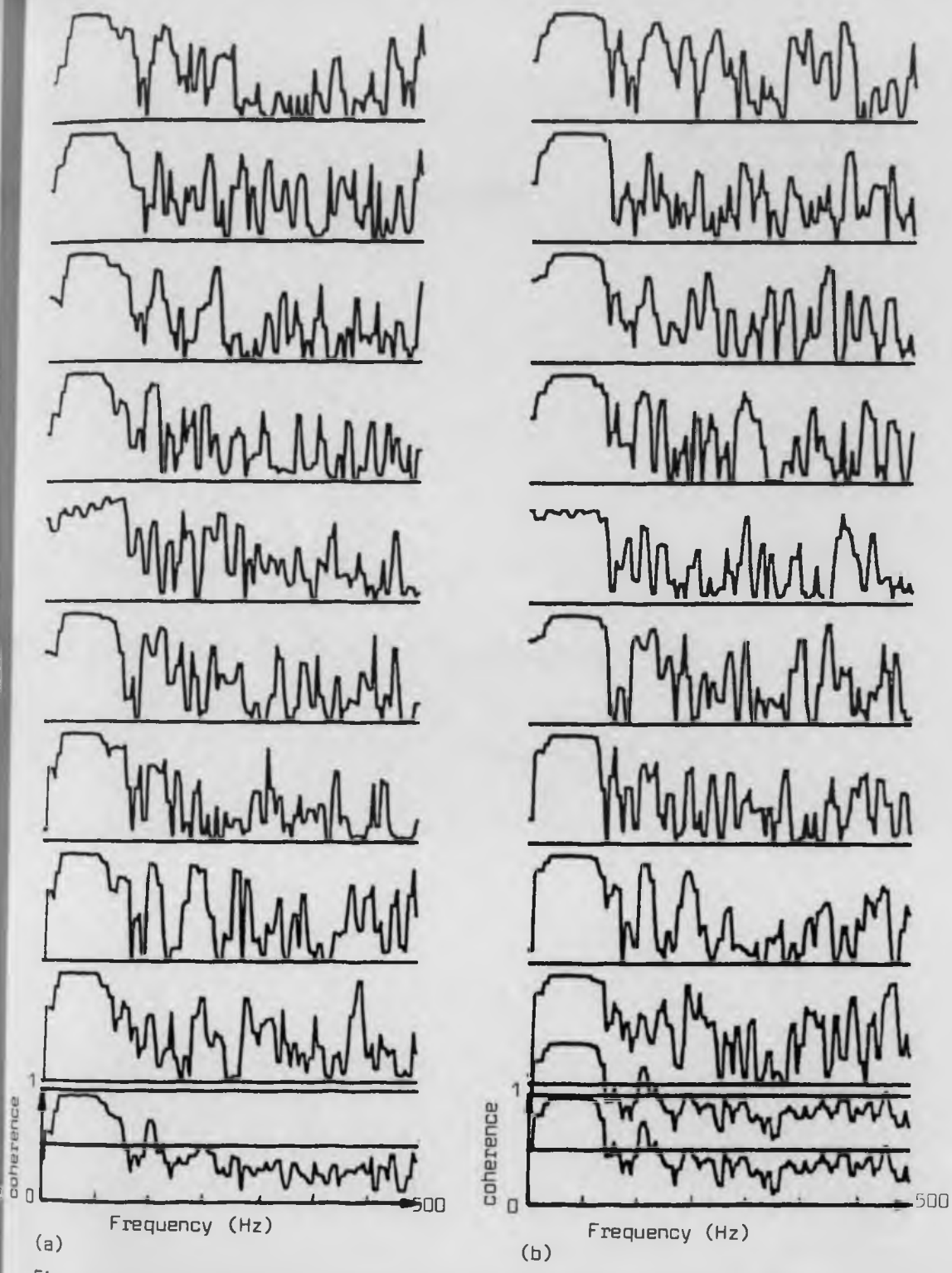

Figure 2.6 Comparison of coherence function between individual ECG cycles between;

(a) channels 2 and 4
(b) channels 3 and 4

The bottom trace is the coherence average of the individual cycles of channels 2,4 and 3,4.

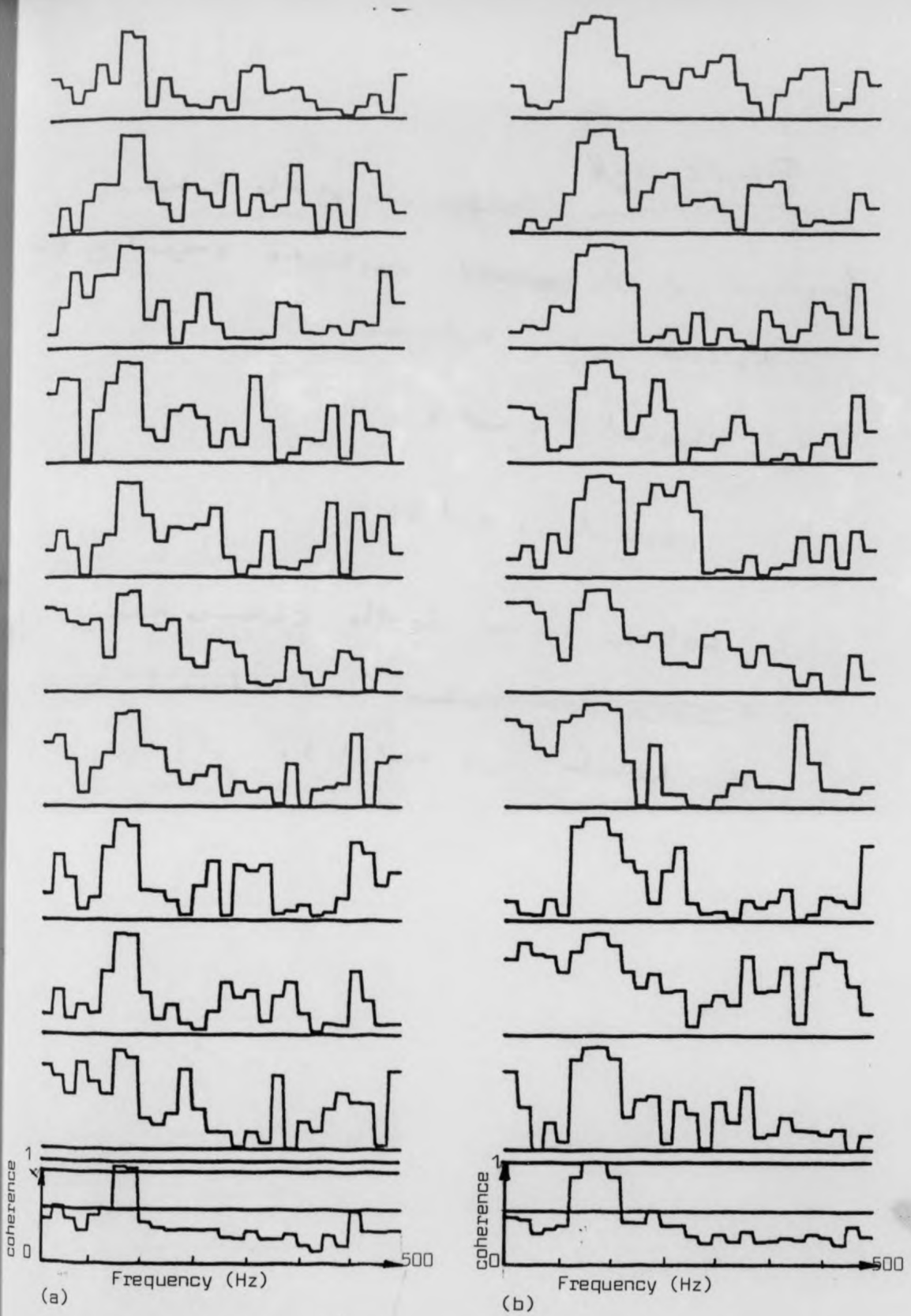

Figure 2.7 Comparison of the coherence function of isoelectric segment of the individual cycles between;

(a) channels 1 and 2
(b) channels 1 and 3

The bottom trace is the coherence average of individual cycles of channels 1,2 and 1,3. NB: resolution poorer due to shorter lengths of record

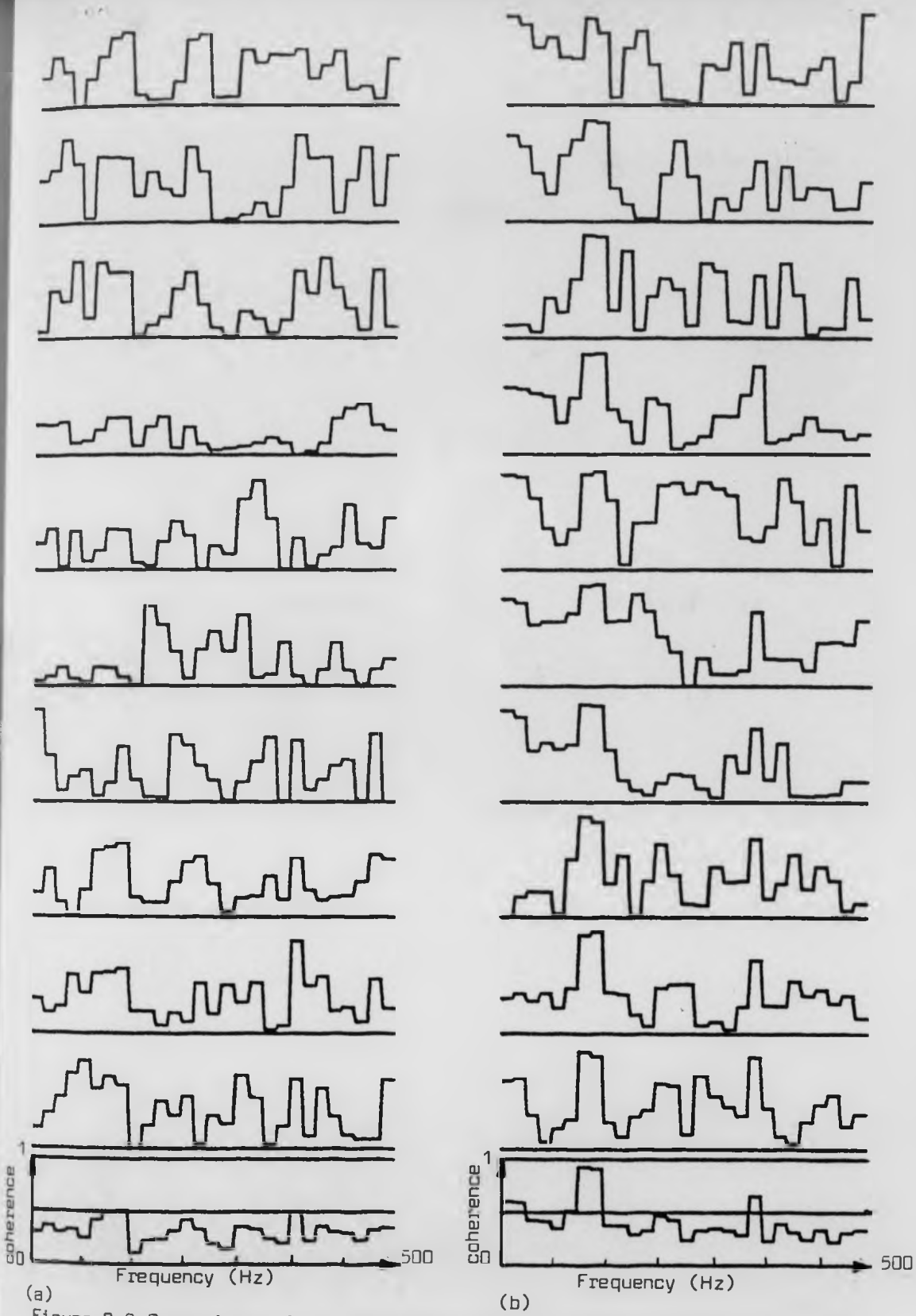

Figure 2.8 Comparison of the coherence function between isoelectric segment of individual cycles between;

(a) channels 1 and 4
(b) channels 2 and 3

The bottom trace is the coherence average of individual cycles of channels 1,4 and 2,3.

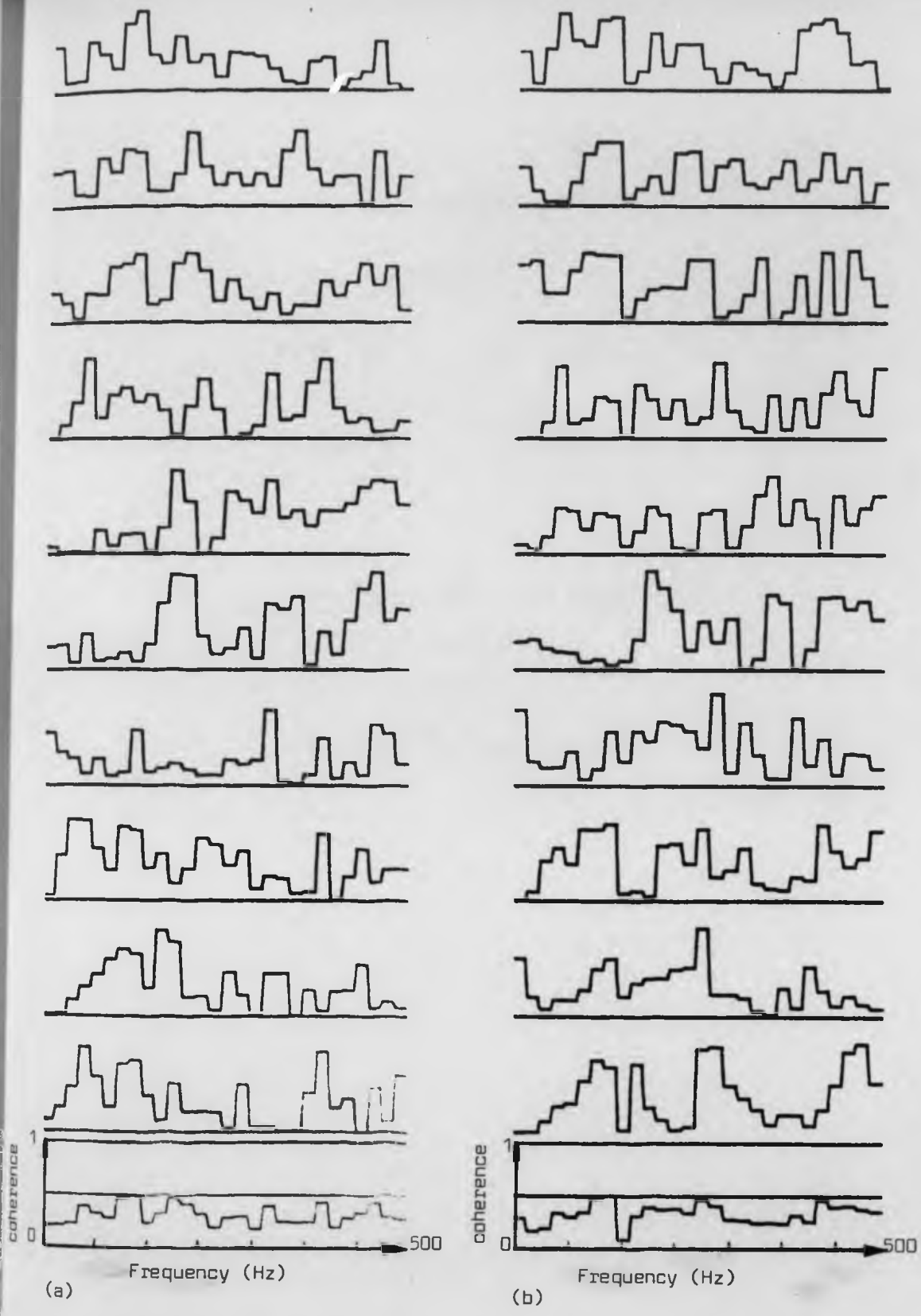

Figure 2.9 Comparison of the coherence function between isoelectric segments of individual cycles between;

(a) channels 2 and 4
(b) channels 3 and 4

The bottom trace is the coherence average of individual cycles of channels 2,4 and 3,4.

Table 2.1

Figure Number	Coherence between channels	100% (Hz)	50% (Hz)
2.6	1 and 2	110-140	10-40 420-440
2.6	1 and 3	90-160	420-440
2.7	1 and 4	-	110-140 360-370
2.7	2 and 3	110-140	330-360
2.8	2 and 4	-	110-140 180-190
2.8	2 and 4	-	110-140 410-430

Table 2.1 shows the coherence function between the four recorded channels for the isoelectric interval.

Table 2.2

Figure Number	Coherence function between channels	100% coherence (Hz)	50% coherence (Hz)
2.4	1 and 2	0- 90 110-130 140-180	270-280 410-420
2.4	1 and 3	30- 90 110-130	210-220 410-420
2.4	1 and 4	10- 90	110-120
2.4	2 and 3	0- 90 120-180	190-250
2.5	2 and 4	10- 90	140-160
2.5	3 and 4	10- 90	140-160

Table 2.2 shows the coherence function between the four recorded channels for the ECG.

2.3.5 AC interference in the electrocardiogram

AC interference is one of the most common types of disturbance encountered in recording ECG's from the surface of the body. This section is concerned with the origins of electrical interference, and the advantages and disadvantages of techniques used to reduce 50Hz interference in surface ECG's (Huhta & Webster, 1973). Many researchers have described, in detail, the mechanisms of coupling of interference (50Hz) in the recording of ECG signals. Webster (1977) has shown that interference may enter the amplifier input leads in three ways:

(i) Capacitative coupling which allows, via displacement, a current to flow in the input leads.

(ii) Inductive coupling between current carrying conductors and the input leads, in which the magnetic field induces an electromotive force in the input leads. Ground loops allow interference by induction into the loops established by injudicious connections to ground.

(iii) Resistive coupling in which a conductive pathway is established between a source of electrical activity and the recording equipment.

Interference can be minimised by various procedures, such as skin preparation, appropriate arrangement of the leads and electrodes, careful earthing and shielding, and also by choosing a high

common-mode rejection amplifier. Many researchers have also used signal processing techniques such as filtering and averaging to remove noise and interference. The results of considering such techniques are presented in Chapter 3.

Figure 2.10a shows the recording of an ECG signal contaminated by 50Hz interference, while figure 2.10b indicates the occupancy of 50Hz interference in the power spectra of figure 2.10a.

(a)

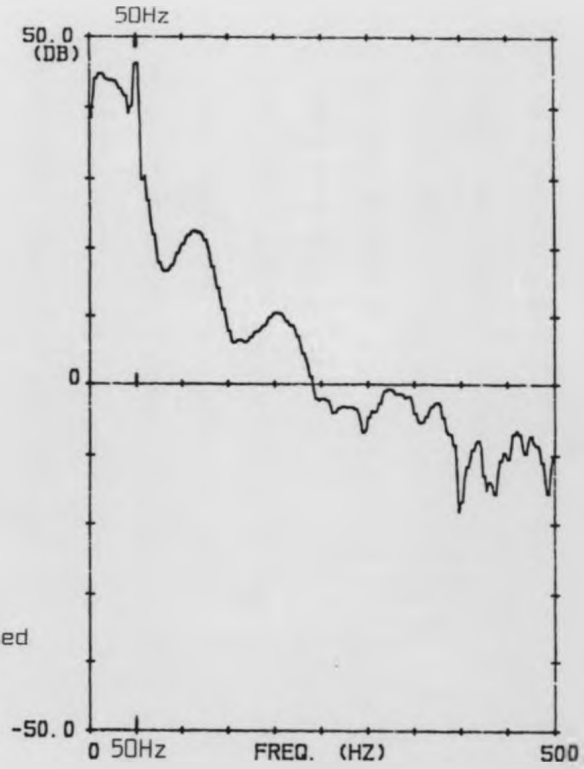

(b)

Figure 2.10 a) The recording of ECG signal contaminated with 50Hz interference

b) The power spectrum of (a) showing the 50Hz spectrum

2.4 Characteristic of noise and artifact present during exercise ECG

The exercise ECG is an important technique for indentifying cardiac disorders that are not apparent from the resting state ECG, but may be precipitated by the physical stress of exercise and then become apparent in the ECG. Although the test may be effective in this respect the attendant muscle activity may, by virtue of the noise produced, obscure events within the ECG. The quality of the recorded ECG's depends upon factors such as electrode-skin preparation, choice of electrodes, lead system and type of exercise test (Betts & Brown, 1976). Movement of the electrodes in relation to the skin may result in base-line fluctuation correlated with periodic bodily activity and other physiological sources of noise such as respiration.

Figure 2.11a shows an example for recording electrodes placed in lead V_1 during exercise ECG. It shows the base-line fluctuation, while figure 2.11b shows the recording of the same lead in the resting state.

Figure 2.11 (a) Example of recording electrode placed at V_1 during exercise testing.
(b) Example of recording electrode placed at V_1 with subject at rest.

2.5 Experimental method for muscle noise measurement studies

The main objective of this part of the study was to obtain ECG recordings corresponding to lead I and leads parallel to lead I in the frontal plane, under specified conditions relating to activation of various major skeletal muscle groups, with a view to selecting appropriate lead positions for the adaptive filter technique.

Four leads were recorded simultaneously, these being defined as follows. For each of the subjects considered a reference electrode, common to all leads was attached to the left leg. The first electrode pair was placed with one electrode in each of the right and left mid-clavicular lines at the level of the sternoclavicular junction and the three remaining electrode pairs placed on the mid-clavicular lines, immediately below the first pair and separated at 80mm centres.

Recording Procedures

(i) With the subject at rest, one minute recordings for each lead were obtained.

(ii) A one minute recording of each lead was obtained with the subject bending his head forward and chin touching the chest so as to activate mainly platysma muscle, splenious capitis muscle and semispinalis capitis muscle.

(iii) A one minute recording was obtained for each lead with the head inclined backwards, so as to activate mainly splenius capitis muscle, semispinalis capitis muscle and the platysma muscle.

(iv) A one minute recording was obtained for each lead with the subject grimacing under conditions in which the sternocleidomastoid muscle and platysma muscles were considered to be activated.

(v) A one minute recording for each lead was obtained with the subject's arms raised, the hands placed behind the neck and the elbows brought forward. Under these conditions the trapezium and deltoid muscles were considered to be activated.

(vi) A one minute recording was obtained for each lead with the subject tensing the abdominal muscles. Under these conditions the major and minor pectoralis muscles, together with the deltoid, serratus anterior and external oblique muscles were considered to be activated.

Results and Discussion

The results presented in this section will be used to predict, on the basis of coherence function, the effectiveness of the methods used in chapters 3 and 4 in cancelling noise and interference in different electrode pairs. Santopietro (1974,1977) clearly assumed the occupancy of the noise and interference to be within the isoelectric intervals. The coherence was implemented for the combination of the four channels in this region. The coherence function was also applied for the ECG signal only.

Figure 2.12 shows the four channel recording of the ECG with the subject at rest, while figure 2.13 shows the coherence function for

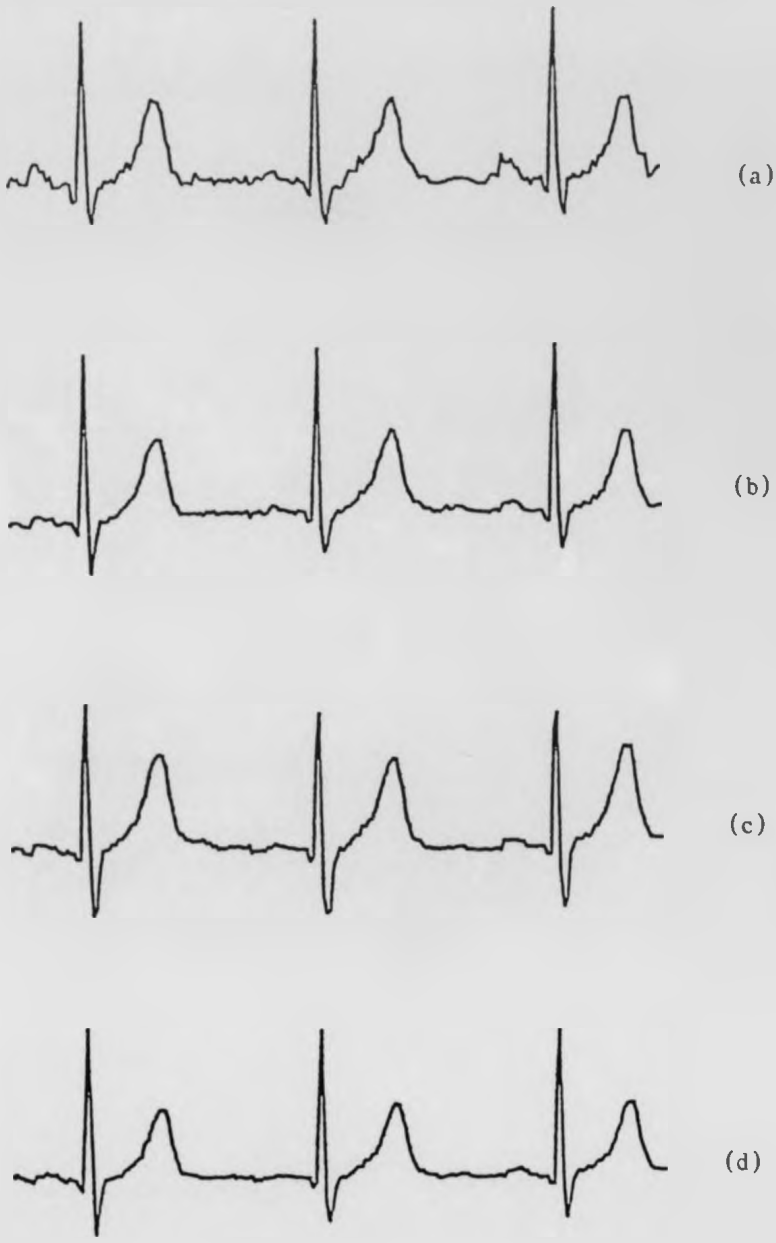

Figure 2.12 The surface recording of four channel of ECG

(a) - channel 1
(b) - channel 2
(c) - channel 3
(d) - channel 4

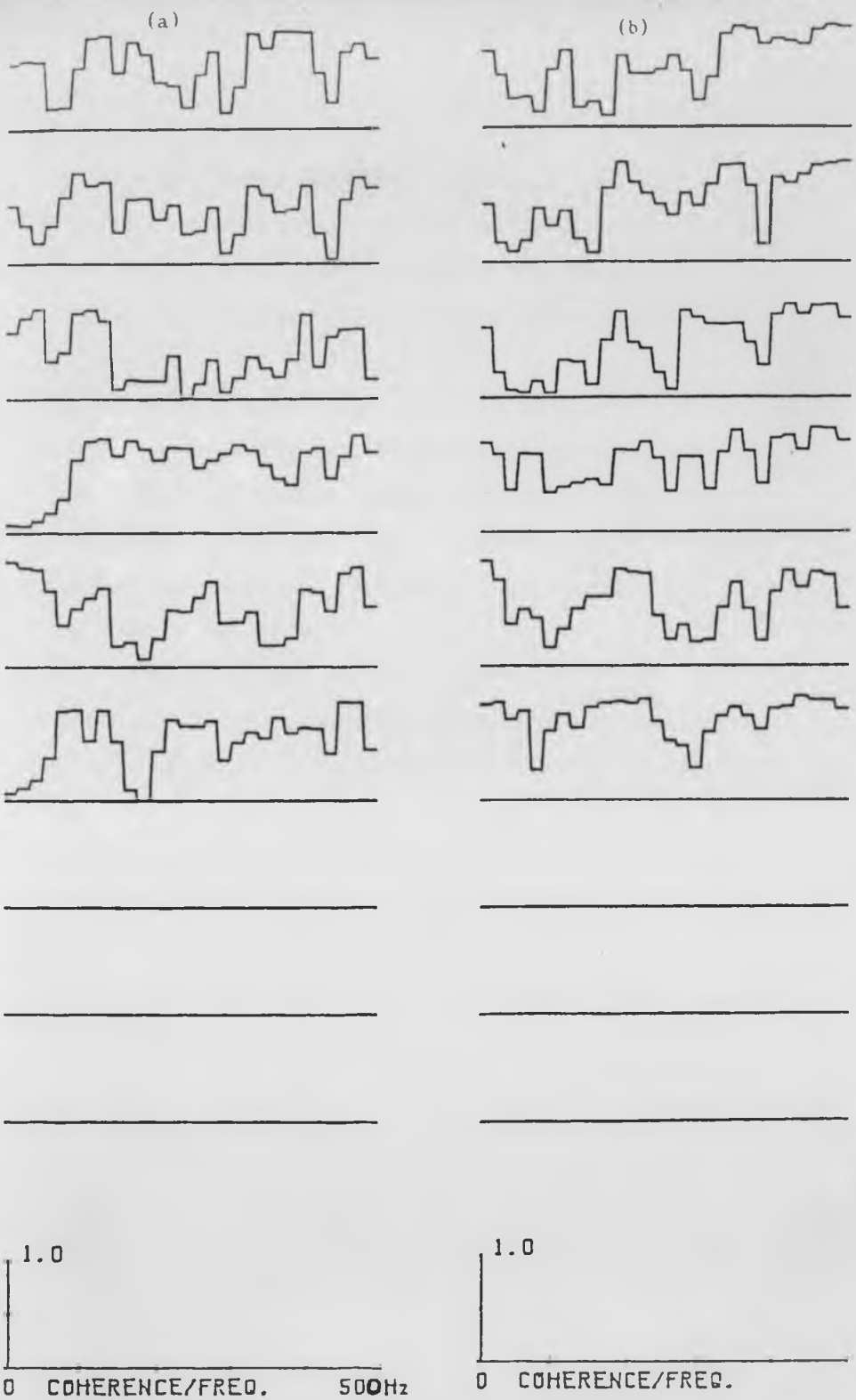

Figure 2.13 Comparison of coherence function of isoelectric intervals between
a - the first isoelectric of channel 1 (2,3,4), and between the individual isoelectric of the same channel
b - the second isoelectric of channel 1 (2,3,4), and also between the second isoelectric of the same channel

the isoelectric intervals of various channel combinations. These results are in good agreement with the results presented in the previous section. As the electrode separation increases the attentuation of components in low frequency region varies.

Figure 2.14 shows the coherence function for recordings derived from the four channels considered. The consistently high coherence value in the frequency range 0-100Hz suggests that this activity is due to the ECG signal. In the mid and high frequency regions the distribution of coherence function may be partly attributed to artifacts and noise.

The slight decease in coherence that occurs as electrode separation increases indicates a decrease in the level of shared activity, or increase in random noise activity. At higher frequencies the activity of the ECG is variable and some poorer coherence might be expected, due to the relatively greater influence of noise.

The summary and general discussion of the result of experiments ii to vi are presented in table 2.3 and 2.4.

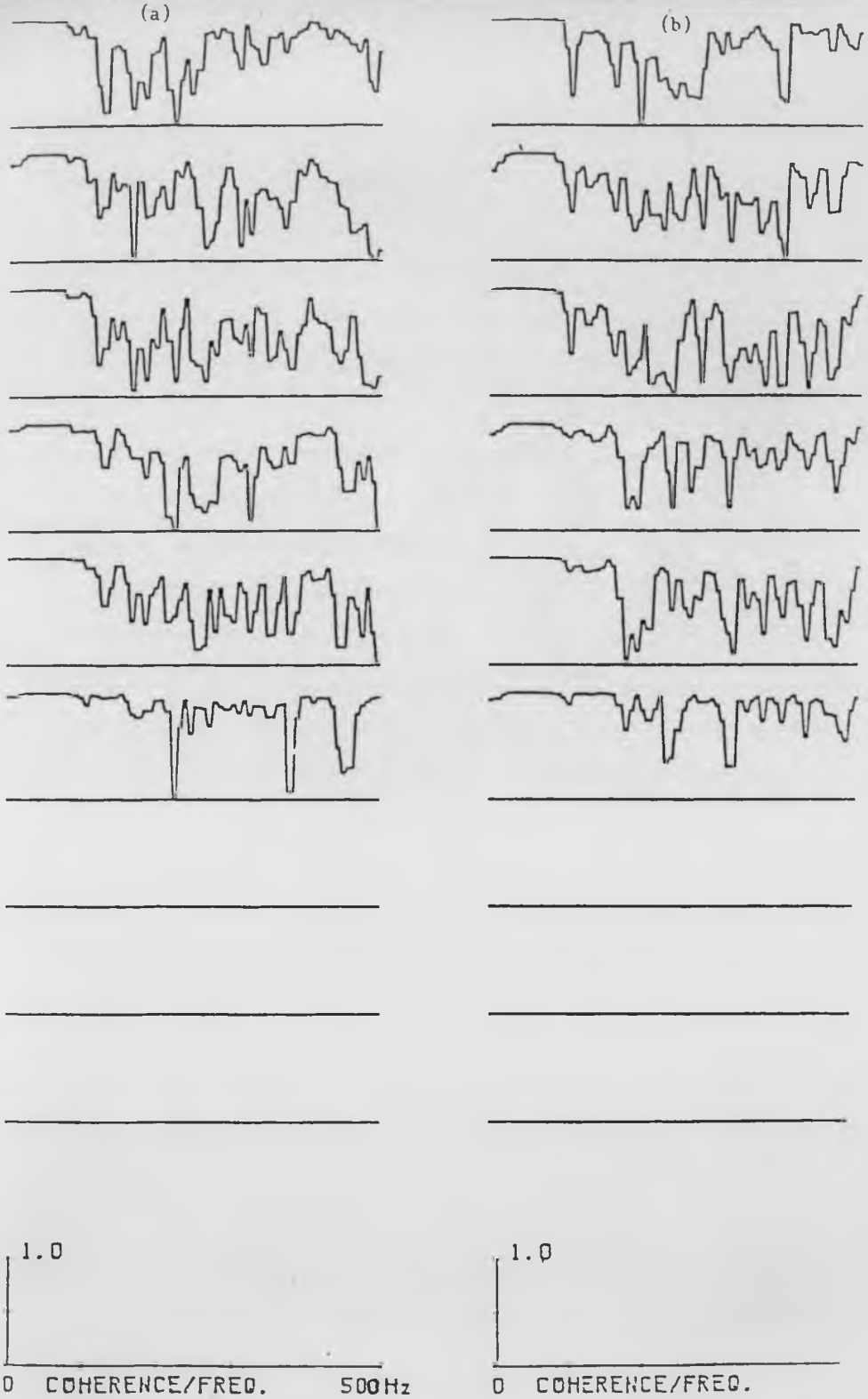

Figure 2.14 Comparison of coherence function of the first ECG cycle between

a - channel 1 (2,3,4) and between the individual cycles themselves
b - the second ECG cycle of channel 1 (2,3,4) and between the individual cycles themselves

2.6 Discussion

The results of the study of noise, interference and artifact have been presented in this chapter. Methods have been desicribed to enable identification of suitable electrode placement for adaptive processing.

A coherence function was used to predict the spatial correspondence between activity in different electrode pairs for both signal and noise independently. It was suggested that a high coherence value in frequency range 0-100Hz is due to the activity of the heart signal only. At frequencies above 100Hz, the ECG activity is small, and lower coherence might be expected due to the greater influence of the skeletal muscle noise and other artifacts. This seems to be in agreement with the consequences arising from the overlap spectra of signal and skeletal muscle shown in figure 8.1

At very high frequencies, in which the coherence function was seen to be approximately 0.25, tape recorder noise and any other random components were considered responsible.

An experiment was conducted to establish the identity of the primary muscle mass activity that contaminates the ECG signal. A summary of the results is presented in tables 2.3 and 2.4.

The results indicate the greater the spatial separation between lead pairs, the lower the coherence; sufficient for selecting appropriate leads for adaptive cancellation.

Table 2.3

Experiment	Coherence between channels	100% Hz	50% Hz
ii	1 - 2	0 - 80	90 - 100 130 - 150 190 - 200
	1 - 3	0 - 50 75 - 90 140 - 150	180 - 200
	1 - 4	0 - 60 180 - 200	70 - 85 130 - 150
iii	2 - 3	0 - 80 100 - 160 180 - 200	160 - 180
	2 - 40	0 - 80	120 - 130 180 - 190 220 - 230
iv	1 - 2	0 - 80	90 - 160
	1 - 4	0 - 40	80 - 140 160 - 200
v	1 - 4	0 - 40 80 - 110 140 - 220	110 - 130

Table 2.3 shows the coherence function between the four selected recorded channels for the complete ECG.

Table 2.4

Experiment	Coherence between channels	100% Hz	50% Hz
ii	1 - 3	0 - 20 120 - 170 180 - 220	70 - 120
	1 - 4	180 - 190 230 - 250	0 - 120
	2 - 4	120 - 180	0 - 35
iii	1 - 4	50 - 65	0 - 20 75 - 130
iv	1 - 2	10 - 45 210 - 230	70 - 120 140 - 150 160 - 200
	1 - 3	0 - 45 150 - 180 210 - 230	70 - 120
	1 - 4	150 - 180 210 - 230	0 - 40
v	1 - 4	0 - 60	90 - 160
	3 - 4		20 - 100 200 - 230

Table 2.4 shows the coherence function between the four recorded channels for the isoelectric intervals.

Chapter Three:Techniques for Noise reduction

3.1 Introduction

The basic approach to the problem of investigating a signal corrupted by interference or noise is to start by passing the corrupted signal through a filter, with a view to suppressing the effect of the noise or interference whilst leaving the signal unchanged.

This chapter provides a review of the previous work that has been done on the extraction of signal from noise based on a priori knowledge of both the signal and the noise. Extraction techniques of this kind are referred to as fixed value filtering. In filtering of this type, the coefficients do not change with the changing of statistical characteristics of the signal.

3.2 Noise reduction using analogue filters

Knott (1974) introduced an analogue filter with the ability to reduce interference at mains frequency and harmonics. This filter was based on the idea of a commutating RC network as shown in figure 3.1. The advantage of this technique was its ability to track changes in the mains frequency, enabling very sharp rejection characteristics by using a low-pass filter. However, the technique has a disadvantage of introducing a phase shift in the pass-band and causes a decrease in the rejection performance. In recent years, advances in digital technology and the development of fast fourier transform algorithms have made the use of digital processing techniques practical for spectral analysis of non-stationary waveforms and filtering.

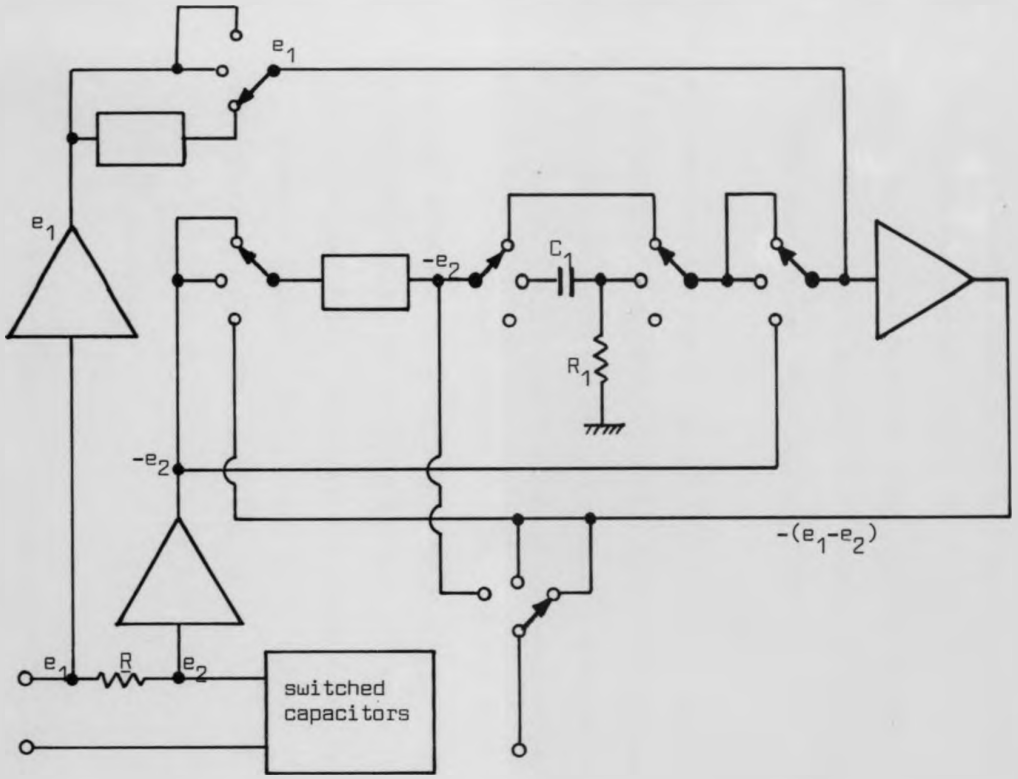

Figure 3.1 A complete block diagram of a practical mains rejection filter.
(adapted from Wireless World, October 1977, figure 9)

3.3 Noise reduction using digital filtering

There is a considerable amount of published work that deals with the acquisition and enhancement of ECG signals from unwanted noise, and has been well reviewed in a number of papers published within the last fifteen years (Furno & Tampkins, 1983; Huhta & Webster, 1973; Johnson et al., 1979; Kaunitz & Widrow, 1973; Ribeiro et al., 1980; Sheild & Kirk, 1981; Weerd & Kap, 1981; Winter, 1966).

In this section, the use of digital filtering as a means of reducing noise is examined. In 1977, Lynn introduced a low-pass recursive digital filter in which the Z-plane poles and zeros are placed inside the unit circle. This filter has the advantage of a linear phase response, but introduces a delay of 0.5s. Weavers et al., (1968) and Lynn (1971) introduced a notch filter design which had the advantages of a negligible delay, but involves a trade off between computer storage and filter delay. Very good results have been obtained by the use of recursive digital filters (Lynn, 1971). However, this type of digital filtering still affects the high frequency signal component and can also introduce 'ringing' if the frequency characteristic cut-offs are very sharp.

Levkov et al.,(1984) introduced a digital method for 50Hz interference elimination. This technique is based upon computing the interference amplitudes and subtracting these data from the original signal. This method tends to preserve the high frequency components of the signal.

Gregory and Willis (1983) introduced a new method of using a notch filter in removing 50Hz interference. This microcomputer based filter involves two stages in the elimination process:

(i) Learning phase, to identify the shape of the noise or interference waveform by sampling the ECG signal during an isoelectric interval, and saving these values as a table within the microcomputer RAM based memory, and

(ii) the filter then synchronously subtracts the values in the table from subsequent input signal samples to form the filter output waveform.

In general, a digital filter operates by weighting and summing a number of sample values of a sampled-data signal. Figure 3.2 shows a diagram of a simple recursive filter.

The relationship between the input $x(t)$ and the output $y(t)$ of a linear digital filter is given by the convolution integral

$$y(t) = \int_{-\infty}^{\infty} h(\tau)x(t - \tau).d\tau \qquad \ldots . 3.1$$

Where $h(\tau)$ is the weighting function of the filter. The frequency response function of the filter, $H(f)$, is the Fourier transform of $h(\tau)$

$$H(f) = \int_{-\infty}^{\infty} h(\tau)\, e^{-j2\pi f\tau}.d\tau \qquad \ldots . 3.2$$

A design for a low pass recursive digital filter is presented in

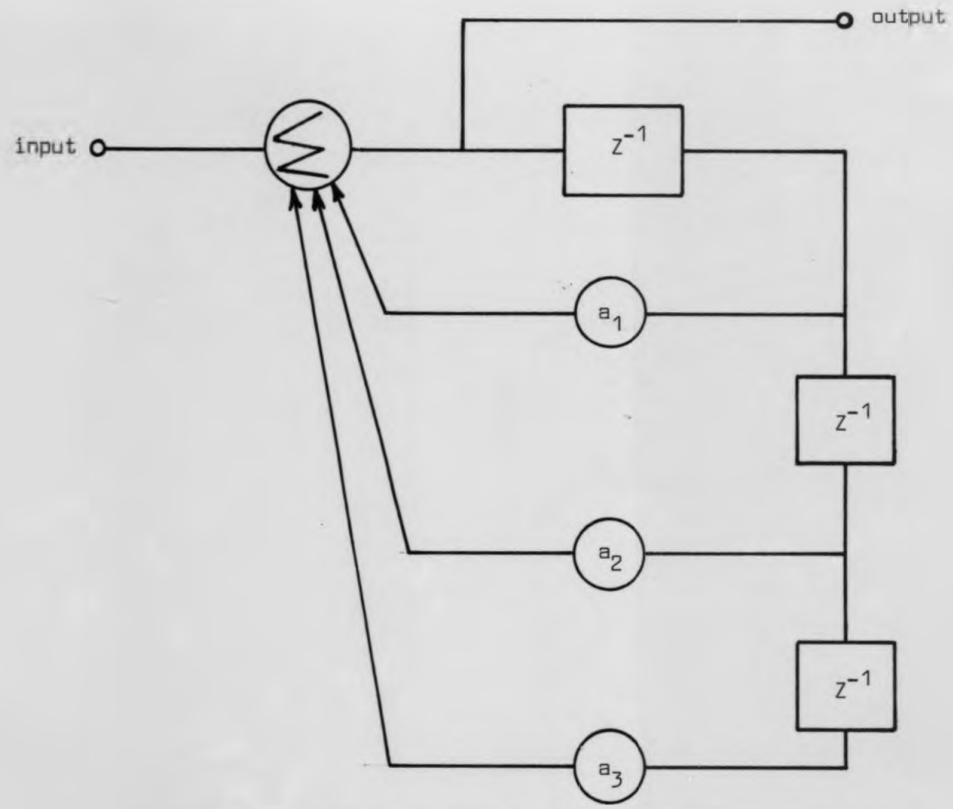

Figure 3.2 A block diagram of Simple Recursive Digital Filter

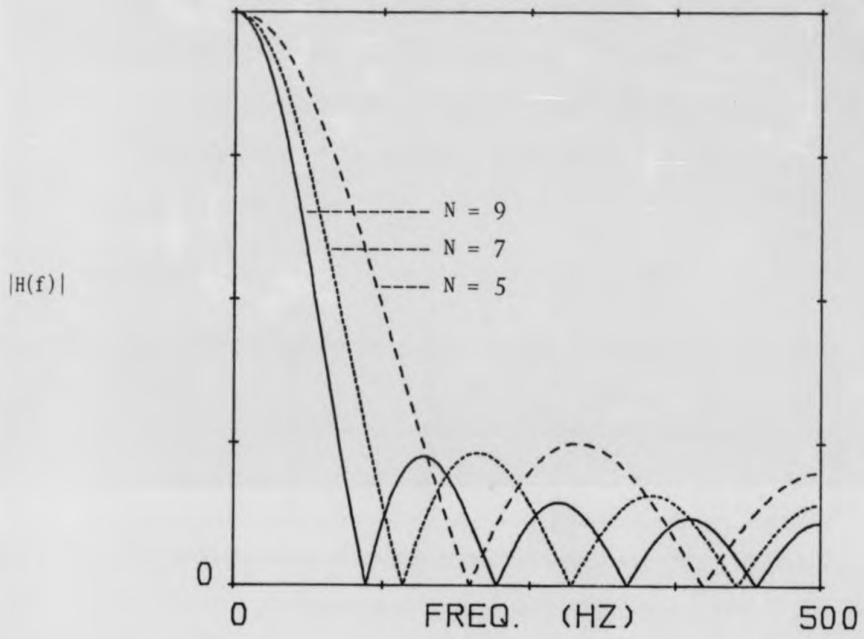

Figure 3.3 Response magnitude vs frequency characteristic of a low pass digital filter with different number of coefficients.

N = 5, 7 and 9

Annex B ,, which uses the same shape of characteristics as those used by Lynn (1977). Figure 3.3 shows the transfer characteristics of the first order recursive digital filter for different coefficients, and the effect of such filter conditioning on a noisy exercise ECG is illustrated in figure 3.4. It can be seen that a higher number of coefficients is better for the reduction of noise, but at the expense of amplitude signal distortion (Taylor & Macfarlane, 1974). Table 3.1 summarises the signal improvement with respect to the number of the filter coefficient.

Table 3.1

Number of coefficient	7	9	15	21
Signal improvement (dB)	13.38	12.27	11.71	9

From the table above it seems that the smaller the coefficient, the greater the signal improvement but with less noise reduction, and vice versa. The amount of signal improvement could be obtained if a known simulated signal was used with different noise levels.

If the noise power lies within the filter pass band, an error will arise in the filter output waveform and since, during exercise tests, their exists some spectral overlap between the noise and the desired signal, the output signal is clearly altered by the action of the filter. This is illustrated in figure 3.4.

It can be seen from figure 3.3 that the amplitude-frequency

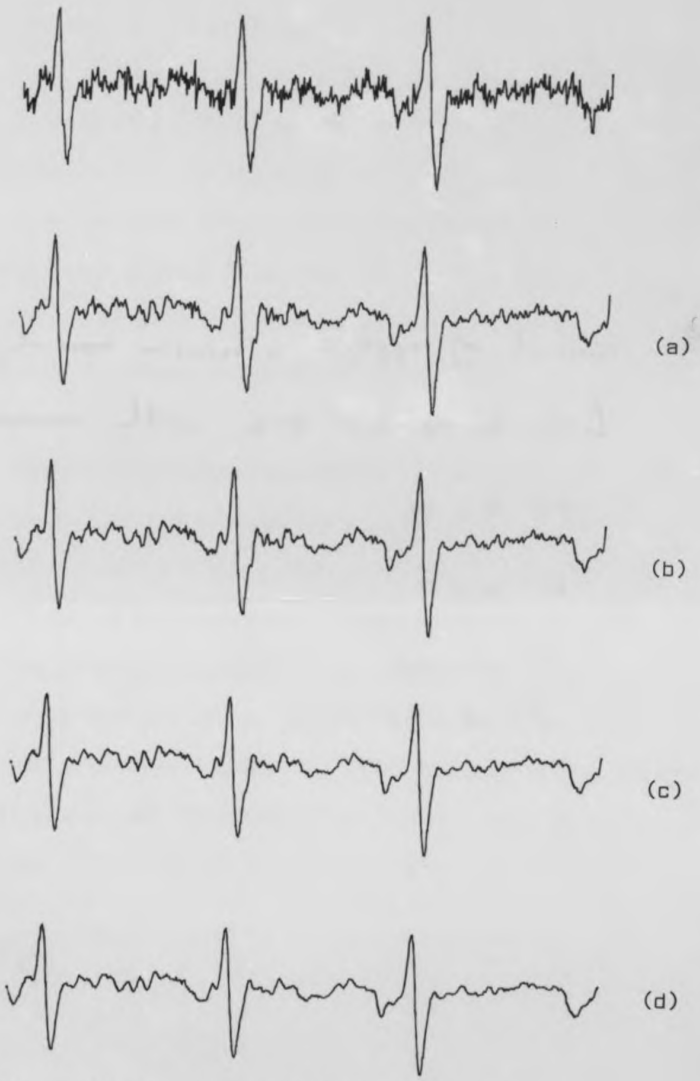

Figure 3.4 Result of applying a recursive digital low pass filter to exercise ECG with number of coefficients

(a) N = 7
(b) N = 0
(c) N = 15
(d) N = 21

characteristic is far from ideal, suffering from a poorly defined cut-off and substantial side lobes, the first side lobe having a peak about 22% of that of the main lobe.

By adding a pole at Z = (1,0) in the unit circle, the side lobe is reduced to about 5.1%, so improving the noise reduction, but at the expense of an increased computational requirement (figure 3.5). One of the advantages of digital filtering over conventional analogue filtering is that the set of weighting coefficients may be altered to match the requirement of the noise characteristic.

Often in recording electrocardiograms (ECG), a narrow band contaminating signal such as 50Hz electromagnetic interference may obscure or degrade the desired signal. The application of a digital notch filter may be used to remove the 50Hz component. Again, this has the effect of removing any 50Hz component within the signal itself, but it is ineffective in removing any of the harmonics associated with the interference component. Since the signal components in wide band electrocardiograms may well occupy a frequency range up to 1 - 2 KHz (Santopietro, 1977), the use of such techniques is limited.

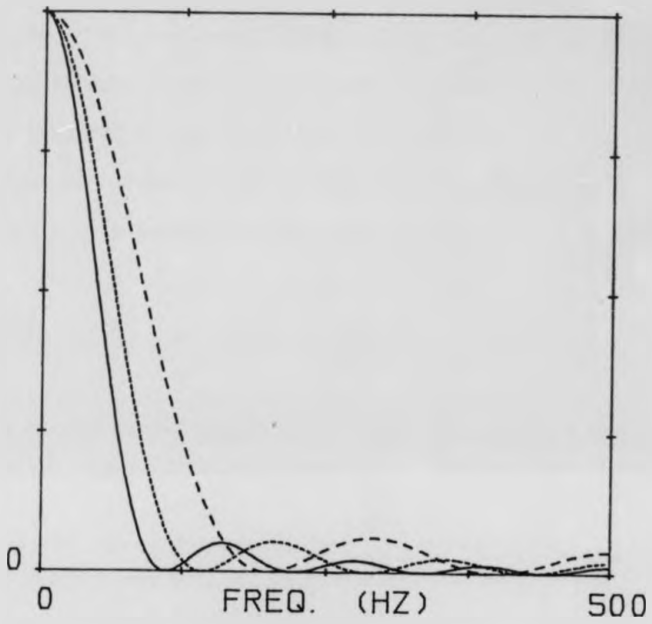

Figure 3.5 Transfer characteristics of the recursive digital filter when the side lobe is reduced by 5.1% for different number of coefficients

3.4 Noise reduction using a transversal filter

One of the techniques examined in this study as a means of eliminating noise from signal recording was the use of transversal filtering. A block diagram of a transversal filter is illustrated in figure 3.6. This type of filter receives input samples which are then delayed and multiplied by a set of weighting coefficients with all the products summed within each time period to form the output samples. Mathematically this process may be represented by the expression:

$$y(t) = \sum_{n=1}^{N} x(t - n)h_n \qquad \ldots . 3.3$$

Where x(t) is the signal input to the N-tap line and the output signal is y(t).

A computer program was written (see Annex C) to enable the calculation of the number of weight coefficients required for a specific transfer function of the filter. Figure 3.7 illustrates the impulse response and transfer function for different weight coefficients of the transversal filter. The performance characteristics for this arrangement are illustrated in figure 3.9.

A greater noise reduction can be obtained by the use of this technique, but such a reduction is at the expense of amplitude signal distortion, especially at low input signal-to-noise ratios. The improvement (SNR) can be estimated using a quantifiable input signal that shows resemblance to the real data, and to which different

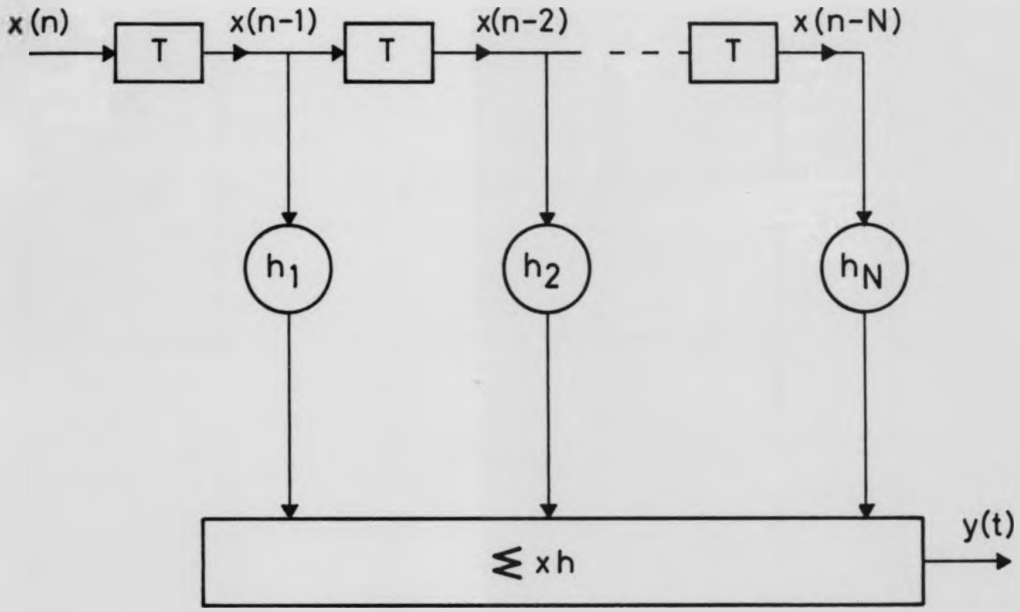

Transversal filter.

Figure 3.6 Diagram of a transversal filter based on a tapped delay line structure. The output y(t) is formed by summing weighted contributions of successively delayed input samples x(n), x(n-1). . . . . x(n-N). T represents a time delay of one sample period, and h_1, h_2. . . . h_N are the filter coefficients.

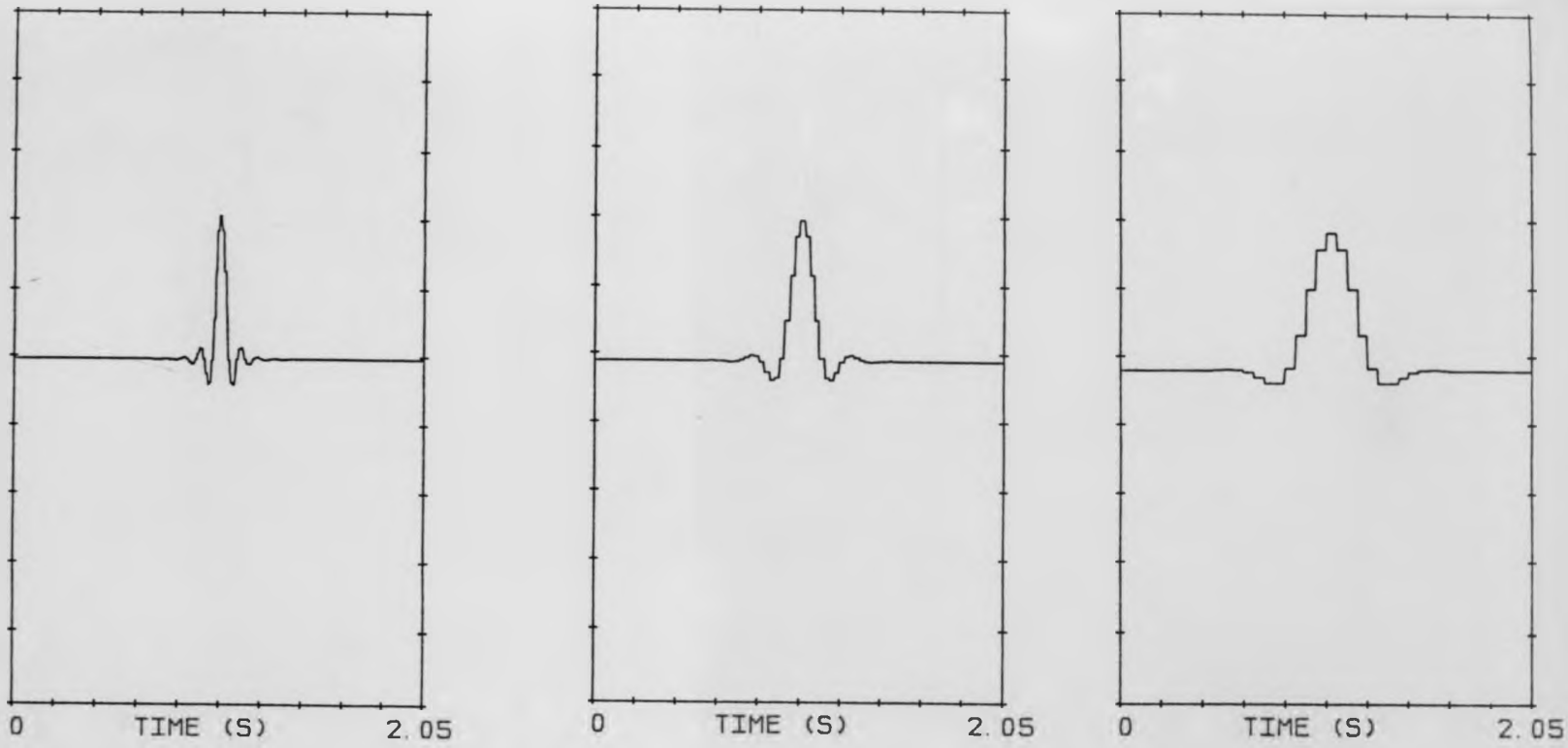

Figure 3.7 The impulse characteristic of a transversal filter with weight coefficients of N = 199, 81 and 13

TIGHTLY
BOUND
COPY

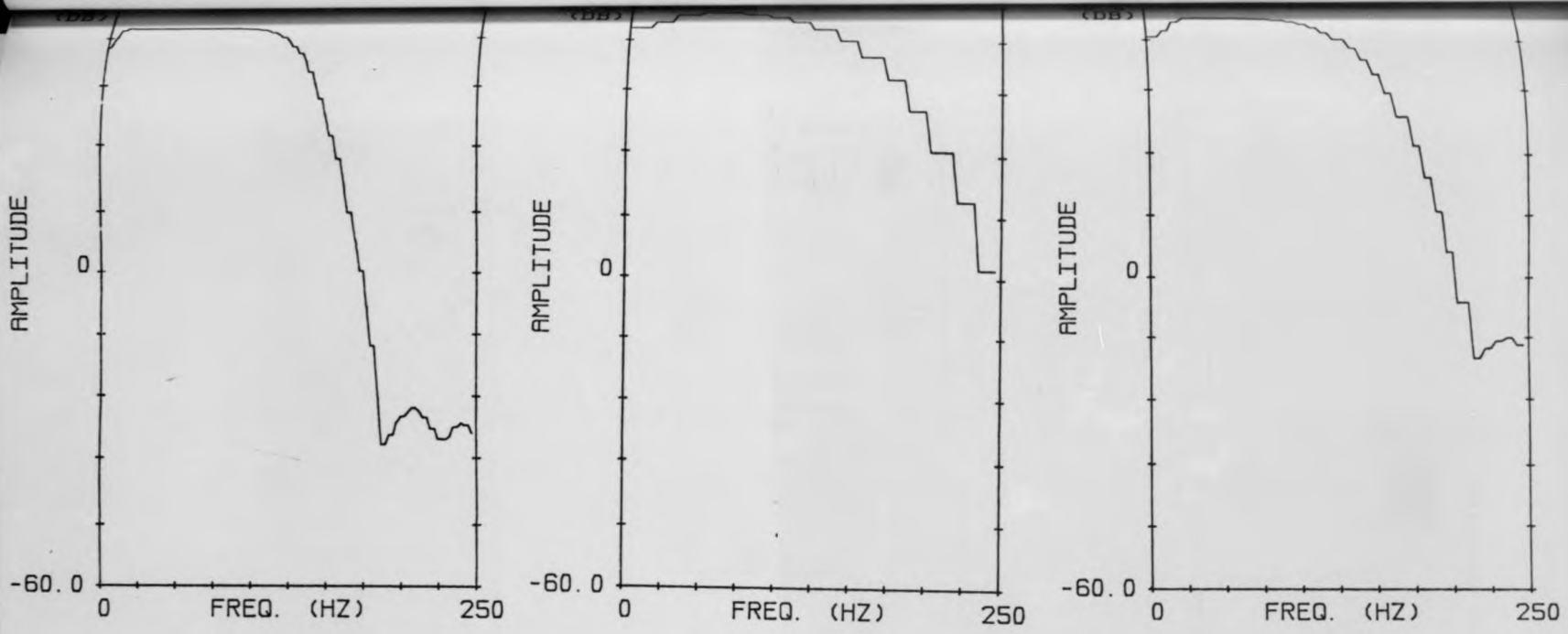

Figure 3.8 The transfer function characteristics of a transversal filter with weight coefficient of N = 199, 13 and 81

Figure 3.8a

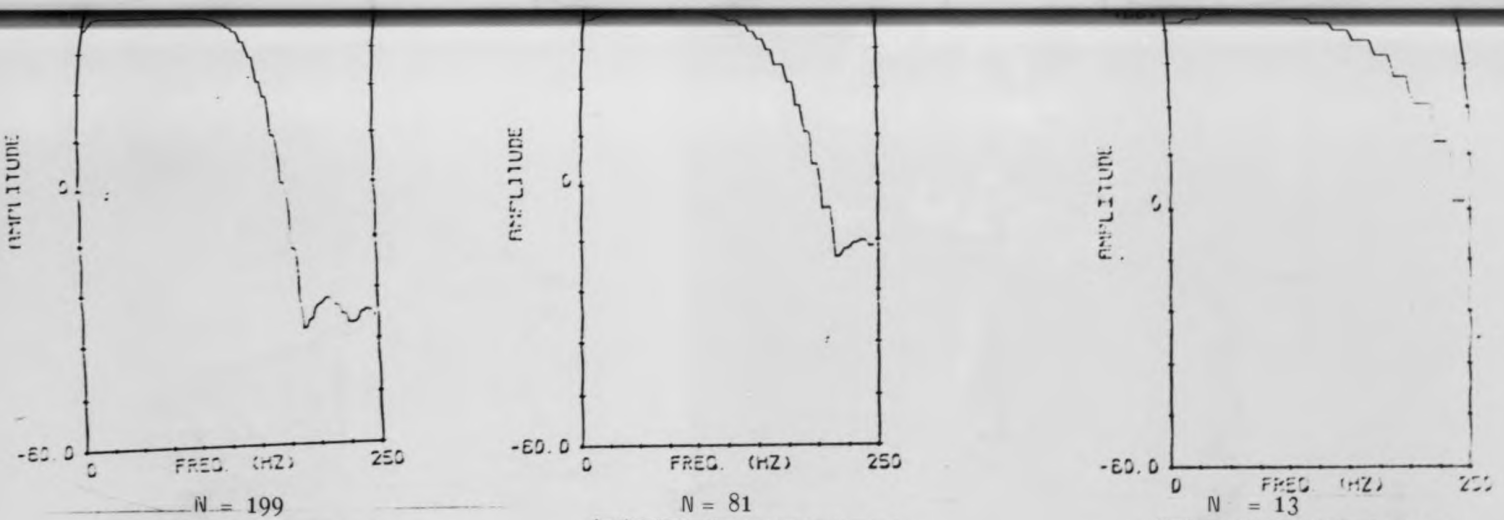

Figure 3.8b

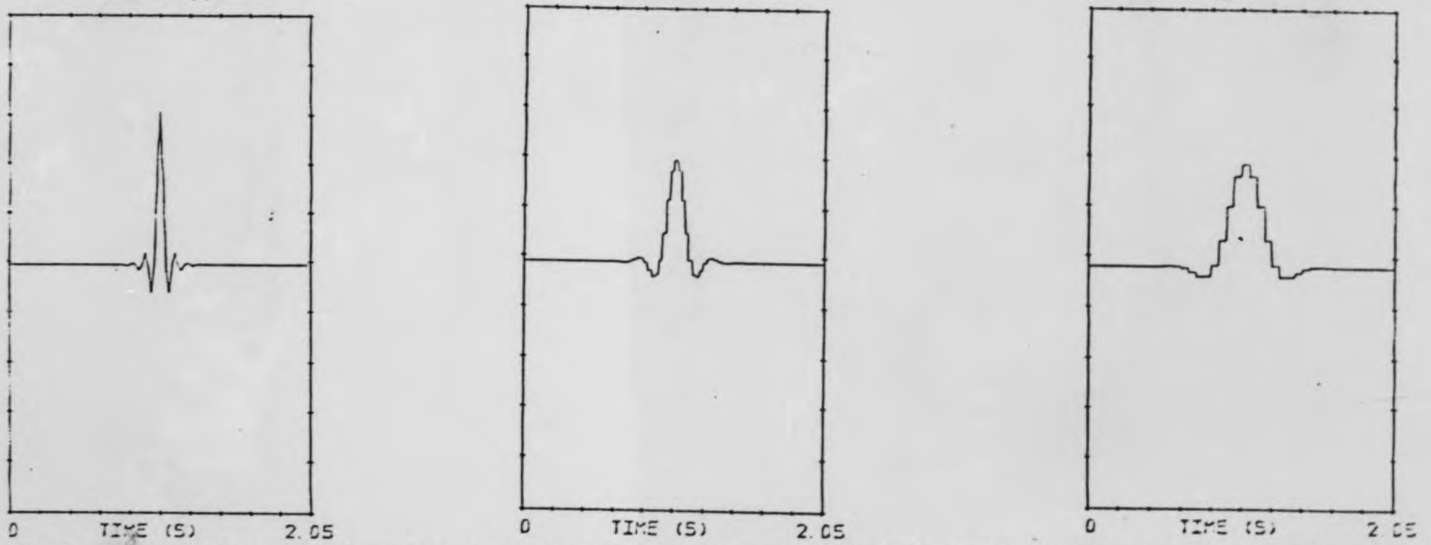

Figure 3.8a The transfer function characteristics of a transversal filter with weight coefficient of N = 199, 81 and 13.
Figure 3.8b The impulse characteristic of a transversal filter with weight coefficent of N = 199, 81 and 13.

Figure 3.9 Results of applying transversal filter with different weight coefficients to exercise ECG.

(a) N = 81
(b) N = 39
(c) N = 13

amounts of noise can be added. Table 3.2 shows a summary of the improvement using this technique for different weight coefficients.

Table 3.2

Number of Coefficient (N)	13	39	81	199
Signal to noise improvement (dB)	13.88	12.27	11.71	11.2

The advantages and disadvantages of transversal filters for achieving improvement in signal-to-noise ratio may be summarised as follows:

Advantages of transversal filter

(i) a greater reduction may be obtained with higher input signal-to-noise ratios.

(ii) Economy in the number of coefficients required to achieve a reasonable improvement compared with other digital techniques mentioned in previous sections.

Disadvantages of tranversal filter

(i) For low signal-to-noise ratios, distortion occurs.

(ii) Inappropriate for non-stationary data.

(iii) Little improvement observed for higher numbers of coefficients.

(iv) The value of coefficients do not vary with the variation of the statistical characteristics of the input signal (fixed value weight).

(v) It is time consuming, and therefore not well suited for an application in real time.

The results in this section clearly demonstrate that the use of transversal filters yields an improved estimate of the signal in terms of reduced noise activity, but with an attendant amplitude distortion.

3.5 The use of Wiener filter for improving signal-to-noise ratios in electrocardiograms.

The Wiener filter is a particular form of digital filter which is used to detect the signals that are masked by noise. The technique has been examined for stationary and non-stationary signal and noise components. The application of the Wiener filter to enhance the signal-to-noise ratio in electrocardiograms is based on a complete knowledge of the spectra of the ECG signal and the unwanted noise. The mathematical basis for the transfer function of the Wiener filter is presented below as a precursor to discussing the relative merits of the technique for signal-to-noise improvement in exercise electrocardiograms.

Assuming that the ECG recorded from the body surface can be expressed as follows:

$$x_i(t) = s(t) + n_i(t) \qquad i = 1,2... \qquad \ldots . 3.4$$

where $s(t)$ is the desired signal ECG and $n_i(t)$ stationary noise with zero mean. The assumption is made that $s(t)$ and $n_i(t)$ are uncorrelated.

Taking the ensemble averaging of equations:

$$\bar{x}(t) = s(t) + \frac{1}{N} \sum_{i=1}^{N} n_i(t) \qquad \ldots . 3.5$$

$0 < t < T$

T is the duration of the ECG cycle.

Taking the Fourier transform of equation 3.2, i.e. transformation of the ensemble average from time domain to frequency domain, denoted by $\bar{x}(\omega)$, the power density spectrum of $\bar{x}(t)$ is

$$\phi\bar{x}\bar{x}(\omega) = \bar{x}^{*}(\omega)\,\bar{x}(\omega) \qquad \ldots\ 3.6$$

Assuming that the noise is not time locked and uncorrelated to the desired signal, the expectations are:

$$E[\phi\bar{x}\bar{x}(\omega)] = E[\phi ss(\omega)] + \frac{1}{N}E[\phi nn(\omega)] \qquad \ldots\ 3.7$$

Where $\phi\bar{x}\bar{x}$, ϕss, ϕnn represent the power density spectra of the average, the ECG signal and the noise respectively.

By averaging the power density spectra of all the individual ensembles:

$$E[\overline{\phi xx}(\omega)] = E[\phi xx(\omega)] = E[\phi ss(\omega)] + E[\phi nn(\omega)] \qquad \ldots\ 3.8$$

Where $\phi nn(\omega)$ is the power density spectrum of $x(t)$.

From equation 3.7 and 3.8, the spectra of signal and noise can be expressed in terms of the average and power density spectrum of $x(t)$:

$$\phi ss(\omega) = \frac{N}{N-1}\left[\phi\bar{x}\bar{x}(\omega) - \frac{1}{N}\phi xx(\omega)\right] \qquad \ldots\ 3.9$$

and

$$\phi nn(\omega) = \frac{N}{N-1}\left[\phi nn(\omega) - \frac{1}{N}\phi\bar{x}\bar{x}(\omega)\right] \qquad \ldots\ 3.10$$

therefore, the transfer functions of Wiener filter given by

$$H(\omega) = \frac{\phi ss(\omega)}{\phi ss(\omega) + \frac{1}{N}\phi nn(\omega)} \qquad \ldots\ 3.11$$

may be expressed in the form:

$$H(\omega) = \frac{N}{N-1}\left[1 - \frac{1}{N}\frac{\Phi xx(\omega)}{\Phi \overline{xx}(\omega)}\right] \quad \ldots . 3.12$$

This is the transfer function of the Wiener filter based on theoretical spectra, and on a priori knowledge of both signal and noise. In general, a priori knowledge of both signal and noise is not always available. In these circumstances equation 3.12 may be expressed in terms of the spectra $\Phi \overline{xx}(\omega)$

$$H(\omega) = \frac{N}{N-1}\left[1 - \frac{1}{N}\frac{\overline{\Phi xx}(\omega)}{\Phi \overline{xx}(\omega)}\right] \quad \ldots . 3.13$$

The main disadvantage of the Wiener filter for use in enhancing the signal-to-noise ratio of exercise ECGs are as follows:

(i) where spectral overlap between signal and noise occurs and the signal is obscured by noise, the Wiener filter cannot distinguish between the signal component and the noise component, especially in the excercise ECG test,

(ii) this technique is suitable for stationary data only,

(iii) a priori knowledge of the signal and noise is necessary for efficient application of the technique, and

(iv) distortion occurs when signal-to-noise ratio is low.

The main reasons that this technique has been considered in this study

is that it provides an optimal estimate of the true signal, has been used successfully for the estimation of evoked potential (de Weerd, 1981; de Weerd & Kap, 1981).

The results presented in section 3.5 indicate that there is no significant difference in separation of noise frequencies from signal frequencies when signal and noise have the same spectral occupancy, as in parts of the exercise ECG's.

3.6 Application of coherent signal averaging to noise reduction in electrocardiograms

3.6.1 Noise reduction

For many years, signal averaging has been used in electrocardiographic studies (Briller et al.,1966). In particular, signal averaging has been used for reducing noise during surface recording of ECGs, for enhancing foetal electrocardiograms in the presence of excessive noise on the maternal electrocardiogram (Hon et al., 1964; Docker, 1971), and for the detection of events of the Specialised Conduction system (Trisawa et al., 1966; Berbari et al., 1973, 1979; Furness, 1976; Vincent et al., 1978,1980).

The surface measured signal is composed of a desired signal component plus an unwanted noise component and, in applications such as those cited above, the noise is usually one or more orders of magnitude larger than the amplitude of the desired signal component. If the frequency content of the noise component is higher or lower than that of the desired signal component, conventional fixed value filters can be used to attenuate the noise. However, if the frequency spectrum of the noise partially overlaps that of the desired signal (figure 3.10), conventional filtering alone is not sufficient to achieve adequate noise reduction.

Coherent signal averaging may be used to enhance the signal-to-noise ratio, provided certain requirements are fulfilled.

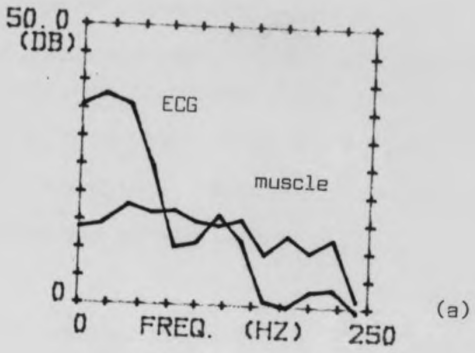

(a)

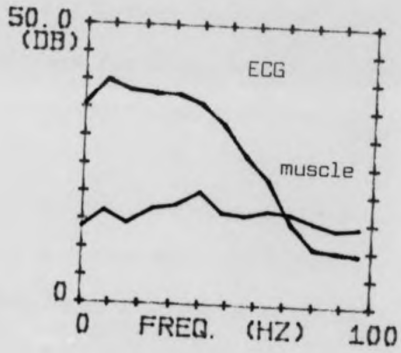

(b)

Figure 3.10 Shows the overlap between ECG spectra and muscle activity.

(a) 250Hz
(b) 100Hz

(i) A length of record with a continuous ECG signal, and

(ii) The proper alignment of the individual signals

Many researchers have investigated methods to determine the reference point by which successive periods of recorded signal are aligned for averaging. These methods include level sensing, slope determination and pattern matching.

Following a detailed examination of signal averaging, a new method was developed for achieving alignment. A lenth of record of successive ECG cycles was stored in the computer memory. The length of record needed for the averaging technique was based on the noise content and heart rate (Furness, 1973). For small signal (1-10μv) investigation during this study, a minimum noise level of 25μv (rms) was found to be present during surface recordings. After determining the length of record required for a particular application, the alignment of the signal for averaging was performed using the following technique.

An appropriate sampling rate was selected to avoid aliasing, and a processing algorithm was used to search for the maximum in each ECG cycle. The input data was segmented into 500 ms segments, the position of peak signal level in each segment was then used to align each cycle. The R wave was selected as the feature in the ECG cycle in which a maximum was sought. After segmenting, the whole record averaging was performed by summing all the segmented data and dividing by the sweep count. Although sections of the isoelectric intervals may overlap as a result of cycle to cycle variation, the PR segments are not affected in this way. In order to gainas much information as possible from the frequency characteristics of the ECG, a sampling rate of 1KHz was chosen.

The coherent average of a signal y(t) can be represented in mathematical terms in the following way:

$$y(t) = \frac{1}{N} \sum_{k=1}^{N} s_k(t) \qquad \ldots\ldots 3.14$$

where $s_k(t)$ is the repetitive signal,

N is the number of segments averaged,

y(t) is the averaging result.

If the signal y(t) contains an additive random noise n(t):

$$y(t) = s(t) + n(t) \qquad \ldots\ldots 3.15$$

then

$$y(t) = \frac{1}{N} \sum_{k=1}^{N} s_k(t) + n_k(t) \qquad \ldots\ldots 3.16$$

If s(t) is repetitive and deterministic,

$$y(t) = s(t) + \frac{1}{N} \sum_{k=1}^{N} n_k(t) \qquad \ldots\ldots 3.17$$

taking the expectation of equation 3.17

$$E[y(t)] = s(t) + \frac{1}{N} \sum_{k=1}^{N} E[n_k(t)] \qquad \ldots\ldots 3.18$$

If we assume the noise is independent and has zero mean, therefore:

$E[y(t)] = s(t)$ signal only 3.19

If the samples were taken every T seconds, equation 3.15 becomes:

$$y(t_k + iT) = s(t_k + iT) + n(t_k + iT)$$
$$= s(i) + n(t_k + iT) \quad \ldots\ldots 3.20$$

Since the noise was assumed to have a zero mean and rms value of σ, on any particular repetition, the signal-to-noise ratio will be

$$S/N = \frac{s(iT)}{\sigma} \quad \ldots\ldots 3.21$$

after N repetitions, equation 3.20 becomes:

$$\sum_{k=1}^{N} y(t_k + iT) = \sum_{k=1}^{N} s(iT) + \sum_{k=1}^{N} n(t_k + iT) \quad \ldots\ldots 3.22$$

Since the noise is random and N samples are independent, the mean square value of the sum of the n noise samples is $N\sigma^2$, and the rms value is $\sqrt{N}\sigma$.

Therefore, the signal-to-noise ratio, after summation is:

$$(S/N)_N = \frac{NS(iT)}{\sqrt{N}\sigma} = \sqrt{N}(S/N) \quad \ldots\ldots 3.23$$

therefore, the summing of N repetitions improves the signal-to-noise ratio by a factor of $\sqrt{N}$.

Thus if the noise exhibits a Gaussian distribution, the improvement in signal-to-noise ratio is $\sqrt{N}$, where N is the number of sweeps of the averaging sequence (Trimble, 1968; Furness, 1976). Often the noise that obscures the signal does not exhibit Gaussian distribution. In such circumstances the improvement in signal-to-noise ratio can be difficult to estimate theoretically.

Signal averaging can be considered as a filtering process in frequency domain, its behaviour being likened to a comb filter (Trimble, 1968; Budo, 1964). The process may be represented as the convolution of the input signal with a train of N unit impulses which, when translated into the frequency domain, yields the characteristic transfer function of a comb filter. Every frequency component of the time locked signal coincides with the centre point of a peak or 'tooth' of the comb filter due to the synchronous pulses that are time locked to the signal, s(t). The bandwidth of each tooth becomes progressively narrower as the number of repetitions increases. In analytical terms the bandwidth of the comb filter peaks satisfy the expression:

$$\Delta f = \frac{0.886}{N\tau} \text{ Hz} \qquad \ldots\ldots 3.24$$

where τ is the period of the periodic signal and N is the sweep count.

3.6.2 Jitter effect

The objective of coherent signal averaging is to improve signal-to-noise ratio to reveal a signal buried in noise. To do this without producing distortion it is important to ensure stable triggering based upon a well defined signal reference. Jitter, due to noise or base line variation, may if present result in deterioration of the average as the number of sweeps is increased. To investigate the effect of jitter due to noise, and to develop a technique for the quantification of jitter, simulated data with various levels of noise was processed using a PDP11/23 computer. Experiments were conducted in order to gain insight into the influence of the noise on peak detection and its manifestation as jitter. The presence of jitter clearly produces smearing in the results of the averaging process, with consequential distortion.

The processing involved the following steps:

(i) The length of record required for the specific improvement in signal-to-noise ratio was determined, and divided into segments corresponding to the number of the repetitive cycles (assuming the size of each segment or cycle to be 500ms).

(ii) A buffer space was allocated equal to the same length of the record as in (i) and divided into 500ms segment lengths.

(iii) A routine was implemented to search for the peak within the first 500ms of data and shifted to place the detected peak in the middle of the buffer space, and fill the right and left of the buffer with the data of the first 500ms.

(iv) The search routine was repeated for the peak of the second 500ms data and re-distributed in the second buffer. The process was repeated until the whole of the data had been processed in this manner.

(v) Different levels of noise were added to the individual buffers.

(vi) The new positions for the peaks produced by additions of the noise were determined.

(vii) The difference between the respective peak positions were determined as a measure of the jitter due to noise.

The simulated results so obtained illustrated that there was no jitter effect when the data has a signal-to-noise ratio greater than 4dB. The jitter was found to be 2ms for data of signal-to-noise ratio less than 4dB.

Figure 3.11 shows a clean recorded ECG signal. With different noise levels added to it, the signal-to-noise ratios were 23.7, 15.7, 9.7, 3.6, -5.86 and -7.2dB. figure 3.12 shows the overlap between a clean QRS complex and a noisy QRS. It also shows the amount of jitter measured in each case.

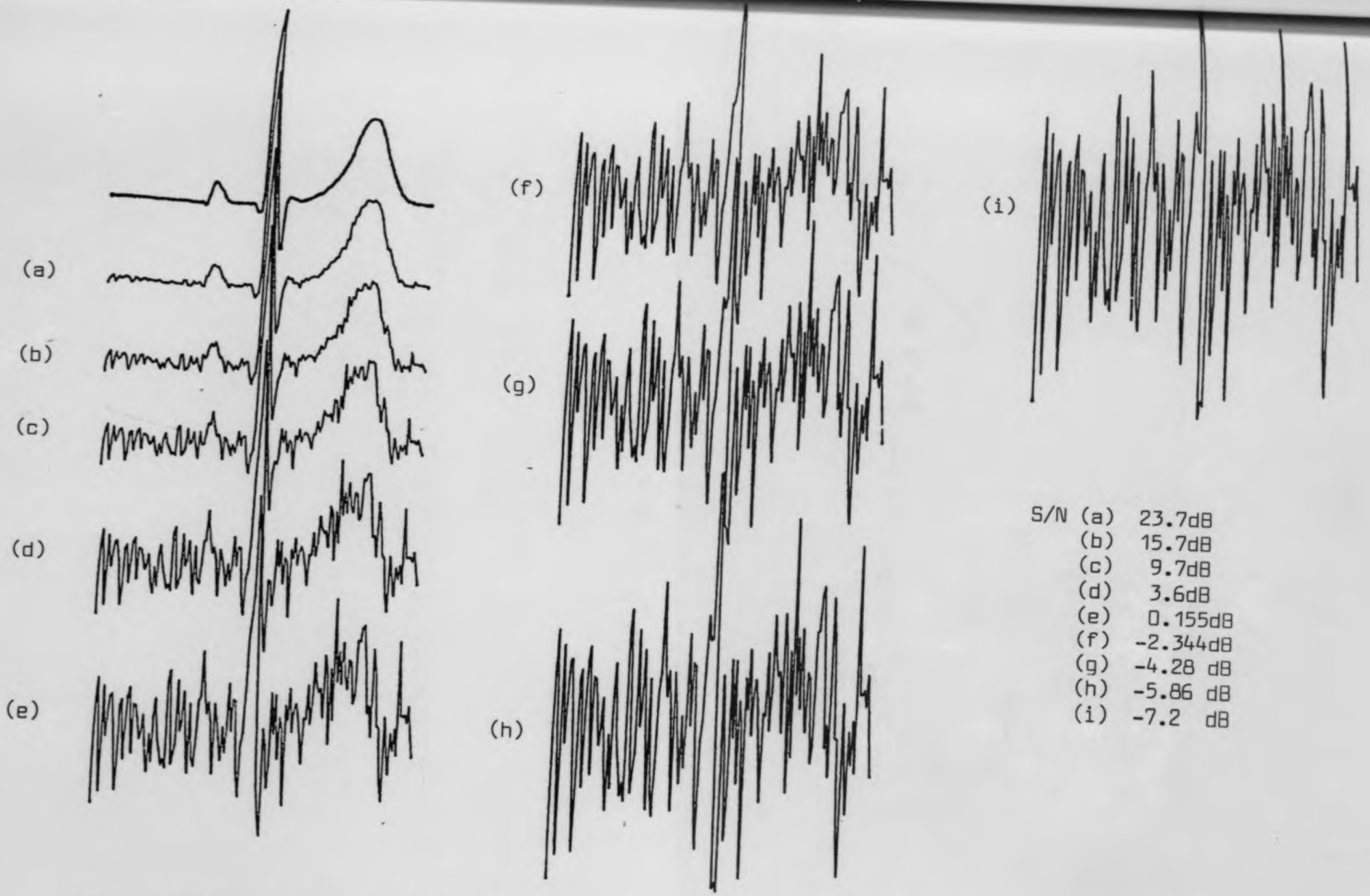

Figure 3.11 ECG signal with different noise levels

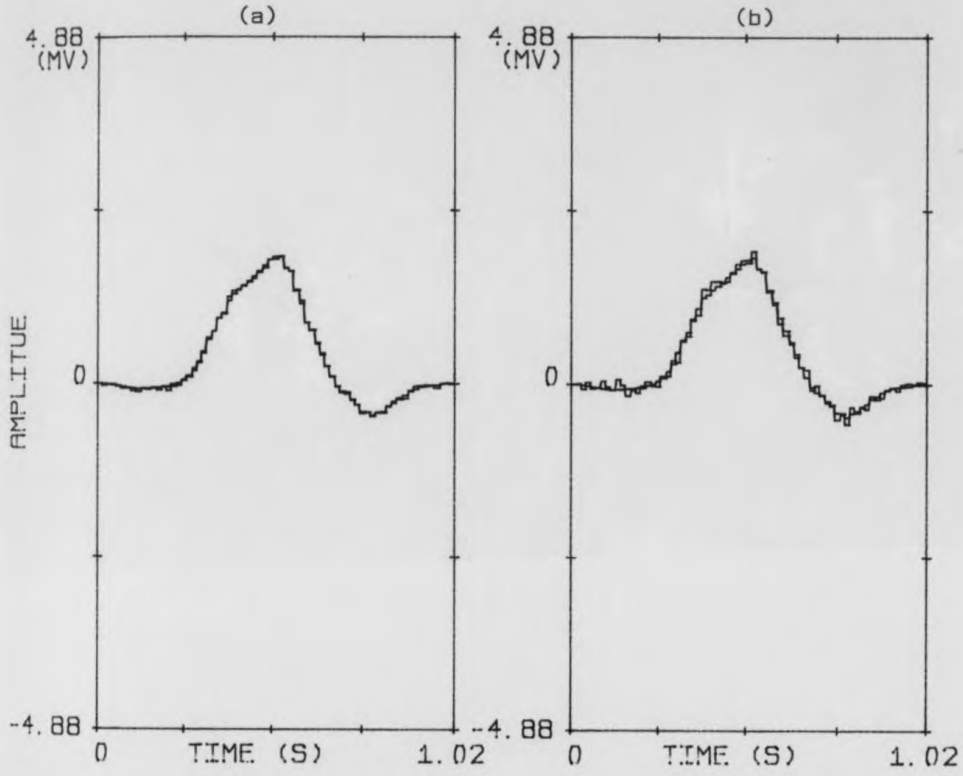

Figure 3.12 The overlap between a clean QRS complex with a QRS added to noise.

(a) S/N = 23.7dB Jitter = 0ms
(b) S/N + 15.7dB Jitter = 0ms

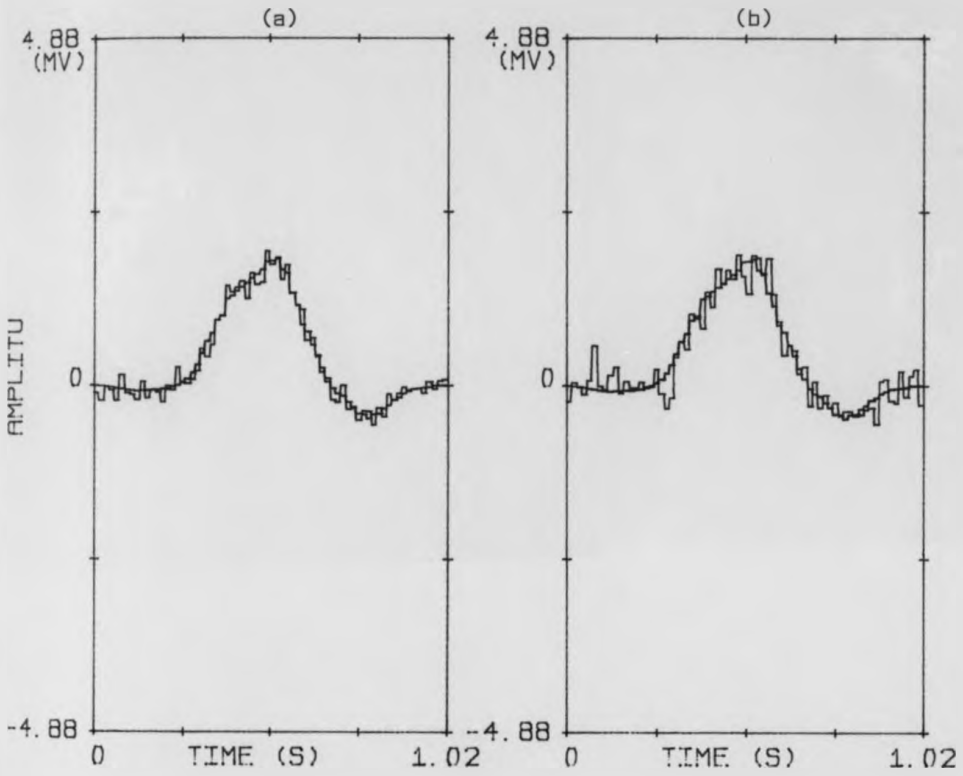

Figure 3.12 The overlap between a clean QRS complex with a QRS added to noise

(a) S/N = 9.7dB Jitter = 0ms
(b) S/N = 3.6dB Jitter = 0ms

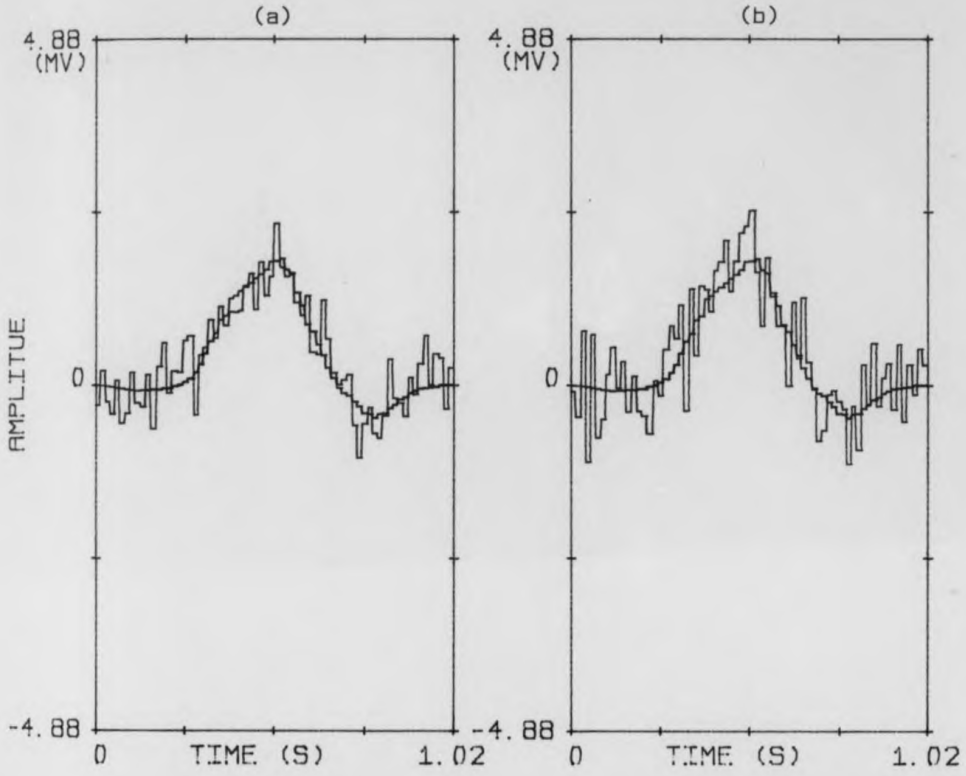

Figure 3.12 The overlap between a clean QRS complex with a QRS added to noise

(a) S/N = 0.155dB Jitter = 1ms
(b) S/N = -2.34dB Jitter = 1ms

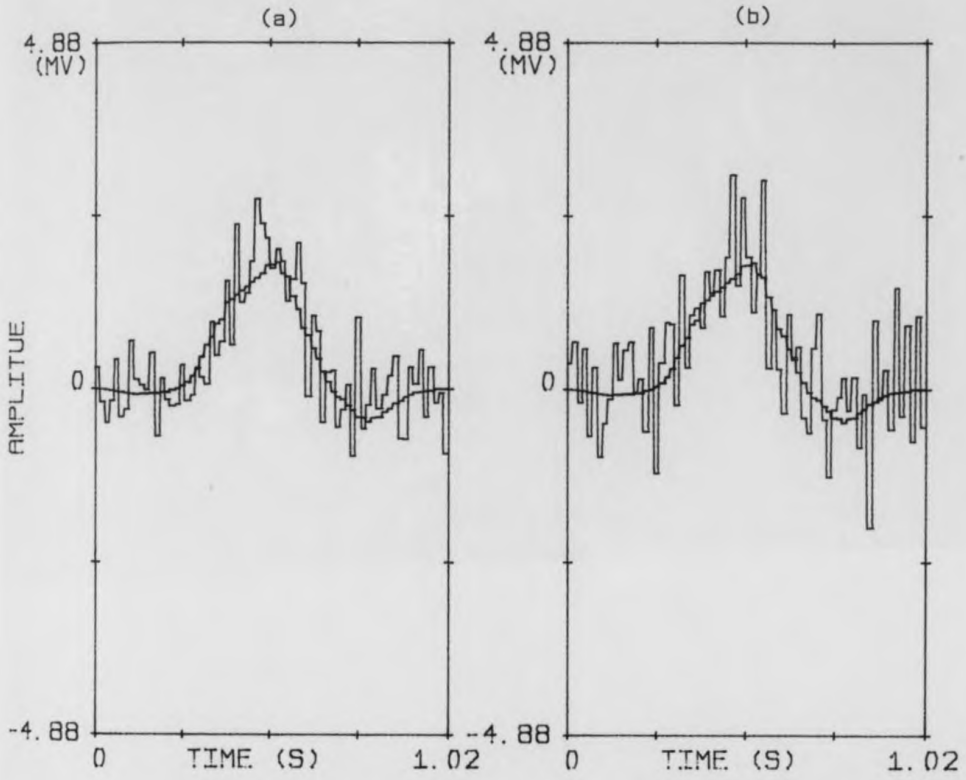

Figure 3.12 The overlap between a clean QRS complex with a QRS added to noise

(a) S/N = -4.28dB Jitter = 2.6ms
(b) S/N = -5.86dB Jitter = 3 ms

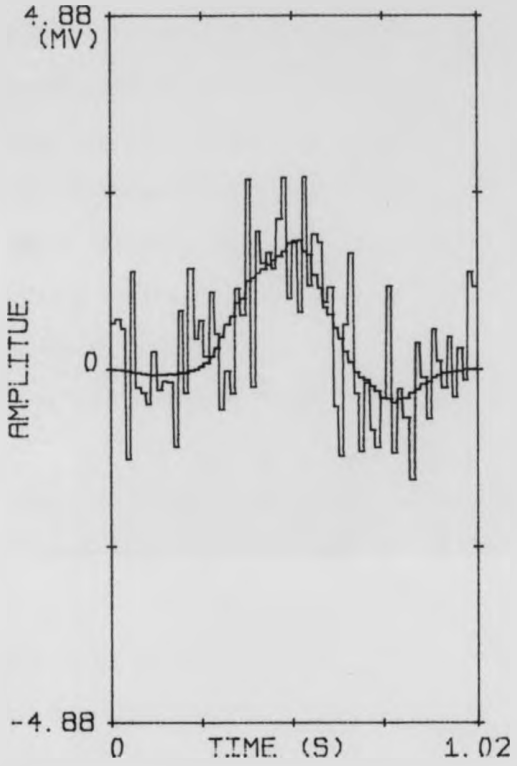

Figure 3.12 The overlap between a clean QRS complex with a QRS added to noise

S/N = -7.2dB Jitter = 3.21ms

3.6.3. Limitations on noise reduction by coherent signal averaging

Noise, in the context of this discussion, is any component other than the signal required. The reduction of such components by this technique can be affected by the following factors:

(i) the nature of the noise present in the input signal,

(ii) the correlation between signal and noise,

(iii) the overlap of the spectral occupancy of the noise and signal,

(iv) the variability in the time interval between the trigger event and the events to be detected,

(v) the jitter effect associated with the trigger routine.

Often the noise masking a signal is not random. The presence of 50Hz interference for example can effectively obscure the signal in many situations. Under these circumstances it may be difficult to estimate how much the noise will be attenuated. The presence of excessive ac interference cannot be reduced effectively unless:

a) a large number of signals are averaged, or

b) most of the interference is filtered out, by using a notch filter.

Figure 3.13 shows a simulated ECG and the averaged output as a result of 400 averages on a signal with 400μv peak-to-peak, 50Hz interference. The result widens the R wave and rounds off the peaks.

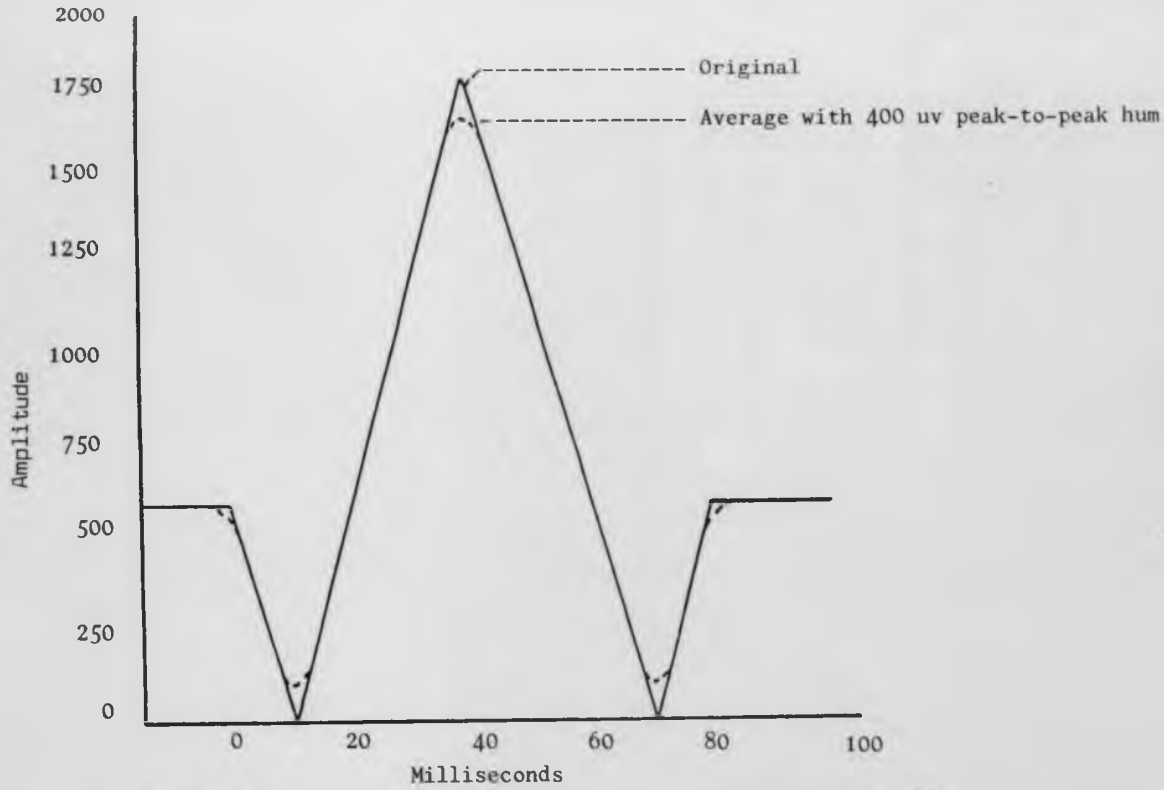

Figure 3.13 Simulated ECG and the averaged output as a result of 400 averages with 400 μv peak-to-peak hum (adapted from figure 5.213(a), Winter, 1966)

3.6.4 Disadvantages of coherent signal averaging

Although signal averaging may provide an improvement in signal-to-noise ratio under appropriate conditions, the technique may not be entirely appropriate for processing electrocardiograms. The various disadvantages include:

(i) The inability to detect transient small signal events within each cycle of an ECG on a beat-by-beat basis.

(ii) In the case of skeletal muscle activity or the exercise ECG test, some of the noise component is correlated with the desired signal and averaging cannot distinguish between the two. Distortion can therefore occur.

3.7 Noise reduction using time-varying filter

In previous sections a Wiener filtering technique was described as a means of reducing noise in the electrocardiogram. As this technique is a time-invariant filtering process, it does not yield an optimal result in dealing with a transient signal. A time-varying filter is needed in order to cope with a transient waveform and to perform in an optimal manner. The advantages of the time-varying filter technique include:

(i) the ability to perform for non-stationary data,

(ii) no a priori knowledge of the signal and noise components is required.

This technique has been fully explained by de Weerd (1981) and successfullly applied to the problem of improving signal-to-noise ratio of evoked potentials. The use of a time-varying filter was investigated in this study as a method for reducing the background noise from surface recorded ECG signals. The filter, which is based upon an estimation of the time-varying power spectra of signal and noise, assumes that the signal is identically repeating but is masked by noise.

The signal and noise may be represented by an equation of the form:

$$y_i(t) = s(t) + n_i(t) \qquad \ldots . \; 3.25$$

$$i = 1,2,3,\ldots\ldots N$$

$$0 < t < T$$

where s(t) represents the signal (ie. the desired ECG signal), $n_i(t)$

represents noise (i.e. unwanted activity, such as muscle noise, and 50Hz interference), T is the duration of each cycle and N is the number of repetitive cycles. The collection of cycles y (t) is referred to as the ensemble.

DeWeerd and Kap (1981) employed time-varying filters in the following ways:

(i) The use of a bank of proportional bandwidth filters, i.e. filters having a bandwidth proportional to their centre frequency.

(ii) By taking Fast Fourier Transform, the power of the signal and noise can be estimated, in each of these regions over the entire record.

(iii) The ensemble average y(t) is modulated by the time-varying coefficients.

(iv) The final estimate can be obtained by taking the sum of (iii). This may be described mathematically:

$$S(t) = \sum_{n=1}^{N} W_n(t).X_n(t) \qquad \ldots . \quad 3.26$$

Where $X_n(t)$ is the ensemble average record in the nth band, $W_n(t)$ is the time-varying filter coefficient in the nth frequency band, and S(t) is the time varying filter (TVF) estimate. Figure 3.14 shows the block diagram of the construction of the time-varying filter.

Time-varying filtering (TVF) was applied to electrocardiograms in order to reduce the background noise, and the results depicted in

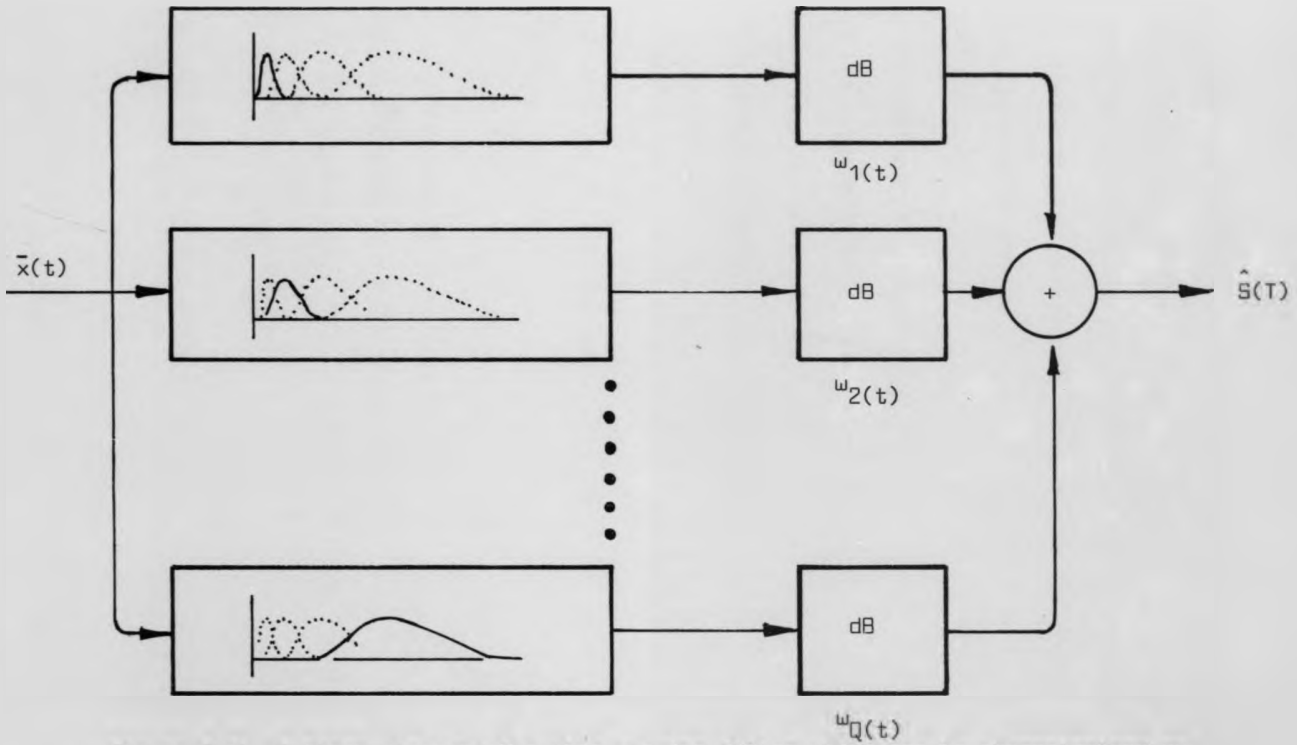

Figure 3.14 A block diagram of a time-varying filter which can be characterised as a bank of constant relative bandwidth filters, followed by time-varying attenuators and a summing network. The attenuators are controlled by the estimated time-varying signal-to-noise power ratio in the corresponding frequency bands (adapted from figure 6.2, De-Weerd, 1081)

figures 3.15 and 3.16 show an improvement in signal-to-noise ratio beyond that of the averaging technique. However, this improvement depends upon the spectro-temporal structure of signal and noise.

Figure 3.19 shows the spectrum of the input signal, after averaging and after the application of the time-varying filter. From the results it can be seen that the time-varying filter is more appropriate than averaging in noise reduction. The technique was applied to exercise ECGs and the results are presented in Chapter 7.

Simulated data was used in order to examine the improvement achieved by using TVF on an artificial signal, to represent an ECG, together with a noise component generated using software. TVF was performed for different levels of added noise. Averaging was also performed for comparative purposes using low sweep count. The results are depicted in figures 3.17 and 3.18. The TVF technique gives better estimation of the simulated signal that the averaging techniques for the sweep count considered.

If signal and noise spectra overlap in time and frequency, as is likely in the applications considered in this study, not only the noise components are attenuated, but the signal components are attenuated as well.

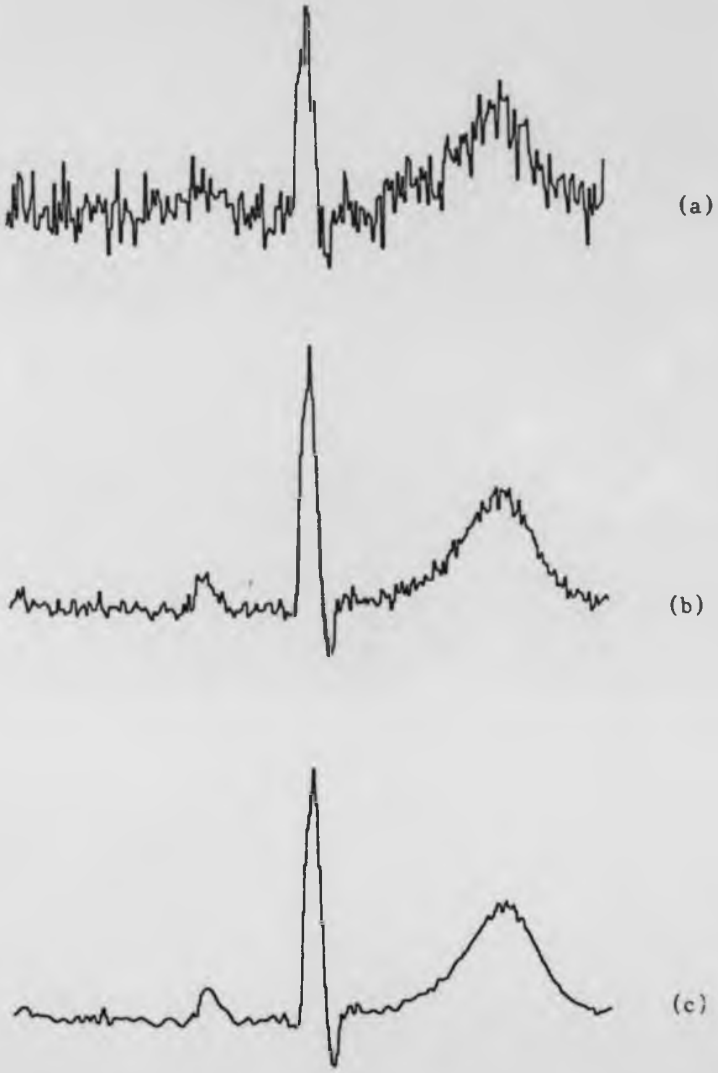

Figure 3.15 Result of averaging and time-varying filter in which the estimate of the mean square error was achieved in 4 cycles.

(a) input signal
(b) result of averaging
(c) result of time-varying filter

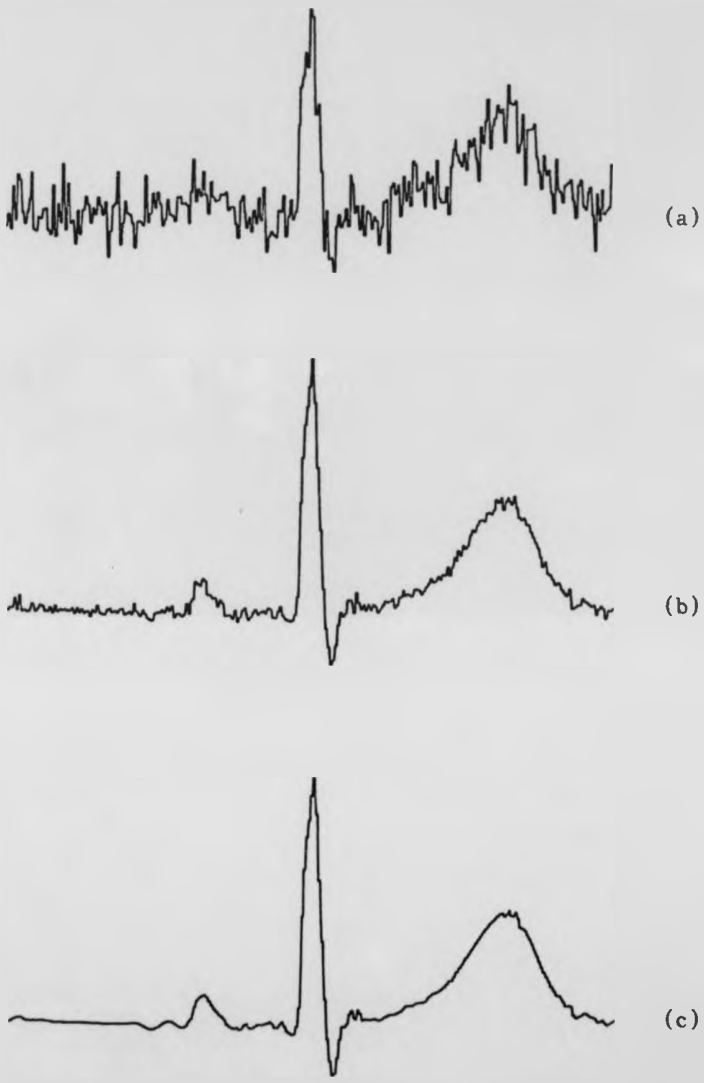

Figure 3.16 Result of averaging and time-varying filter in which the estimate of the mean square error was achieved in 64 cycles

(a) input signal
(b) averaging result
(c) time-varying filter result

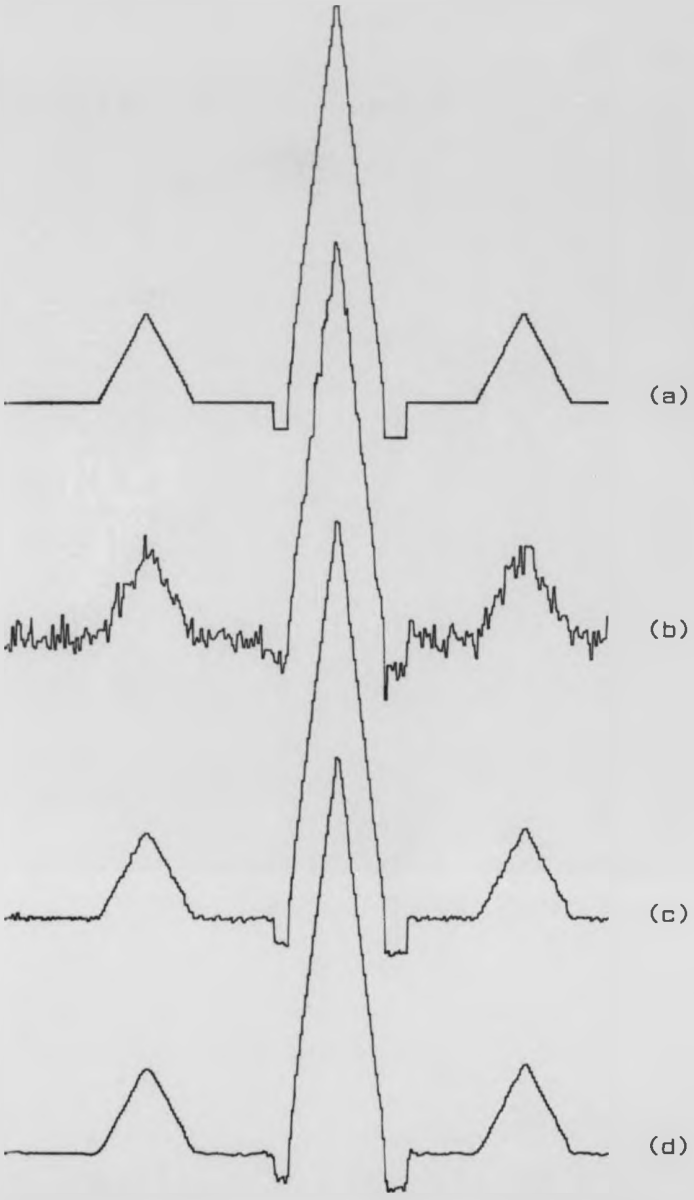

Figure 3.17 Results of averaging and time-varying filter in which the estimate of the mean square error was achieved in 32 simulated cycles

(a) simulated input signal
(b) simulated signal and noise
(c) result of averaging
(d) result of time-varying filter

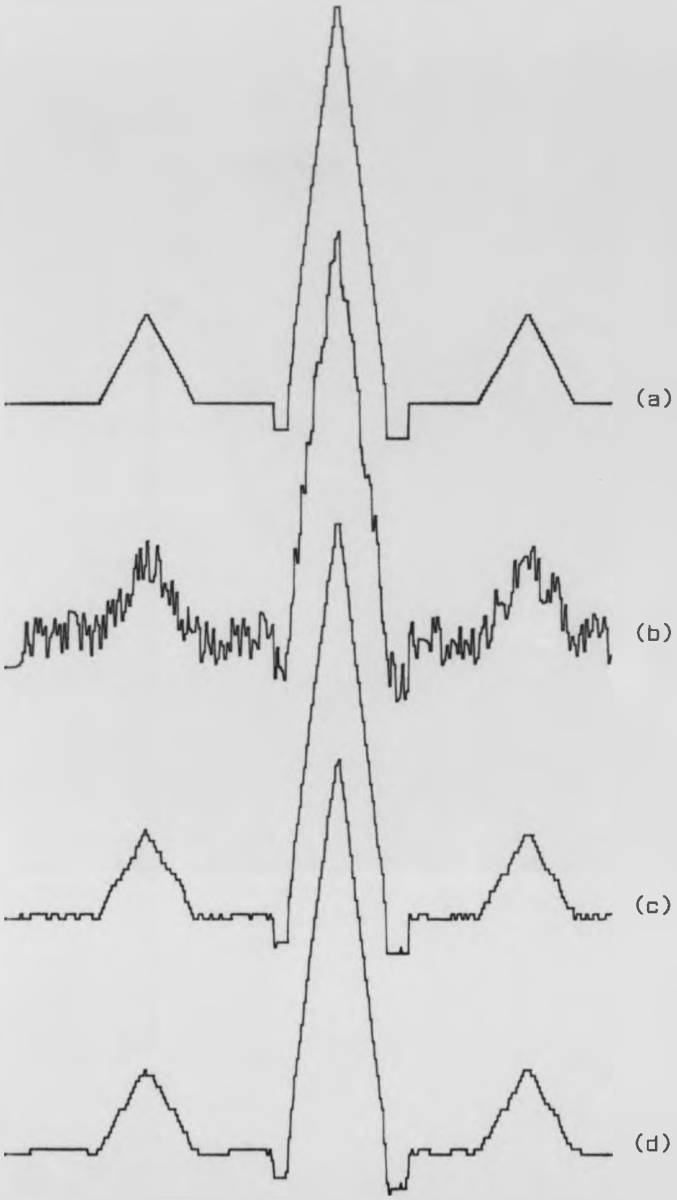

Figure 3.18 Results of averaging and time-varying filter in which the estimate of the mean square error was achieved in 64 simulated cycles

(a) simulated input signal
(b) simulated signal and noise
(c) result of averaging
(d) result of time-varying filter

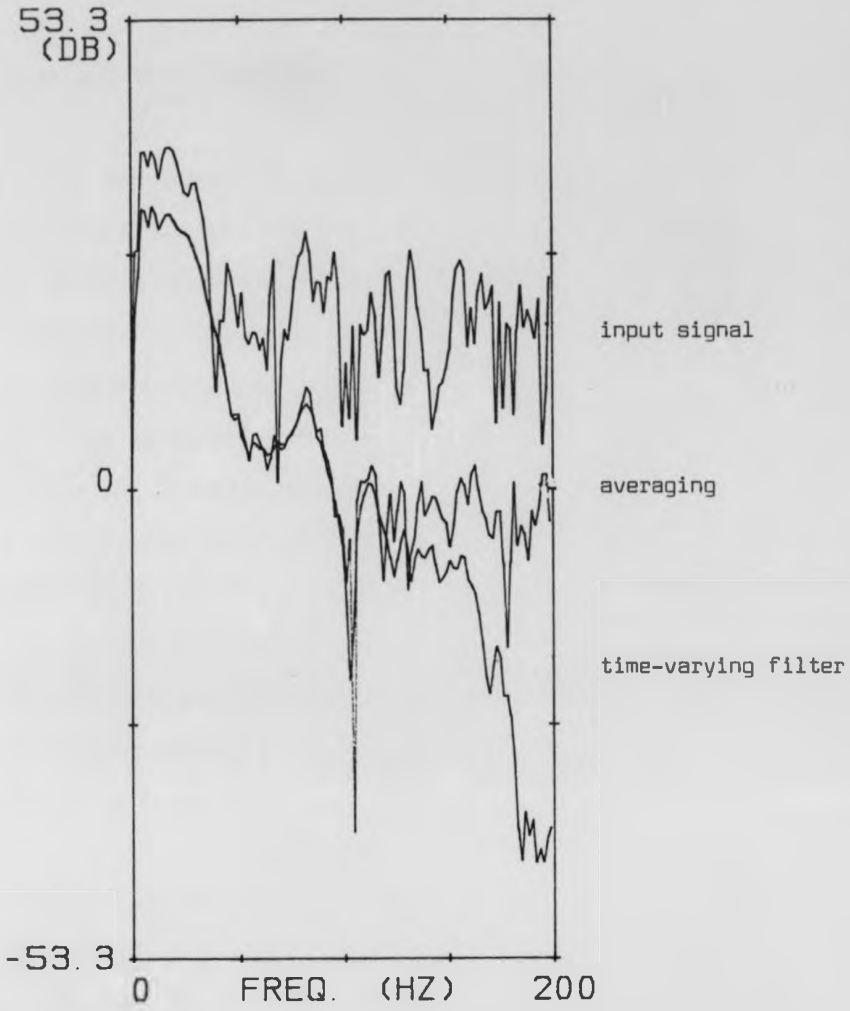

Figure 3.19 The spectra of the input signal, averaging and time-varying filter

3.8 Discussion and conclusion

This chapter has been concerned with the description and application of different filtering techniques for noise removal from ECGs. Although the techniques mentioned provide improvements in signal-to-noise ratio, it is often at the expense of signal distortion. This distortion may be considered to be due to the inability of these techniques to change their characteristics to follow the variation in the signal and noise. In situations where signal fidelity is important, the distortion due to conditioning must be minimised.

It has been noted that even inaccurate results can be obtained through the use of averaging procedures in certain circumstances, but an attempt was made to improve the way of conducting the technique.

A need was identified for a technique which has the ability to improve signal-to-noise ratio and avoid signal distortion. Such a technique requires the coefficients of the transfer function to vary with the variation of signal and noise. Techniques of this kind may be collectively referred to as adaptive filters and are considered in detail in the following chapters.

Chapter Four: Theory of Adaptive Filters

4.1 Introduction

The review of techniques used to extract a signal (ECG) from the unwanted activity (noise) revealed that while improvments could be obtained by use of time-varying filtering or transversal filtering, the improvement was less than adequate for the applications in mind. Two main reasons may be considered to account for this result:
(i) Lack of a priori knowledge of the signal and noise, and
(ii) The non-stationary nature of the signal.

A need was therefore recognised for a technique that could track or follow the variation of the signal and noise, and have the ability to perform without any a priori information of the signal and noise. This type of filter was first introduced by Widrow (1966) and the group of filters in this category are known collectively as adaptive filters. Adaptive filters are essentially self-design filters in which the coefficients of the filter are internally and automatically adjusted, based upon estimated statistical characteristics of input and output signals. The statistics are not measured explicitly and then used to design the filter. The filter design is achieved by means of a recursive algorithm which automatically updates a set of coefficients (weights) with the arrival of each new data sample.

An example of an adaptive transversal filter consists of a tapped

delay line, a variable weight change facility based upon the signal information at the delay-line taps, a summer to add the weighted signals, and circuitry to adjust the weights automatically. The impulse response, determined by the coefficient settings and the adaptation process. The latter automatically seeks an optimal response through adjustment of the coefficients.

Figure 4.1 shows a diagram of a transversal adaptive filter.

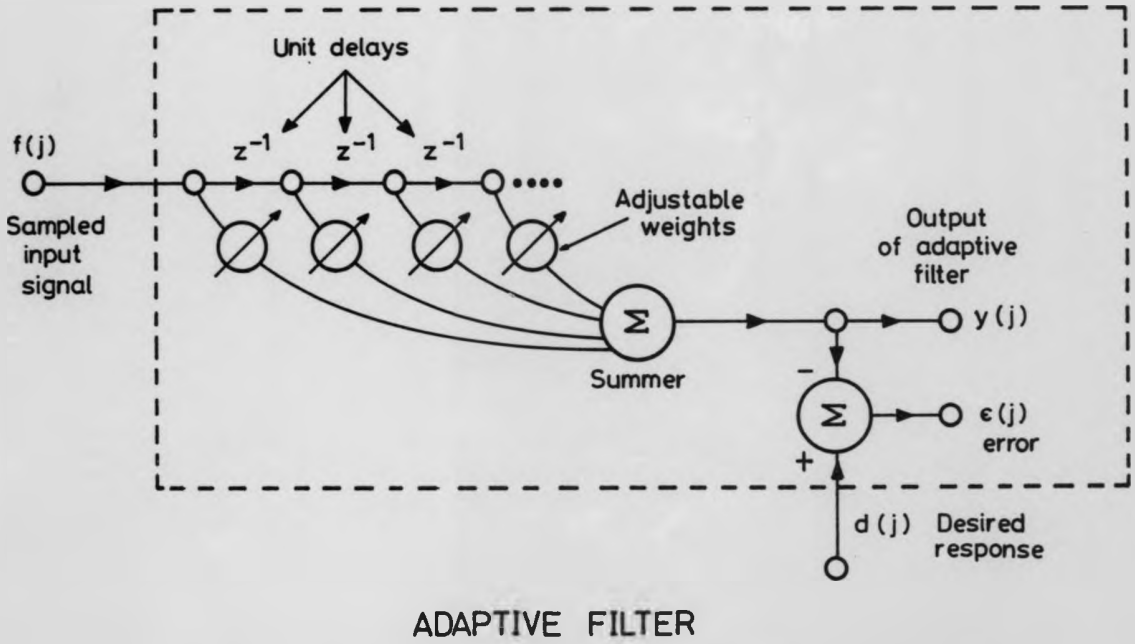

Figure 4.1 Diagram of an adaptive transversal filter which uses a set of successively delayed input samples as the input to the adaptive linear combiner.

4.2 The concept of adaptive filtering

An essential feature of the adaptive filter (AF) is the adaptive linear combiner as is illustrated in figure 4.2. A stationary input signal $X_j(t)$ is sampled to form n sampled measurements X_{ij}, where j is the time index. Each measurement is multiplied by a corresponding weighting coefficient W_j, and the weighted measurements are combined to form an output y_j. This output is compared with a desired response d_j to form the error signal $E_j(d_j)$ and is used to train the adaptive filter.

Two main objectives are sought in the operation of this type of filter

(i) to choose the weighting coefficient in order to minimise the error signal, E_j , and

(ii) to find the weighted sum of input signals that best matches the desired response, d_j.

The jth output signal of the combiner is given by

$$y_j = \sum_{i=1}^{n} W_j X_{ij} \qquad \ldots\ldots 4.1$$

and the error signal is given by

$$E_j = d_j - y_j = d_j - \sum_{i=1}^{n} W_j X_{ij} \qquad \ldots\ldots 4.2$$

The analysis in this section is based upon a stationary input signal.

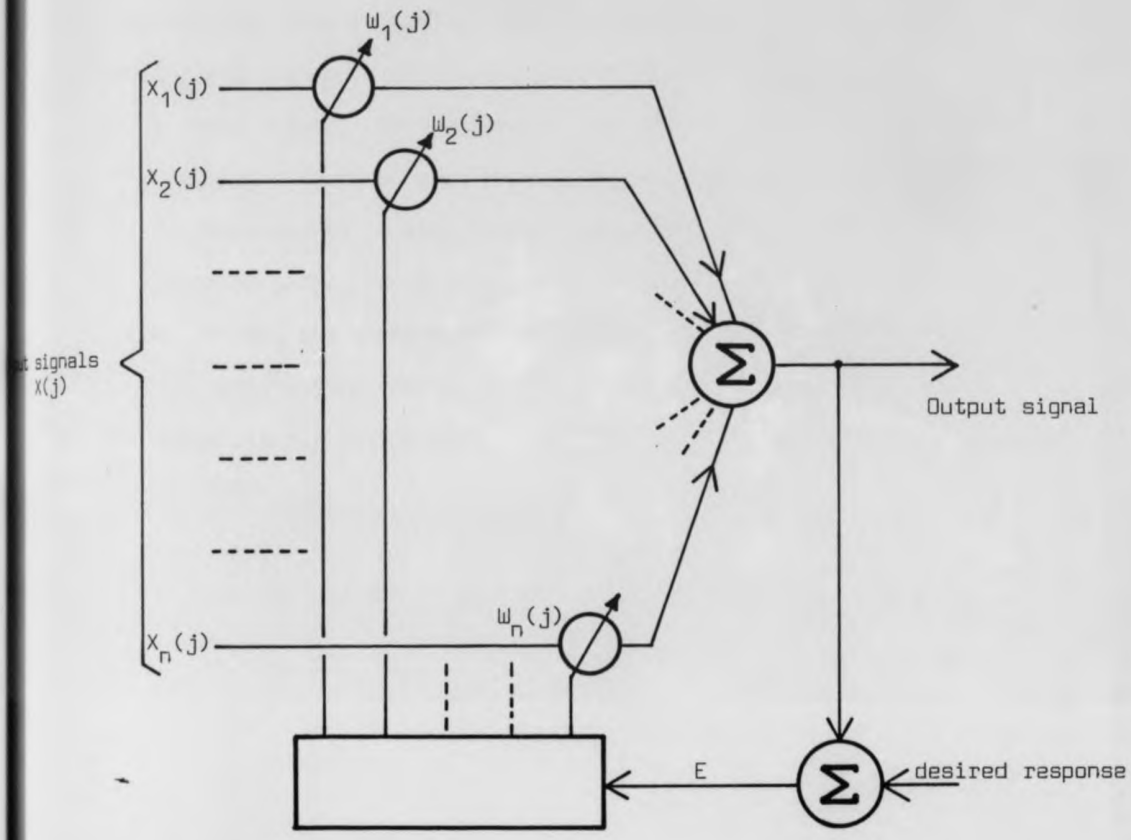

Figure 4.2 An adaptive filter based on the adaptive linear combiner. The control algorithm samples the input and output signals and adjusts the weights to obtain the desired filter function.

There are various ways of configuring the input signal $X_j(t)$. For example, if the inputs are taken from a tapped delay-line, the linear combiner will form a transversal or finite impulse response (FIR) filter, and the whole structure will be known as an adaptive transversal filter, (ATF) (Widrow et al.,1976). Such configurations have been used to model an unknown system (Widrow et al., 1975) to reduce interference in communication systems (Widrow, 1981), reduce or eliminate periodic interference in electrocardiography (Widrow & McCool, 1976), and broadband interference in the sidelobes of an antenna array (Widrow et al., 1976), to separate periodic and broadband signals and detect very low level periodic signals (Widrow et al.,1974).

4.3 The LMS adaptive algorithm

Two main processes may be recognised in the operation of adaptive filters; training (adaptation) and operation. In the training process the weights are readjusted, while in the operation process the output signals are formed by weighting the tap delay-time signals (figure 4.1) using the weights resulting from the adaptation.

In optimising a filter it is necessary to either minimize the mean square error to approach the best of linear filtering, as in Weiner's theory of optimal filters, or maximize the signal-to-noise ratio (Shensa, 1979).

Referring to figure 4.1, one can develop the theory of an adaptive filter by using the mean square error approach. The output in terms of the filter input and weights, equation 4.1, may be rewritten using a matrix notation.

$$y_j = \underline{X}_j^T \underline{W} = \underline{W}^T \underline{X}_j \qquad \ldots\ldots 4.3$$

$$\text{where } \underline{X}_j^T = [X_j, X_{j-1}, X_{j-2}, \ldots X_{j-N}] \qquad \ldots\ldots 4.4$$

$$\text{and } \underline{W} = W_1, W_2, W_3, \ldots\ldots W_N \qquad \ldots\ldots 4.5$$

The main requirements of the adaptive algorithm are to select the weights necessary to minimise the mean square error (MSE). By squaring equation 4.2 and taking the mean over the ensemble the MSE can be formed.

$$E[e_j^2] = E[d_j^2] - 2E[d_j \underline{X}_j^T]\,\underline{W} + \underline{W}^T E[X_j X_j^T]\underline{W} \qquad \ldots\ldots 4.6$$

which may be written as:

$$E[e^2_j] = E[d^2_j] - 2\underline{P}^T\underline{W} + \underline{W}^T\underline{R}\,\underline{W} \qquad \ldots\ldots 4.7$$

$$E[d_j X_j] = E\begin{bmatrix} d_j X_{1j} \\ d_j X_{2j} \\ d_j X_{nj} \end{bmatrix} \triangleq P \qquad \ldots\ldots 4.8$$

$$E[X_j X^T_j] = E\begin{bmatrix} X_{1j}X_{1j} & X_{1j}X_{2j} & \cdots \\ X_{2j}X_{1j} & X_{2j}X_{2j} & \cdots \\ \cdot\ \cdot & \cdot\ \cdot & \\ \cdot\ \cdot & \cdot\ \cdot & \\ \cdot\ \cdot & \cdot\ \cdot & X_{nj}X_{nj} \end{bmatrix} \triangleq R \qquad \ldots\ldots 4.9$$

Where P is the cross correlation vector between the input signals and the desired response, and R is the input correlation of the X- input signals.

Since the input and the output are assumed to be statistically stationary, the MSE is a quadratic function of the weights (McCool & Widrow, 1976). This function has a minimum that can be obtained by differentiating the MSE equation 4.7 with respect to the weight factor.

to obtain the gradient vector $\nabla E[e_j^2]$

Therefore:

$$\nabla E[e^2_j] = -2\underline{P} + 2\underline{\underline{R}}\underline{W} \quad \ldots\ldots 4.10$$

By setting the gradient to zero, the optimal weight vector is obtained;

$$\underline{W}^* = \underline{R}^{-1}\,\underline{P} \quad \ldots\ldots 4.11$$

This is the matrix form of the Wiener-Hopf equation.

The exact solution from equation 4.11 can be obtained, but is impractical if the number of weights is large, or the data rate is high since the process involves an NxN matrix and may require as many as $\frac{N(N+1)}{2}$ autocorrelation and cross correlation measurements. Moreover, in the case of a non-stationary signal, a continuously repeated process is necessary.

In general autocorreaction and crosscorrelation functions are normally unknown, and the Wiener-Hopf algorithm does not compute the correlation matrices or matrix manipulations but requires that the weight vector be adjusted from the estimates of the gradient to approach the Weiner solution.

The LMS algorithm is commonly based upon gradient estimation even though it tends to be noisy compared with taking a true gradient value. However, it can be minimised through careful application of the adaptive algorithms for steepest descent (Widrow et al., 1976).

4.3.1 Method of gradient estimation

This method measures the gradient of the mean square error by differentiating the MSE with respect to the weight vector.

If $\bar{E}_j^2$ is the mean square error, the differential with respect to the weight vector is:

$$\frac{\delta \bar{E}_j^2}{\delta W_i^2} \simeq \frac{\delta E_j^2}{\delta W_i^2} = 2E_j \frac{\delta E_j}{\delta W_i} \qquad \ldots\ldots 4.12$$

Differentiating equation 4.2 with respect to W_i, gives

$$\frac{\delta E_j}{\delta W_i} = -X_{ij} \qquad \ldots\ldots 4.13$$

substituting 4.13 into 4.12 will give

$$\frac{\delta \bar{E}_j^2}{\delta W_i^2} \simeq \frac{\delta E_j^2}{\delta W_i^2} = -2E_j X_{ij} \qquad \ldots\ldots 4.14$$

Therefore the gradient vector can be approximated as

$$\nabla \bar{E}_j^2 \simeq \nabla E_j^2 = -2E_j \underline{X}_j \qquad \ldots\ldots 4.15$$

In order to estimate the gradient, the present input vector and the error should be known according to equation 4.15. This method (gradient estimation) introduces noise (Widrow, 1976), into the weight

vector which is proportional to the speed of adaptation and to the number of weights. This effect can be expressed in terms of a dimensionless quantity called misadjustment (Widrow, 1966)

4.3.1.1. Misadjustment due to gradient noise

It is evident from the previous section that, for adaptation by minimising the mean square error, the faster the system adapts the poorer will be the expected performance. For the Wiener optimum solution the weights are adjusted according to equation 4.11 and are based upon a priori knowledge of the statistics of the signal (an ideal system). When the LMS algorithm is used, the expected level of the mean square error will exceed that of the ideal system and the Wiener solution of equation 4.11. The longer the time constants for adaptation the closer the expected performance is to the Wiener optimum performance.

In using the LMS algorithm an excess of mean-square error will develop which is called misadjustment and can be represented in the following equation.

$$\text{Misadjustment} = M \triangleq \frac{\bar{y}_i - \bar{e}^2_{min}}{\bar{e}^2_{min}} \qquad \ldots\ldots 4.16$$

A simplified formula for misadjustment may be expressed in the form:

$$M = \frac{1}{2} \sum_{p=1}^{n} \frac{1}{\tau_p} \qquad \ldots\ldots 4.17$$

where n is the number of weights, τp is the settling time and N time constant of the filter adjustment weights (Widrow, 1966). The time constant of the pth mode, τp, is related to the pth eigenvalue λp of the input correlation matrix R and also to the convergence, μ. It may

be expressed in the form:

$$\tau_{Pmse} = \frac{1}{4\mu\lambda_p} \qquad \ldots . 4.18$$

Where λ is a convergence factor that controls stability and rate of adaptation. In a special case when all the eigenvalues are equal, all the time constants will also be equal. This case only occurs when all the input signal components are uncorrelated and are of equal power.

Under these conditions the time constant may be expressed as:

$$\tau_{mse} = \frac{1}{4\mu\lambda} \qquad \ldots . 4.19$$

In the above case the misadjustment will be proportional to the number of weights and inversely proportional to the time constant and may be written:

$$M = \frac{1}{2} \sum_{p=1}^{n} \frac{1}{\tau p} = \frac{n}{2\tau} = \frac{n}{4\tau_{mse}} \qquad \ldots . 4.20$$

$\tau p = \tau$ for all p

Substituting equation 4.19 into equation 4.20, the misadjustment may be expressed as:

$$M = n\mu\lambda \qquad 0 < \mu < \frac{1}{\lambda_{max}} \qquad \ldots . 4.21$$

Where λ max is the largest eigenvalue. Widrow et al.(1974, 1976) suggested that a 10% misadjustment is satisfactory for many applications. An increase in the number of weights will improve the performance of the adaptive filter but at the expense of an increase in misadjustment at a fixed rate of convergence.

It has been shown from more general considerations that for many adaptive LMS systems, the misadjustment for small values of M($\simeq$ 0.25) is approximately equal to

$$M = \frac{\text{number of filter coefficients}}{\text{number of training samples}}$$

4.3.1.2. Stability of LMS algorithm

It has been shown in the previous section that misadjustment can be related to the speed of adaptation and to the number of weights being adapted. It has also been shown (Widrow, 1976) that unconditionally stable operation of LMS algorithm can be obtained if $0 < \mu < \frac{1}{\lambda_{max}}$ where λ max is the maximum eigenvalue of the input signal correlation matrix (R). This eigenvalue can often be difficult to obtain. However, stability can be assured without knowing λ max as long as μ is kept within certain bounds.

For stability μ is kept $< \lambda$ max. However, another important property which can influence stability is the convergence time. This has been shown experimentally with the time constant, τ_p, (Widrow, 1976; Shensa, 1979) related to by the approximate relation:

$$\tau_p \approx \frac{1}{2\mu\lambda_p} \qquad \ldots . 4.23$$

The overall convergence is also limited by the smallest of the eigenvalues, λ min, and this sets the lower bound of the condition. For stability;

$$\tau_{min} = \frac{\lambda_{max}}{4\lambda_{min}} \qquad \ldots . 4.24$$

Thus when the LMS algorithm is stable, transients must die out. If the algorithm is unstable on the other hand, the weight vector will grow.

4.3.1.3. Choosing the number of coefficients

The choice concerning the number of weights depends upon the application of the adaptive filter and, in accordance with the sampling frequency, the desired filter frequency resolution. Based upon these two parameter values, the number of weights may be expressed as;

$$N = \frac{2 \text{ sampling frequency}}{\text{resolution}} \quad \ldots . 4.25$$

Choosing a large number of weights for a transversal filter will ensure a close approximation to the impulse response of the ideal Wiener filter. However, increasing the number of weights also slows the adaptive process (increases misadjustment) and increases the cost of implementation.

In practice, misadjustment is often chosen first, set accordingly and the value of the delay then chosen so that the filter weights peak at the centre of the weight vector.

4.3.2 Method of steepest descent

The LMS algorithm for minimising the error function can be based upon the method of steepest descent. This involves adjusting the present weight vector by an amount opposite in sign and proportional to the value of gradient vector, thus;

$$\underline{W}_{j+1} = \underline{W}_j - \mu(\underline{\nabla}_j)) \qquad \ldots . 4.26$$

where $\underline{\nabla}_j$ is the gradient vector and μ the convergence factor which controls the stability and rate of adaptation.

The gradient estimate takes the gradient of the square of a single error sample, thus;

$$\underline{\nabla}_j = -2e_j\underline{X}_j \qquad \ldots . 4.27$$

where $\underline{X}_j$ is the input vector.

The LMS algorithm can be written as

$$W_{j+1} = W_j + 2\mu E_j X_j \qquad \ldots . 4.28$$

where W_{j+1} is the next weight vector.

For convergence of the LMS algorithm it is necessary that $\frac{1}{\lambda_{max}} > \mu > 0$ where λ_{max} is the maximum eigenvalue.

Since the individual eigenvalues are rarely known and as R approaches

positive: $t_r R > \lambda max$

where $t_r R$ is the total input power.

Therefore, $\frac{1}{t_r R} > \mu > 0$

is quite sufficient condition for convergence.

In seeking the minimum mean-square error (i.e. $\overline{\Sigma^2_{min}}$), the method of steepest descent could be conducted as follows:

(1) Initial guess of where the **minimum** point of the $\overline{\Sigma_j^2}$ surface may be. Then measure the gradient vector $\nabla\overline{\Sigma_j^2}$ at the point on the performance surface corresponding to those in the set of initial values of the weights.

(2) the next guess is then obtained from the present guess by making a change in the weight vector in the opposite direction to the gradient vector.

If each change in the weight vector is made proportional to the error-surface gradient vector:

$$\underline{W_{j+1}} = \underline{W_j} + \mu \underline{\nabla\Sigma_j^2}$$

W_j is the present guess

The performance function ($\overline{\Sigma_j^2}$) is **quadratic**, the gradient is a linear function of weights.

$$\therefore \nabla\overline{\Sigma_j^2} = \underline{-2\Phi(x_1 d)} + 2W_j[\Phi(x_1 x)]$$

4.4 Efficiency of adaptive algorithm

The Widrow-Hoff method of steepest descent is most widely used in the adaptive algorithm, in spite of its slow convergence and reduced efficiency due to the misadjustment and rate of adaptation (Widrow, 1966). Widrow has introduced a measure for the efficiency of the adaptation process (algorithm) called efficiency measure (EM) and can be written in the following form:

$$EM = \frac{N}{t.M} \qquad \ldots . 4.29$$

where N is the number of coefficients, M is the misadjustment and t is the settling time. The latter may be defined in terms of the longest adaptive time constant, τ_{max} as;

$$\text{settling time} \simeq 3\tau_{max} \qquad \ldots . 4.30$$

For fixed adjustment EM increases with reduction of settling time per number of weights.

For the situation in which all the eigenvalues are equal (ie. the same time constant) equation 4.29 becomes;

$$EM = \frac{N}{3\tau(N)(\overline{2\tau})} = \frac{2}{3} \qquad \ldots . 4.31$$

However, when the time constants are different from one another;

$$EM = \frac{N}{3\tau_{max}\frac{1}{2}\sum_{p=1}^{N}\frac{1}{\tau_p}} = \frac{2}{3}\frac{1}{\frac{1}{N}\sum_{p=1}^{N}\frac{\tau_{max}}{\tau_p}} \qquad \ldots . 4.32$$

and since

$$\frac{1}{N}\sum_{p=1}^{N}\frac{\tau_{max}}{\tau_p} \geq 1 \qquad \ldots\ldots 4.33$$

$$\text{therefore } EM < \frac{2}{3} \qquad \ldots\ldots 4.34$$

It may be concluded that the higher the difference between the eigenvalues of R the lower will be the efficiency of the adaptation process, and the longer the settling time for the same level of misadjustment for the same number of weights.

In a case when data can be stored and used again and again for the LMS algorithm to adapt, the weights will approach the Wiener-Hoff solution;

$$W^* = R^{-1}P = R^{-1}P \qquad \ldots\ldots 4.35$$

The process will have misadjustment of

$$M = \frac{n}{N} = \frac{\text{number of weights}}{\text{number of weights of independent training system}} \qquad \ldots\ldots 4.36$$

In this case, the system settling time, or averaged time is N sample periods. The efficiency measures of this data (repeated again and again) for the adaptive process is therefore;

$$EM = \frac{n}{\frac{N(n)}{(N)}} = 1 \qquad \ldots\ldots 4.37$$

It may be concluded that for one-pass data the efficiency measure is 1/3 less than the repeated data. In order to have the same level of misadjustment, the one-pass-data would have to be 50% longer than the average time of the repeated data process.

4.5 Adaptive noise cancellation

The adaptive noise canceller (ANC) is one form of adaptive filter that attempts to estimate a signal corrupted by noise. The performance of adaptive noise canceller, illustrated in figure 1.4, has been studied within the framework of Wiener filter theorem (Glover, 1977; Shensam, 1979, 1980; Widrow, 1976). The ANC consists of two input channels and one output channel, the primary input $d_j(t)$ contains a signal s(t) combined with an uncorrelated noise, $n_0(t)$, and a reference input $x_j(t)$ which contains the noise $n_1(t)$ which is uncorrelated to the signal s(t) but correlated in some unknown way with the noise $n_0(t)$. The noise $n_0(t)$ is filtered to produce an output y(t) that is as close a replica as possible to $N_0(t)$. This output is subtracted from the primary input $s(t) + n_0(t)$ to produce the system output.

$$Z(t) = s(t) + n_0(t) - y(t) \quad \ldots\ldots 4.38$$

The function of an adaptive noise canceller is to use the reference input to optimally cancel the correlated components of the noise, $n_0(t)$ so providing a better estimate of s(t) at the output.

This could also be done by a fixed value filter, but a priori knowledge of a signal statistics is needed. Such information is not often available for such a filter. So the use of an adaptive filter, which automatically adjusts its impulse response through an algorithm to minimise the error signal, is needed.

An explanation of how an ANC attempts to minimise the mean square error when the signal statistics are unknown is presented below.

Assuming that s, n_0, n_1 and y are statistically stationary and n_1 is correlated with n_0, but uncorrelated with s, the output is;

$$Z = s + n_0 - y \qquad \ldots . 4.39$$

squaring;

$$Z^2 = s^2 + (n_0 - y)^2 + 2s(n_0 - y) \qquad \ldots . 4.40$$

Taking expectation of both sides of equation 4.40 yields the relationship;

$$E[Z^2] = E[s^2] + E[(n_0 - y)^2] + 2E[s(n_0 - y)] = E[s^2] + E[n_0 - y^2] \qquad \ldots . 4.41$$

$2E[s(n_0 - y)] = 0$ because s is uncorrelated to n_0 and y.

In minimising $E[Z^2]$ the signal power $E[s^2]$ will be unaffected, therefore;

$$\min E[Z^2] = E[s^2] + \min E[(n_0 - y)^2] \qquad \ldots . 4.42$$

When the filter has adapted, the filter output, y, is approximately the least squares estimate of the primary noise n_0 .When $E[(n_0 - y)^2]$ is minimised, $E[(Z - s)^2]$is also minimised and from equation 4.39;

$$(Z - s) = (n_0 - y) \qquad \ldots . 4.43$$

Adjusting the filter to minimise the total output power causes the output, Z, to be a best least square estimate of the signal, s, and since the signal at the output remains constant, minimising the total output will maximise the output signal-to-noise ratio.

For the situation when the reference input n_1 is completely

uncorrelated with the primary input n_0, the adaptive noise cancellor will turn itself off and will not increase the output noise. In this case the filter output, y, will be uncorrelated with the primary input n_0.

Therefore the output power will be

$$E[Z^2] = E[(s + n_0)^2] + 2E[-y(s + n_0)] + E[y^2] = E[(s + n_0)^2] + E[y^2] \quad \ldots\ldots 4.44$$

Minimising output requires minimisation of $E[y^2]$ (all the weights have zero value to bring $E[y^2]$ to zero).

It was considered important to examine the behaviour of this type of filter under the following conditions:

(i) uncorrelated random noise present in both inputs,

(ii) signal components present in the reference input

4.5.1. Uncorrelated noise present in both inputs

Figure 4.3 shows a single channel adaptive noise canceller with correlated n_0, n_1 and uncorrelated m_0, m_1 noise present in both primary and reference inputs respectively. The primary input contains the signal $s_j + n_{0j} + m_{0j}$ while the reference input consists of a sum of two other noises, m_{1j} and n_{1j} where

$$n_{1j} = n_{0j} * h(j) \qquad \ldots . 4.45$$

where $h(j)$ is the impulse response of the reference channel whose transfer function is $H(Z)$.

n_{0j} and n_{1j} are uncorrelated since this originates from the same source.

m_{0j} and m_{1j} are uncorrelated noise present in both channels.

The Wiener solution will be:

$$W^*(Z) = \frac{\delta xd(Z)}{\delta xx(Z)} \qquad \ldots . 4.46$$

where $\delta xd(Z)$ is the input cross correlation function and $\delta xx(Z)$ is the input autocorrelation function where:

$$\delta xx(Z) = \delta m_1 m_1(Z) + \delta n_0 n_0(Z) \, |H(Z)|^2 \qquad \ldots . 4.47$$

and

$$\delta xd(Z) = \delta n_0 n_0(Z) \, H(Z^{-1}) \qquad \ldots . 4.48$$

the Wiener transfer function becomes:

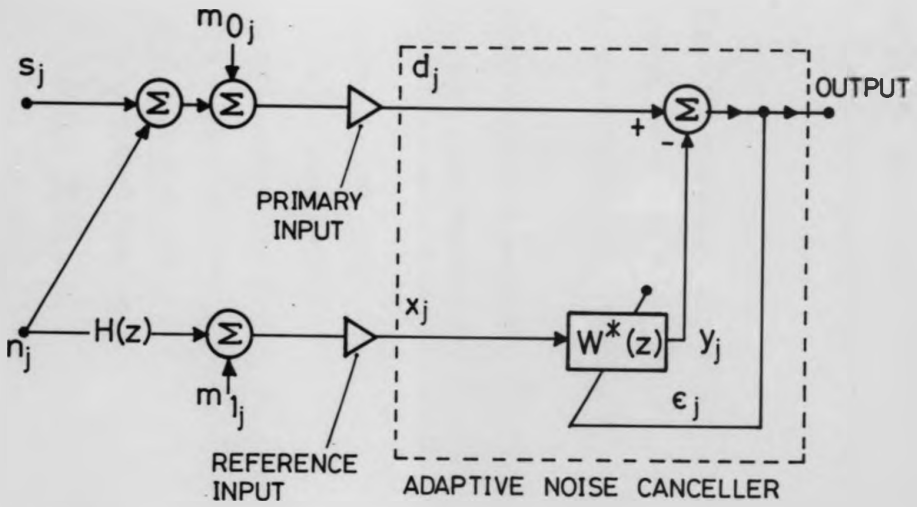

Figure 4.3 Single channel ANC with correlated and uncorrelated noises in the primary and reference I/P

$$W^*(Z) = \frac{\delta n_0 n_0(Z) H(Z^{-1})}{\delta m_1 m_1(Z) + \delta n_0 n_0(Z)\,|H(Z)|^2} \quad \ldots\ 4.49$$

Equation 4.49 is independent of the primary signal spectrum $\delta ss(Z)$ and of the primary uncorrelated noise spectrum $\delta m_0 m_0(Z)$. If m_1 is zero then $\delta m_1 m_1(Z)$ is zero, therefore equation 4.50 will become the optimal transfer function of equation 4.49

$$W^*(Z) = \frac{1}{H(Z)} \quad \ldots\ 4.50$$

The adaptive noise canceller will filter the noise in the primary input leaving the uncorrelated noise, m_1, to pass while changing the noise m_2 by the filter transfer function at the output.

Widrow (1976) derived an expression for the improvment in signal-to-noise power density ratio where signal-to-noise density ratio is:

$$= \frac{\text{Signal power density}}{\text{noise power density}}$$

therefore the output signal-to-noise power density $\rho_{out}(Z)$ to the primary input signal-to-noise power density $\rho_{pri}(Z)$ is

$$= \frac{\text{Primary noise power spectrum}}{\text{output noise power spectrum}} \quad \ldots\ 4.51$$

$$\frac{\rho_{out}(Z)}{\rho_{pri}(Z)} = \frac{[A(Z) + 1][B(Z) + 1]}{A(Z) + A(Z)B(Z) + B(Z)} \quad \ldots\ 4.52$$

$$\text{where } A(Z) = \frac{\delta\, m_0 m_0(Z)}{\delta\, nn(Z)} \quad \ldots\ 4.53$$

$$\text{and} \quad B(Z) = \frac{\delta m_1 m_1(Z)}{\delta nn(Z)\,|H(Z)|^2} \qquad \ldots\ldots 4.54$$

Equation 4.52 represents the performance of the ideal noise canceller which can be limited by the ratio of the uncorrelated noise density at primary input to the correlated noise density at the reference input.

When both A(Z) and B(Z) are zero, an infinite improvement for the noise canceller can be obtained. When A(Z) and B(Z) are small, misadjustment occurs (discussed for the adaptive filter in the previous section).

4.5.2 Effect of signal components present in the reference input

Figure 4.5 represents an adaptive noise canceller (ANC) in which the reference input contains signal components and both the primary and reference inputs contain additive correlated noise. For simplicity in the following analysis the uncorrelated noise has been ignored ($m_0 = m_1 = 0$). The reference input has a different pathway with a transfer function of I(Z), and the unconstrained Wiener solution is that of equation 4.46 where:

$$\delta xd(Z) = \delta ss(Z)\, I(Z)^{-1} + \delta nn(Z)\, H(Z^{-1}) \qquad \ldots . 4.55$$

and

$$\delta xx(Z) = \delta ss(Z)|I(Z)|^2 + \delta nn(Z)|H(Z)|^2 \qquad \ldots . 4.56$$

which will converge to the solution of equation 4.50 when I(Z) approaches zero. The transfer function of the propagation route from the signal input to the noise canceller is $[1 - I(Z)\, W^*(Z)]$, and that from the noise input to the canceller output is $[1 - H(Z)\, W^*(Z)]$

Therefore in considering the signal and noise components present at the output of the noise canceller, it is instructive to determine the signal-to-noise density ratio $\rho_{out}(Z)$ where:

$$\rho_{out}(Z) = \frac{\delta nn(Z).|H(Z)|^2}{\delta ss(Z).|I(Z)|^2} \qquad \ldots . 4.57$$

which can be written as:

$$\rho_{out}(Z) = \frac{1}{\rho_{ref}(Z)} \qquad \ldots . 4.58$$

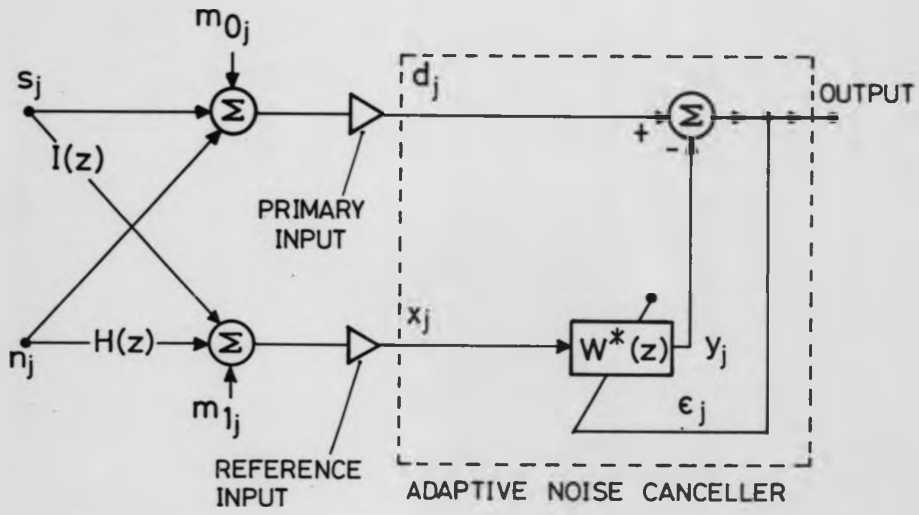

Figure 4.4 Adaptive noise canceller with signal components in the reference input.

where $\rho_{ref}(Z) = \dfrac{\delta ss(Z)\ |I(Z)|^2}{\delta nn(Z)\ |H(Z)|^2}$ 4.59

From equation 4.58 it can be seen that the output signal-to-noise density ratio is inversely proportional to the reference input signal-to-noise density ratio at all frequencies when convergence occurs.

Ferrara & Widrow (1981) have derived an expression for signal distortion due to the presence of the signal component in the reference input, and the amount of such distortion will depend upon the amount of signal propagation through the adaptive filter.

The signal component that appears at the filter output is $-I(Z)\ W^*(Z)$. If $I(Z)$ is small then:

$$-I(Z)\ W^*(Z) \simeq \frac{-I(Z)}{H(Z)} \quad \ldots . 4.60$$

The spectrum of signal components which propagate to the noise canceller output through the adaptive filter is:

$$\delta ss(X)\left|\frac{I(Z)}{H(Z)}\right|^2 \quad \ldots . 4.61$$

Ferrar & Widrow (1981) have defined a measure of such distortion, $D(Z)$, expressed as the ratio of the spectrum of the output signal components that propagate through the adaptive filter to the spectrum of the signal components at the primary input;

$$D(Z) = \frac{\delta ss(Z)\ |I(Z)W^*(Z)|^2}{\delta ss(Z)} \quad \ldots . 4.62$$

$$D(Z) = I(Z)\, W(Z) \qquad \ldots . 4.63$$

For simplicity, equation 4.63 can be rewritten as:

$$D(Z) = \frac{\rho_{ref}(Z)}{\rho_{pri}(Z)} \qquad \ldots . 4.64$$

Equation 4.64 indicates that low distortion occurs when signal-to-noise ratio at the reference input is low, and high at the primary input.

4.6 Introduction to the adaptive signal enhancer

Another form of adaptive noise canceller, introduced by Widrow and Ferrara (1981), is the adaptive signal enhancer. This type of adaptive configuration seeks to enhance the signal against an additive noise and makes use of two input channels containing correlated signal components but uncorrelated noise components. The advantage of this technique is that the input or correlated signal need not be of the same waveform. This technique may be extended to adapt more than two channels. Using the multichannel adaptive signal enhancer approach, the more input channels available, containing correlated components, the higher will be the signal-to-noise ratio improvement and the lower the distortion. The adaptive channel enhancer having two or more input channels will discriminate the signal and noise on the basis of the channel-to-channel correlation.

4.6.1 The concept of adaptive signal enhancement

The principle of the adaptive channel enhancer may be examined for the two channel arrangement illustrated in figure 4.5. The zeroth-input channel contains signal s_0 and noise n_0 which are uncorrelated. Input to channel one contains a signal s_1 plus noise n_1, which are also uncorrelated but s_0 and s_1 are assumed to be related but not necessarily of the same waveform and the noise components, n_0 and n_1, are assumed to be uncorrelated with each other and with both signals s_0 and s_1. Once the filter has adapted its impulse response, through the LMS algorithm of the adaptive filter, and the power of the error is minimised the filter output is then a best least square estimate of s_0, (since n_0 is uncorrelated with the input s_1 and n_1).

A time delay is used to compensate for the various signal arrival times. It is equal to half the adaptive filter length (number of coefficients x update time) in the 'derived response' channel. From figure 4.5 the error signal will be;

$$E_j = d_j - y_i \qquad \ldots . 4.65$$

The unconstrained Wiener solution (discussed in previous sections) is;

$$W^*(Z) = R^1(Z)\, P(Z) \qquad \ldots . 4.66$$

Considering now the multichannel signal enhancer of figure 4.6 and assuming that the input signal is statistically stationary, the adaptive filter will, after convergence, closely approach the Wiener filter solution. If the inputs of figure 4.6 are x_{ij},------x_{kj} and the output y_i, the error signal ε_i will be;

$$\varepsilon_i = d_j - y_i \qquad \ldots . 4.67$$

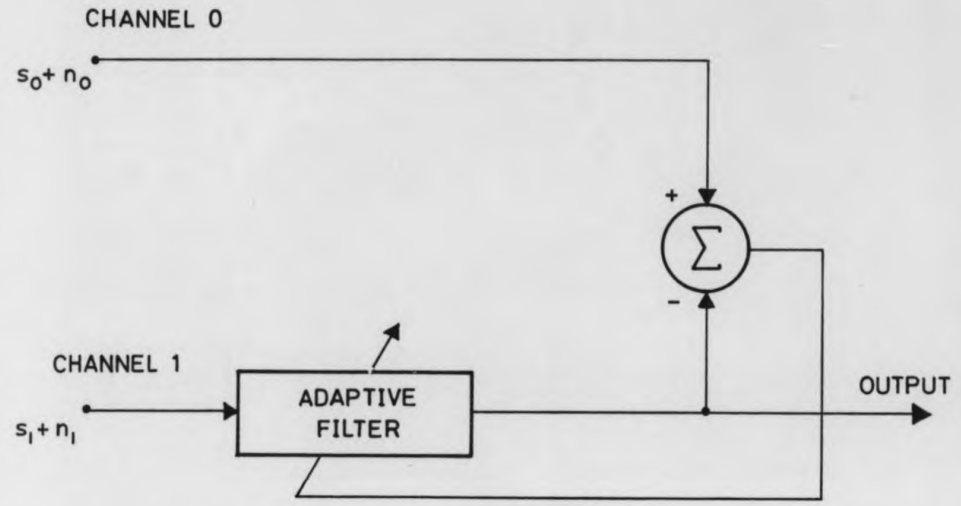

Figure 4.5 A block diagram of an adaptive signal enhancer. The adaptive filter attempts to form a best least square estimate of S_0 by enhancing the correlated signal components with respect to the uncorrelated noises N_0 and N_1.

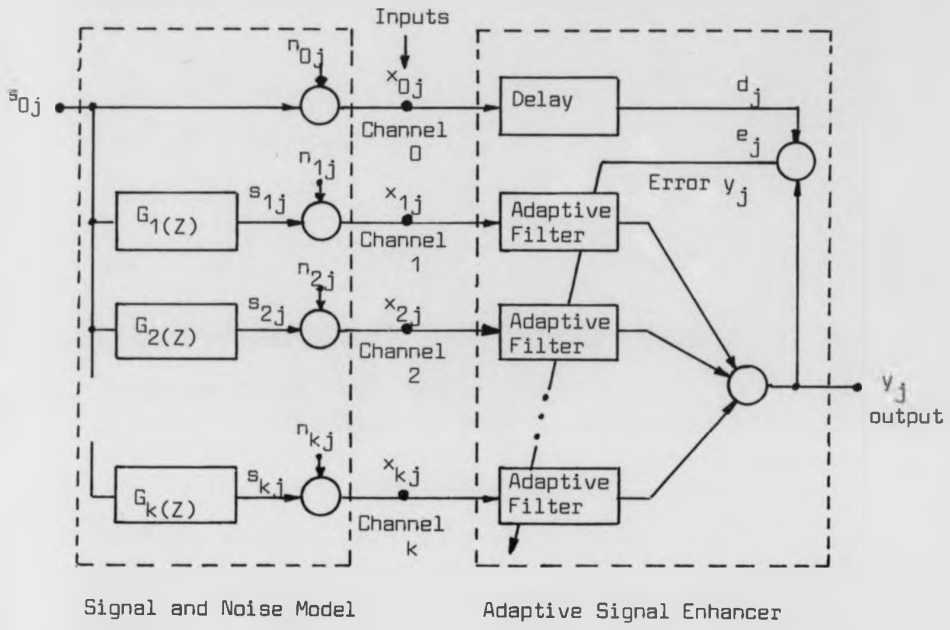

Figure 4.6 Model for analysis of multichannel signal enhancer.

where d_j is the desired response. For simplicity it is assumed that the adaptive filter is noncasual.

Considering further the Wiener solution; $W^*(Z) = R^1(Z)P(Z)$ 4.68

R(Z) is the input spectral function which can be defined as;

$$R(Z) = \begin{bmatrix} \varphi x_1 x_1(Z) \\ \varphi x_2 x_1(Z) \\ \cdot\cdot \\ \cdot\cdot \end{bmatrix} \begin{bmatrix} \varphi x_1 x_2(Z) \cdot\cdot\cdot \\ \varphi x_2 x_2(Z) \cdot\cdot\cdot \\ \cdot\cdot \\ \cdot\cdot \quad \varphi x_k x_k(Z) \end{bmatrix} \quad \ldots . 4.69$$

Here the power density function is expressed as a Z-transform at the real frequencies only (Widrow, 1976).

Where $\varphi x_1 x_1(Z)$ is the auto power density spectrum of the input x_1, since the input signal contains signal plus correlated noise, equation 4.69 can be rewritten as;

$$R(Z) = \begin{bmatrix} \varphi n_1 n_1(Z) \cdot\cdot\cdot \\ \cdot\cdot\cdot \quad \cdot\cdot\cdot \\ \cdot\cdot\cdot \quad \cdot\cdot\cdot \\ \cdot\cdot \varphi n_k n_k(Z) \end{bmatrix} + \begin{bmatrix} \varphi s_1 s_1(Z) \cdot\cdot\cdot \\ \cdot\cdot\cdot \quad \cdot\cdot\cdot \\ \cdot\cdot\cdot \quad \cdot\cdot\cdot \\ \cdot\cdot \varphi s_k s_k(Z) \end{bmatrix} \quad \ldots . 4.70$$

Since inputs s_{oj}, are related to the other inputs by the transfer function of $G_k(G)$, equation 4.70 can be written;

$$R(Z) = \Omega(Z) + \varphi s_0 s_0(Z) \begin{bmatrix} \bar{G}_1(Z)G_1(Z) & \bar{G}_1(Z)G_2(Z) \\ \bar{G}_2(Z)G_1(Z) & \\ & \bar{G}_k(Z)G_k(Z) \end{bmatrix} \quad \ldots\ldots 4.71$$

$$G(Z) = \begin{bmatrix} \bar{G}_1(Z) \\ G_2(Z) \\ G_3(Z) \end{bmatrix} \quad \ldots\ldots 4.72$$

and

$$R(Z) = \Omega(Z) + \varphi s_0 s_0(Z)\, \bar{G}(Z)\, \bar{G}(Z)^T \quad \ldots\ldots 4.73$$

where $\Omega(Z)$ is the input noise spectral density function and $P(Z)$ is the cross spectral density function;

$$P(Z) = \begin{bmatrix} \cdot \\ \varphi x_1 d(Z) \\ \cdot \\ \cdot \\ \varphi x_k d(Z) \end{bmatrix} = \begin{bmatrix} \varphi s_1 s_0(Z) \\ \varphi s_2 s_0(Z) \\ \cdot \\ \cdot \\ \varphi s_k s_0(Z) \end{bmatrix} = \varphi s_0 s_0(Z)\, G(Z) \quad \ldots\ldots 4.74$$

Therefore the signal-to-noise ratio at the input of the ith adaptive filter is;

$$SNR_i(Z) = \frac{\varphi s_i s_i(Z)}{\varphi n_i n_i(Z)} \quad \ldots\ldots 4.75$$

which can be written as;

$$SNR_i(Z) = \frac{G_i(Z)\overline{G}_i(Z)\varphi s_0 s_0(Z)}{\varphi n_i n_i(Z)} \quad \ldots\ldots 4.76$$

The effective signal-to-noise ratio SNR_{eff} may be defined (Ferrara, 1981);

$$SNR_{eff}(Z) = \sum_{i=1}^{k} SNR_i(Z) \quad \ldots\ldots 4.77$$

$$\text{The output } SNR(Z) = \frac{\text{output signal spectrum}}{\text{output noise spectrum}} \quad \ldots\ldots 4.78$$

$$\simeq \frac{\varphi s_0 s_0(Z)}{\varphi nn(Z)} \quad \ldots\ldots 4.79$$

$$\simeq SNR_{eff}(Z) \quad \ldots\ldots 4.80$$

Assuming that the effective signal-to-noise ratio is much greater than 1, the output signal-to-noise ratio is approximately equal to the sum of the SNR of the individual filter inputs.

4.7 Summary

In this chapter the concept of adaptive filters, employing adaptive transversal structure were reviewed, with regard to a brief derivation of the Widrow-Hoff LMS adaptive algorithm.

The parameters which influence the operation of adaptive filters, such as the convergence factor and filter order, are discussed in chapter eight. The misadjustment due to the method of gradient estimation noise, together with the stability of the algorithm, were derived in this chapter.

The use of adaptive filters to perform noise cancelling and adaptive signal enhancement were also reviewed, expressions for the predicted improvement in signal-to-noise ratio were derived. The results of the application of adaptive filters can be seen in chapters six, seven and eight.

Chapter Five: Theory and application of time-sequence adaptive filters

5.1. Introduction

Chapter four dealt with the theory of the adaptive filter for dealing with stationary signals corrupted by noise. In this chapter another important form of adaptive filter, usually used for non-stationary data, is examined. This filter is also based upon the use of the LMS algorithm for improvement in signal-to-noise ratio. The time-sequence adaptive filter is applied mainly for two reasons;

(i) for use in the conditioning of non-stationary signals having recurring, but not necessarily periodic statistical characteristics. With a rapid change in the statistics of the signal, all the weight vectors have to change freely in time in order to accommodate the variation. This necessitates the operation of the filter with slow convergence.

(ii) all the filters previously mentioned yield a substantial reduction in noise but often at the expense of signal distortion, especially with a low signal-to-noise ratio.

The time-sequence adaptive filter (TSAF) uses a multiple set of adjustable weights (Ferrara, 1977). At each point in time, one and only one set of weights is selected to form the filter output and is adapted using the LMS algorithm. The selection of the set of weights is continually synchronised with the recurring statistical character of the filter input in order that each set is associated with a particular error surface. After many adaptations of each set of

weights, the minimum point on each error surface is reached, resulting in an optimal time-varying filter. A priori knowledge of the recurrence of each segment of the input data is needed in order to synchronise the selection of the set of weights.

Ferrara and Widrow (1981, 1982) developed this technique and verified its validity both theoretically and by computer simulation.

5.2 The time-sequence adaptive filter (TSAF)

The adaptive transversal filter (ATF), consists of a tapped delay line connected to an adaptive linear combiner which adjusts the weights applied to the signal, derived from the taps of the delay line, and combines them to form the output signal. A modified version of the adaptive transversal filter includes a separate input, which when muliplied by a bias weight and summed with other weighted signals, forms the output. A bias weight is often used when both the filter input and the desired response have a non-zero mean.

Suppose that the input signal vector X_j of the adaptive linear combiner is defined as;

$$X_j^T = [1, x_j, x_{j-1} \text{-----} x_{j-(n-1)}]^T \qquad \ldots . 5.1$$

These input signal components are assumed to appear simultaneously in time.

The weighting coefficients w_0, w_i $\text{-----}w_n$, are adjustable.

The weight vector W is;

$$W^T = [w_0, w_1 \text{-----} w_2 \text{-----} w_n]^T \qquad \ldots . 5.2$$

The filter output Y_i is equal

$$Y_i = X_j^T W = W^T X_j \qquad \ldots . 5.3$$

The error E_j which can be defined as the difference between the desired response d_j and Y_i and can be written as;

$$E_j = d_j - Y_i = d_j - X_j^T W = d_j - W^T X_j \quad \ldots\ldots 5.4$$

The mean square error at time t_j can be defined by ξ_j which is given by;

$$\xi_j = E[(E_j^2)] \quad \ldots\ldots 5.5$$

$$= E[(d_j - W_j^T X_j)^2] \quad \ldots\ldots 5.6$$

$$= E[d_j^2] - 2W_j^T P_j + W_j^T R_j W_j \quad \ldots\ldots 5.7$$

The Wiener weight vector W_j, which minimises the mean-square error may be related to the correlation and cross-correlation matrices by;

$$W_j^* = R_j^{-1} P \quad \ldots\ldots 5.8$$

Define R_j as a correlation matrix at time t_j,

$$R_j = E[X_j X_j^T] \quad \ldots\ldots 5.9$$

and P_j a cross-correlation matrix,

$$P_j = E[d_j X_j] \quad \ldots\ldots 5.10$$

For non-stationary data R_j and P_j are unknown. In using a time-sequence adaptive filter the input data (non-stationary data) may be considered to be composed of a finite number of stationary segments, of known duration with respect to the signal recurrence moment. Under these conditions, in which the R_j and P_j are considered to be constant for stationary data, the solution for each stationary segment is derived for a particular associated error surface.

In practice a time-sequence filter may be considered to be composed of

a bank of LMS adaptive filters and has the ability to track rapid changes in the data input. The form of the TSAF is illustrated in figure 5.1.

The number of weight vectors is finite, each corresponds to an error surface which can be denoted by W_0, W_1, W_2 ----W_n. Only one weight vector is selected at anyone time and depends upon the error surface required at that time. The error will be minimised by the LMS algorithm when, after many adaptations, it becomes identical to that of the Wiener weight factor. This results in the filter output being the best least square match to the desired output.

In operation, a sequence number ζ_j is required to determine the weight vector necessary at time j. When $\zeta_j = i$ the ith error surface is selected to form the filter output.

The time sequence adaptive algorithm is;

$$Y_j = X_j^T W_{\zeta_j}(j) \qquad \ldots . 5.11$$

and

$$W_{i(j+1)} = W_{i(j)} + 2\mu_i E_j x_j \qquad \text{for } \zeta_j = i \qquad \ldots . 5.12$$

$$\text{or} = W_{i(j)} \text{ otherwise.}$$

Where $W_{i(j)}$ is the value of the i^{th} weight vector at time j.

Ferrara (1977) suggested that by using a different value for μ, for each weight vector, an identical loss in steady-state performance (misadjustment) for each weight vector will occur. Also when the LMS

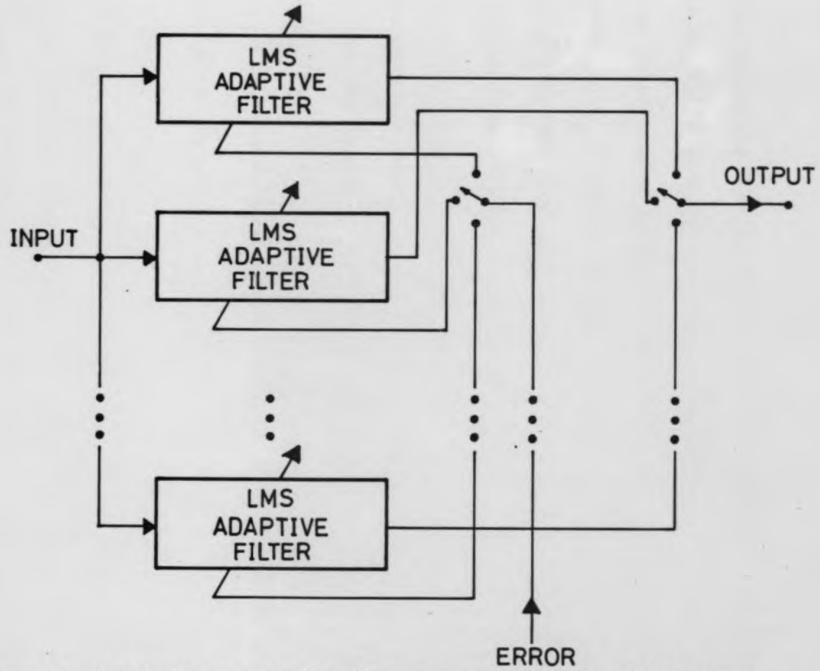

Figure 5.1 Block diagram of the time-sequence adaptive filter may be notionally depicted as a set of separate adaptive filters which are operated in sequence, with the output taken from each in turn. An external sequencing signal controls the commutator.

algorithm is used, a different weight vector for each error surface in the time sequence filter will be required in order to eliminate the Wiener weight vector tracking error present, particularly for a non-stationary signal.

In order to reduce the effect of misadjustment, a slower adaptation is required. Different kinds of error may arise in a time-sequence adaptive filter. One source of error is due to the jitter and may be influenced by ζ_j. The error may be overcome if ζ_j can be chosen perfectly in order that the time sequence adaptive filter can converge in an optimal manner and is performed slowly.

A simple example using a computer simulated recurring signal can illustrate the method of selecting the weight vector. It is important, for TSAF to perform correctly, to choose the timing signal (sequence number) ζ_j correctly, otherwise an error signal will arise and distortion occur.

If each cycle of the ECG has the same period, then it is easier to define one general weight vector for all the experiments conducted. This signal is chosen before TSAF is applied and the way in which it is chosen is as follows;

(i) select a suitable length of record,

(ii) apply two cursors, a fixed and a variable one,

(iii) select an appropriate point of measure within the record (e.g. beginning of Q point),

(iv) move the second cursor to the right until the end of S point,

(v) Register the amount of bins, (1 bin = 1 msec)

(vi) move the first cursor into the position of the second cursor, and start to move the second cursor for the next segment, and

(vii) repeat until the end of the record.

Figure 5.2 shows the application of TSAF applied to recover a signal . This figure also shows the placement of the weight vector.

Figure 5.2(a) shows the signal S to be recovered.

Figure 5.2(b) shows the white Gaussian noise added to the signal and used as the filter input X_j.

Figure 5.2(c) shows the switching of the filter on and off during the recurring pulses of X_j by choice of the weight vector.

Figure 5.2(d) shows the result of time-sequence adaptive filter to recover signals of figure 5.2(a).

The effect of adding more noise is illustrated in figure 5.3(b), and in applying time-sequence adaptive filtering, the results shown in figure 5.3(d) were obtained.

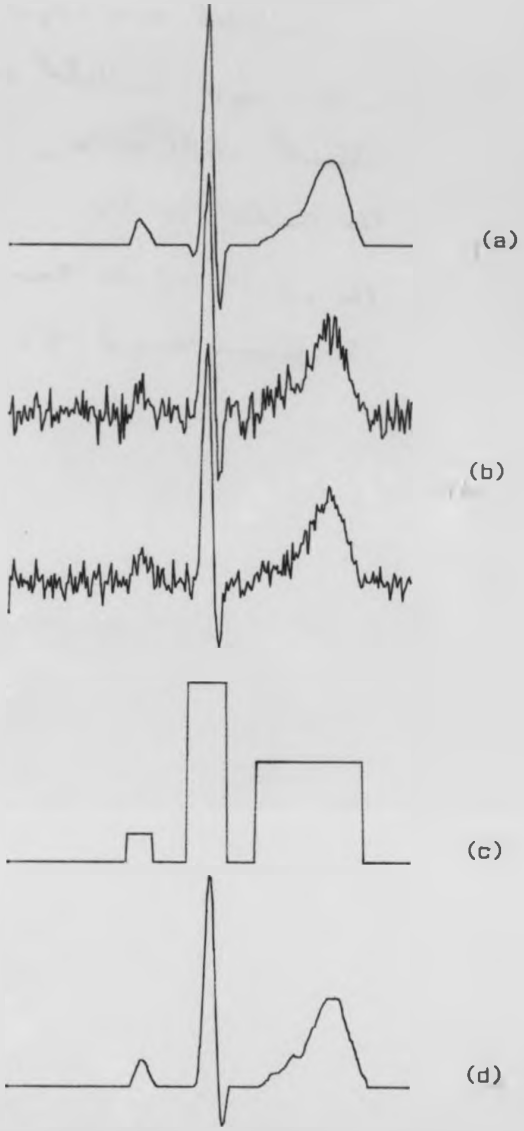

Figure 5.2 Result of applying time-sequence adaptive filter to a noisy input, the figure shows:

(a) the simulated ECG signal only S
(b) the two input simulated ECG added to a different white noise
(c) the control vector
(d) the result of the time-sequence adaptive filter to recover signal S.

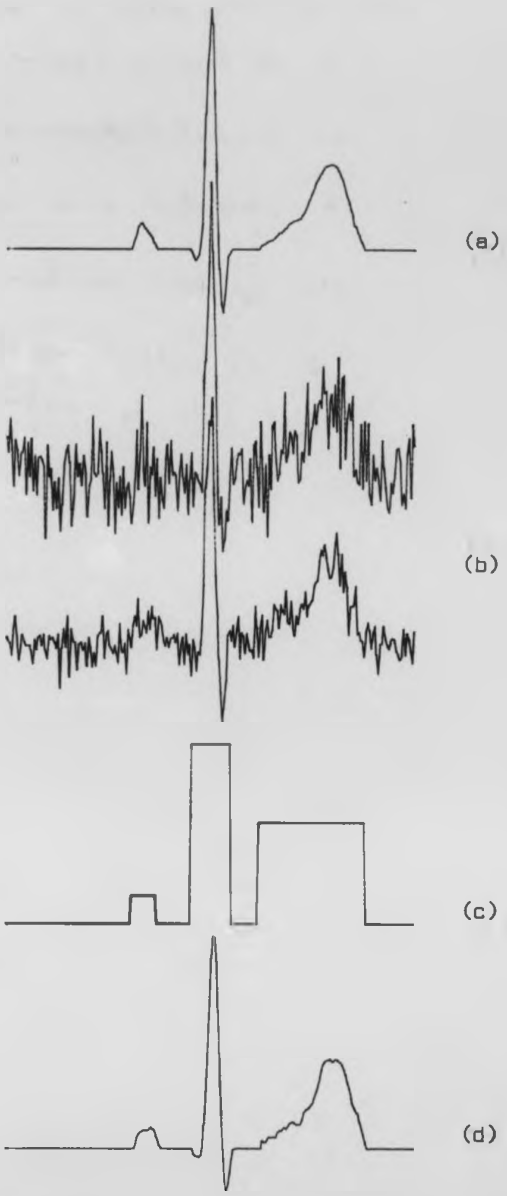

Figure 5.3 Result of applying time-sequence adaptive filter when the noise added is twice as large as in Figure 5.2, the figure shows:

(a) simulated ECG only
(b) simulated ECG added to a white noise
(c) control vector
(d) the output vector of time-sequence adaptive filter to estimate the signal at figure 5.3a simulated

5.3 Summary and conclusion of TSAF

The time-sequence adaptive filter described in the previous section is another form of adaptive filter (AP) suited for non-stationary data having a recurring statistical character. This sort of filter requires no prior knowledge of the signal except the time of occurrence of the statistically stationary segments in order to set the weight vector for the appropriate filter operation.

The time-sequence adaptive filter (TSAF) may seem to require longer computing time compared to that of the conventional LMS filtering, but in actual fact it is essentially the same. However, the memory requirements are quite different. The amount of input data needed for the TSAF to converge to time-varying solution is greater than that of the LMS adaptive filter to converge to time-invariant solution. Therefore, more memory is required for the TSAF.

One of the disadvantages of the TSAF is that it does not offer better approximation in the case of fast adaptation to a transient signal compared to an LMS adaptive filter, if more than two error surfaces are involved. This problem may be alleviated to some extent by the use of only two error surfaces, one to accommodate noise and one to accommodate a recognised signal segment. This may be referred to as the minimal time-sequence adaptive filter (MTSAF).

5.4 Minimal time-sequence adaptive filter (MSAF)

The minimal time-sequence adaptive filter is based upon similar theoretical considerations to those of the other adaptive filters considered and the use of the LMS algorithm, but differs slightly in the way the weight vector (W_i) is derived. As a result, the MSAF provides a better performance than AF or multi-error surface TSAF, under transient conditions.

It will be shown in this section, that in terms of non-stationarity and transient signal considerations,the minimal time-sequence adaptive filter is more appropriate for the ECG applications examined in this study than the other versions of adaptive filter identified. The results using real data have supported the view that the minimal time-sequence adaptive filter can offer better recovery of the signal than the other filters. The results of the application to electrocardiography are presented in Chapter 8.

5.4.1 The concept of minimal time-sequence adaptive filter

The objective of this part of the study was to obtain some experimental evidence regarding the use of the minimal time-sequence adaptive filter for the enhancement of the ECG signal and, having established the non-stationarity and transient characteristics of the input signal, to use such techniques in order to achieve an optimal estimation of the signal. The structure of the minimal time-sequence adaptive filter (MTSAF) is based upon a similar configuration to that of the TSAF described at the beginning of this chapter. It differs in the sense that it uses only two sets of weights, one for the non-stationary segments of the signal and the other for the stationary noise segments.

The use of the control signal is essential for the weight set to converge to the optimal solution for each segment. To illustrate this, a block diagram (figure 5.4) shows how an ECG signal can be classified into two main segments. One represents the noise which mainly occupies the so-called isoelectric intervals, which are considered to be stationary and the other is the signal expressed in the QRS complex as non-stationary (Santopietro, 1974).

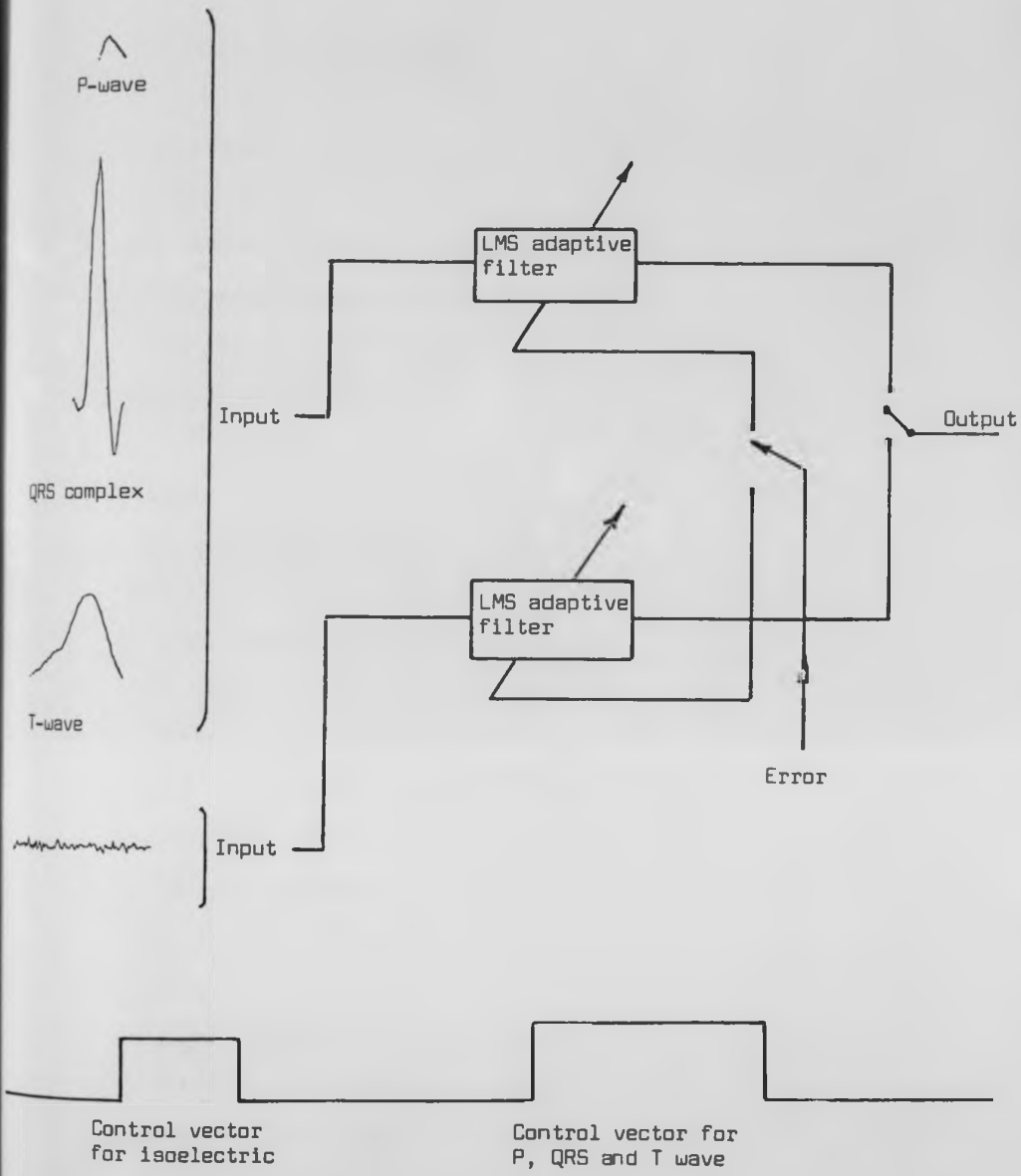

Figure 5.4 (a) Shows how the minimal time-sequence adaptive filter is applied to the ECG signal

(b) Shows the control vector for minimal time-sequence adaptive filter.

5.4.2 Filter performance

In the adaptive filter only one set of coefficients was used throughout adaptive filtering. In the MTSAF only two set of coefficients were used. During the isoelectric intervals, the noise statistics are stationary and the first set of weights adapts accordingly, whilst the other set remains unchanged until a signal segment is detected.

Although this technique is simple to implement, it also uses a fewer number of weights compared to the multi-vector TSAF, as shown diagramatically in figure 5.3. The mean square error (MSE) was computed for both stationary and non-stationary signals forming the filter output. This procedure was repeated for different coherence values ranging from 0.2 - 1.0 in a 0.2 step, i.e. 0.2, 0.4, 0.6, 0.8 and 1.0. In addition, results were obtained by using three different levels of SNR, approximately 4, 9 and 16dB. Each filter was also applied using two values of μ, equal to 0.1 and 0.001, to permit the effect of adaptation speed to be examined.

Figures 5.5 and 5.7 show typical filter outputs for selected cases. The first is the primary input, followed by two groups of 3 records corresponding to AF, TSAF and MTSAF outputs used with two other convergence factors, μ at 0.1 and 0.001 (i.e. low and high adaptation speeds).

The TSAF performs in the same manner as the MTSAF, but is not as

Figure 5.5 Comparison of three adaptive filters (AF, TSAF and MTSAF) using low SNR (SNR = 3.58dB), the figure shows:

(a) the two input signals and noise
(b) the result of adaptive filter
(c) the result of time-sequence adaptive filter
(d) the result of minimal time-sequence adaptive filter
the convergence factor is 0.1.

Figure 5.6 Comparison of three adaptive filters (AF, TSAF and MTSAF) using low SNR (SNR = 9dB), the figure shows:

(a) the two input signal and noise
(b) the result of adaptive filter
(c) the result of time-sequence adaptive filter
(d) the result of minimal time-sequence adaptive filter
the convergence factor is 0.001.

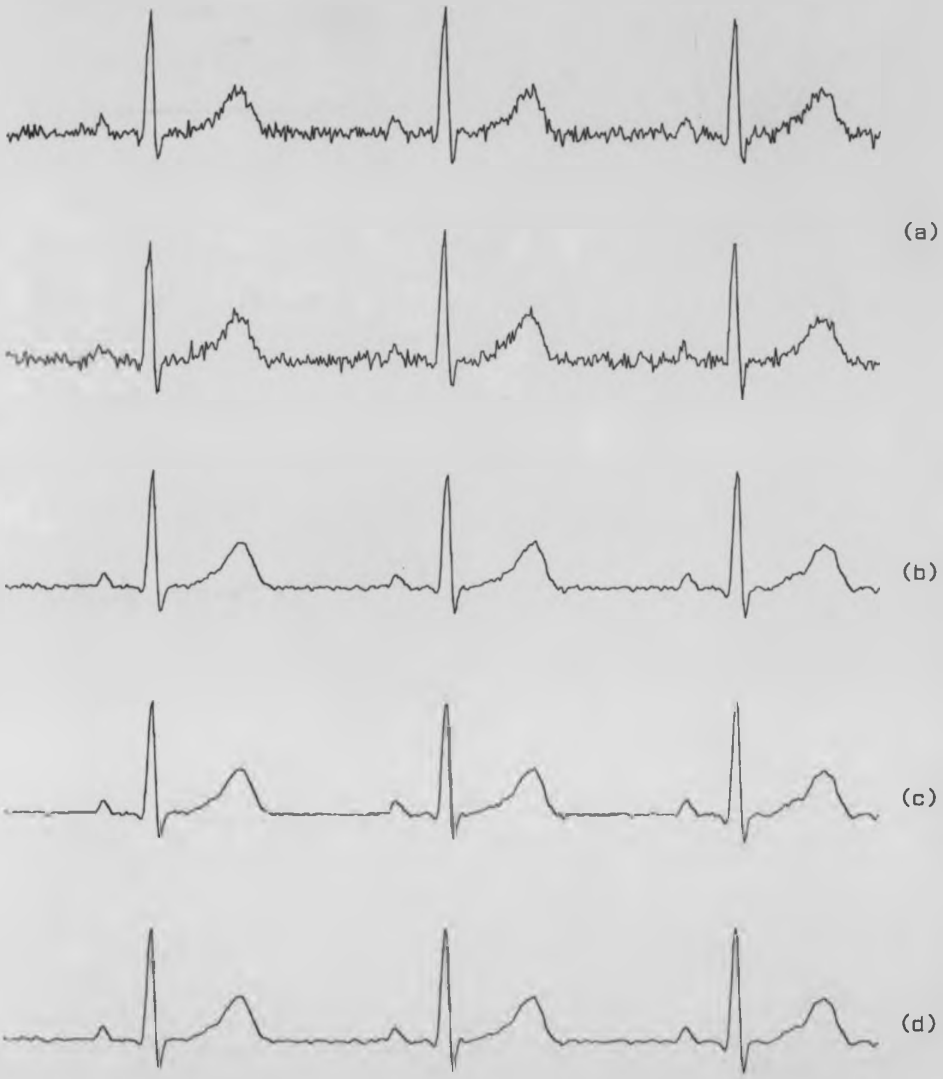

Figure 5.7 Comparison of three adaptive filters (AF, TSAF and MTSAF) using low SNR (SNR = 14.4dB), the figure shows:

(a) the two input signal and noise
(b) the result of adaptive filter
(c) the result of time-sequence adaptive filter
(d) the result of minimal time-sequence adaptive filter
the convergence factor is 0.01.

effective in removing noise in the non-stationary segments. The results in figures 5.5 and 5.6 suggest that the repetitive transient signal corrupted by stationary noise can be filtered better by using the minimal time-sequence adaptive filter than by either the basic AF or TSAF, especially when the signal energy is high.

5.5 Summary

The MTSAF is based upon a similar principle to that of the multi-vector TSAF, but uses only two sets of weights. It also uses a synchronous control signal in order to control the adaptation of each set of weights.

The results presented have shown that the MTSAF is more appropriate than the basic AF or multi-vector TSAF for a non-stationary and transient data, especially when signal amplitude is high.

An experimental investigation was performed for the MTSAF using computer-simulated data to represent the ECG signal. The experiment was conducted under a wide range of conditions including low and high correlation between the noise records, three levels of SNR and two adaptation rates. The results of the experimental study confirmed that MTSAF yielded superior cancellation in almost all cases and with less distortion compared to other unmodified filters. The results improve with higher coherence and SNR.

Although signal distortion may occur in this technique, it is less, under the conditions examined, than that introduced by the basic AF. Further comparison of results on signal distortion is presented in Chapter 8.

Chapter Six: Applications of adaptive filters in Electrocardiography

6.1 Introduction

In order to establish confidence and gain experience in the use of adaptive filters of the form described in Chapters 4 and 5 for applications in electrocardiography, various reported uses were re-examined. New applications directed at the extraction of signals from skeletal muscle noise and the identification of cyclo-stochastic perturbations have been identified and investigated.

Adaptive filtering was chosen for the following reasons:

(i) to overcome the limitations imposed by conventional fixed value filters when the signal exhibits non-stationarity,

(ii) to yield more effective results without a priori information concerning the nature of the signal or noise, and

(iii) to accommodate situations in which the spectral occupancy of the signal overlaps with that of the noise.

Applications of adaptive filters in electrocardiography have, to date, included cancellation of AC interference (Clark, 1976), cancellation of electro-surgical interference (Yeldman et al., 1983), separation of donor and recipient electrocardiograms obtained from heart transplant patients (Widrow, 1976) and enhancement of foetal electrocardiograms by cancellation of the maternal ECG (Widrow et al., 1975).

The principles applied in these applications were examined and the technique extended to the use of adaptive filters to detect events arising from the specialised conduction system of the heart, previously achieved using signal averaging (Berbari et al, 1973; Ellis, 1976; Hoopen & Reuver, 1972; Oldenburg & Macklin, 1977; Rhyne, 1969). Consideration was also directed at the use of adaptive filters for detecting cyclo-stochastic perturbations in surface electrocardiograms. (Simulated signals were used to determine the effectiveness of the technique for both these applications.)

A comprehensive study was also undertaken to determine the effectiveness of adaptive filtering for the removal of skeletal muscle activity from exercise electrocardiograms. This study is reported in full in the following chapter. The results of the pilot studies and simulations presented in this chapter provided the basis for proceeding with the exercise ECG investigation.

6.2 Applications of basic adaptive filters in Electrocardiography

6.2.1 Adaptive cancellation of AC interference

A problem often encountered in the recording of electrocardiograms (ECG's) from the surface of the body is the presence of unwanted 50Hz interference. An adaptive noise canceller which has been described in detail in Chapter 4 is one of the techniques which has been used in this study to overcome (or remove) this noise. In this application the primary input to the adaptive noise canceller is taken from the ECG amplifier, and reference input (safely derived) from a suitable 50Hz source.

Being a single frequency noise component, only two weights are required to cancel AC interference, one operating on the zero phase shifted version of the reference and one operating on a 90 degree phase shifted version of the reference, as illustrated in figure 6.1. The two weighted versions of the reference are summed to form the filters output, which is subtracted from the primary input containing the ECG signal and an AC interference.

Choosing combinations of the values of the weights allows the reference waveform to be changed in magnitude and phase in such a way that it cancels the AC interference in the primary channel. A sampling rate of 1KHz was used in the study undertaken. Effective cancellation can be achieved within one to two cycles of the electrocardiogram. Figure 6.2 shows a result of AC interference cancellation with low signal distortion.

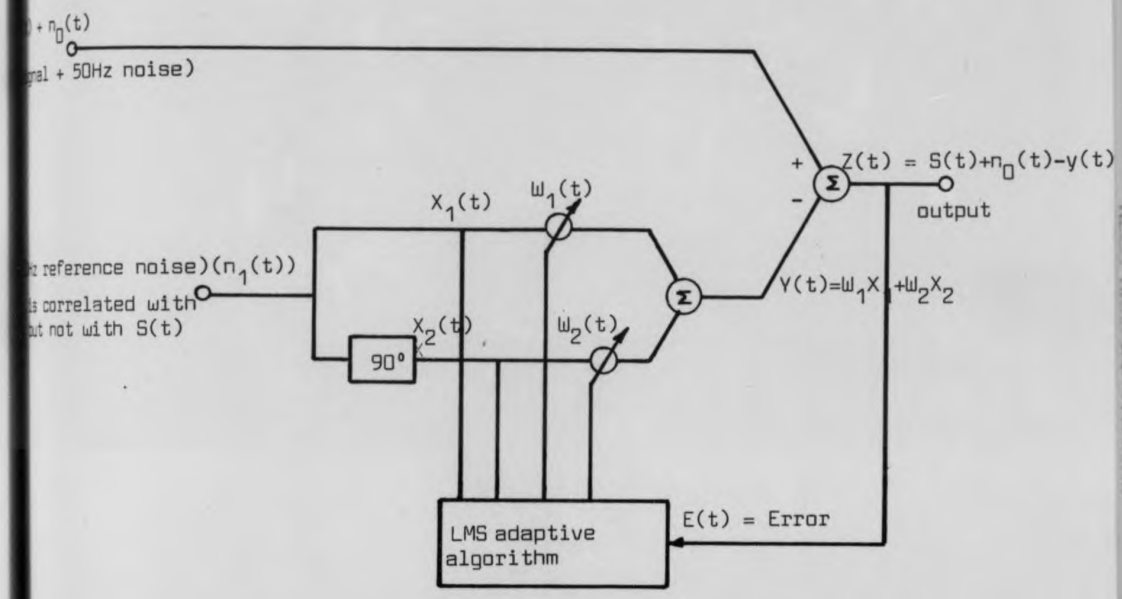

Figure 6.1 A block diagram of two weight adaptive filter in removing 50Hz interference.
(Adapted from Widrow, 1975, fig. 6)

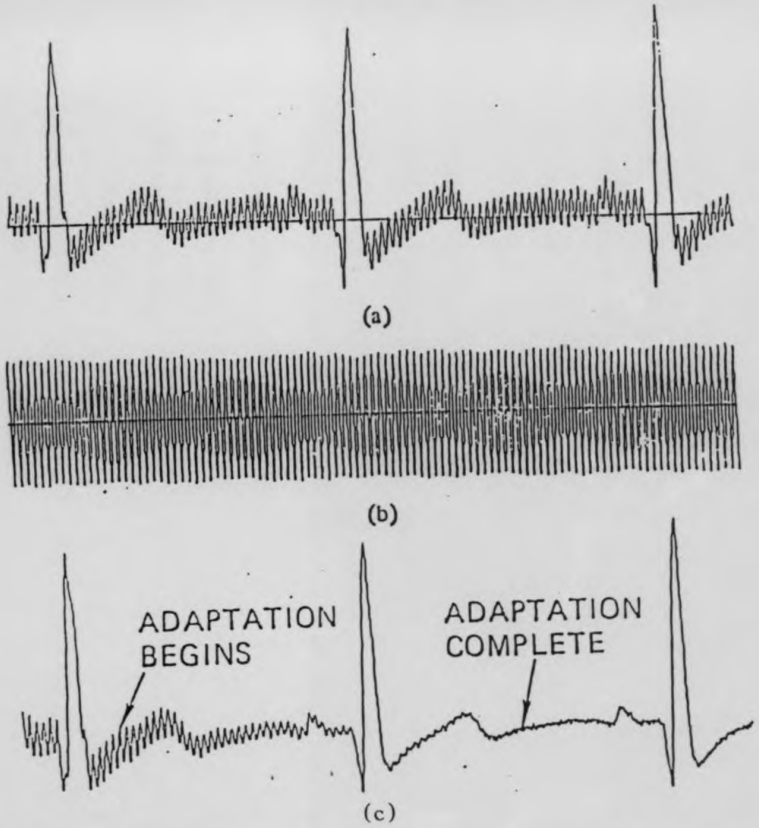

Figure 6.2 Application of adaptive noise canceller in removing 50Hz interference, in which

(a) is the ECG signal contaminated by 50Hz
(b) the reference channel of 50Hz only
(c) the output of adaptive noise canceller. (Adapted from Widrow 1975, fig.11, page 1702)

6.2.2 Signal extraction from skeletal muscle noise by adaptive filtering

Skeletal muscle activity is a source of noise that can present problems, especially in exercise electrocardiograms and wide-band ECG's. As a precursor to the full study of adaptive filtering for exercise ECG enhancement, this section will only deal with the basic technique of adaptive channel enhancement to extract the ECG signal from the skeletal muscle noise. The requirement for this technique is two correlated signals, but uncorrelated noise components.

An investigation was undertaken to identify two channels in which the ECG signals were correlated and the muscle noise uncorrelated. It was found that a 100mm electrode distance was quite appropriate for this application. Two channels were recorded, the primary input was taken from a conventional lead I, and a bipolar lead in the frontal plane at the level of the 10th rib, as a reference input. The skeletal muscle activity in these leads was found to be sufficiently uncorrelated to allow the application of the adaptive process and an estimate of the signal-to-noise ratio improvement in lead I to be obtained.

The experiments were carried out for five subjects with a record length of 2048 bin values, and a sampling rate of 1KHz. It was found that the most effective improvement in signal-to-noise ratio was achieved with a convergence factor, μ, of 0.001 and 64 weights. Unfortunately this was not without some signal distortion. A full investigation of the signal distortion is presented in Chapter 8.

After selecting the appropriate lead position as described in section 2.6, the adaptive channel enhancement was first tested using simulated data in which the primary input was composed of a simulated ECG added to simulated white noise. The reference input consisted of the same simulated ECG added to a different amount of white noise.

The amount of noise added into both channels was sufficient to yield a very poor signal-to-noise ratio. The reason for this was to examine how the channel enhanement technique would behave under conditions of low signal-to-noise ratio. Figure 6.3(a) shows the computer simulated signal, while figure 6.3(b) shows the simulated white noise components. Figure 6.3(c) shows the two inputs to the channel enhancer, the primary and the reference inputs. Figure 6.3(d) shows the filter output of the channel enhancer. From the result indicated in figure 6.3(d), it is seen that there is a large improvement in signal-to-noise ratio.

The effect of adding more noise to the simulated signal is shown in figures 6.4(c) and 6.5(c).

Table 6.1 summarises the improvement in SNR expressed in dB's with respect to the amount of noise added to the input signals.

Table 6.1

Input signal-to-noise ratio (dB)	Improved S/N ratio (dB)
3.47	3.4
9.3	4.9
15.0	11.8

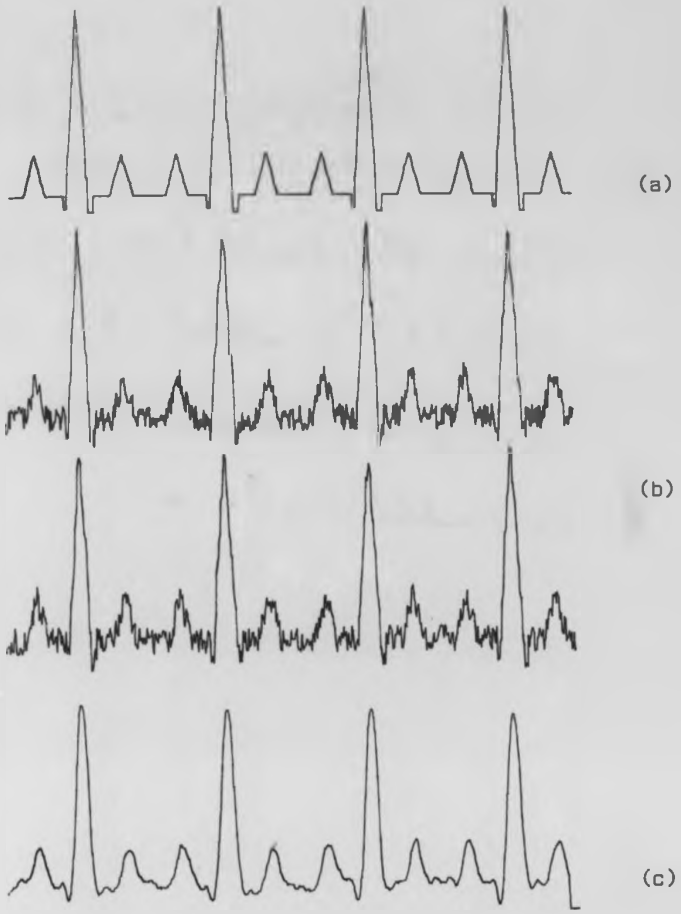

Figure 6.3 Result of applying adaptive filtering technique to simulated data (SNR = 15dB)

(a) shows the simulated ECG signal
(b) the simulated ECG added to white noise
(c) the output of adaptive filter to estimate the simulated signal in (a)

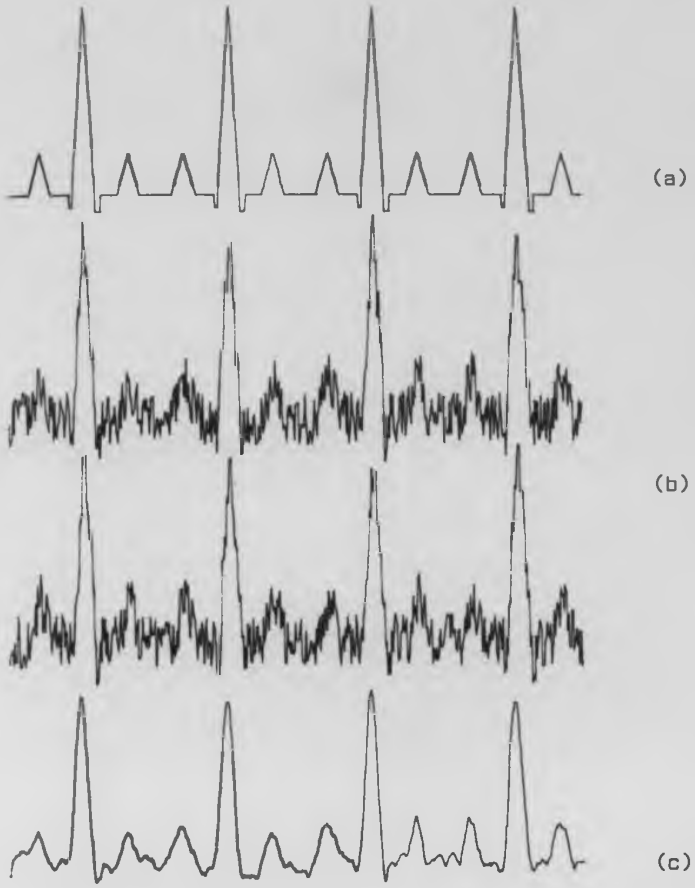

Figure 6.4 Result of applying adaptive filtering technique to simulated data (SNR = 9.3dB)

(a) shows the simulated ECG signal
(b) simulated ECG added to a white noise
(c) the output of adaptive filter to estimate the simulated signal in (a).

Figure 6.5 Result of applying adaptive filtering technique to simulated data (SNR = 3.47dB)

(a) shows the simulated ECG signal
(b) simulated ECG signal added to a white noise
(c) the output of adaptive filter to estimate the simulated signal in (a).

It is seen that the improvement is high with high input signal-to-noise ratio. The experiment was conducted with the input signal in both primary and reference channels of the channel enhancer being identical and well defined. The experiment was also carried out with the weight vector having 64 weights together with the convergence factor of 0.001 to yield the best signal-to-noise improvement.

The adaptive channel enhancer described earlier was also applied to real data. The data was obtained from electrodes placed in the frontal plane on mid-clavicular lines at the level of the 10th rib, and at the level of the first intercostal space, and yielded the primary and reference inputs respectively.

Figure 6.6(a,b) shows the two input channels to the enhancer, while figure 6.6(c) indicates the improved output. As shown in figure 6.4(c) the improvment in signal-to-noise ratio was 6.6dB, but in this case the amount of muscle noise was not severe. The filter was also tested under conditions where the muscle noise was high, so providing a lower input signal-to-noise ratio. The improvement measured at the output was in this case found to be 9.9dB and 10.7dB respectively and the effects are illustrated in figures 6.7 and 6.8 respectively.

It can be concluded that, providing the input channels are not highly contaminated with muscle artefact, the improvement in SNR (>8dB) can be considerable.

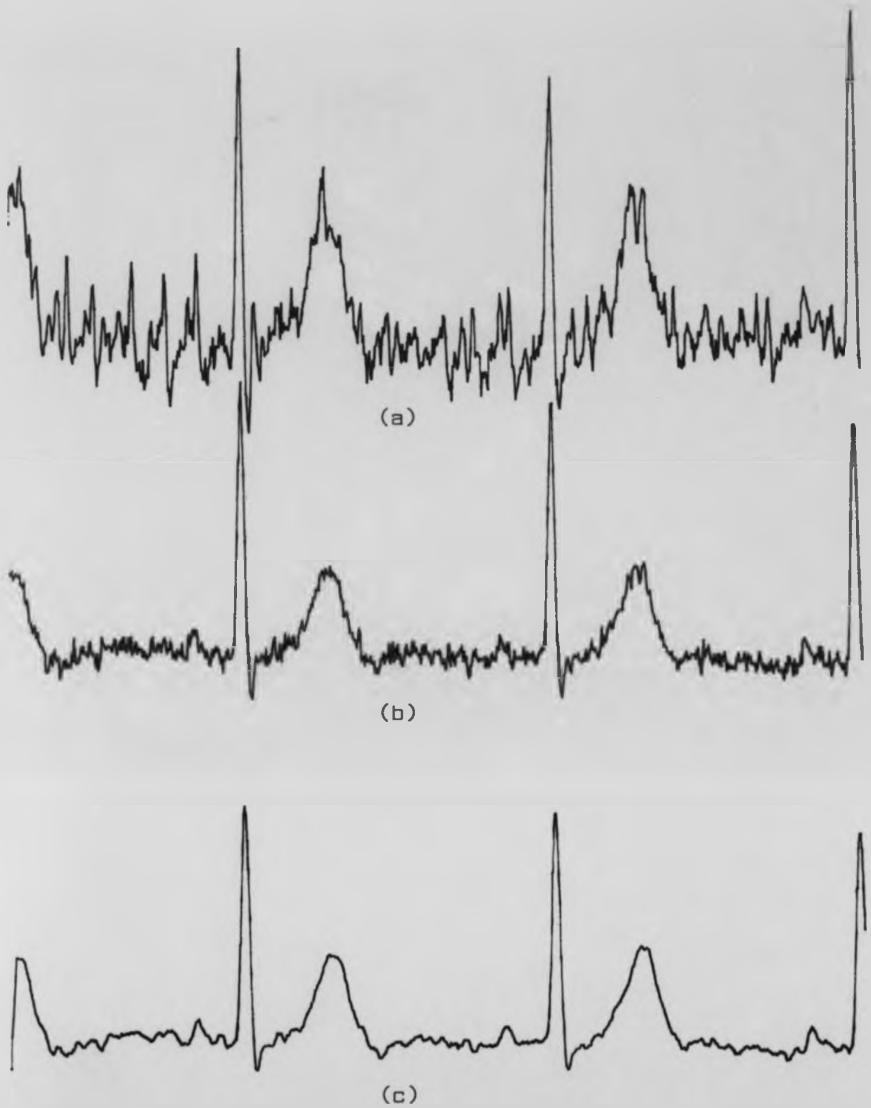

Figure 6.6 Result of multichannel enhancement to reduce skeletal muscle component. the figure shows:

(a) frontal plane lead in which electrodes positioned in mid-clavicular line at level of 10th rib.
(b) frontal plane lead in which electrodes positioned in mid-clavicular line at level of 1st intercostal space.
(c) adaptively enhanced frontal plane lead (b)

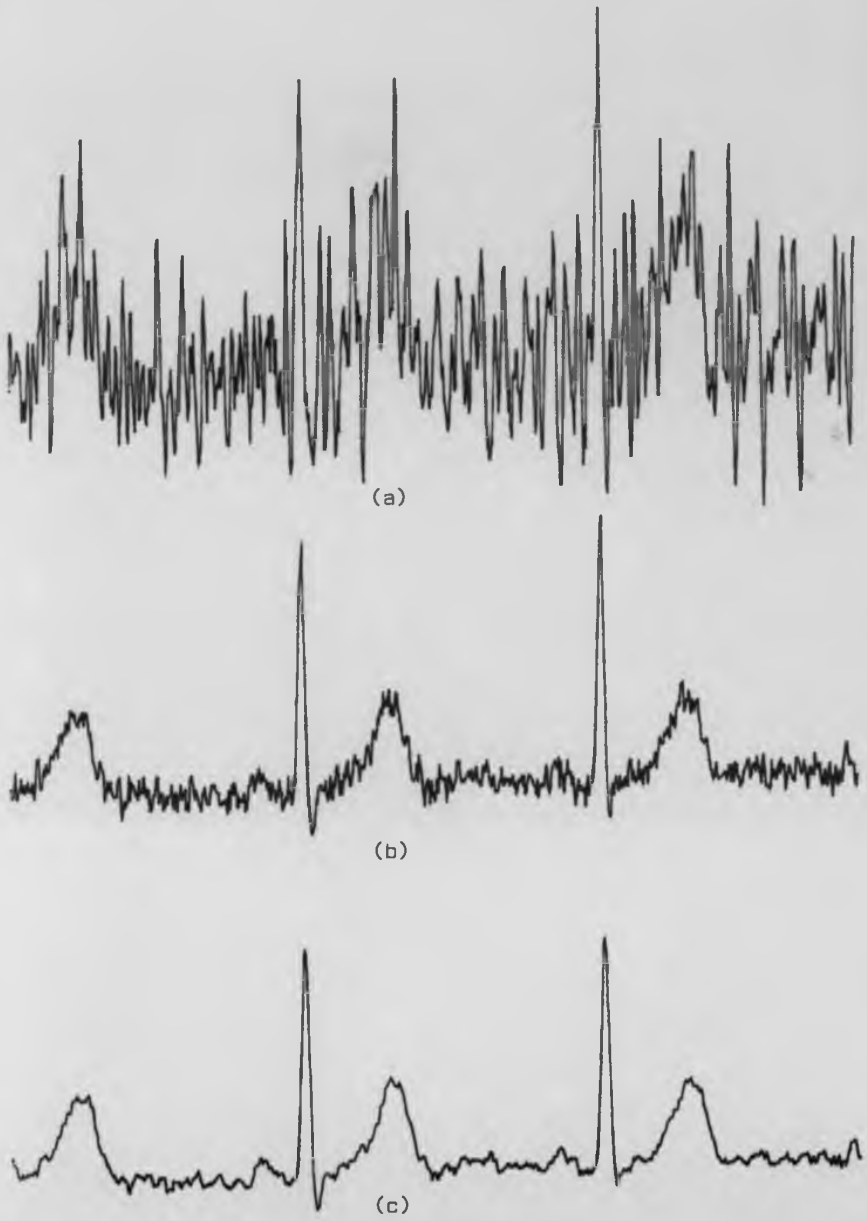

Figure 6.7 Result of multichannel enhancement to reduce skeletal muscle component. the figure shows:

(a) frontal plane lead in which electrodes positioned on mid-clavicular line at level of 10th rib.
(b) frontal plane lead in which electrodes positioned on mid-clavicular line at level of 1st intercostal spece.
(c) adaptively enhanced frontal plane lead (b)

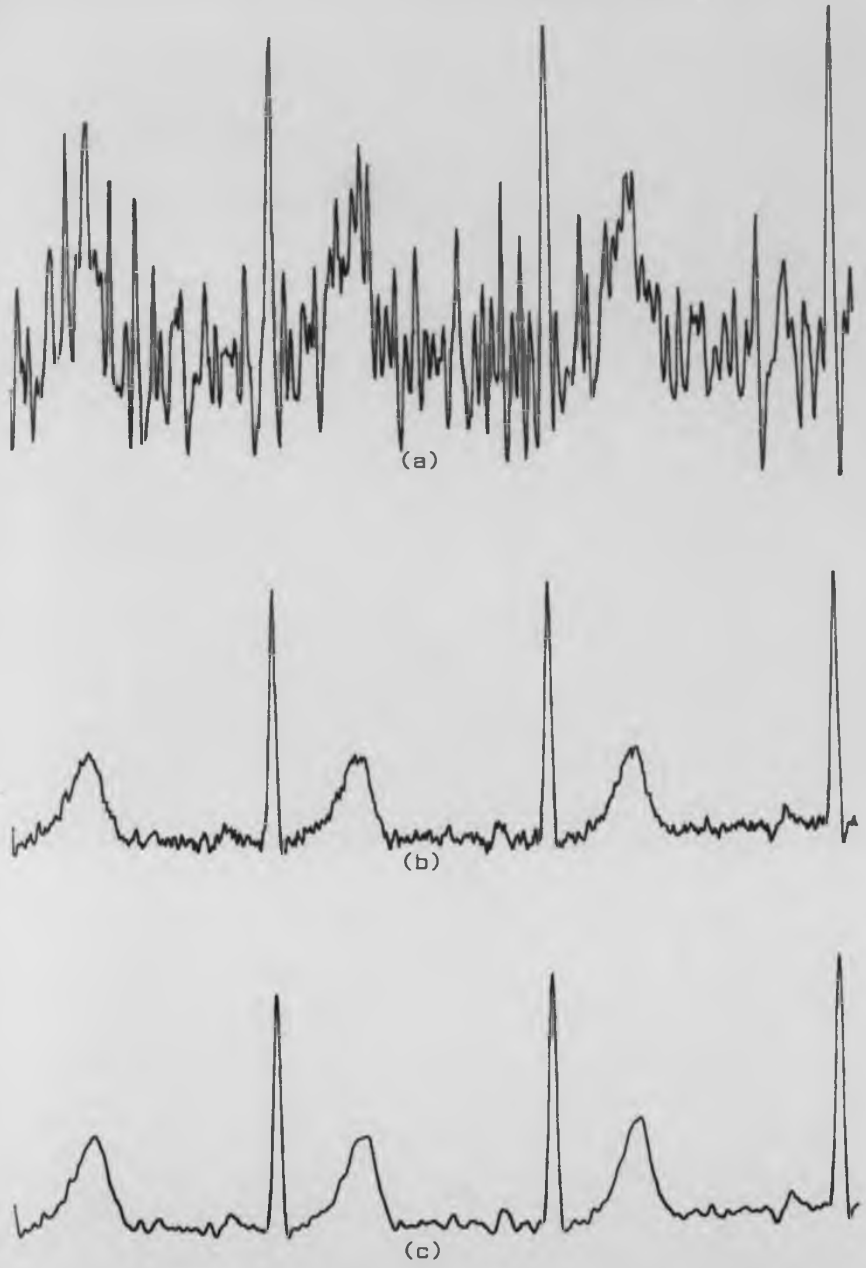

Figure 6.8 Result of multichannel enhancement to reduce skeletal muscle component, the figure shows:

(a) frontal plane lead in which electrodes positioned on mid-clavicular line at level of 10th rib.
(b) frontal plane lead in which electrodes positioned on mid-clavicular line at level of 1st intercostal space.
(c) adaptively enhanced frontal plane lead (b).

6.2.3 Application of adaptive filtering to enhance the foetal electrocardiogram

Widrow (1975) has shown how adaptive filtering may be used to extract the foetal ECG from the mixed foetal and maternal ECG by using an adaptive filter (AF). By taking the primary input to be the lead taken from the abdominal electrodes of the mother and the chest lead to be the reference input containing, in effect, the maternal ECG only, AF may be applied to extract the foetal signal.

It may appear in the first instance that a simple subtraction would be sufficient for enhancement, providing that all records are simultaneous and there are no variations in amplitude or phase component. In reality the situation is more complex as the recording of these two channels will include interference and noise components due to muscle activity or 50Hz interference for example. Two simple simulations to model this situation were examined. Figure 6.9(a) shows a reference input which contains the simulated maternal ECG (chest lead), and figure 6.9(b) shows the primary input which contains the reference input plus the simulated foetal ECG. Figure 6.9(c) shows the result of the noise cancellation in which the foetal signal is clearly enhanced.

A more exacting application in which both channels contain signals heavily contaminated with noise was also examined. Figure 6.10(a) and figure 6.10(b) show the input to the noise canceller, while figure 6.10(c) shows the output of the ANC. Figure 6.10(c) shows that the adaptive filtering is quite limited in cases there the signal to noise ratio is low, as in foetal ECG recordings, for example.

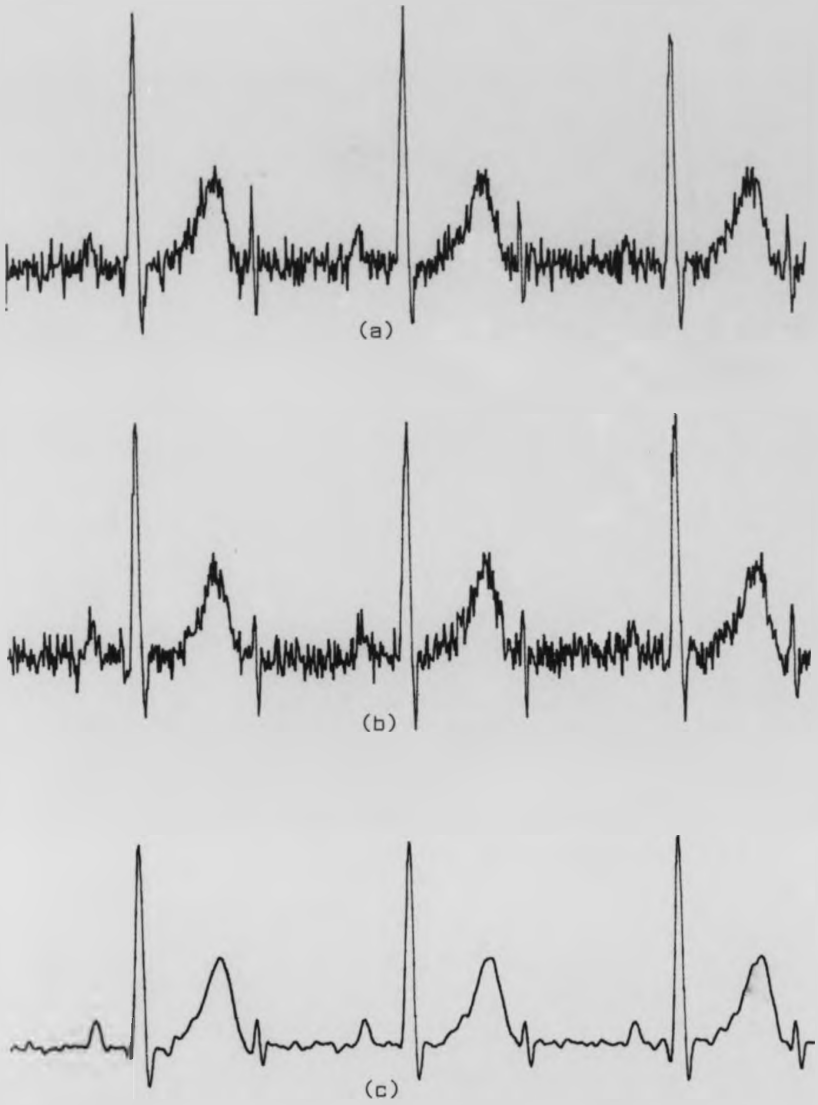

Figure 6.9 Shows the application of the adaptive filter to the foetal ECG (simulated)

(a) Reference input, simulated maternal ECG (chest lead)
(b) Primary input containing reference input plus simulated foetal ECG.
(c) Enhancement of foetal signal by noise cancellation

Input Signal/Noise ratio 7.2d8., signal improvement 11.95d8.

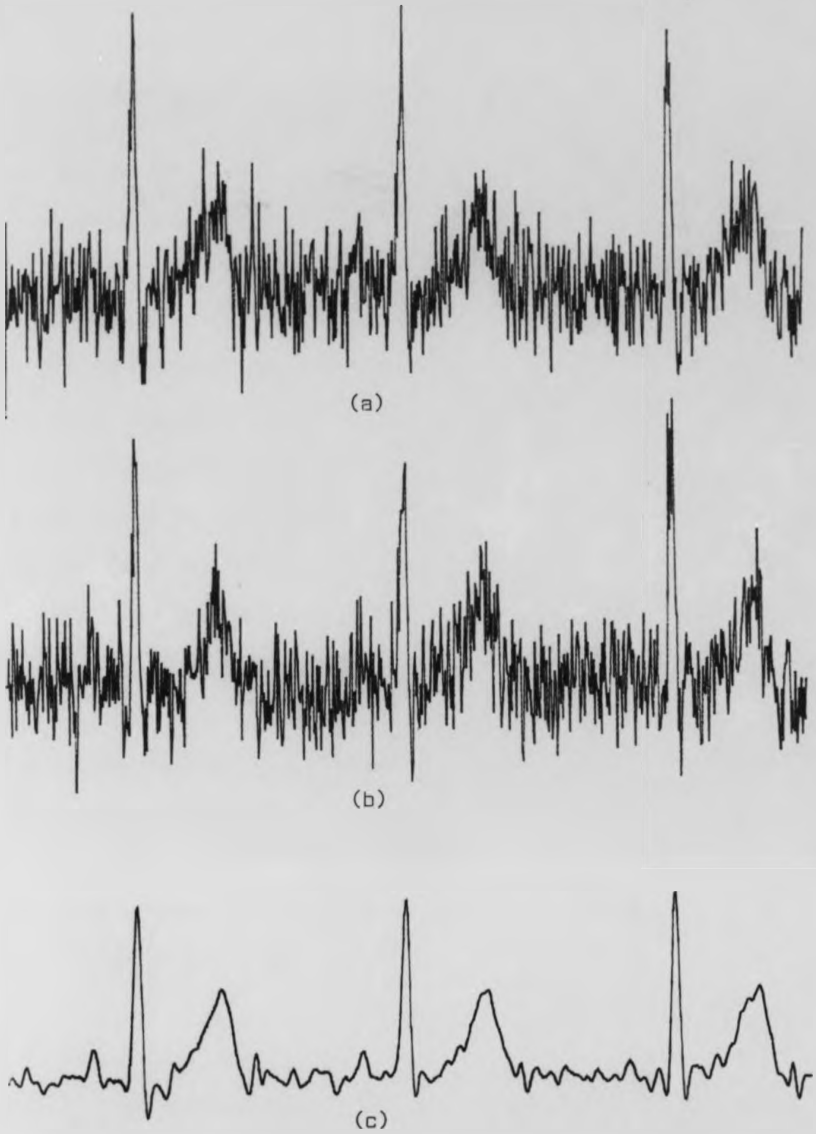

Figure 6.10 Shows the application of the adaptive filter to the foetal ECG (simulated)

(a) and (b) input to noise canceller,
(c) Enhancement of foetal signal by noise cencellation.

Input Signal/Noise ratio 1.8dB., signal improvement 10.7dB.

6.2.4 Application of adaptive filtering in the identification of cyclo-stochastic perturbations

The early detection of ischaemic heart disease and other cardiac disorders can have an important bearing upon the treatment and/or managment of the condition. Various, ECG based, techniques have been proposed and investigated for this purpose (Prasad et al., 1978) and the phase invariant signature algorithm (PISA) (Prasad & Gupta, 1980) is one of them. The basis of the PISA technique involves the consideration of the surface ECG both as a function of time and as a function of phase, (from 0 to 2π).

If $X(\Phi)$ is the surface recorded ECG which contains $S(\Phi)$ the ECG signal generated by a healthy heart, $N(\Phi)$ the background noise which is not correlated with $S(\Phi)$, $P(\Phi)$ the perturbation due to the disorder in the heart which is coherent with $S(\Phi)$, then

$$X(\Phi) = S(\Phi) + N(\Phi) + P(\Phi)$$

The PISA technique involves the detection of $P(\Phi)$ from $X(\Phi)$, assuming that only $S(\Phi)$ is stationary, $P(\Phi)$ is phase-locked to the cardiac cycle and also that $N(\Phi)$ has a random distribution.

To implement this technique, the following procedure is adopted;

(i) Acquisition of a recording of 50 or more cycles of ECG,

(ii) digitisation and conversion from the time domain to the phase domain,

(iii) acquisition of the average, in order to obtain $S(\Phi)$ from $X(\Phi)$,

(iv) subtraction of $S(\Phi)$ from $X(\Phi)$, to obtain $N(\Phi)$ and $P(\Phi)$, and

(v) the power in the random components is then averaged over many heartbeats as a function of phase (Φ).

The power distribution of $N(\Phi)$, which is independent of the phase, is uniformly distributed over the phase (Φ) $0 - 2\pi$, while the power of distribution of the random component of $P(\Phi)$, which is phase-locked to the cardiac cycle, appears as peaks occurring at the particular phase of the cardiac cycle. Small or low PISA signatures are considered indicative of a healthy heart and vice versa (Prasad & Gupta, 1981).

Detection of small random peaks or events within the ECG may be more effectively achieved by use of adaptive filters. The use of adaptive filters may be considered superior to other forms of filtering for ECG perturbation analysis for a number of reasons;

(i) The collection and analysis of real data revealed the virtual impossibility of recording a set of ECG cycles without any variation in the amplitude of the QRS complex, even for a healthy normal person. This variation contributes to $P(\Phi)$.

(ii) Perturbations may be removed by averaging, so precluding the technique as a means of detecting them.

(iii) In using adaptive filtering it was found that less data was necessary to achieve the same results as the PISA method.

Figures 6.11 - 6.15 show a set of recorded ECG cycles which were aligned in order for averaging to be performed. The vaiation in amplitude of the QRS complex is clearly apparent. The result of the

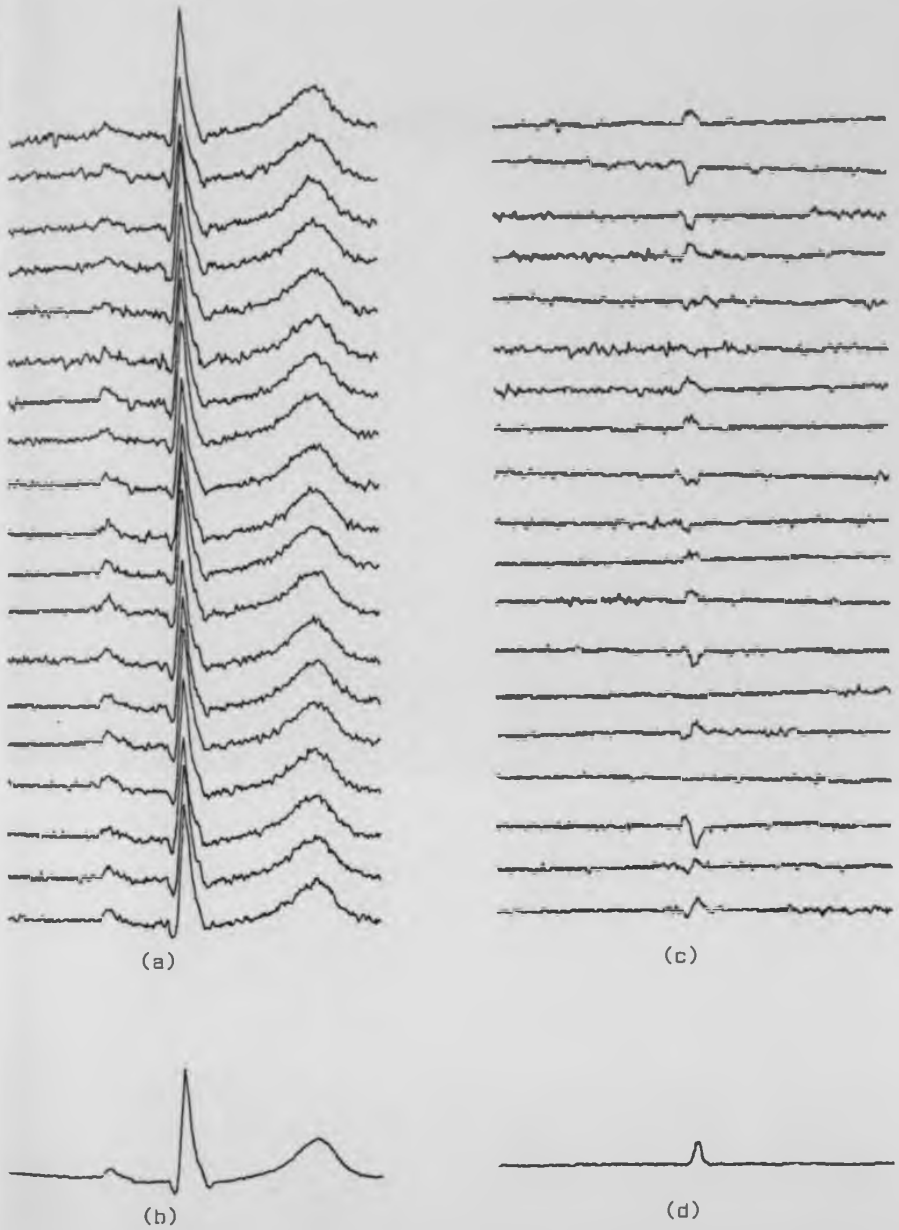

Figure 6.11 The result of applying PISA to raw data of ECG, the figure shows:

(a) the individual ECG
(b) the average of all the ECG's in (a)
(c) the difference between the average and the individual cycle.
(d) the result of PISA.

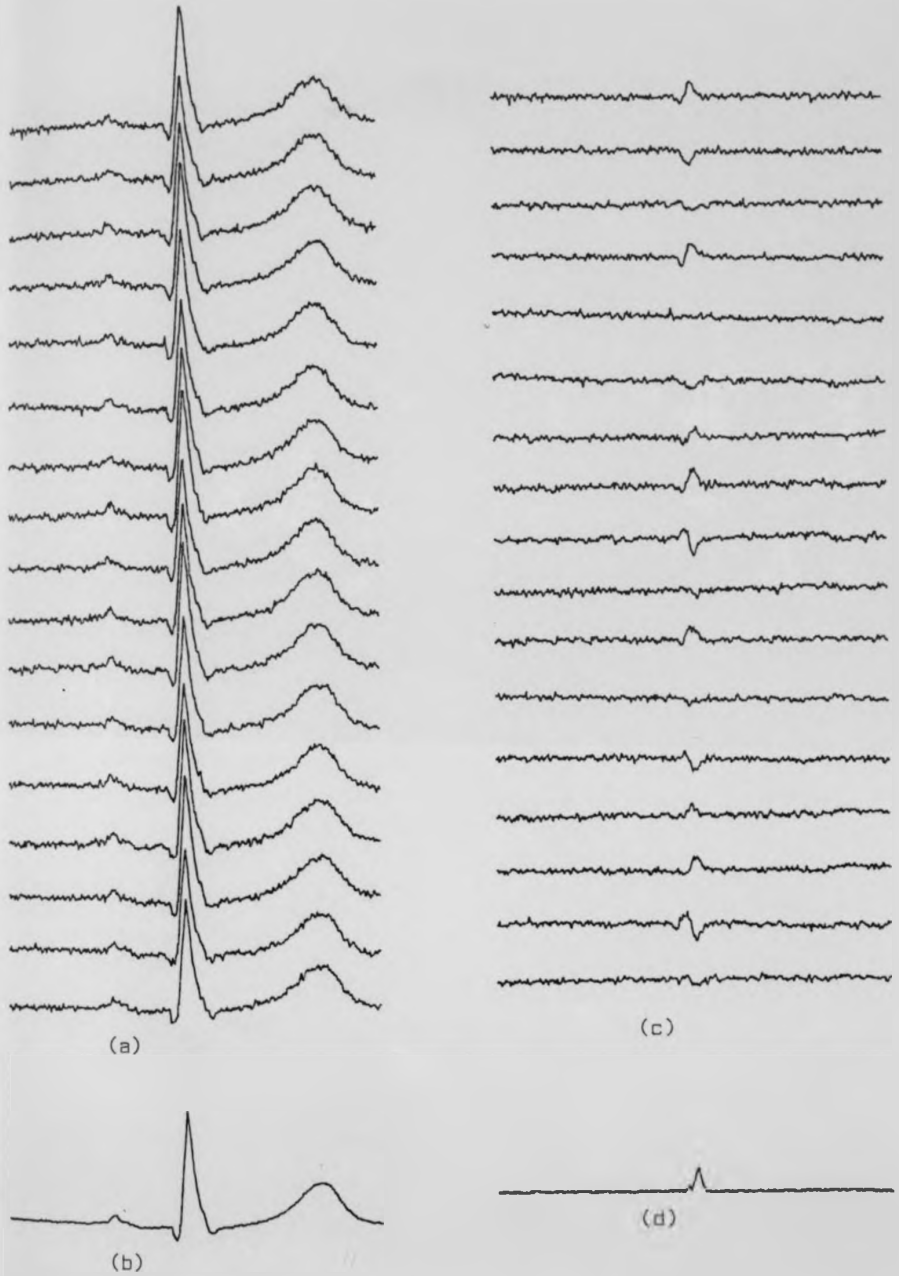

Figure 6.12 The result of applying PISA to raw data of ECG, the figure shows:

(a) the individual ECG
(b) the average of all the ECG's in (a)
(c) the difference between the average and the individual cycle
(d) the result of PISA

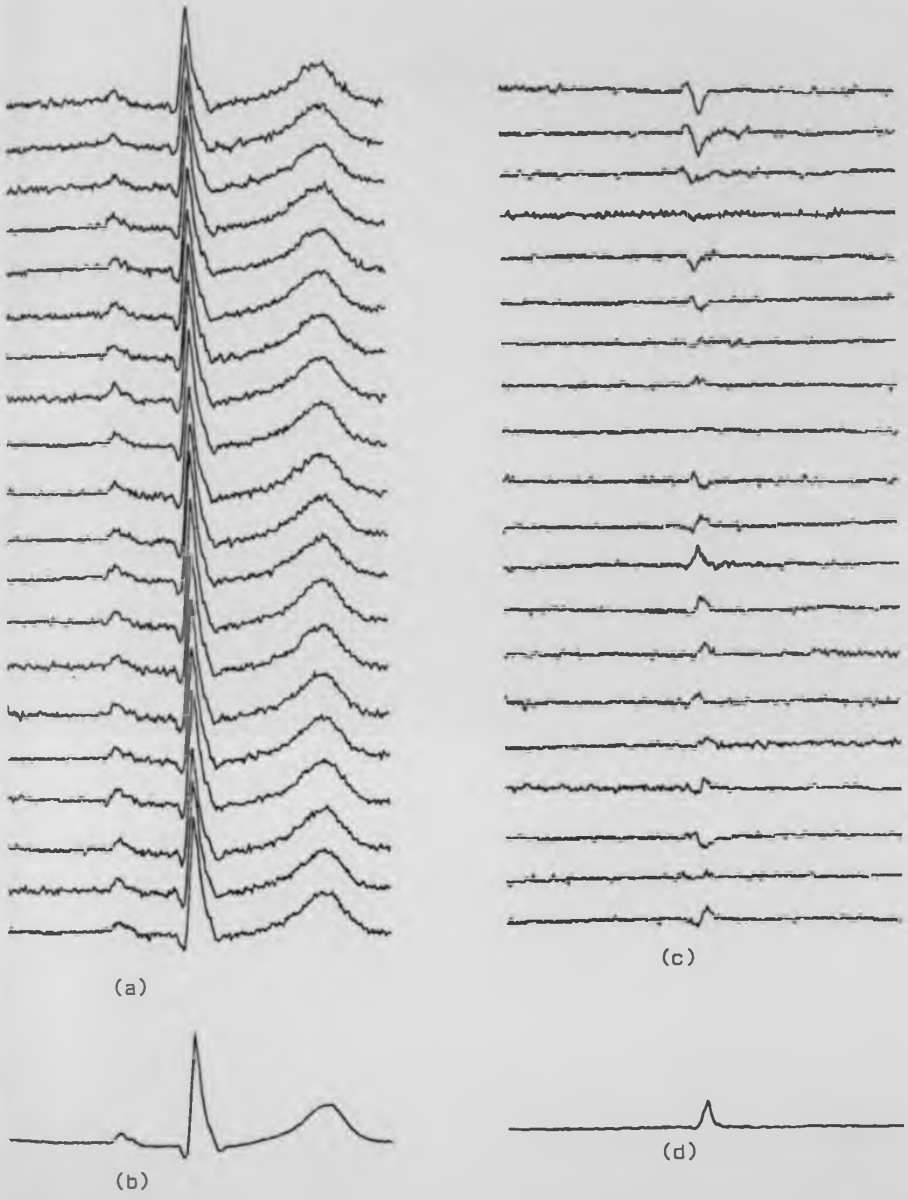

Figure 6.13 The result of applying PISA to raw data of ECG, the figure shows:

(a) the individual ECG
(b) the average of all the ECG's in (a)
(c) the difference between the average and the individual cycle
(d) the result of PISA.

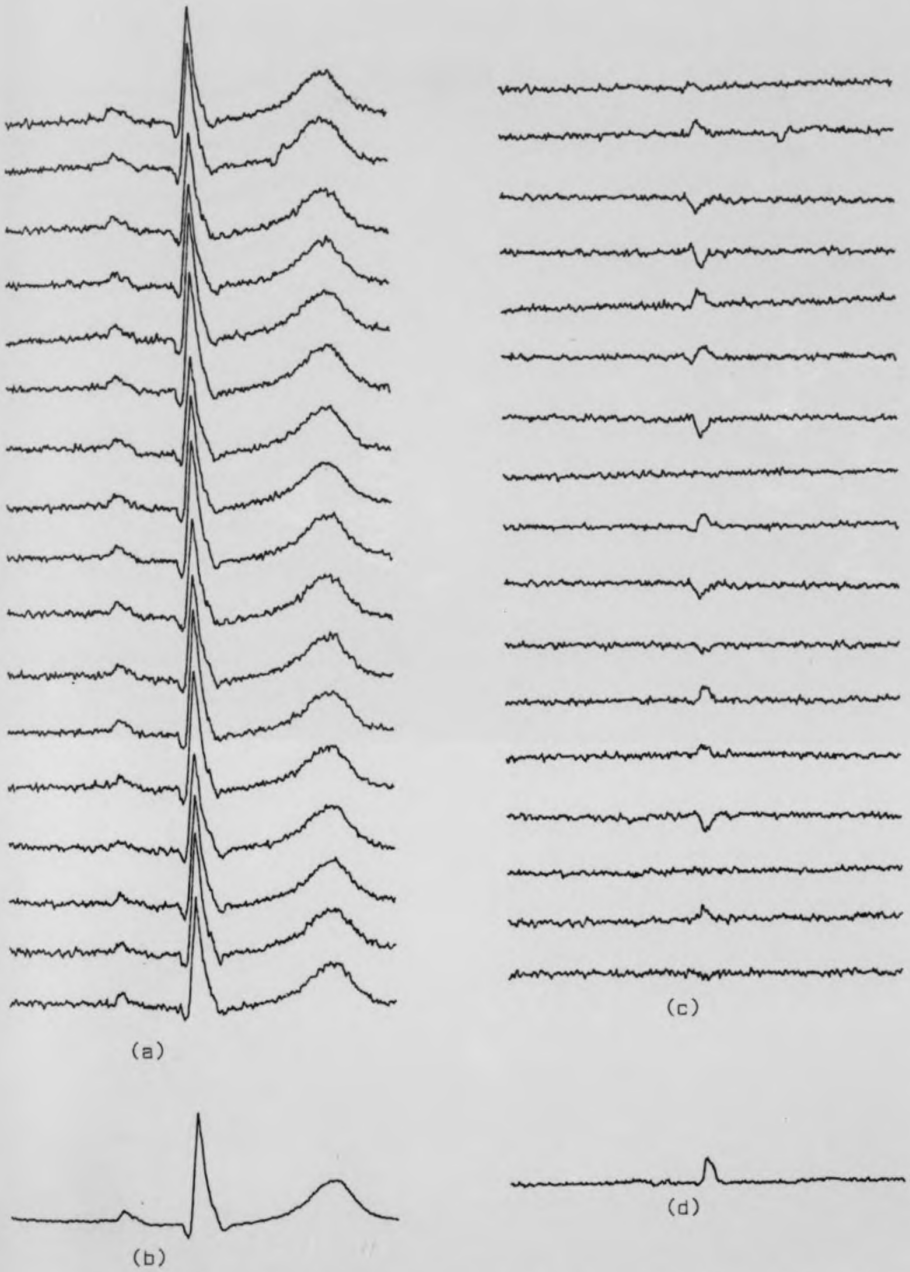

Figure 6.14 The result of applying PISA to raw data of ECG, the figure shows:

(a) the individual ECG
(b) the average of all the ECG's in (a)
(c) the difference between the average and the individual cycle
(d) the result of PISA

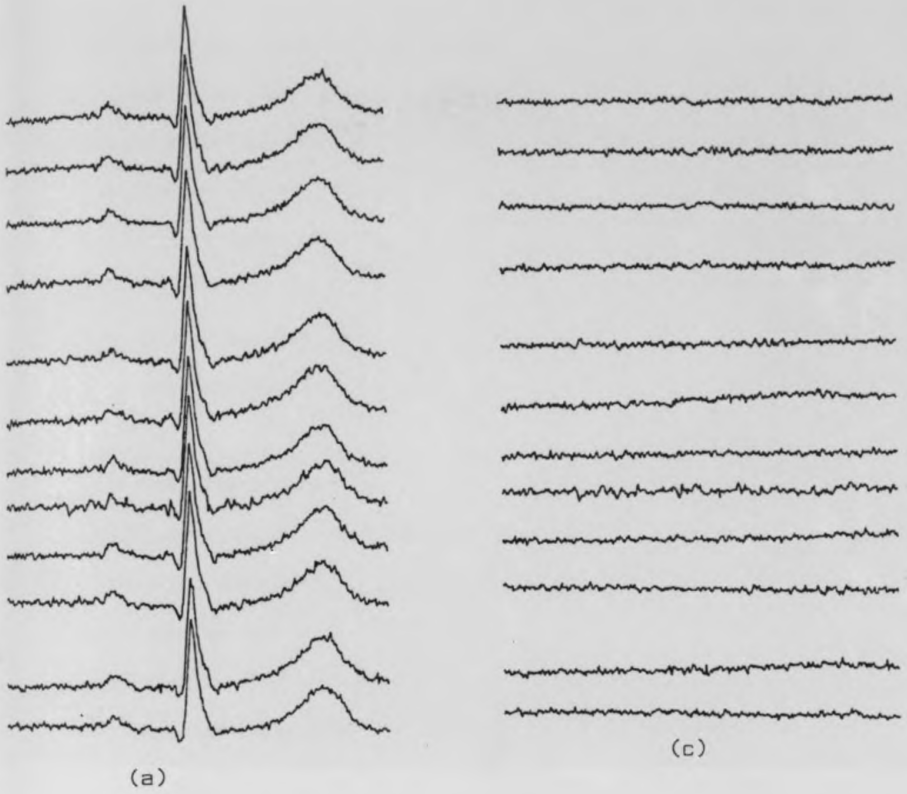

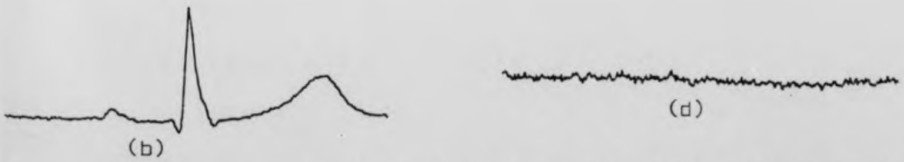

Figure 6.15 The result of applying PISA to raw data of ECG, the figure shows:

(a) the individual ECG
(b) the average of all the ECG's in (a)
(c) the difference between the average and the individual cycle
(d) the result of PISA

PISA technique can be seen in figures 6.11(d) - 6.15(d). The result of the PISA in this case is due to the variation of the QRS complex and may therefore constitute a serious artifact in applying the technique in the clinical situation. It has been difficult to record data from patients in which the PISA technique could be applied, as shown in previous figures (6.11 - 6.15). PISA technique was applied to a normal recorded signal and it is concluded that there will always be an artefact due to QRS variation.

To investigate the usefulness of PISA to detect small events within the QRS complex, 12 individual ECG cycles, selected from figures 6.11 - 6.15 were examined, in which the difference between the average of the 12 cycles with respect to the individual selected cycles was almost zero. This is shown clearly in figure 6.12. Note that there is no artefact appearing since there is no QRS variation.

Taking the same set of selected cycles, simulated low level signals were added to each cycle (figure 6.17a) and the PISA technique was once again applied to the composite signals (figure 6.17b). The results are shown in figures 6.17d and 6.17e. Thus the PISA technique is shown to be effective in revealing the embedded signals.

It is quite apparent from figure 6.17e that the peak which appears within the area of QRS is due to the variation of the simulated signal of figure 6.17a.

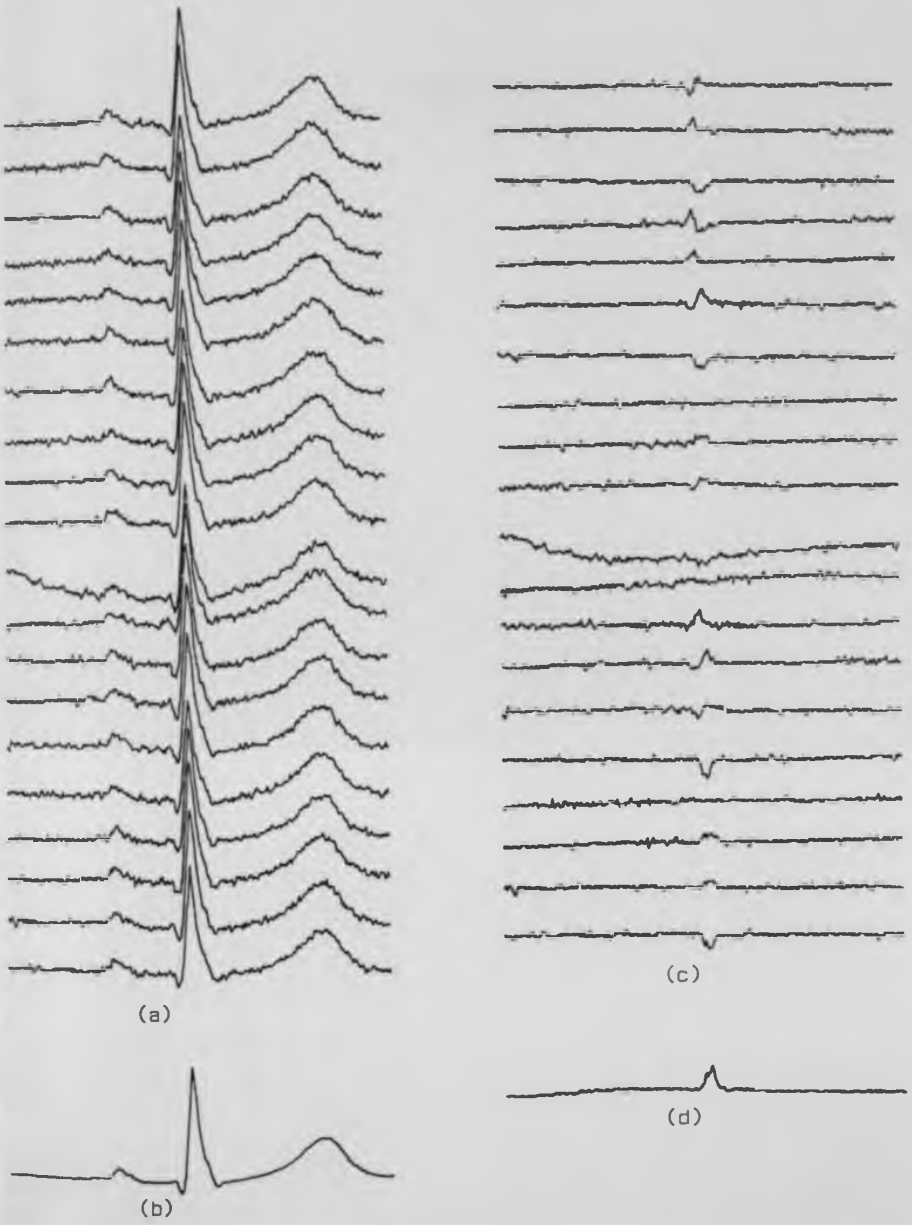

Figure 6.16 The result of applying PISA to raw data of ECG, the figure shows:

(a) the individual ECG
(b) the average of all the ECG's in (a)
(c) the difference between the average and the individual cycle
(d) the result of PISA.

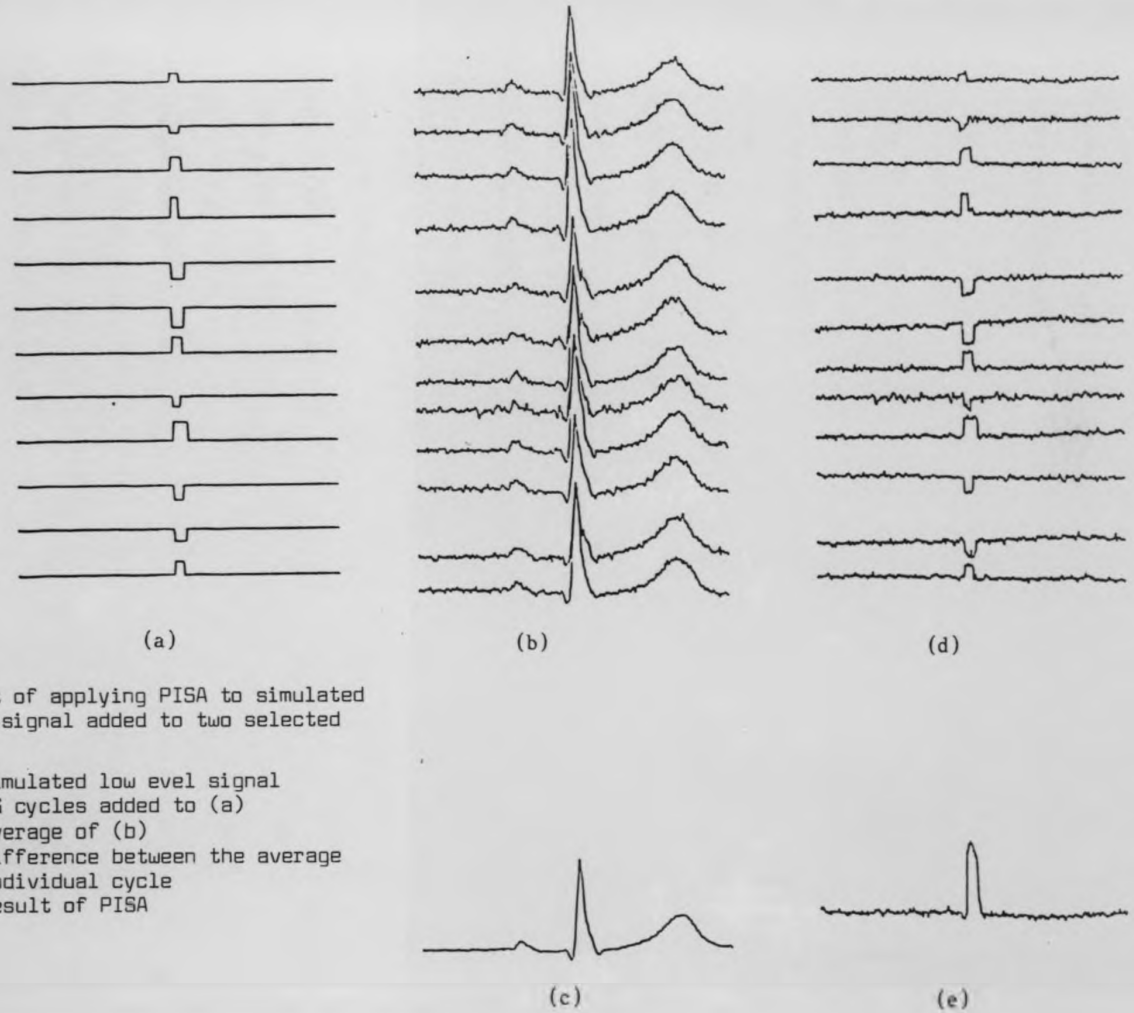

Figure 6.17 The result of applying PISA to simulated low level signal added to two selected data

(a) the simulated low evel signal
(b) 12 ECG cycles added to (a)
(c) the average of (b)
(d) the difference between the average and individual cycle
(e) the result of PISA

6.3 Application of time sequence adaptive filtering to Electrocardiography

The application of time sequence adaptive filtering (TSAF) for noise reduction is introduced in this section. Several experiments were performed using the TSAF. Computer simulations were performed and results compared with the results obtained using basic LMS adaptive filtering.

The TSAF technique was applied using simulated data for two particular ECG signal recovery applications, enhancement of the foetal ECG and detection of cyclo-stochastic perturbations. Using real data, the technique was applied to enhance exercise electrocardiograms by adaptive cancellation of skeletal muscle noise. In this case the two recorded channels contained signal components for which the precise waveforms could differ, but exhibited correlation with each other. The skeletal muscle noise components were uncorrelated with each other and with the signal waveform from channel to channel. Figure 6.18 shows two recorded channels and the result can be seen in figure 6.18c. The best estimation of the signal was obtained by time-sequence adaptive filter (figure 6.19c). The operation of time-sequence adaptive filter was carried out under the control of the selected weight vectors. Figure 6.20 illustrates how the weight vectors relate to the ECG cycle.

The presence of high amplitude signal components (QRS complex), can cause a significant disturbance in the filter weights and hence result

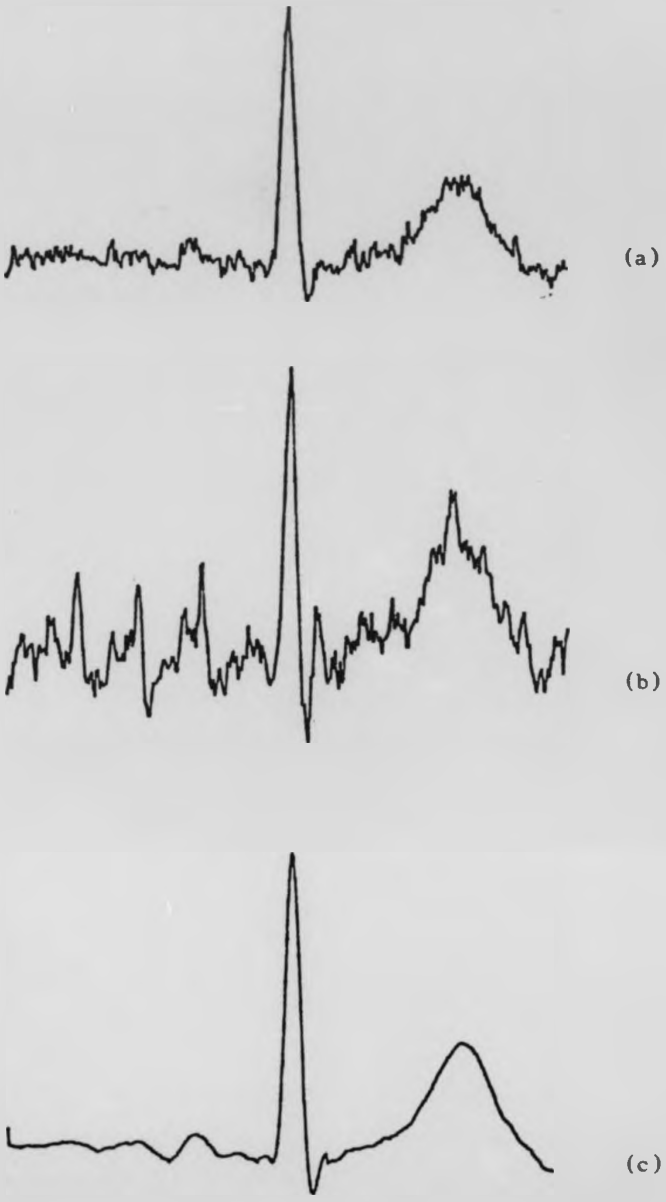

ure 6.18 Results representing time-sequence adaptive filter to reduce skeletal muscle activity, the figures show:

(a) Frontal plane lead on mid-clavicular line at level of 1st intercostal space
(b) Frontal plane lead, electrodes positioned on mid-clavicular line at level of 10th rib
(c) Time-sequenced , enhancing frontal plane lead (a)

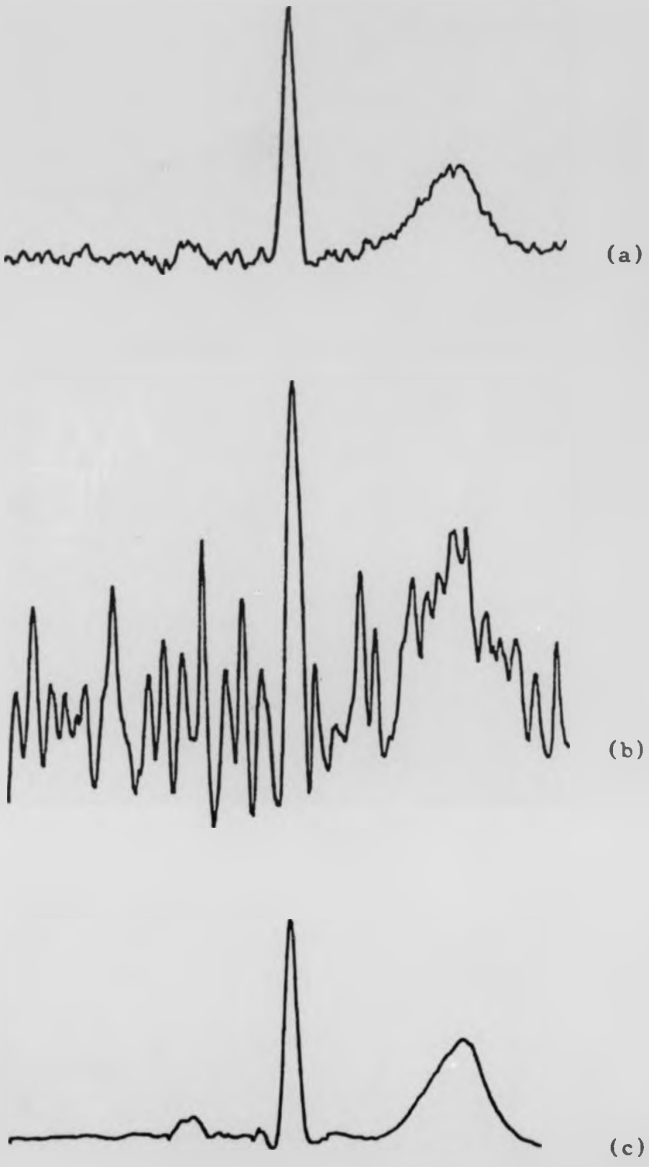

re 6.19 Results representing time-sequence adaptive filter to reduce akeletal muscle activity, the figures show:

(a) Frontal plane lead on mid-clavicular line at level of 1st intercostal space
(b) Frontal plane lead, electrodes positioned on mid-clavicular line at level of 10th rib
(c) Time-sequenced, enhancing frontal plane lead (a)

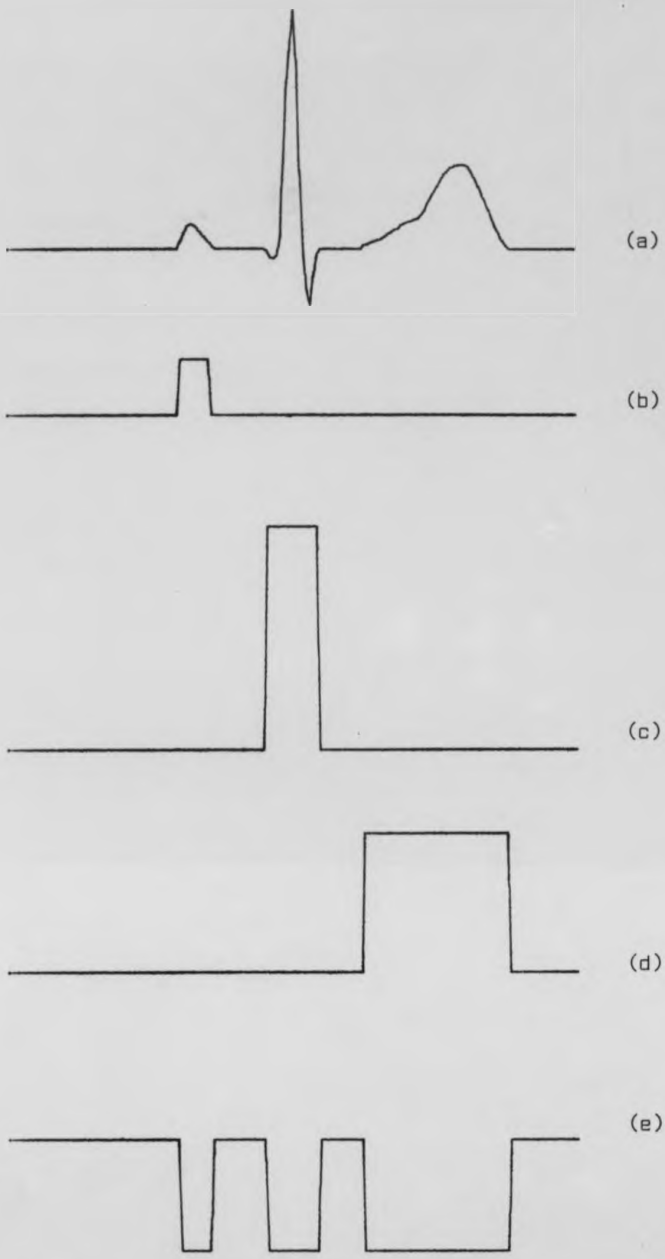

Figure 6.20 Time-sequence weight selection control vector, the figures represent:

(a) ECG waveform
(b) QRS weight set
(c) T weight set
(d) P weight set
(e) isoelectric weight set

in poor filter performance, as in basic adaptive filtering (figure 6.21). The TSAF is more appropriate for filtering repetitive transient signals.

Simulations have clearly demonstrated that TSAF is superior both to basic AF and averaging in most conditions, and yields a much improved estimate of the signal in terms of signal-to-noise ratio.

Figure 6.21 Comparison of adaptive and time-sequence adaptive filter using simulated data, the figures represent:

(a) the simulated ECG
(b) the simulated signal added to different simulated noises
(c) the results of adaptive filtering
(d) the results of time-sequence adaptive filtering

The number of weights was 64, and the adaptation speed was 0.001

6.3.1 Application of time-sequence adaptive filtering to foetal ECG (Simulated data only)

In recording the foetal ECG using electrodes placed on the abdomen of the mother, the foetal component can be obscured by skeletal muscle noise and the maternal ECG. Basic LMS adaptive filtering may be used to enhance the foetal ECG by channel enhancement, but the complex, non-stationary nature of the signal results in severe signal distortion. Further improvement may be achieved by using time-sequenced adaptive filtering. For both the AF and TSAF methods for enhancing the foetal ECG, two abdominal leads are recorded, one constitutes the desired response and the other the filter input.

Because the foetal ECG signal components are correlated between the two channels, but the interference due to muscle noise uncorrelated, the adaptive filter will attempt to pass the foetal ECG input signal component while at the same time attenuating uncorrelated muscle noise. By using a conventional LMS adaptive filter, a substantial reduction of the background muscle noise may be achieved, but not without severe foetal ECG signal distortion. The main reason for this is that the LMS adaptive filter is unable to track the fast recurring but variable features of the foetal ECG (non-stationary). Thus a time-sequence adaptive filter was considered for overcoming this problem.

Figure 6.22 shows two simulated channels of abdominal ECG in which there are substantial amounts of muscle noise. Figure 6.22c shows the

Figure 6.22 A computer simulation result of applying time-sequence adaptive filters to detect the simulated foetal ECG of SNR = 10.3dB. The figure shows:

(a) the simulated ECG with foetal ECG
(b) the two input channels
(c) the result of time-sequence adaptive filtering

result of TSAF in attempting to reduce the noise without distorting the simulated foetal ECG. The signal-to-noise ratio was 10.9dB and the improvement in SNR due to time-sequence adaptive filter, 15.2dB.

Figure 6.23 shows the results of a computer simulation in which SNR is 3.9dB, and figure 6.23c shows the result of applying time-sequence adaptive filtering to the simulated foetal ECG only.

All the weight vectors in the TSAF contain 64 weight values plus a bias weight, and the filter operates with a convergence factor of 0.001. In both cases the recurring simulated foetal ECG was obscured by the addition of white noise (S/N = 3.9dB) and subsequently extracted using the TSAF (S/N = 10.9dB). The output of the time-sequence adaptive filter after convergence is shown in figure 6.22c and 6.23c.

It can be seen from the result of figures 6.22 and 6.23 that the time-sequence enhancing of the simulated foetal ECG does not employ cycle-to-cycle averaging. The individual variation in a simulated foetal shape, and cycle-to-cycle intervals, can be retained. In a real situation, the technique of time-sequence adaptive filtering will not be effective unless the foetal ECG can be identified and the control vector set accordingly.

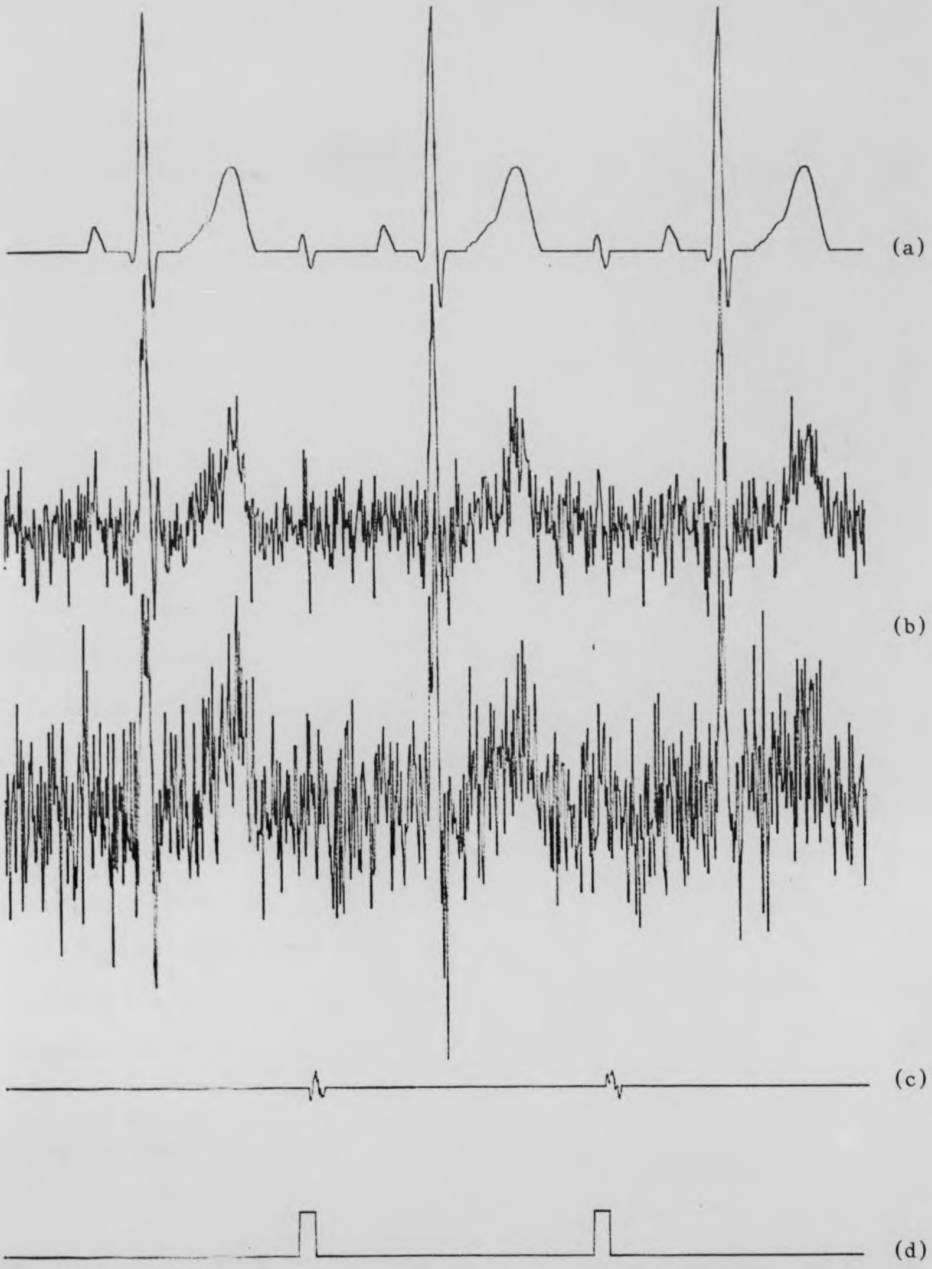

Figure 6.23 A computer simulation result of applying time-sequence adaptive filters to detect the simulated foetal ECG of SNR = 3.9dB, the figures show:

a - the simulated ECG with the foetal
b - the two input channels
c - the result of time-sequence adaptive filters
d - the control vector.

6.3.2 Time-sequence adaptive filter applied to cyclo-stochastic perturbation

The prevalence of heart disease in our society has emphasised the importance of early identification (Prasad et al., 1978; Gupta, 1980). A diagnostic technique with a low risk is of obvious advantage over the presently available diagnostic techniques which have certain limitations and are inappropriate for detecting heart disease in its early stages.

This section deals with a further application of time-sequence adaptive filtering for extraction and detection of the abnormal events within the electrocardiogram. These abnormal events generally occur within the QRS complex and are indicative of cardiac muscle damage.

The study of this application was conducted on simulated data in which two simulated ECG's with different noise levels were used. Small signals were introduced within the QRS complex to represent the abnormality due to cyclo-stochastic perturbation. Adaptive filtering was applied in the time-sequence mode to detect these events.

Results depicted in figure 6.24 illustrate the output of TSAF after convergence. The results suggest that the TSAF technique would be a valuable diagnostic tool for the detection of such disorders. Currently no other technique is available that effectively detects such perturbations, except from PISA (phase-invariant signature algorithm) averaging. The limitation of the PISA technique due to artifact has been demonstrated in section 6.2.4.

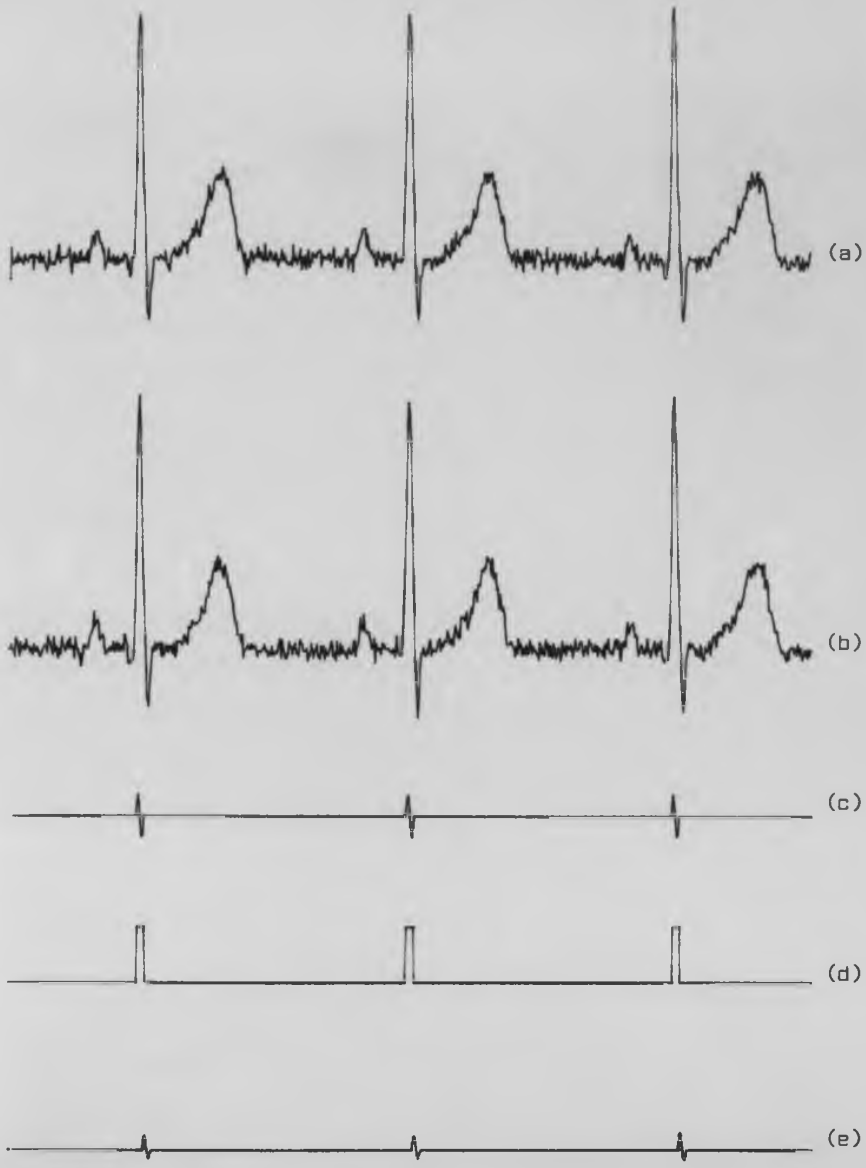

Figure 6.24 (a) and (b) Inputs to time-sequence adaptive filter
(c) Simulated perturbation in (a) and (b)*
(d) Control vector
(e) Output of time-sequence adaptive filter

*(c) amplified 100 times.

6.4 Conclusions

This chapter has been concerned primarily with a review of the application of adaptive and time-sequence adaptive filters to some previously recognised problems, together with two new applications. One is for the extraction of skeletal muscle noise from exercise ECG's by use of two chest leads, and the application of an adaptive signal enhancer and the second for the detection of cyclo-stochastic perturbations.

Although the time-sequence adaptive filter is only an extension of the adaptive filter principle, it has particular advantages for the application considered. However, for optimal estimation of a non-stationary signal having a recurring statistical character, knowledge is required of the time of occurence of the recurring signal, in order for the filter to switch between weight vectors. No other a priori knowlege is required.

A wide range of conditions were examined and encompassed high and low correlations between the noise records. The results of the study confirm the superiority of TSAF cancellation in the cases presented, compared to the basic AF. This advantage is most significant when the coherence and SNR are high.

The results presented in this chapter also show the spatial use of time-sequence AF which, in comparison with the conventional LMS method, yields less distortion and better S/N performance.

Chapter seven: Application of adaptive filters in exercise electrocardiography

7.1 Introduction

In previous chapters, the case for using adptive filters for enhancement of the ECG signal derived from a subject in the resting state has been presented, with particular attention to the use of time-sequence adaptive filters in the form of channel enhancers. In this chapter a full study of these techniques, applied to exercise ECG tests, is presented.

The ECG is an integral part of exercise testing in which the objective is the assessment of the functional efficiency of the heart and circulation. Continuous recording during exercise is essential both for safety and for the recognition of changes that could otherwise be missed if ECG's were obtained on a sample basis throughout the exercise period. Using the ECG, various indices may be derived that can be related to functionality. Various features and factors such as ST segmented variations, QU/QT ratio, changes in T-wave morphology and variations in TU segment and U-wave morphology provide clinical information that forms part of the functional assessment (Gupta & Prasad, 1980; Journee & Manen, 1984; Goovaets et al., 1978).

Whilst careful preparation for ECG recording is mandatory in exercise testing, muscle activity during exercise may yield sufficient noise that important features of the ECG become obscured. Adaptive

filtering is seen as being of potential value in helping to cancel out such noise and so provide clear ECG's under exercise conditions.

In the previous chapter, the choice of parameter values for the adaptive filter techniques was considered and values selected from the earlier studies. The same choice of parameter values has been used in the application to exercise electrocardiography. Having established how best to apply the signal enhancer and the time-sequence adaptive filter in the form of channel enhancer, the results of filtering a large number of records from twenty-two subjects, male and female aged between 30 and 50, have been obtained.

The presence of base-line variation within the record, due in part to respiratory effects has, to some extent, an effect upon the performance of the adaptive filter technique. This kind of effect, along with the presence of different noise components arising from the exercise test, were studied and their effect upon the adaptive filter performance examined.

7.2 Types of noise present in exercise electrocardiograms

The presence of noise, artefacts and baseline variations are the main causes of signal masking in exercise electrocardiograms, and care must be taken to minimise the influence of the noise components upon the signal. The tests were carried out with data recorded during:

(a) bicycle ergometer tests and,

(b) the Master Step tests.

These techniques are adequately described elsewhere (Rautaharju, 1965; Thakor, 1978; Winter, 1966, 1969; Worthuis et al., 1979). Adaptive filtering was used for the extraction of the noise components produced by exercise test and the base-line variations.

In this section two sets of experiments are reported, based upon recordings obtained from a group of patients in which two bipolar lead configurations were used. One set involved recordings from the conventional V leads system in which V_1 and V_5 were taken. The second set of recordings was obtained using the chest leads in which one of the electrodes was placed in the frontal plane and positioned in mid-clavicular line at the level of the 10th rib, while the other was positioned on the mid-clavicular line at the level of the first intercostal space.

7.3 The effect of the base-line variation

A problem may arise when adaptive filtering techniques are applied to exercise ECG data obtained in the presence of base-line variation. The variations are mainly due to the presence of the electrode movement and respiration effects, both of which can affect filter performance. The most prominent base-line variation is a periodic variation due to respiration (Ferrara & Widrow, 1981) and in applying conventional signal averaging the signal derived can be severely distorted.

Since adaptive filtering of the Exercise ECG is restricted to a specific length of record, the removal of the dc and low frequency components is an important pre-requisite to applying the adaptive filter. This is not possible if continuous filtering has to be performed.

Several methods have been considered in this study to remove the DC and base-line fluctuations, one of which involves their removal from cycle-to-cycle of the data record. This was done by using five second data segments, and resulted in much smaller base-line fluctuations.

Figures 7.1 and 7.2 show the influence of DC and base-line fluctuations through successive cycle segments of the data record. In performing the experimental work, some difficulties were encountered in applying the above method. By processing each cycle independently discontinuities occur at the boundaries and this method is therefore

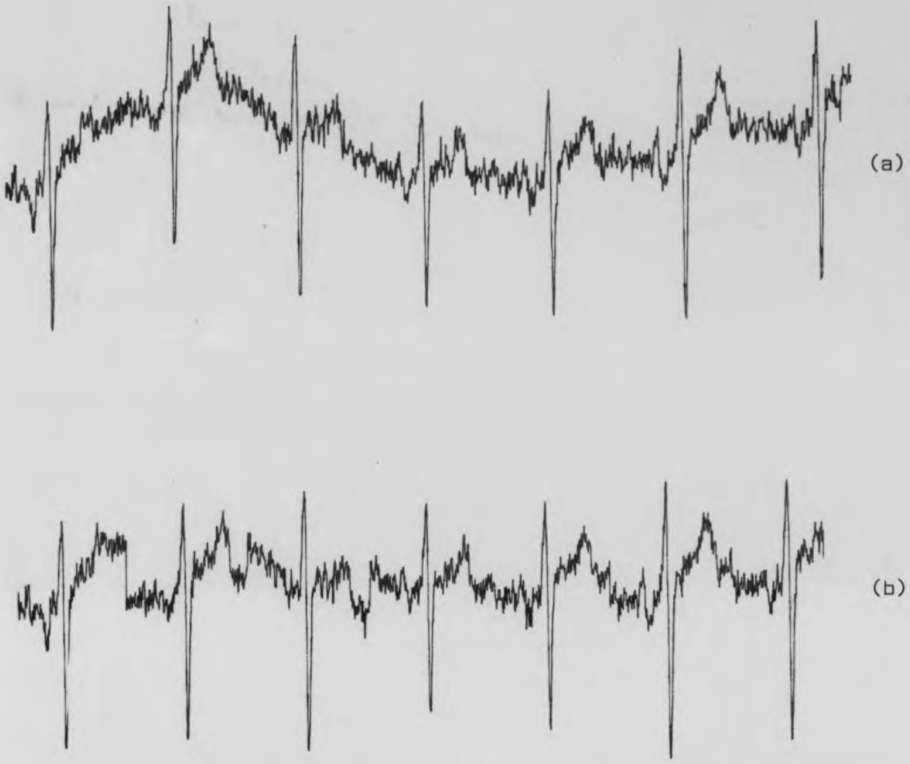

Figure 7.1 Shows the influence of dc and baseline fluctuations through successive cycle segments

(a) the recording of lead V_1

(b) the result of the removal of dc and baseline fluctuations

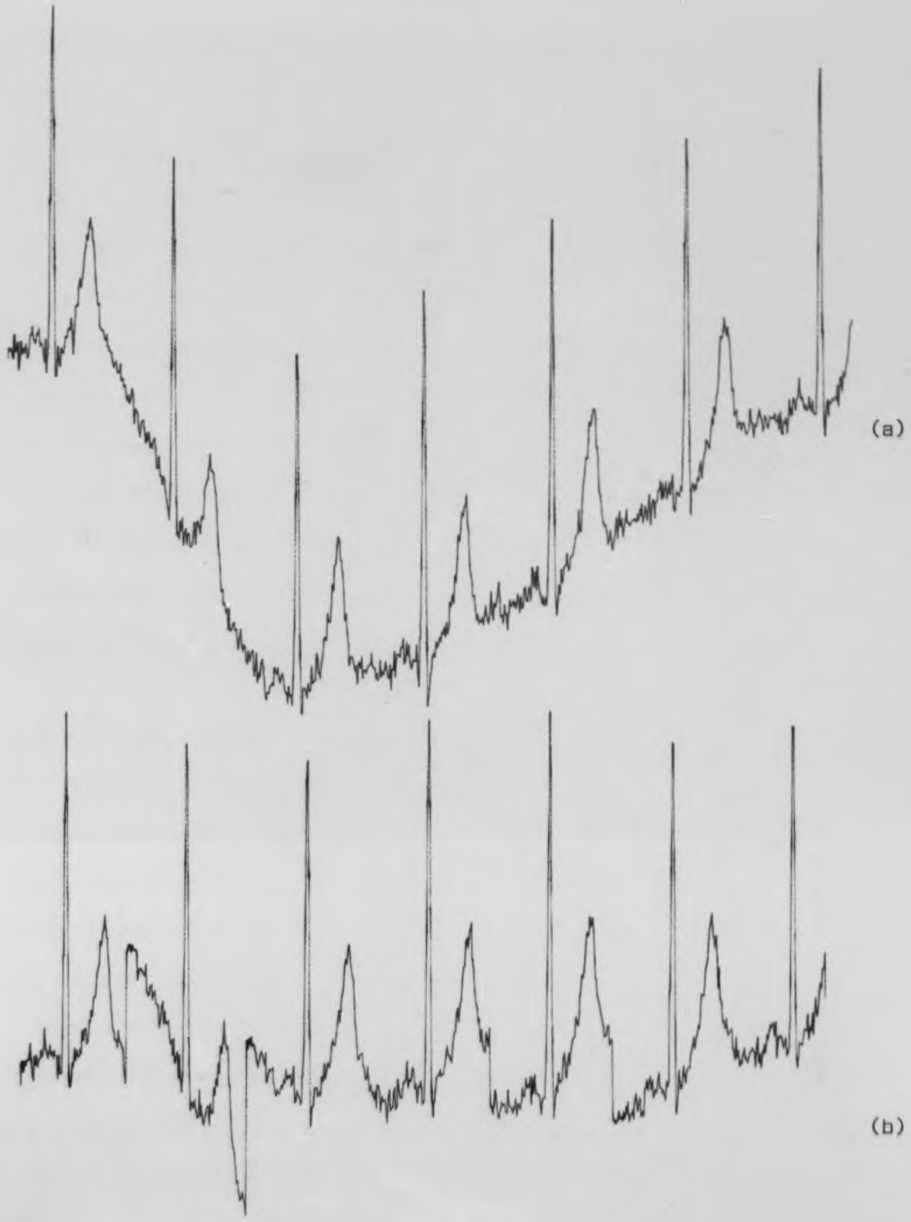

Figure 7.2 Shows the influence of dc and baseline fluctuations through successive cycle segments

(a) the recording of lead V_5

(b) the result of the removal of dc and baseline fluctuations

inappropriate for on-line processing.

Ferrara (1981, 19829 suggested that the problem of DC drift may be overcome if an additional bias weight is added in the adaptive filter that will track and remove the dc component. The function of this bias weight is to cause the filter to behave as a notch filter at DC. Figure 7.3 shows the result of applying an additional bias weight. Although the bias approach introduced by Ferrara and Widrow (1977) was used in the adaptive filtering of exercise ECG data, it was found that the method could give inferior results, especially in cases where the exercise activity is high.

By using a simple recursive high pass stage prior to the adaptive filter, removal of low frequency variation can be achieved without distorting the signal (figure 7.4). This method has the advantage of allowing continuous filtering. The high pass recursive filter is similar to that described by Lynn (1977). The application of this method in removing the base-line fluctuation was found to be more effective than the method suggested by Ferrara and Widrow (1981). The improvements in signal-to-noise ratio through the use of the high pass stage suggests that this method is an effective way of handling the base-line fluctuations, as shown in figures 7.5 and 7.6.

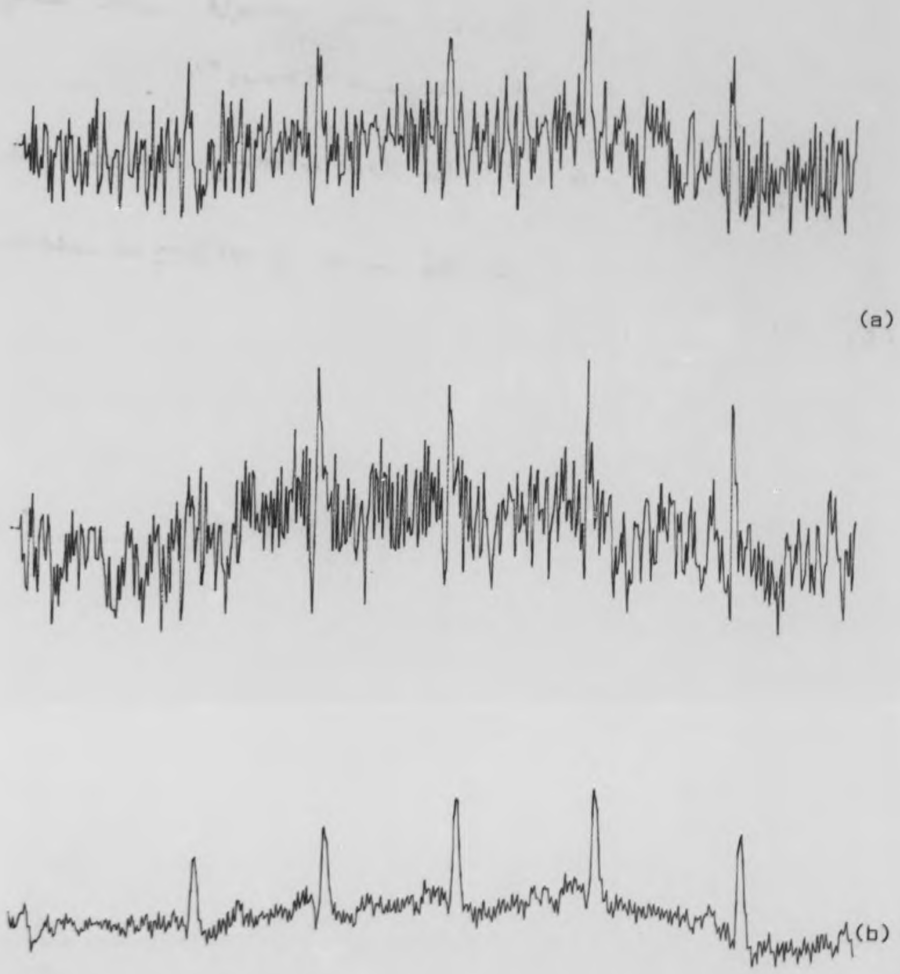

Figure 7.3 Shows the result of applying an additional bias weight with adaptive filters, the figure shows:

(a) the two necessary recorded channels
(b) the result of applying an additional weight

(a)

(b)

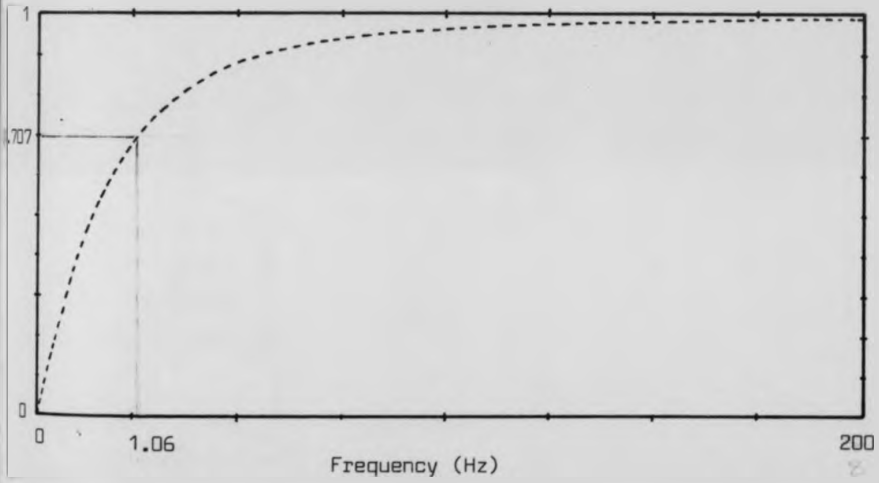

Figure 7.4(a) A block diagram of a high pass filter prior to an adaptive filter in order to remove the dc drift

(b) Magnitude response characteristics of a recursive digital high pass filter

Figure 7.5 Shows the result of applying high pass filter followed by adaptive filtering, the figure shows:

(a) the recorded channel
(b) the result of applying the technique

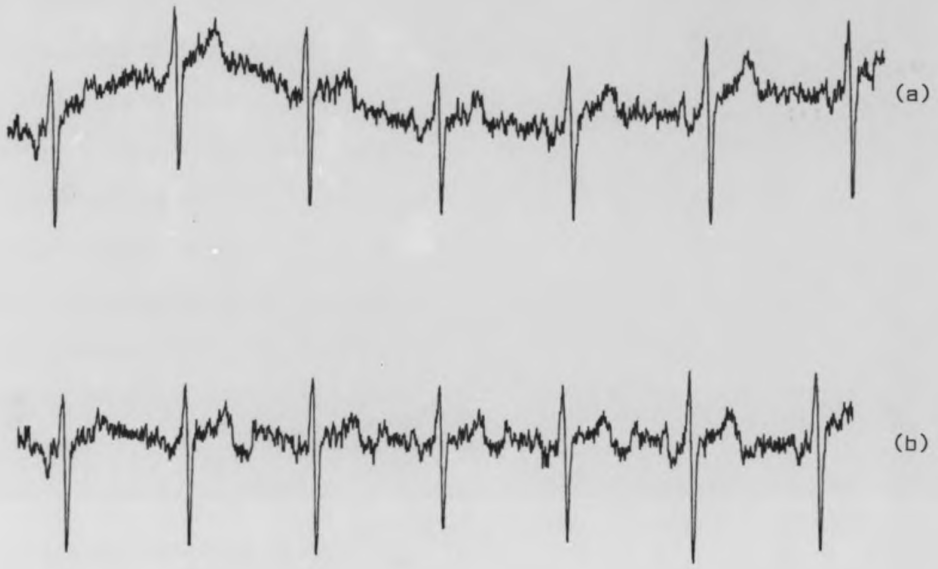

Figure 7.6 Shows the result of applying high pass filter prior to adaptive filtering, the figure shows:

(a) the recorded channel
(b) the result of applying the technique

7.4 Application of adaptive filters to exercise ECG using a bipolar lead configuration

Many problems may be encountered in recording exercise electrocardiograms (Winter, 1966). They include the choice of stress test, movement of the subject, the choice of electrodes, choice of lead configuration and the limitation of the technique and processing systems. Artefacts and interference can, to some extent, be reduced by momentary cessation of the exercise whilst the recording is obtained (Thakor, 1978). Although the choice of electrodes and lead systems for exercise electrocardiography have been investigated by others (Webster, 1977; Thakor & Webster, 1980), it was considered necessary to re-examine these choices in considering the application of adaptive filtering.

By using a non-conventional lead configuration such as presented in figure 7.7, the signals developed between any two pairs of electrodes may be regarded as almost identical. However, the noise arising at each of these electrode pairs can be found to be largely uncorrelated, depending upon the distance of separation between electrode pairs. For the exercise study, the first pair of electrodes was placed in the mid-clavicular line at the level of the first intercostal space and the second pair placed at the positions of the 10th rib, as shown in figure 7.7. The recordings obtained from these two lead configurations were digitised and entered directly into a computer memory for analysis. The subjects were, in each case, asked to exercise for exactly the same period of time as that stipulated in the

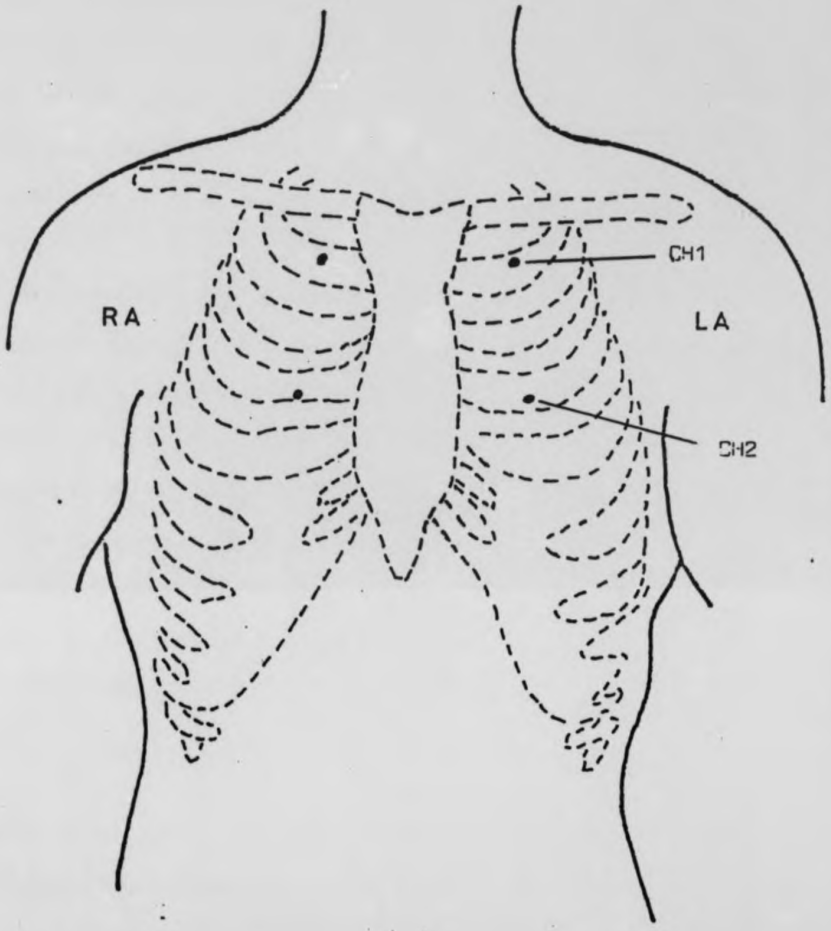

Figure 7.7 Two channels are recorded

CH1 the electrodes placed in the mid-clavicular line at the level of the 1st intercostal space.

CH2 the electrode placed in the mid-clavicular line at the position of the 10th rib.

exercise programme, to a state where they could safely do no more.

After recording the data, the base-line variations were removed and three types of adaptive filtering were applied, in order to enhance the ECG signal above the noise. The experiments were conducted simply to establish the ability and behaviour of the adaptive filter technique with regard to the enhancement of the signal in the very noisy conditions produced by muscle activity during exercise.

The results obtained showed a substantial reduction of noise for all three types of adaptive filter and provided an ECG recording in which underlying cardiac abnormalities could be more readily recognised. Comparisons with processed ECG's from normal healthy subjects indicated that the technique was not introducing artefacts that could be mistaken for cardiac abnormalities. The improvement of signal-to-noise ratio of the minimal time sequence adaptive filter appeared to be much higher than the time-sequence adaptive filter and the adaptive channel enhancer. However some signal distortion was observed.

Three sets of results are presented in this section, for the three types of filtering considered. These are:

(i) when the subject was at rest,

(ii) when the subject was exercising under the load of 75W, and

(iii) when the subject was exercising under the load of 150W.

The loadings are representative of those imposed during exercise testing and the higher the load, the more noise due to muscle activity

was encountered. The ECG signal however appears to exhibit little change in magnitude with respect to loading. Figures 7.8 - 7.17 show the selected results of the 22 patients investigated using the adaptive filter technique. The number of weights was chosen to be 64 and the convergence factor 0.001 for all the data used.

From the results of this analysis it is quite apparent that distinct improvements can be made in the reduction of noise by adaptive filtering. Improvements in the signal-to-noise ratio of the exercise ECG can be achieved using real-time technique of adaptive filtering. This technique can also retain information on a cycle-to-cycle basis.

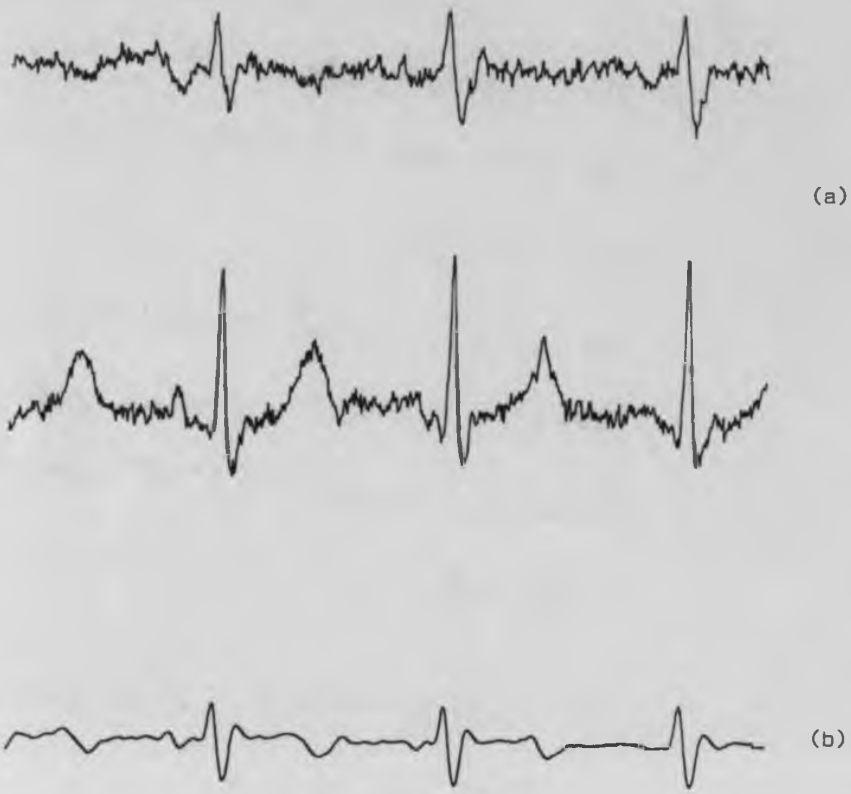

Figure 7.8 The result of applying high pass filter to remove dc and baseline fluctuations and then applying the adaptive technique to remove the skeletal muscle activity, the figure shows:

(a) the two recorded channel necessary for adaptive filter to perform, the convergence factor was 0.001, and it was 64 weight coefficients

(b) the result of high pass filter prior to adaptive filter for V_1 lead

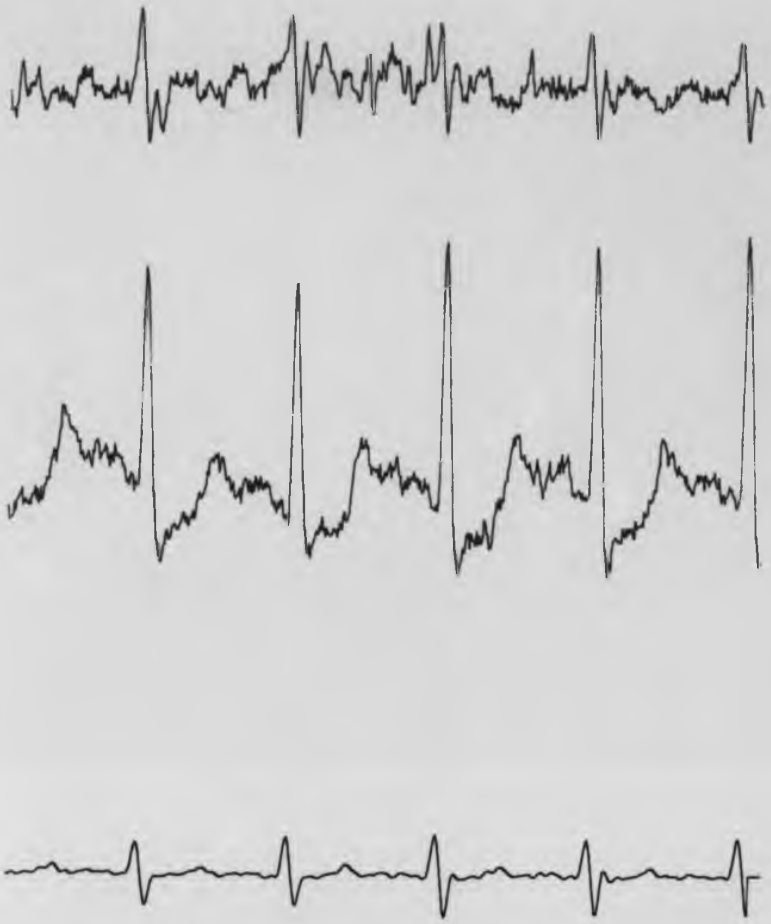

Figure 7.9 The result of applying high pass filter to remove dc and baseline fluctuations and then applying the adaptive technique to remove the skeletal muscle activity, the figure shows:

(a) the two recorded channels necessary for adaptive filter to perform, the convergence factor was 0.001, and it was 64 weight coefficients

(b) the result of high pass filter prior to adaptive filter for V_1 lead

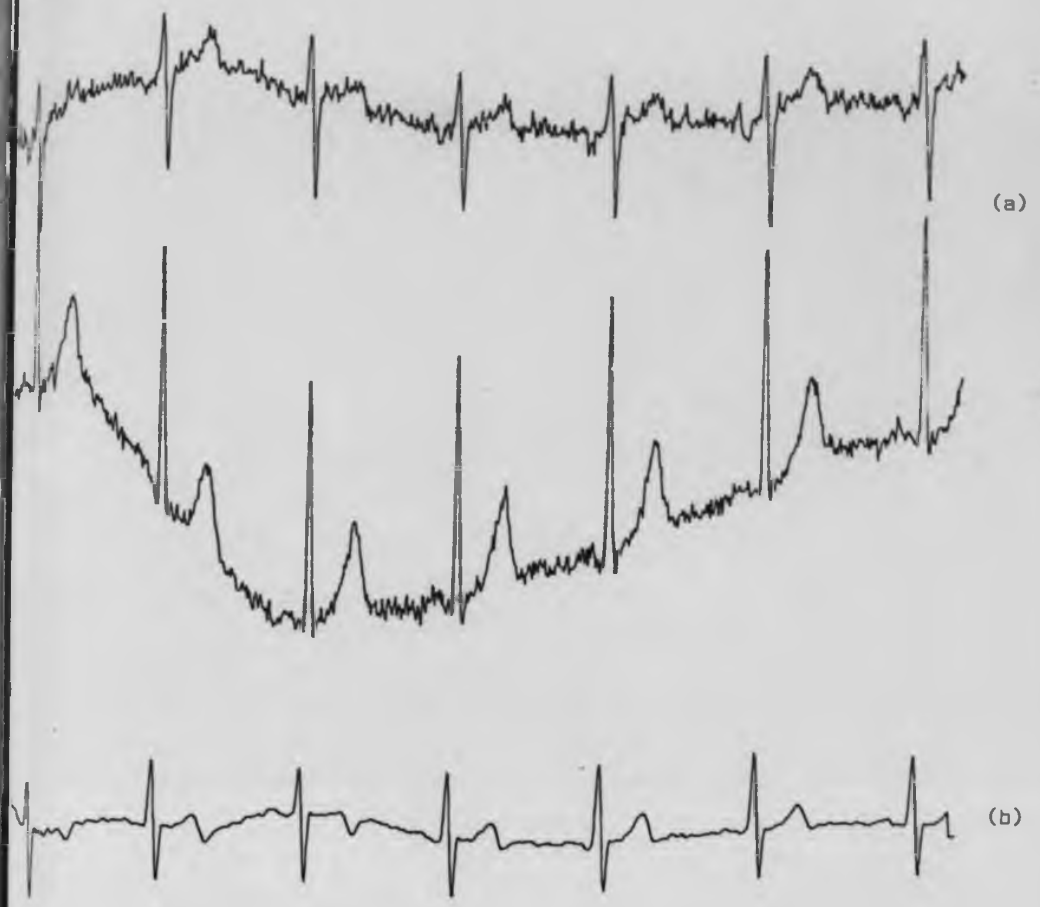

Figure 7.10 The result of applying high pass filter to remove dc and baseline fluctuations and then applying the adaptive technique to remove the skeletal muscle activity, the figure shows:

(a) the two recorded channels necessary for adaptive filter to perform, the convergence factor was 0.001 and it was 64 weight coefficients

(b) the result of high pass filter prior to adaptive filter for V_1 lead

Figure 7.11 The result of applying high pass filter to remove dc and baseline fluctuations and then applying the adaptive technique to remove the skeletal muscle activity, the figure shows:

(a) the two recorded channels necessary for adaptive filter to perform, the convergence factor was 0.001 and it was 64 weight coefficients

(b) the result of high pass filter prior to adaptive filter for V_1 lead

Figure 7.12 The result of applying high pass filter to remove dc and baseline fluctuations and then applying the adaptive technique to remove the skeletal muscle activity, the figure shows:

(a) the two recorded channels necessary for adaptive filter to perform, the convergence factor was 0.001 and it was 64 weight coefficients

(b) the result of high pass filter prior to adaptive filter for V_1 lead

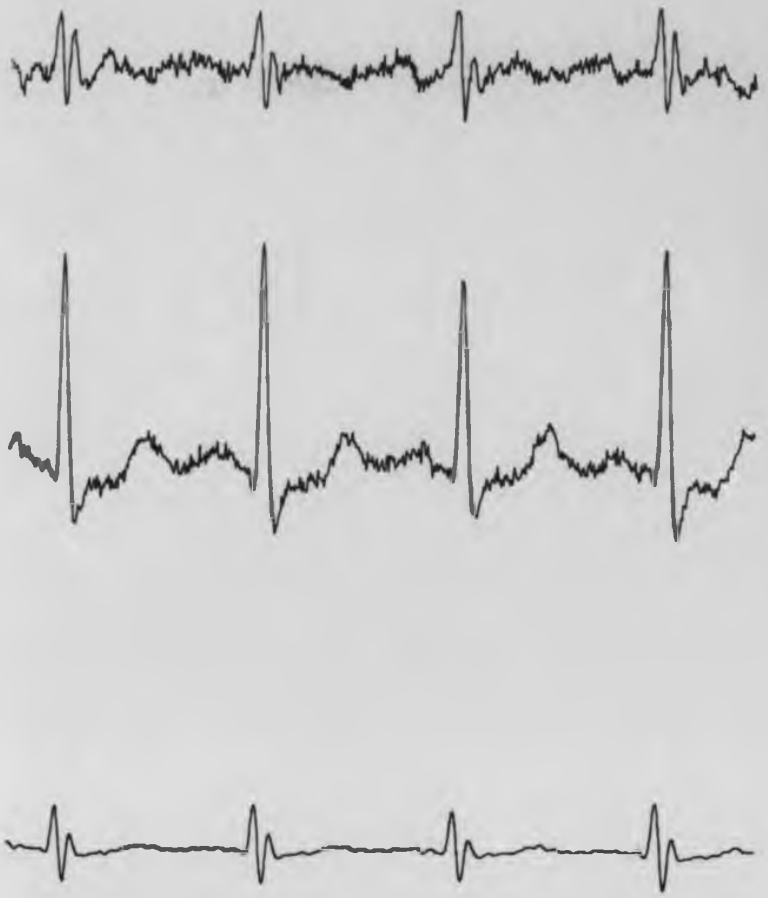

Figure 7.13 The result of applying high pass filter to remove dc and baseline fluctuations and then applying the adaptive technique to remove the skeletal muscle activity, the figure shows:

(a) the two recorded channels necessary for adaptive filter to perform, the convergence factor was 0.001 and it was 64 weight coefficients

(b) the result of high pass filter prior to adaptive filter for V_1 lead

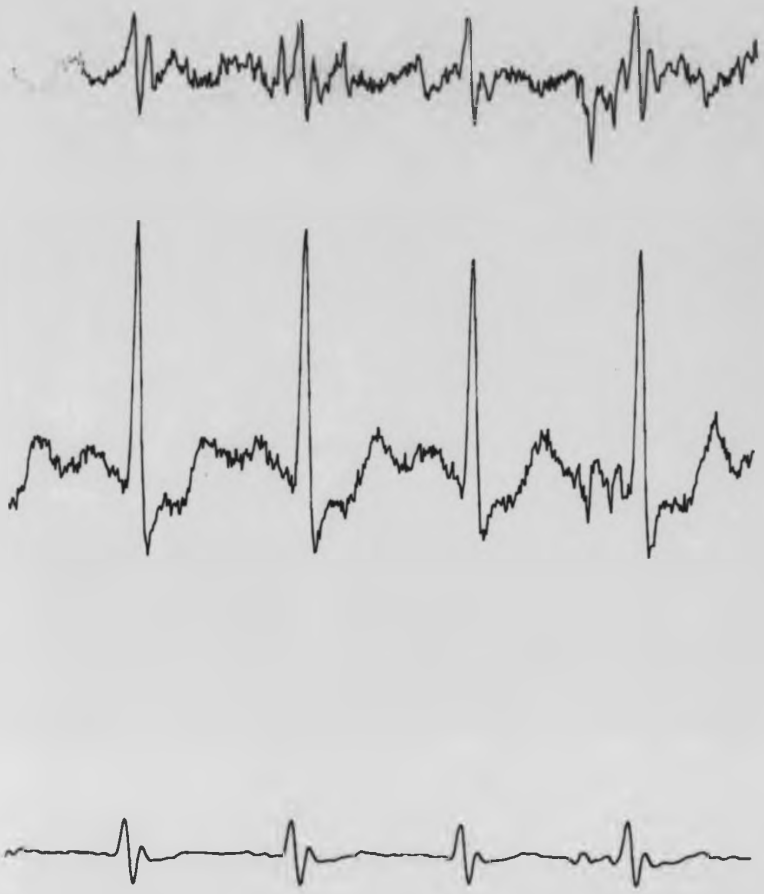

Figure 7.14 The result of applying high pass filter to remove dc and baseline fluctuations and then applying the adaptive technique to remove the skeletal muscle activity, the figure shows:

(a) the two recorded channels necessary for adaptive filter to perform, the convergence factor was 0.001 and it was 64 weight coefficients

(b) the result of high pass filter prior to the adaptive filter for the V_1 lead

Figure 7.15 The result of applying high pass filter to remove dc baseline fluctuations and then applying the adaptive technique to remove the skeletal muscle activity, the figure shows:

(a) the two recorded channels necessary for adaptive filter to perform, the convergence factor was 0.001 and it was 64 weight coefficients

(b) the result of high pass filter prior to the adaptive filter for the V_1 lead

Figure 7.16 The result of applying high pass filter to remove dc baseline fluctuations and then applying the adaptive technique to remove the skeletal muscle activity, the figure above shows:

(a) the two recorded channels necessary for adaptive filter to perform, the convergence factor was 0.001 and it was 64 weight codfficients

(b) the result of high pass filter prior to the adaptive filter for the V_1 lead

Figure 7.17 The result of applying high pass filter to remove dc baseline fluctuations and then applying the adaptive technique to remove the skeletal muscle activity, the figure above shows:

(a) the two recorded channels necessary for adaptive filter to perform, the convergence factor was 0.001 and it was 64 weight coefficients

(b) the result of high pass filter prior to the adaptive filter for the V_1 lead

7.5 Adaptive filter applied to the V-lead data

Having developed the technique for bipolar leads and examined the performance for data obtained from healthy subjects, attention was directed to data obtained from the exercise test clinic. Data was recorded from 22 patients varying in age between 30 - 56 years. The objective was to adaptively filter the exercise ECG's and reveal abnormalities that would otherwise be obscured by noise. Some of the patients exhibited a normal ECG, but the majority of the recordings indicated the existence of a cardiac abnormality.

The data was collected from the patients using a V-lead configuration (V_1 - V_6), but the channel recordings were taken from only two leads, lead V_1 and lead V_5. This was considered adequate to test the technique. The recording procedure and the preparation of patients were carried out in a conventional manner.

The exercise programme was conducted using a bicycle ergometer with the provision of 2-4 stages of loading. The patients were asked to peddle for three minutes under the starting load of 75W, then the load was increased to 100W, 150W, 200W for three minutes each. Recordings were obtained for each load and a rest of 5 minutes was allowed between loadings. The recordings were of one minute duration and the data was recorded onto magnetic tape using an FM tape recorder (specification in Annex D). The data was played back for the application of the adaptive filtering techniques. After the removal of the DC base-line, variations in the data were subjected to the

three types of adaptive filtering described in section 7.4.

Analysing the results obtained from the data, it was found that adaptive filters provide an effective means of achieving noise reduction and allowed the identification of ECG abnormalities otherwise obscured. From the results depicted in figures 7.8 - 7.17 it can be seen that the adaptive filter exhibits the best performance in terms of noise reduction and minimisation of distortion, with a signal-to-noise improvement of 8.6dB's.

In examining other techniques for extracting noise from exercise ECG's, it was found from the results in figures 7.18 - 7.20, that an improvement in the signal-to-noise ratio can be achieved by using signal averaging but prevents identification of beat-to-beat changes. The time-varying filter exhibited a significant improvement in the signal-to-noise ratio (5.5dB), but this technique also exhibited loss in signal-to-noise information, as in the averaging process.

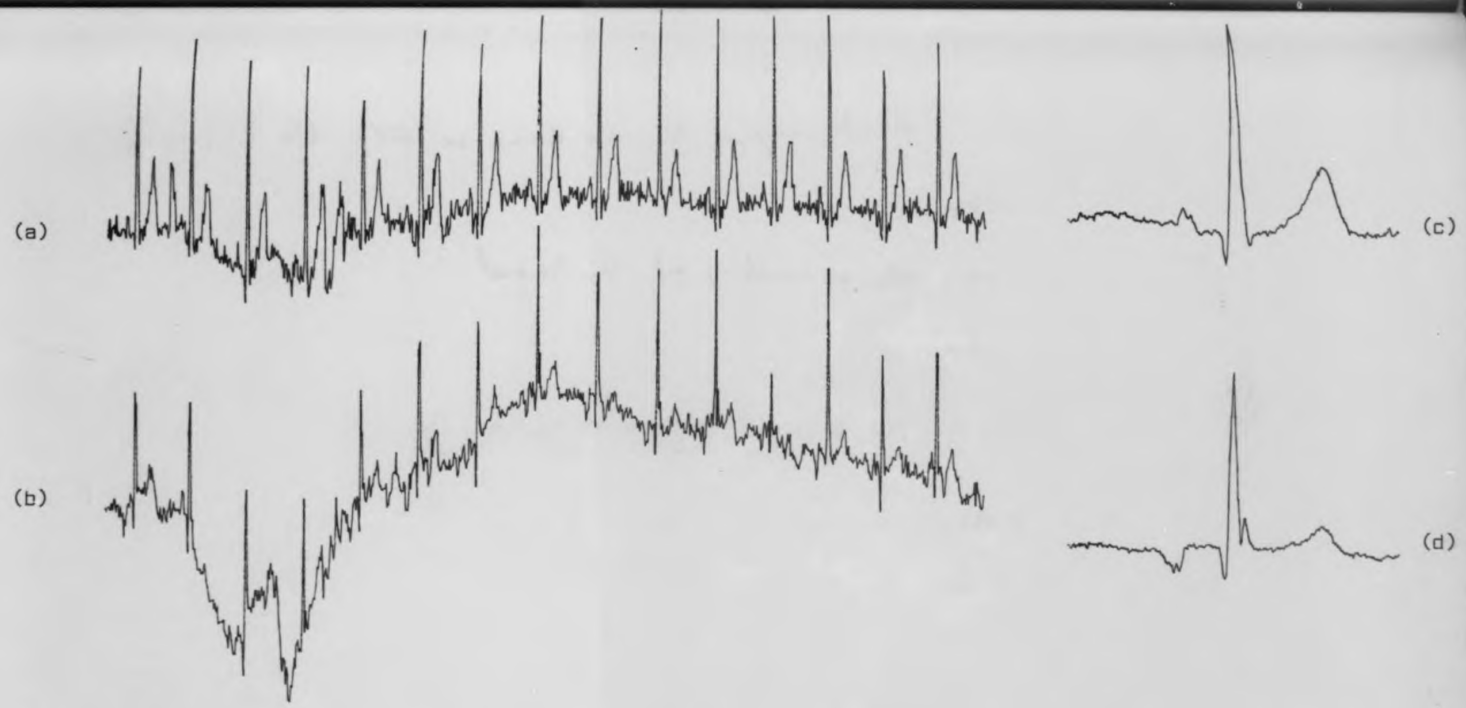

Figure 7.18 Result of applying an averaging technique to an exercise ECG, the figure shows:

(a) the recording of V_1 lead

(b) the recording of V_5 lead

(c) the result of averaging V_1

(d) the result of averaging V_5

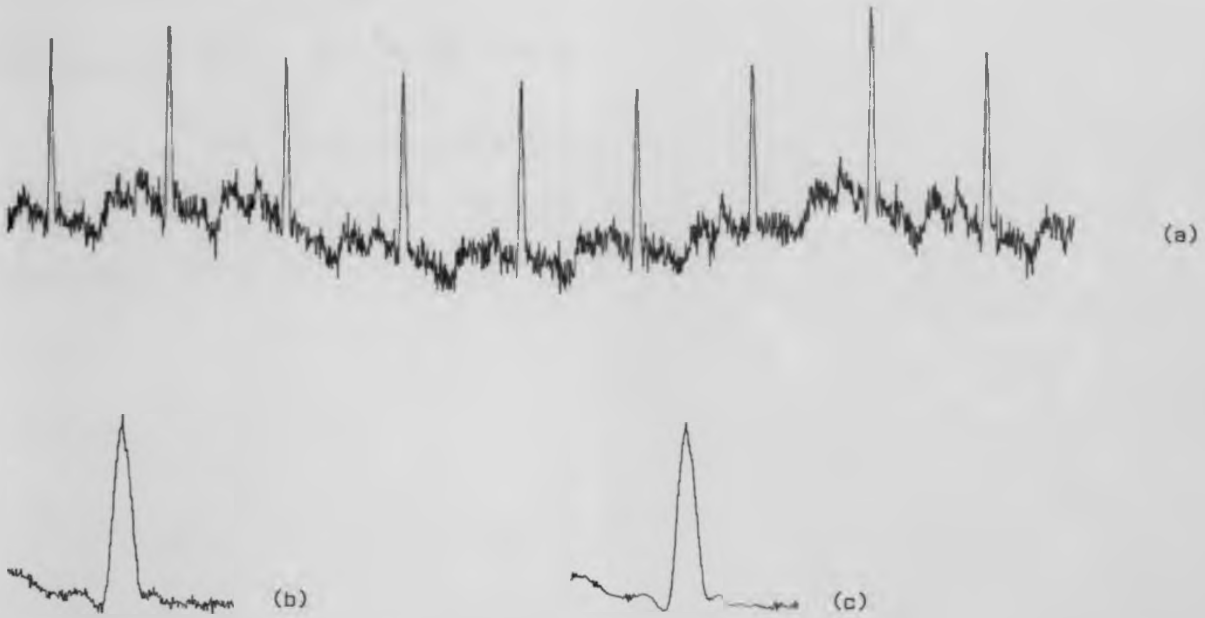

Figure 7.19 Result of applying averaging and time-varying filter to exercise ECG lead V_1, the figure shows:

(a) the recorded V_1

(b) the result of averaging

(c) the result of time-varying filter

Figure 7.20 Result of applying averaging and time-varying filter to exercise ECG lead V_5, the figure shows:

(a) the recorded V_5

(b) the result of averagigng

(c) the result of time-varying filter

7.6 Summary and conclusion

As indicated in chapter two, a number of simple precautions have to be taken in order to achieve good ECG recordings, especially during exercise testing. These factors include:

(i) electrode-skin preparation

(ii) choice of electrode

(iii) choice of lead system

(iv) type of exercise test

(v) possible sources of interference.

In this chapter the results for the removal of the base-line variations have been presented. The presence of these variations dramatically degrade the effectiveness of the adaptive filter. The results obtained after conditioning for base-line variations suggest that of the techniques employed and characteristics chosen (i.e. parameter, number of coefficients, convergence factor μ), the adaptive filtering technique provides better objective results than the other forms of filter mentioned in chapter three.

Chapter Eight: Comparison of adaptive filtering techniques

8.1 Introduction

In previous chapters the application of filtering techniques for the reduction of the noise and artefact that corrupt the ECG signal, especially during exercise testing, have been studied and results presented. In this chapter a complete examination of the spectral occupancy of noise and signal is presented together with their use in the choice of adaptive filtering for particular applications.

The advantages which can be gained by using adaptive filtering have already been described. It was shown in Chapter three that many filtering techniques and signal averaging for the raw data are the most common signal processing methods applied. These achieve noise and artefact reduction by removing frequency components which lie outside the signal bandwidth, but also reduces components that overlap with the signal components. It is in this latter respect that these previous methods are of limited use.

In this chapter experimental work is described which establishes the manner in which adaptive filters may be best applied for ECG conditioning, in order to achieve improvement in signal-to-noise ratio with the minimum of distortion. The amounts of distortion for each of the adaptive filters examined are also presented.

8.2 Spectral analysis of the electrocardiogram

Spectral analysis provides information about the frequency content of a particular signal. The results of spectral analysis may be of use in electrocardiography in;

(i) in devising and using efficient processing techniques that will reduce interference and noise, and

(ii) in helping to devise techniques that will improve the diagnostic capabilities of the high frequency and exercise electrocardiogram.

Spectral analysis usually requires long data records and the statistical property of stationarity. In order to accommodate non-stationarity, data was partitioned into segments in which stationarity could be considered to apply.

Previous investigations have shown that most of the power in the ECG signal lies below a frequency of 40Hz, while a very small amount of power has been measured in some patients at frequencies up to 500Hz (Santopietro, 1971; Berbari et al., 1976). Many researchers concluded that the low level energy at higher frequencies was not of clinical importance. Figure 8.1 shows the spectrum for skeletal muscle activity at frequencies above 100Hz, between 40 and 60dB below the level of the peak spectral components of the ECG signal.

To obtain the spectral estimates of the signal the auto-spectra of the two channel records from the surface of the the body were derived using the discrete Fourier transform (DFT). The cross-spectral

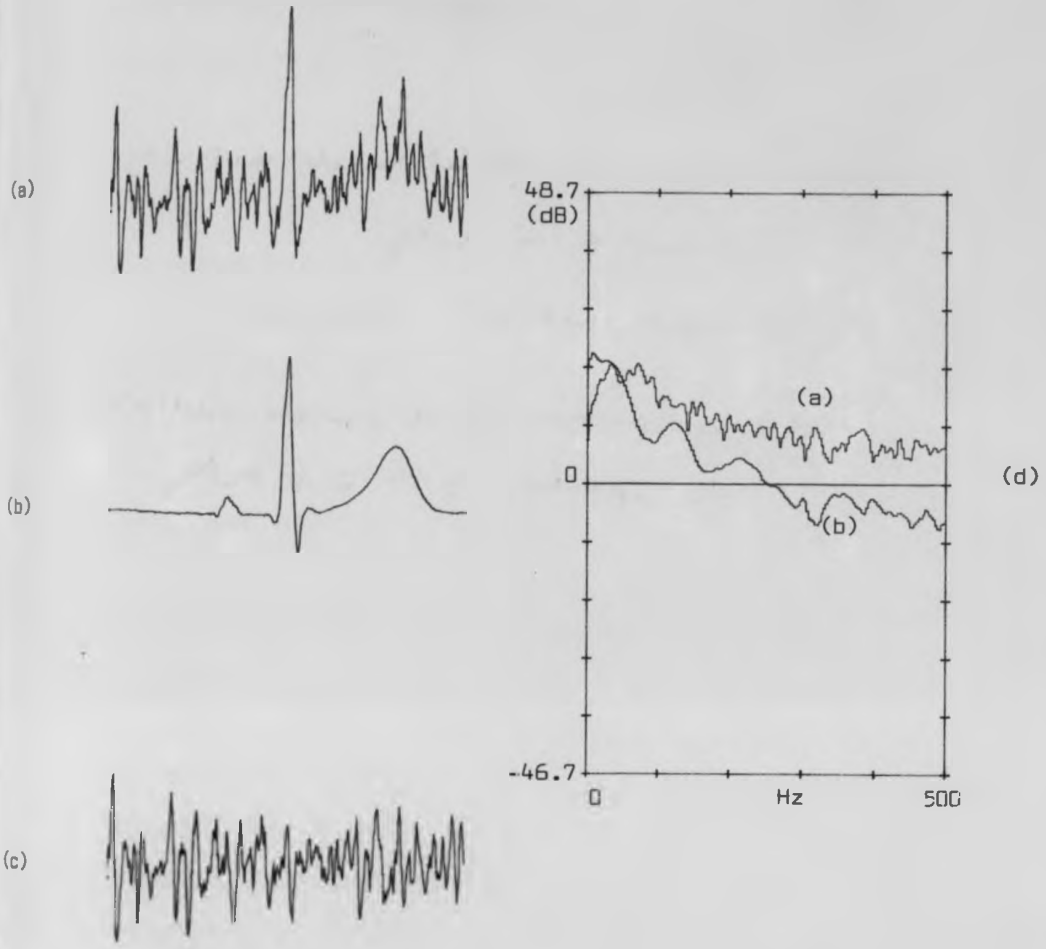

Figure 8.1 Shows the recording of clean and heavily contaminated ECG with skeletal muscle, the figures show:

(a) ECG with skeletal muscle activity

(b) clean ECG only

(c) muscle activity only

(d) the spectrum of the muscle activity and the spectrum of the ECG only

estimates were also computed for these two channels to determine the coherence between them. The discrete Fourier transform (DFT) was calculated using the Fast Fourier Transform algorithm (FFT).

Two major limitations of FFT spectral analysis have been identified (Levy & Linkens, 1984; Linkens, 1982).

(i) The extent to which the Fourier Transform is a limitation on frequency resolution.

(ii) In using the FFT analysis, windowing of the data is inherent in the method. This causes leakage which gives the impression that energy in the main lobe of the spectrum leaks into the side lobes, obscuring and distorting the spectral structure.

A full cosine window was applied in order to reduce the effect of spectral leakage.

In this study some observations were made on the recorded, analysed data obtained from 22 subjects. The results indicated a clear difference in the occupancy of the spectral content of the noise/interference. They also indicate a small range of variation for spectral content of the ECG signals, derived from the population of the subjects examined.

The main ECG signal power occupied the frequency range 0 - 80Hz and the noise power was 40 - 60dB below the main signal for frequencies over 100Hz. The results also indicated some overlap between the spectrum of the noise and spectrum of the signal especially over the

mid-band of occupancy of the ECG Signal.

In the attempts at noise reduction by the different filtering techniques mentioned in Chapters 3, 5 and 6, distortion was observed due to the spectral overlap between the signal and noise components.

8.3 Coherence analysis

The coherence function was derived for two important reasons;

(i) it incorporates both the auto- and cross-spectral information of the signal and noise, and

(ii) it provides an estimate of the degree to which the two channels correspond in the frequency domain.

The coherence function was derived using the auto- and cross-spectral estimates according to the expression:

$$\text{coherence function (spectrum)} = \frac{Sxy(f)^2}{Sx(f)Sy(f)}$$

Coherence function is a measure of the spectral corresponence between two signals, presented as a parameter, normalised at each frequency independently (Roth, 1971).

A coherence of unity indicates that the signals in two channels correspond perfectly in spectral terms over the frequency range considered whilst a coherence of zero, indicates that the signal in both channels are not related at all. Intermediate values between 0 and 1 indicate the degree to which the spectral contents compare (Bendat, 1962, 1964). Intermediate values may arise through:

(i) presence of extraneous noise,

(ii) a non-linear process relating the two sources of signal (and hence introducing non-linearity related components), and

(iii) additional inputs.

The coherence functions computed for the experimental data shown in

figures 8.2 - 8.4 clearly illustrate that from 100 - 500Hz there is a lack of coherence between the two channels, but at low frequencies from 0 - 100Hz the coherence is 1, indicating a 100% correspondence between the two channels.

The coherence functions computed for signals derived from electrodes placed as shown in figures 8.5 for a given value of separation, were found not to differ for the frequencies between 0 - 100Hz. However, they do exhibit small variations depending on the distance between the electrodes, over the range 100 -500Hz. This can be seen in figure 8.6. As the distance between electrodes is reduced, so the coherence functions between them tend to 1. These results suggest the use of coherence as the basis for selecting electrode placement for particular adaptive filtering procedures.

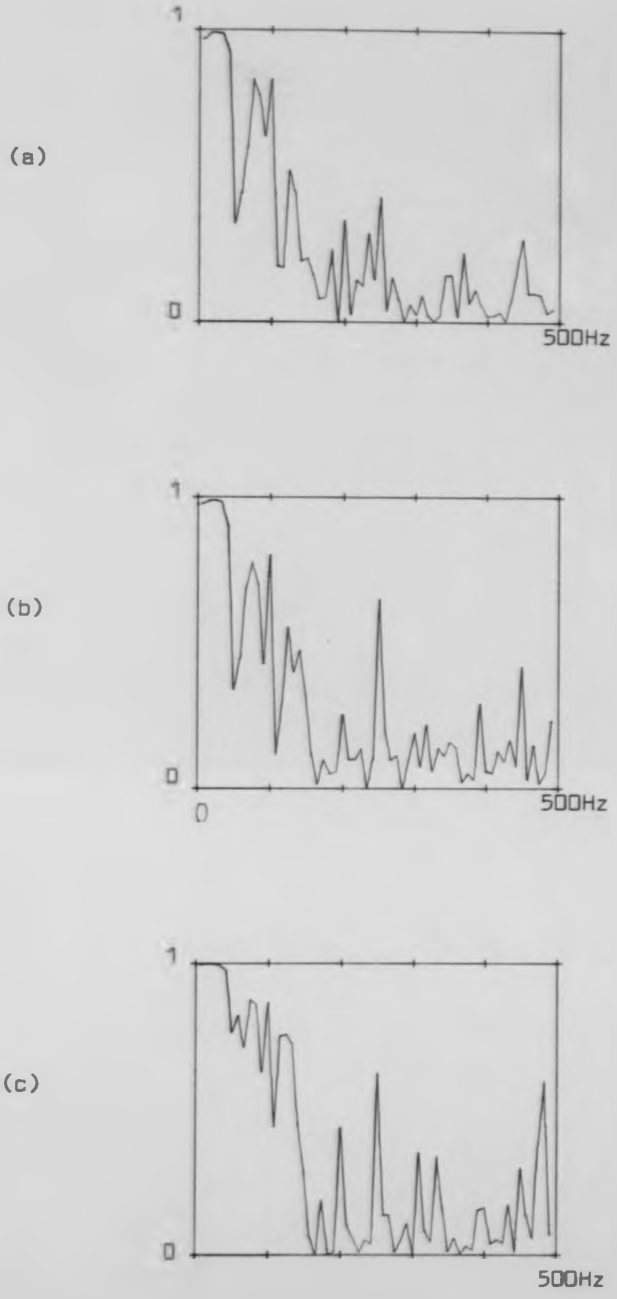

Figure 8.2 The comparison of the coherence function between three recorded sets of data, separated by 8cm

(a) the coherence function between channel 1 and channel 2 (set 1)

(b) the coherence function between channel 1 and channel 3 (set 2)

(c) the coherence function between channel 2 and channel 3 (set 3)

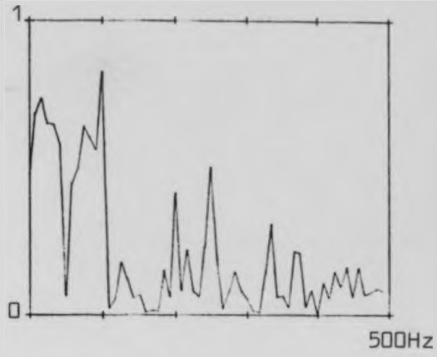

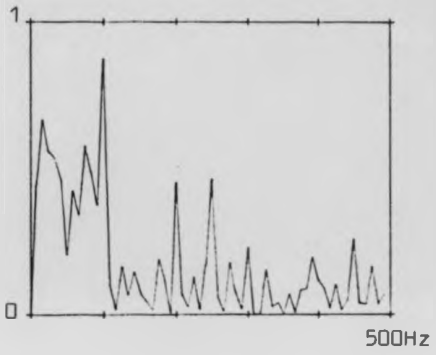

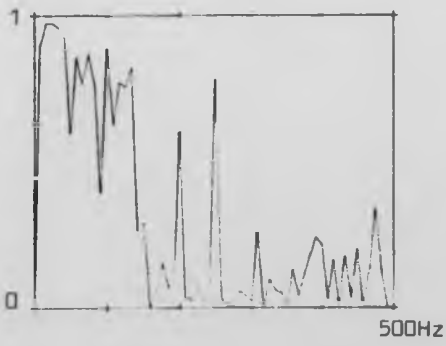

Figure 8.3 The comparison of the coherence function between three sets of recorded data, separated by 8cm.

(a) the coherence function between channel 1 and channel 2 (set 1)

(b) the coherence function between channel 1 and channel 3 (set 2)

(c) the coherence function between channel 2 and channel 3 (set 3)

(a)

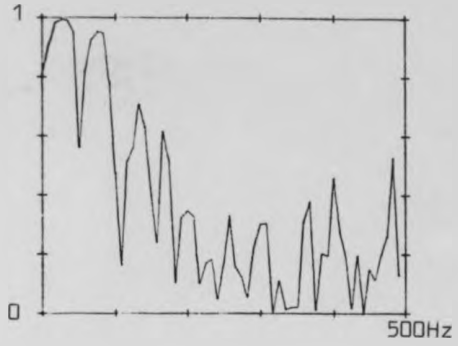

(b)

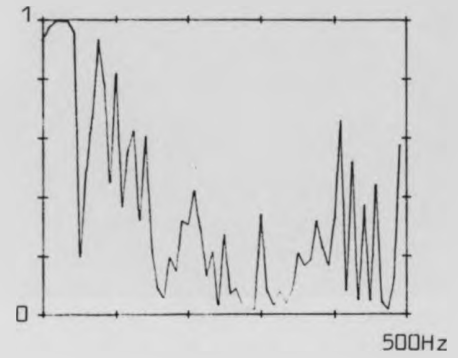

(c)

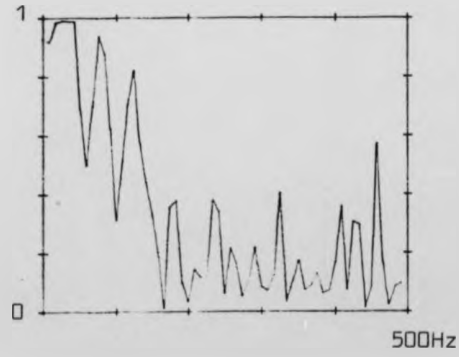

Figure 8.4 The comparison of the coherence function between three sets of recorded data, separated by 8cm.

(a) the coherence function between channel 1 and channel 2 (set 1)

(b) the coherence function between channel 1 and channel 3 (set 2)

(c) the coherence function between channel 2 and channel 3 (set 3)

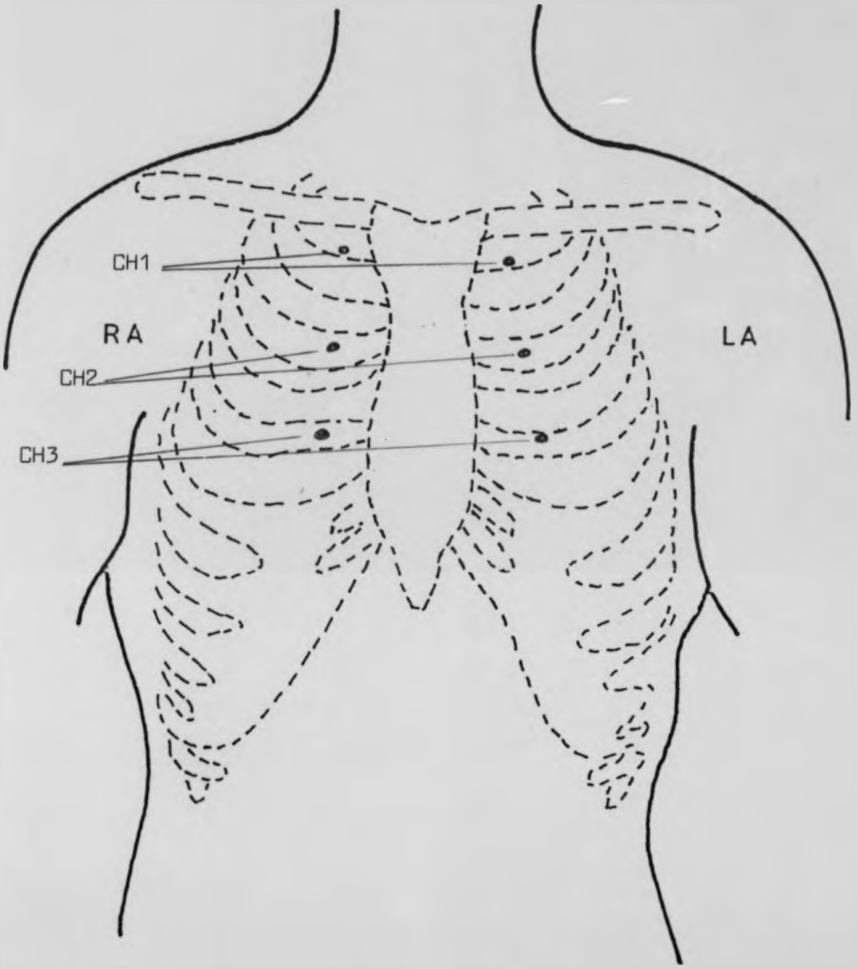

Figure 8.5 Three channels are recorded, electrodes placed as shown. There is a distance of 10mm between each pair of electrodes.

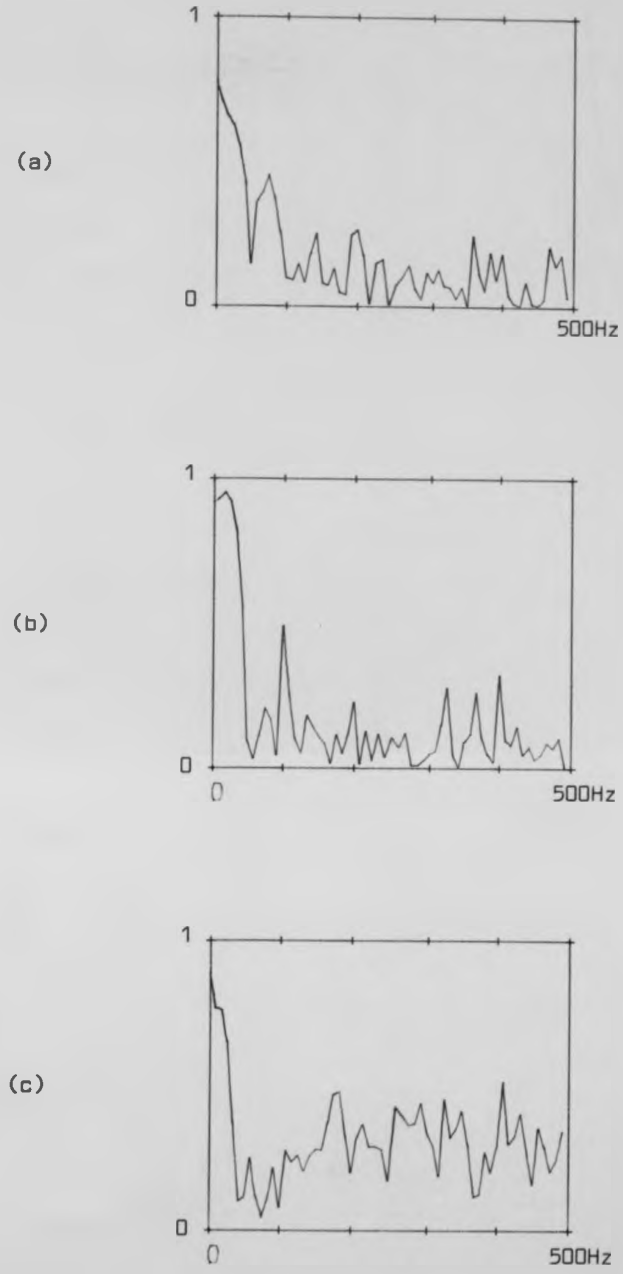

Figure 8.6 The comparison of the coherence function between three sets of recorded data, separated by 16cm.

(a) the coherence function between channel 1 and channel 2 (set 1)

(b) the coherence function between channel 1 and channel 3 (set 2)

(c) the coherence function between channel 2 and channel 3 (set 3)

8.4 Choice of adaptive filter

This section deals with the choice of algorithm and adaptive filter technique, based upon a study of characteristics of both signal and noise in typical surface electrocardiograms. Many algorithms have been derived and investigated for particular applications (Nuttal, 1981). In this study the LMS algorithm was selected for its stability and ease of use and found to be quite adequate.

One of the factors influencing the choice of adaptive filter is the nature of the signal itself and the degree to which the signal is statistically stationary. The use of LMS algorithm used in this study was found adequate to accommodate the slow statistical changes of ECG signal.

The results presented in previous sections show that a significant improvement can be obtained by using the LMS algorithm and an appropriate choice of adaptive filter configuration. To achieve satisfactory performance selection of the parameter values that influence the accuracy and resolution of the filter constitute an important initial consideration. Their choice is considered in the following section.

8.5 Initial selection of filter parameter values

Two main parameters affect the adaptive filter performance. These are the number of weights and the convergence factor which together control the accuracy of the adaptive filter and the speed to convergence. Widrow et al. (1975) have reported that the number of weights can be determined based upon the ratio of the sampling frequency to the desired frequency resolution.

Once the number of weights has been determined, the initial value of convergence factor can be chosen according to the percentage of misadjustment that can be tolerated. This is normally chosen to be approximately 10%. Selection in this way is only acceptable when the data is stationary. If the signal is non-stationary the initial selection of μ is inappropriate since the convergence factor μ should track the variation of non-stationary data.

Experimentally it was found that a number of weights, N, between 32-64 gave satisfactory results. Whilst it is quite difficult to determine the value of the convergence factor, μ, theoretically it is relatively easy to obtain the value experimentally. For the filter used in this study it was found that the best convergence could be achieved when μ has a value of 0.001, but faster convergence requires a higher value.

The results presented in figures 8.7 and 8.8 show that when N is set to 64, better cancellation can be achieved for a μ value of 0.001 than can be achieved for values of 0.1 and 0.01. This indicates that

Figure 8.7 A comparison of the effect of the filter convergence factor upon adaptive filter, the filter order N = 64

(a) the two input channels required for adaptive filter

(b) convergence factor = 0.001

(c) convergence factor = 0.01

(d) convergence factor = 0.1

Figure 8.8 A comparison of the effect of the filter convergence factor upon adaptive filter, the filter order N = 64.

(a) the two input signals

(b) convergence factor = 0.01

(c) convergence factor = 0.001

slower convergence is to be recommended for this type of application. A further study was conducted to investigate the effect of filter order upon the performance of the adaptive filter. The convergence factor μ was chosen to be 0.001 and the same data filtered for various values of N (128, 64, 32, 16, 8). Table 8.1 summarises signal-to-noise improvement with respect to filter order.

Table 8.1

Signal-to-noise ratio with respect to filter order (N).

Filter order (N)	Signal-to-noise improvement (dB)
8	5.84
16	7.62
32	8.35
64	11.77
128	8.10

The results are presented in figures 8.9 and 8.10. The degree of improvement in noise reduction is clearly influenced by the number of weights, and the use of 64 yielded the best results in the study conducted. Figure 8.10 shows a plot representing the signal-to-noise ratio improvements with respect to the number of weights employed.

Two main factors influence the performance of the adaptive filter. One is the choice of the convergence factor μ which must be selected to obtain an optimal convergence without the risk of instability. The experimental results show that when μ is 0.001, convergence appears optimal. The other factor is the choice of filter order N. This must be large enough to accommodate all significant statistical changes in the signal.

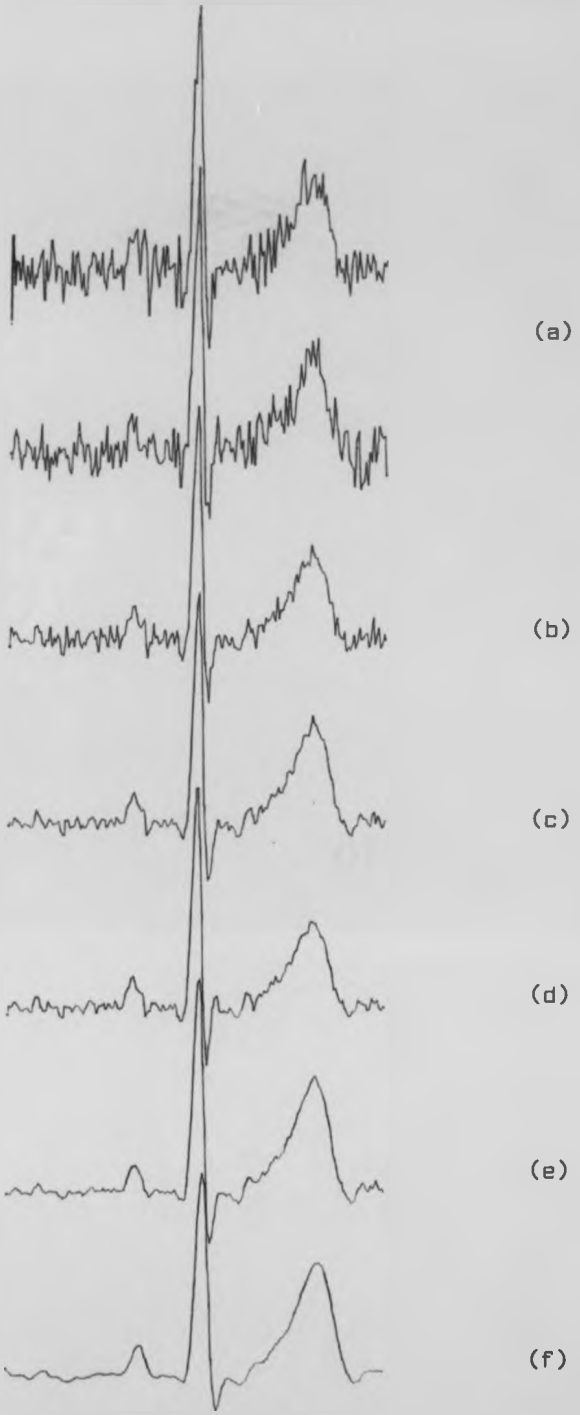

Figure 8.9 A comparison of the effect of filter order upon adaptive filter of ECG signal, the convergence factor μ = 0.001

(a) the two input channels required for adaptive filter
(b) filter order N = 8
(c) filter order N = 16
(d) filter order N = 32
(e) filter order N = 64
(f) filter order N = 128

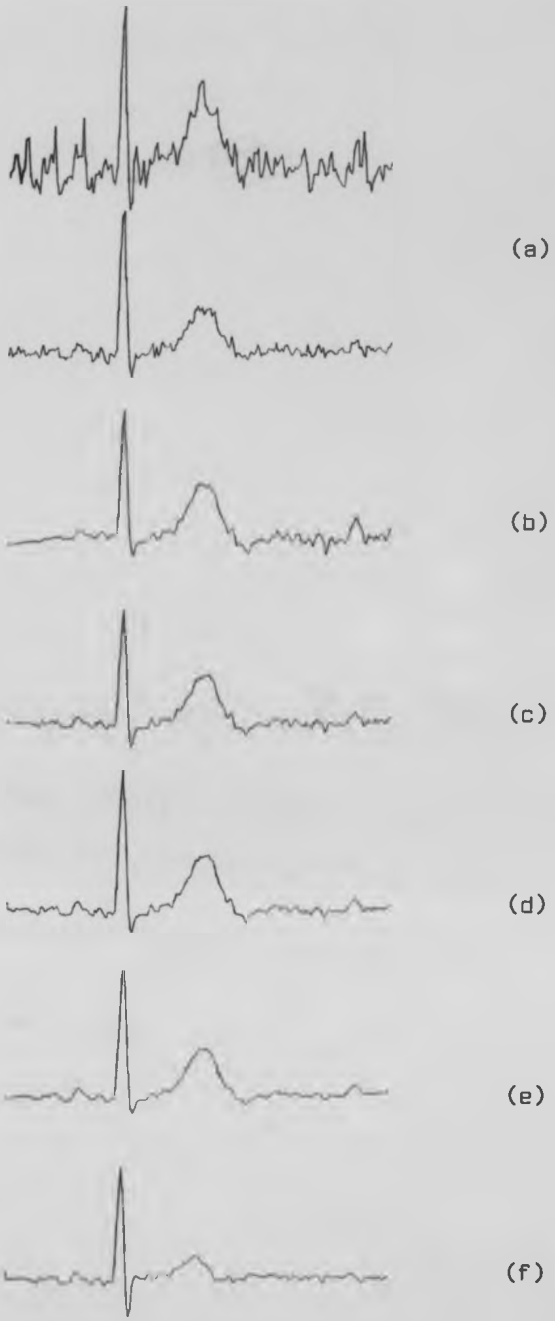

Figure 8.10 A comparison of the effect of filter order upon adaptive filter of ECG signal, the convergence factor μ = 0.001

(a) the two input channels required for adaptive filter
(b) filter order N = 8
(c) filter order N = 16
(d) filter order N = 32
(e) filter order N = 64
(f) filter order N = 128

8.6 Comparison of the adaptive filtering results

Several experiments concerning the application of adaptive filters are presented below. Firstly a computer simulation comparing the results of various adaptive filters in channel enhancement form. Secondly, the three versions of adaptive filter were applied to reduce skeletal muscle noise in exercise electrocardiograms.

The aim of the comparison was to determine which filter was likely to be most effective for achieving noise reduction with least signal distortion. Two channels of simulated ECG signal were mixed with different but known levels of noise and the noise reduction performance determined for various filter configurations. The results indicate that although in all three filter types there is an improvement in signal-to-noise ratio, considerable distortion occurs especially in using the basic LMS channel enhancer (figures 8.11 and 8.14).

In a further comparison, three filters were examined in applications to minimise noise due to skeletal muscle activity in static and exercise ECG's.

The parameter values were chosen to be the same for each filter; $N = 64$ and $\mu = 0.001$. The bandwidth of the signal was 500Hz and sampled at a rate of 1KHz. Figure 8.15 shows signal-to-noise improvement versus noise for the three adaptive filters.

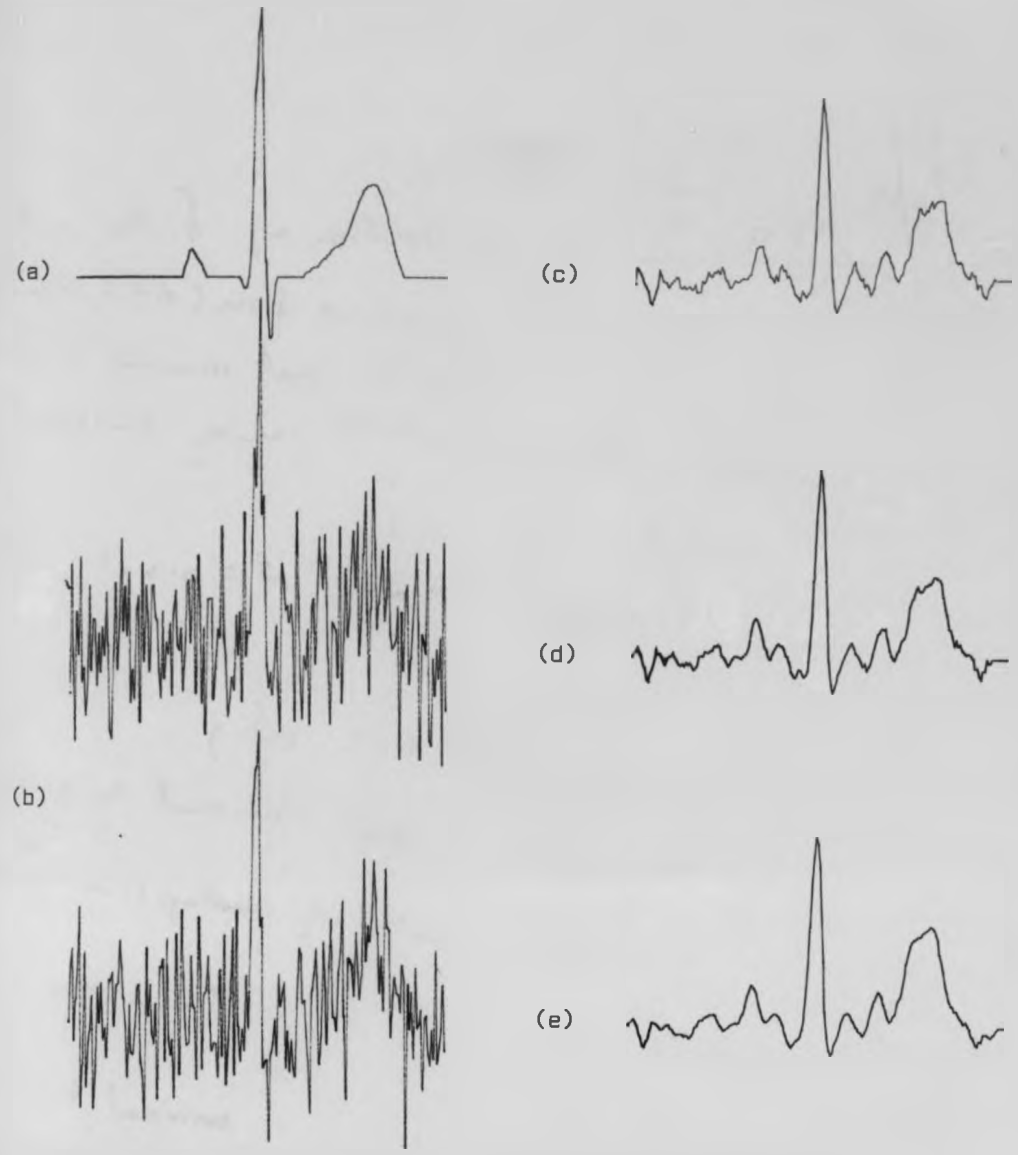

Figure 8.11 Comparison of filter outputs for the basic adaptive filter (AF), time-sequence adaptive filter (TSAF) and minimal time-sequence adaptive filter (MTSAF) using simulated data, SNR = 0.5dB, adaptation speed μ = 0.001, filter order N = 64

(a) simulated ECG only
(b) the two input channel to adaptive filter
(c) the result of adaptive filter
(d) the result of time-sequence filter
(e) the result of minimal time-sequence adaptive filter

Figure 8.12 Comparison of filter outputs for the basic adaptive filter (AF), time-sequence adaptive filter (TSAF) and minimal time-sequence adaptive filter (MTSAF) using simulated data, SNR = 5.5dB, adaptation speed μ = 0.001, filter order N = 64

(a) simulated ECG only
(b) two input channels to adaptive filter
(c) result of adaptive filter
(d) result of time-sequence filter
(e) result of minimal time-sequence adaptive filter

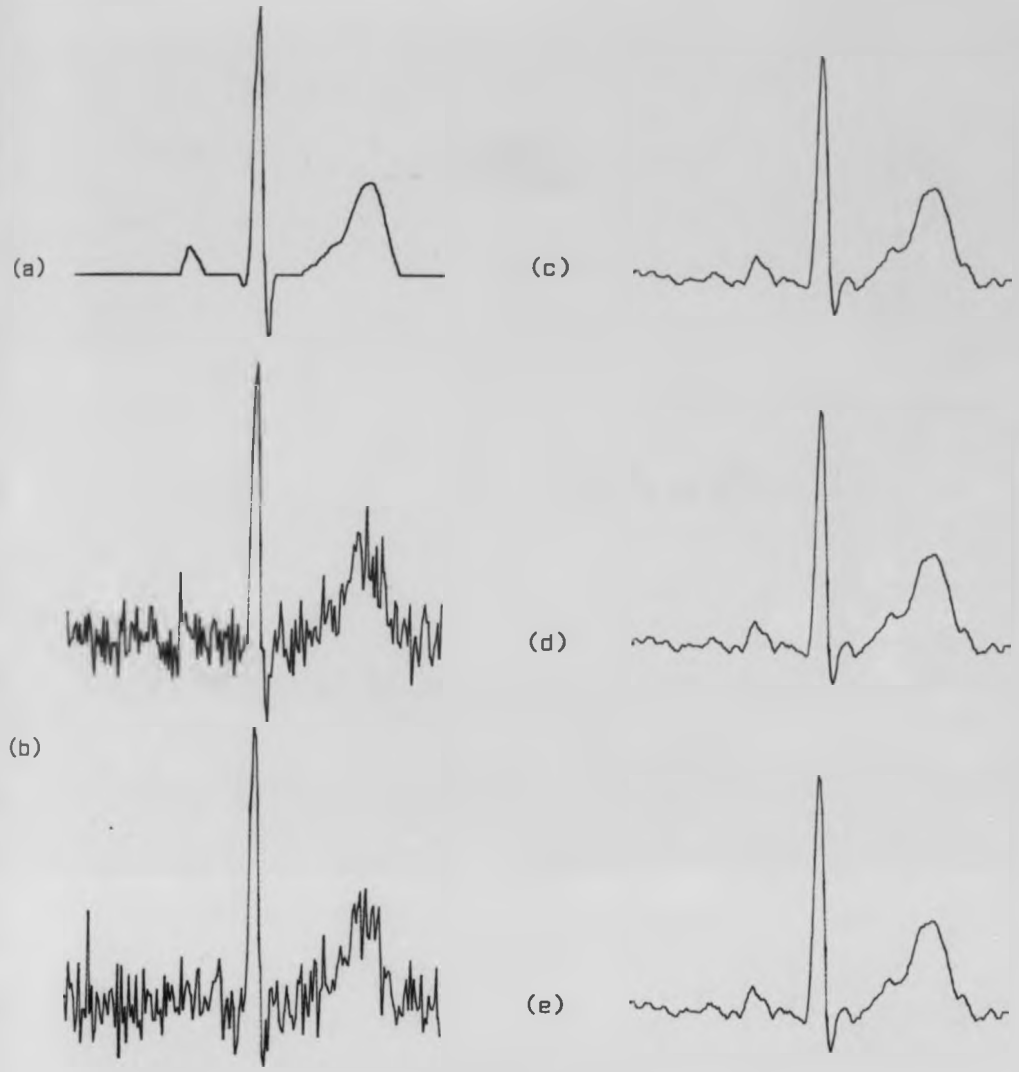

Figure 8.13 Comparison of filter outputs for the basic adaptive filter (AF), time-sequence adaptive filter (TSAF) and minimal time-sequence adaptive filter (MTSAF) using simulated data, SNR = 7.7dB, adaptation speed μ = 0.001m filter order N = 64

(a) simulated ECG only
(b) two channel input to adaptive filter
(c) result of adaptive filter
(d) result of time-sequence adaptive filter
(e) result of minimal time-sequence adaptive filter

Figure 8.14 Comparison of filter outputs for the basic adaptive filter (AF), time-sequence adaptive filter (TSAF) and minimal time-sequence adaptive filter (MTSAF) using simulated data, SNR = 13.24dB, adaptation speed μ = 0.001, filter order N = 64

(a) simulated ECG only
(b) two input channels to adaptive filter
(c) result of adaptive filter
(d) result of time-sequence adaptive filter
(e) result of minimal time-sequence adaptive filter

Figures 8.16 show the results of applying these filters in exercise tests. They again illustrate the advantage of the time-sequence and minimal adaptive filter in revealing signal buried in noise. The results also illustrate the ability to extract a signal from lead V_5 in comparison with lead V_1, where the signal components are from the same source but exhibit different structural features.

In applying a filter for noise reduction, distortion will invariably occur, the amount depending upon the filter used. Two reasons may be suggested for this:

(i) low signal and high noise levels, and

(ii) overlap of signal and noise spectra.

In order to develop techniques in which sensible convergence with minimal distortion could be achieved, a method was devised for measuring the amount of distortion. This is presented in the following section.

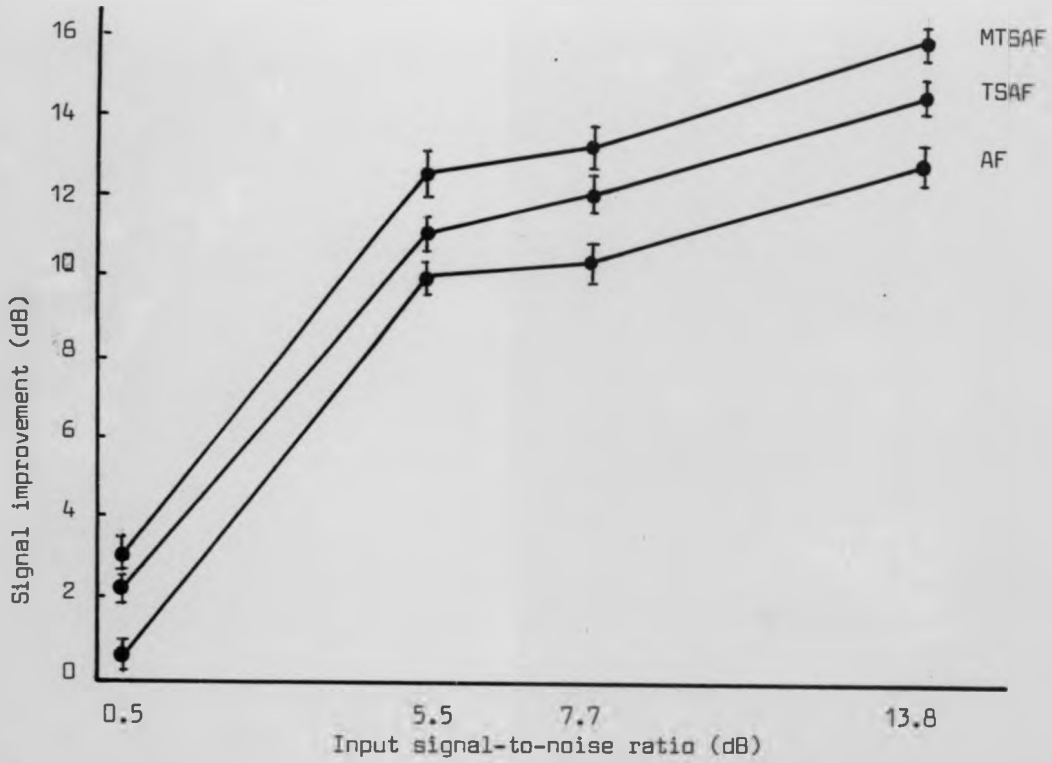

Figure 8.15 Shows the improvement of signal-to-noise ratio for three different adaptive versions, AF, TSAF, and MTSAF.

Figure 8.16 Comparison of filter outputs for the basic adaptive filter (AF), time-sequence adaptive filter (TSAF) and minimal time-sequence adaptive filter (MTSAF) using real exercise ECG. The adaptation speed μ = 0.001, filter order N = 64

(a) the input channels to the adaptive filter
(b) result of adaptive filter
(c) result of time-sequence adaptive filter
(d) result of minimal time-sequence adaptive filter

8.7 Signal distortion

Signal distortion can be defined as the extent to which a system or component fails to reproduce accurately at its output, the form of the input. At least two channels are required for the application of the basic adaptive filter, the primary channel which contains the signal and noise, and a second input that contains a noise-free reference signal which is correlated to the noise in the primary input. The available reference input may contain low-level signal components in addition to the correlated noise in the primary input and still be accommodated by the adaptive noise canceller. However, under these conditions the low-level signal components will cause some cancellation of the primary input signal and distortion will occur at the filter output.

In applying the time-sequence or multichannel adaptive filter for the applications stated earlier, the requirement for cancellation is for two input channels in which both can contain signal plus noise. However, for effective results the noise components should be uncorrelated, and the signals, which need not be of the same waveshape, should exhibit the same frequency spectra.

Signal distortion normally occurs in the use of these adaptive filters when the spectra of the signal and the noise overlap. For Example, figure 3.10 shows that in the lower frequency range 0 - 70Hz, the noise components overlap with the ECG signal components (although the noise is 22dB below the signal power). The amount of noise depends upon the activity of the skeletal muscles, as discussed fully in Chapter two, and of the interference from external sources. Therefore the amount of distortion depends upon:

(i) signal-to-noise ratio at the input,

(ii) the amount of overlap between signal and noise spectral components, and

(iii) the channel propagation characteristics for the signal in propagating through the adaptive filter.[4]

The results indicate that the higher the signal-to-noise ratio at the input, the lower will be the distortion at the output.

Two separate sets of experiments were carried out to examine distortion in the P, QRS and T waves. The first of these involved the use of simulated data mixed with white noise as a filter input. Different levels of white noise were added to the same simulated ECG signal and the performance of the filters examined. Figure 8.17 shows the simulated ECG which is represented by a dotted line, superimposed upon the filtered result of a simulated ECG corrupted by noise. The figure shows;

(a) the signal and noise with different noise levels in the top trace,

(b) the results of using an LMS adaptive filter in the middle trace,

(c) the results of time-sequence adaptive filtering in the bottom trace.

The distortion values were calculated and are presented in graphical form in figure 8.18. In this figure the top trace indicates the distortion in applying adaptive filter for four noise levels in the P, QRS and T waves, while the bottom trace shows the same signals after applying the time-sequence adaptive filter. It is clear that less distortion arises in using the time-sequence adaptive filter than the

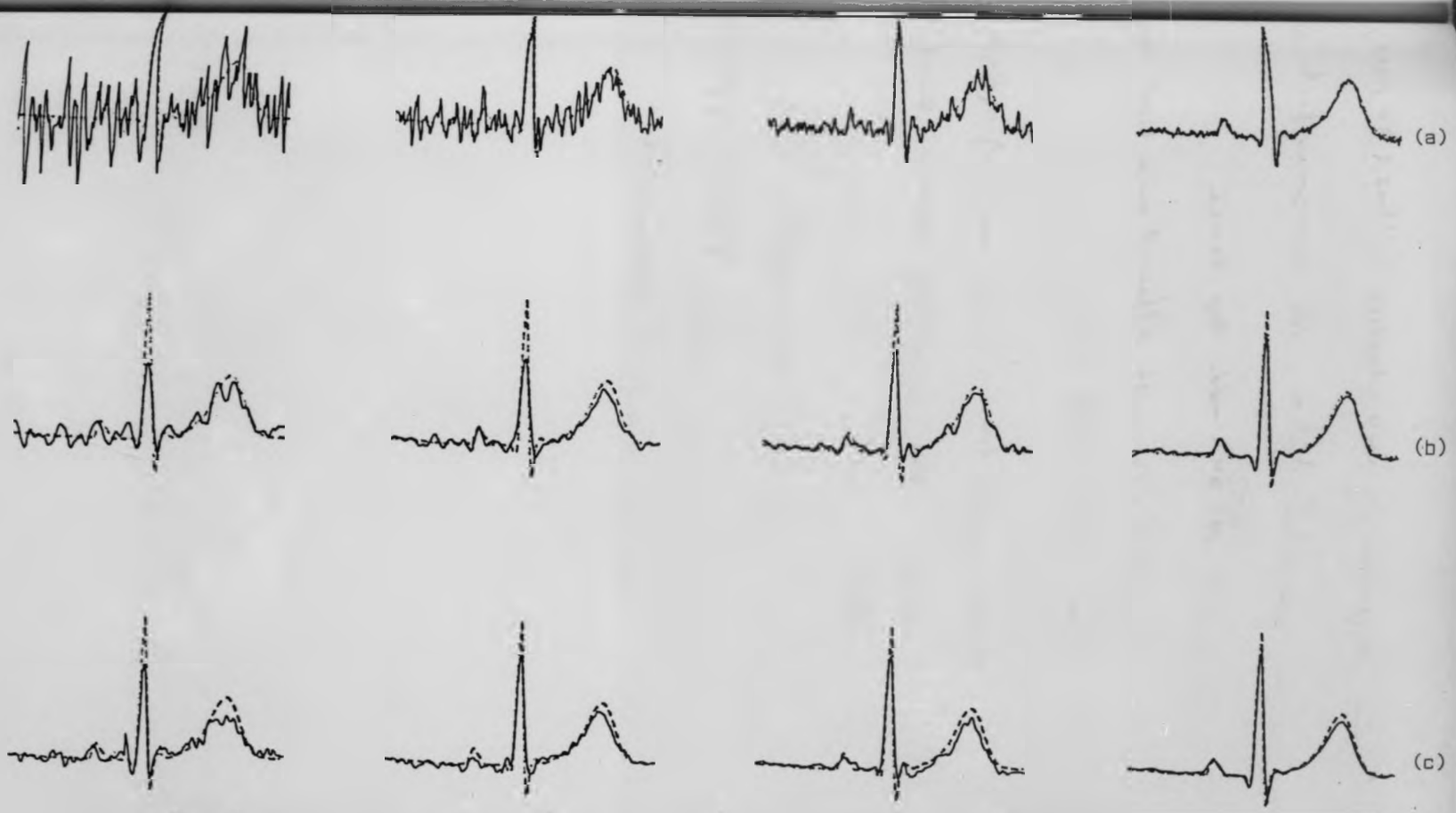

Figure 8.18 Comparison of two adaptive filters (AF, TSAF) using simulated data, the convergence factor $\mu = 0.001$

(a) simulated ECG with different noise levels superimposed upon dotted simulated ECG
(b) result of applying adaptive filter, noise level superimposed on dotted simulated ECG
(c) result of applying time-sequence adaptive filter, noise level superimposed on dotted simulated ECG.

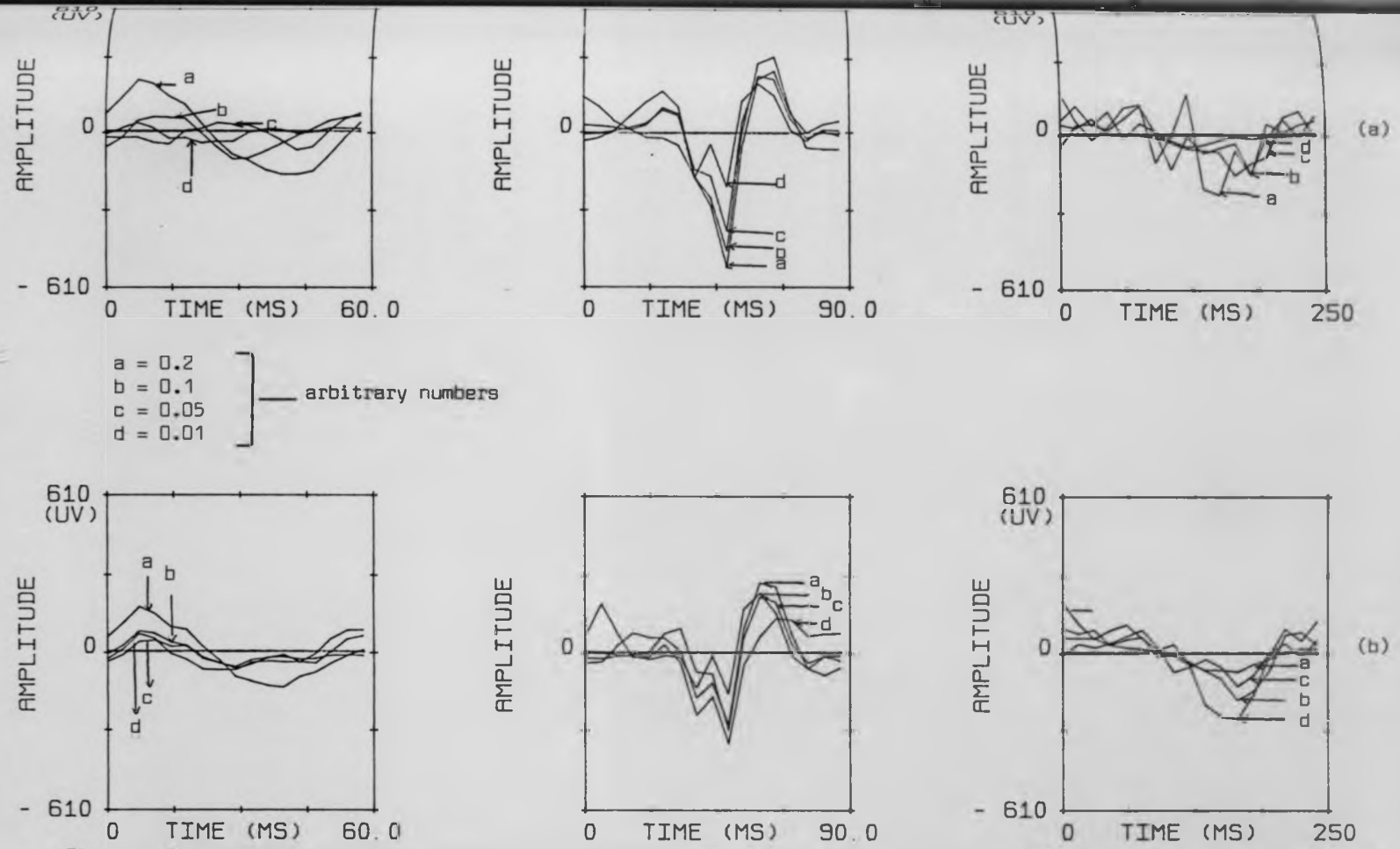

Figure 8.18 Comparison between amplitude distortion through the use of adaptive and time-sequence adaptive filter for four different noise levels.

(a) indicates the distortion in the P, QRS and T waves in applying adaptive filter for different noise levels

(b) indicates the distortion in the P, QRS and T waves in applying time-sequence adaptive filter for different noise levels

use of the basic adaptive filter in a channel enhancer form. This is due mostly to the fact that in the use of the channel enhancer the adaptive filter may start to converge very effectively within the isoelectric intervals, but on entering the QRS or T waves the coefficients become disturbed, and distortion occurs. However, in the time-sequence adaptive filter, each segment is controlled by a particular set of weights and disturbance of the weights is avoided.

The results of the real data study are presented in figures 8.20 and 8.19. Again, the advantages of time-sequence adaptive filter over channel enhancer are well indicated, although the use of more than two input channels in the channel enhancer methods can reduce distortion considerably, but at the expense of increased cost.

Figure 8.21 shows the percentage improvement in distortion of the time-sequence adaptive filter over the channel enhancer. It also shows that the amount of distortion is increased in both techniques as the noise level is increased. Experimentally, the amount of distortion is found to be approximately 2%. The output noise level can be reduced if more than two input channels are used with the appropriate choice of adaptive filter.

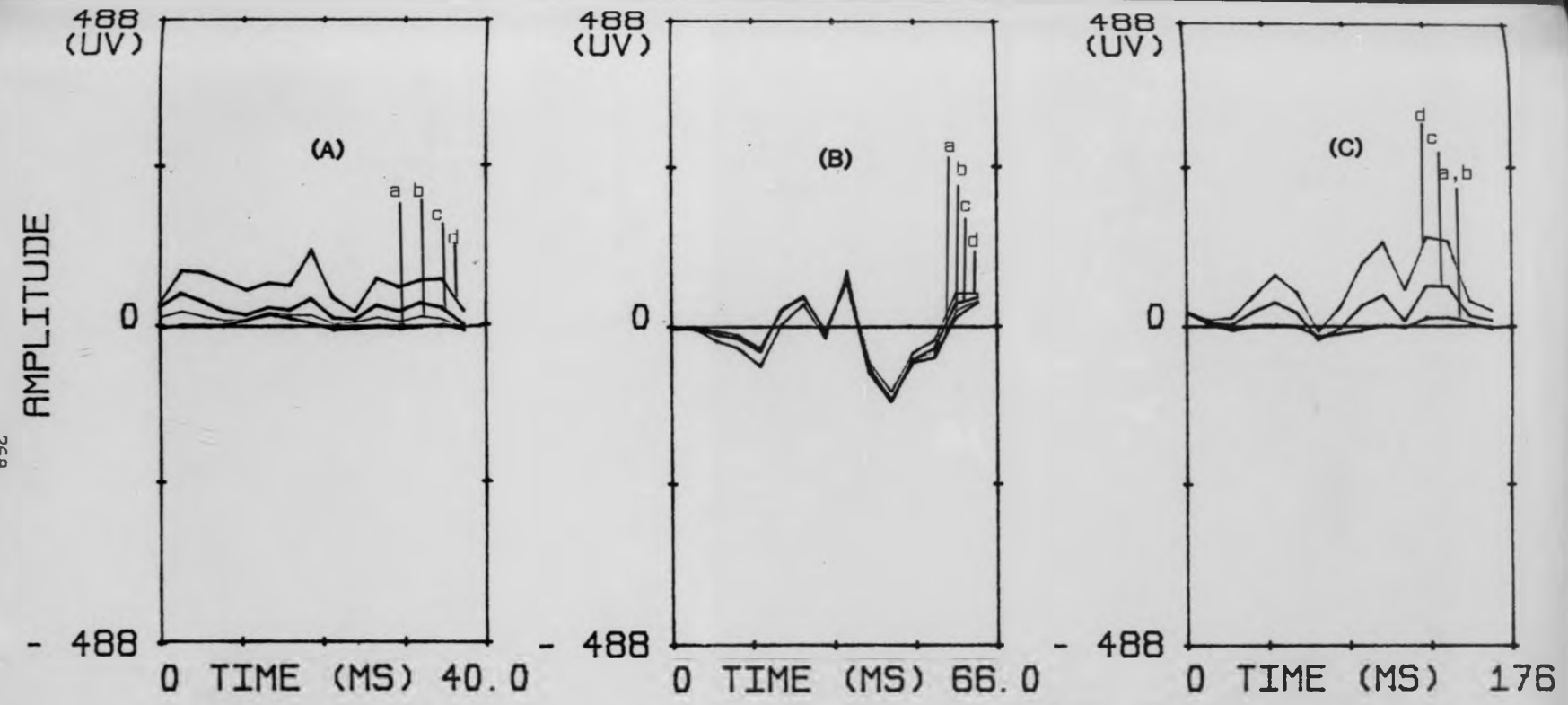

Figure 8.19 Result of amplitude distortion in applying time-sequence adaptive filter, using real data for four different noise levels (a = 0.2, b = 0.1, c = 0.05, d = 0.01)

(A) amplitude distortion in P wave
(B) amplitude distortion in QRS complex
(C) amplitude distortion in T wave

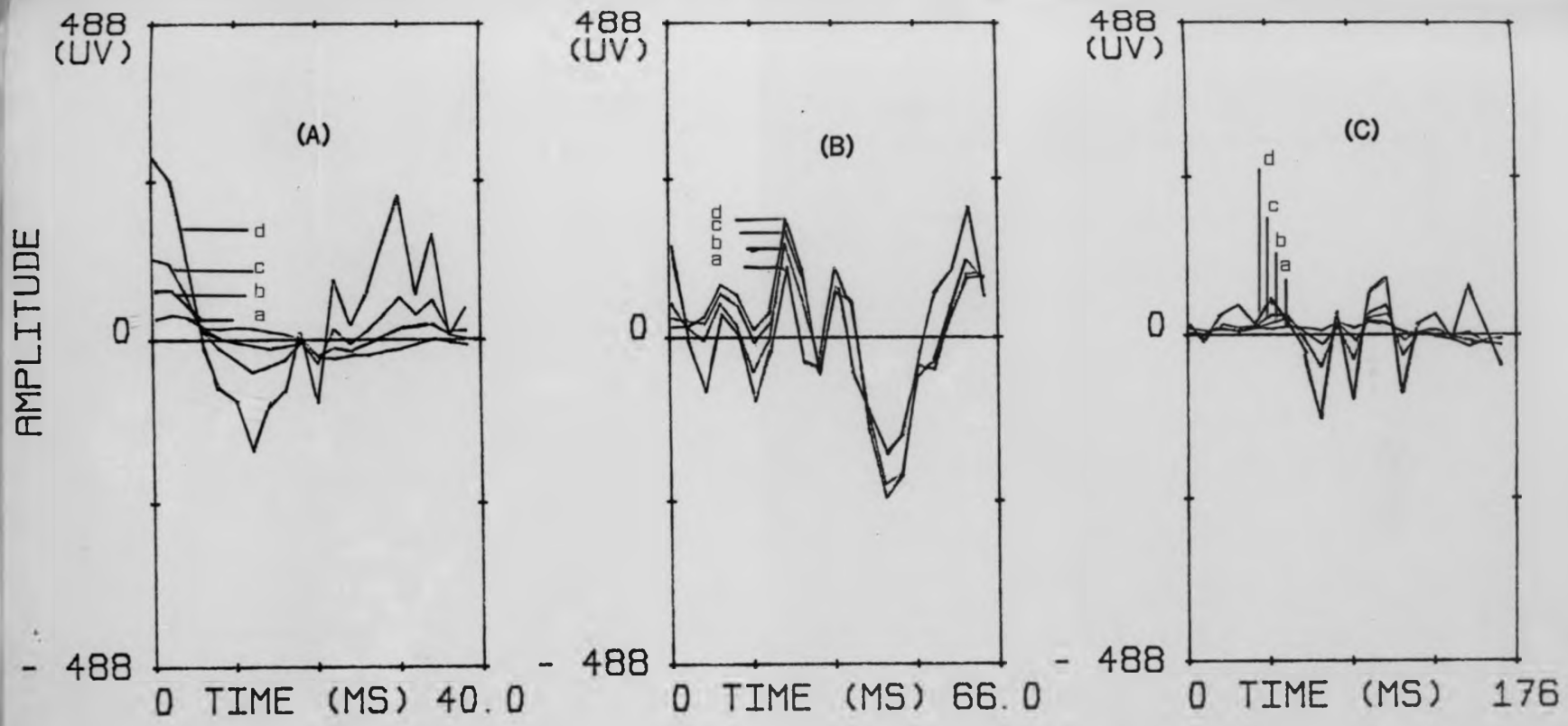

Figure 8.20 Result of amplitude distortion in applying adaptive filter, using real data for four different noise levels (a = 0.2, b = 0.1, c = 0.05, d = 0.01)

(A) amplitude distortion in P wave
(B) amplitude distortion in QRS complex
(C) amplitude distortion in T wave

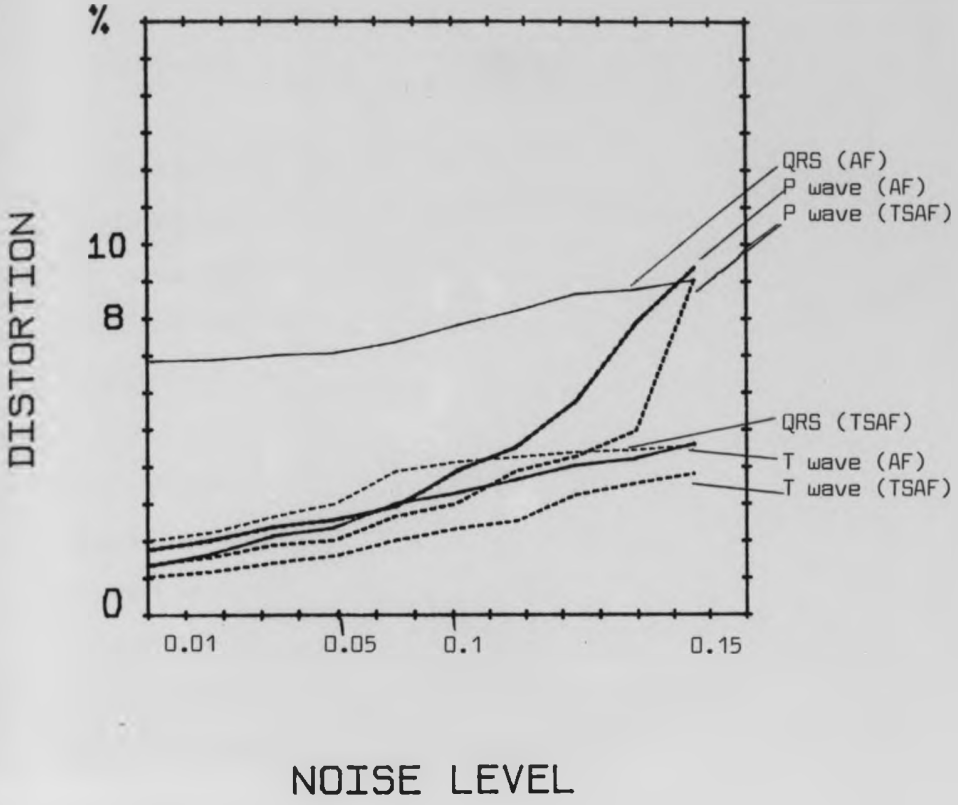

Figure 8.21: Represents the percentage improvement in distortion of adaptive and time-sequence adaptive filters.

The distortion is measured by taking the root mean square (RMS) value of the output to the RMS value of the input.

8.8 Conclusion

The presence of noise and artifacts can obscure important features in ECG records during patient monitoring and during exercise testing. Several approaches to ECG filtering have been proposed in Chapter Three, and adaptive filtering selected as a technique for further study.

Since, in practice, both noise and artifacts may overlap within the frequency band of ECG 0.005 - 100Hz, complete separations of signal and noise using the non-adaptive filtering techniques mentioned in Chapter Three is impossible. Adaptive filtering may overcome this problem but the result is a compromise between distortion of the signal and reduction of noise and artifact.

In this chapter the result of adaptive filtering technique in the form of channel enhancer and time-sequence adaptive filtering have been presented for both simulated and real data. The amount of distortion arising as a result of filtering after applying the appropriate parameter values, has been calculated and presented. The results suggest that the time-sequence adaptive filter can reduce noise and artifacts with less signal distortion, especially in P and T waves, compared with adaptive channel enhancer.

Chapter Nine: Conclusions

9.1 General Discussion of results

The experimental results in the previous chapters have demonstrated that significant improvment in the recording of ECG can be obtained by enhancement of the ECG signal from the skeletal muscle activity using the application of adaptive filtering. The results also demonstrated the superiority of the adapitive filtering over the other filtering processes, including signal averaging.

The ability to use adaptive filtering in the applications considered is based upon the observation that the ECG signals in two discrete leads are highly correlated, whilst the noise is largely uncorrelated particularly if the leads are well separated. In applying the adaptive techniques, a number of assumptions were made. Among these it was assumed that two channels could be distinguished in which the noise contents were uncorrelated with respect to each channel and to the ECG signal. The results indicated that such channels could indeed be distinguished.

Perfect cancellation can be obtained if the conditional requirement of adaptive channel enhancer is fully met. In practice, perfect cancellation cannot be achieved. If, for any reason, some of the background noise components were in one way or another correlated with signal components, then distortion occurs. Distortion for various versions of adaptive filters were examined and the results were

presented as in figures 8.18 - 8.20. Time-sequence adaptive filters were found to exhibit less distortion than the basic adaptive filter. It was also found that higher signal-to-noise improvement can be obtained if more than two channels are used in the adaptive filtering process.

The use of time and minimal sequence adaptive filters appear to have been justified as a means of tackling the problem of the non-stationarity of a signal and its effect upon the performance of the enhancement process. Although at one stage consideration was given to applying faster algorithms, appropriate selection of the convergence factor obviated this need.

The most important application considered for adaptive filtering in this study was its use in exercise electrocardiography. The study has shown that successful noise cancellation can be accomplished and it is likely to be accepted as an important attribute in obtaining good exercise ECG's. Although some difficulties were encountered in these experiments especially in cases where excessive base line variation was evident, a method was developed to overcome this problem. These results indicated a substantial improvement by use of adaptive filtering and the superiority of the technique over many others, especially for precordial leads when two channels such as V_1 and V_5 are readily available for inputs to the adaptive filters.

Detection of low level signals, representative of those associated with the specialised conduction system, may be facilitated by the use

of adaptive filters. The initial results, based upon simulated data, indicate the possible advantages of using this method. Further research is required.

Some difficulties with the use of adaptive filters were overcome in the early stages of this research. These involved the proper selection of filter order and the convergence factor. The study has shown in general that successful noise cancellation can be achieved and the results presented in Chapters six, seven and eight indicate the best parameter values for adaptive filtering.

In most of the experiments reported in the study, it has been found that the minimal time-sequence adaptive filter can exhibit a superior result in signal-to-noise improvement compared with the basic and time-sequence adaptive filter.

In practical terms, the technique could be applied to reveal microvolt events within the ECG, providing attempts are made to obtain recordings that exhibit high initial values of signal-to-noise ratio.

9.2 Suggestions for further work

There are a number of issues arising out of this investigation that could form the basis of future research. One is the application of the adaptive filtering process for the detection, further study and verification of cyclo-stochastic perturbations. These perturbations and the associated abnormalities have been investigated by the PISA method (Prasad & Gupta, 1981, 1981). Simulations of cyclo-stochastic perturbations in noise have been used as the basis of enhancement studies using adaptive filtering and the results appear quite promising.

Because of the importance of the specialised conduction system in determining the sequence of activation of the working myocardium and in turn to the mechanical events of the heart, the surface acquisition of potential variations related to the system are likely to be of diagnostic value.

A further area for future study is the use of dual channel minimal time-sequence adaptive filters to cancel out the noise due to skeletal muscle activity during exercise electrocardiography, by using different convergence factors in each particular segment of the ECG. Further improvements in signal-to-noise ratio and reduced distortion may be expected.

Further research is required on the use of multichannel recording, especially with respect to precordial leads in which the signals

occupy the same frequency spectrum, but exhibit different morphology. Having achieved good results with simulated data, it is expected that the application will improve the signal-to-noise ratio, dependent upon the number of channels used.

The principal conclusion to be derived from this study is that the channel enhancer together with time and minimal sequence adaptive filters provide the basis for improvement of ECG recording systems capable of reducing high levels of noise, of differing characteristics. Moreover, it provides the basis for systems that could extend the clinical usefulness of surface derived ECG's by revealing events that are otherwise obscured. Such systems would initially find application in research studies, but the results may eventually lead to the use of such techniques in routine clinical practice.

Annex A

The specification of instrumentation amplifier

Introduction

The 4430 instrumentation amplifier used in this study (Ormed Limited) is primarily designed for ECG with ten standard lead positions and provides patient isolation and protection from diathermy burns. This amplifier is not connected to any input circuit within the cabinet, but it has its own front panel input socket.

The full specifications for the amplifier are listed below:

Specification	
Sensitivity	Input of 30µv/division to 250µv or 1.5mV to 12.5mV for 1volt across 10K ohms load.
Gain Steps	2.5mV, 5mV inputs for 1volt across 10K ohms load, or 50µv, 100µv, 200µv/division. Fine gain control gives 0.25 to 1.75 times each range.
Gain Accuracy	+2% range to range.
Gain Stability	+0.03%/°C over the range 0°C to 40°C.
Zero Stability	Less than 0.7% of f.s.d./°C.
Input Circuit	Differential, 10Mohms resistance isolated from ground. Common mode, input capacitance 170pF in parallel with 68 ohms. A five-way isolated ECG socket is mounted on the front panel.
Leakage Current	12µA with 240 volts at 50Hz applied to the input circuit.

H.F. Frequency	-3dB at 5kHz.
H.F. Cut	-3 dB at 10, 25 and 50Hz +20%, with 6dB octave roll-off.
Time Constant	3.5 seconds, +20%.
CMR Ratio	Greater than 100,00:1 (100dB) at 1.5Hz and 50Hz.
	Electrode resistance imbalance less than 2Kohms.
Common Mode	+500 volts peak, d.c to 50Hz.
Voltage Range	
Nominal Output	+1 volt.
Maximum Output	+2.5 Volts.
Maximum Output	+1.2mA.
Slew Rate of	Greater than 50mV/µS.

Output Resistance 130 ohms

Noise Level	Less than 0.5 division on chart or 20µV peak-to peak at maximum band-width on oscilloscope, with 1 Kohm source.
	The unit can withstand an input overload of 5kV, phase or anti-phase, for up to 1.5mS.
Anti-blocking	Automatic anti-blocking mutes the amplifier for one second in the presence of an overload signal. The amplifier is muted when the lead selector switch is operated.
Calibration	A 1mV +2% internal calibrate signal can be injected in series with the input.
Power Requirements	+12V at 77 A, -12V at 52mA. Pump supply, 4.25MHz +1% at 1V peak-to-peak +2% and 0.5mA.

The ADC has a range of -5 to +5 volts, while the tape recorder has a maximum output of approximately 1.4volts rms, an additional pre-amplification was used in order to provide a full use of the ADC resolution.

In order to process the data recorded using PDP 11/23, it is necessary to sample and store the raw data. To do this a sampling rate of 1 and 2 msec. was chosen. To avoid error is sampling due to aliasing, it is well-known that signal components must not exist above half the sampling frequency, which is known as Nyguist frequency.

Annex B

A Design for a low-pass digital filter

A low-pass digital filter was designed similar to the filter presented by Lynn (1971), with a linear phase in which the poles and zeros lie on the unit circle in the $\bar{z}$-plane. The pole-zero configuration of a low-pass digital filter can be seen in Figure B1.

A low-pass filter with an integral constant k = 3 can be described by its $\bar{z}$-plane transfer function $H(\bar{z})$, which may be expressed in terms of a set of $\bar{z}$-plane poles and zeros as follows:

$$H(Z) = \frac{k(\bar{z}-z_1)(\bar{z}-z_2)(\bar{z}-z_3)\ .....}{(\bar{z}-p_1)(\bar{z}-p_2)(\bar{z}-p_3)\ .....} = \frac{Y(\bar{z})}{X(\bar{z})} \quad .... B1$$

where $z_1, z_2, z_3, ...$ are $\bar{z}$-plane zeros.

$p_1, p_2, p_3, ...$ are $\bar{z}$-plane poles.

k is a constant

$X(\bar{z})$ is the $\bar{z}$-transform of the input

$Y(\bar{z})$ is the $\bar{z}$-transform of the output.

The recursive filter relationship in the time domain is:

$$Y(n) = Y(n-3) - 3Y(n-2) + 3Y(n-1) - X(n-21) + 3X(n-14) - 3X(n-7) + X(n) \quad ... B2$$

where Y(n) represents the present output sample value,

Y(n-1) represents the previous output value, and so on, and the X terms represent input sample values.

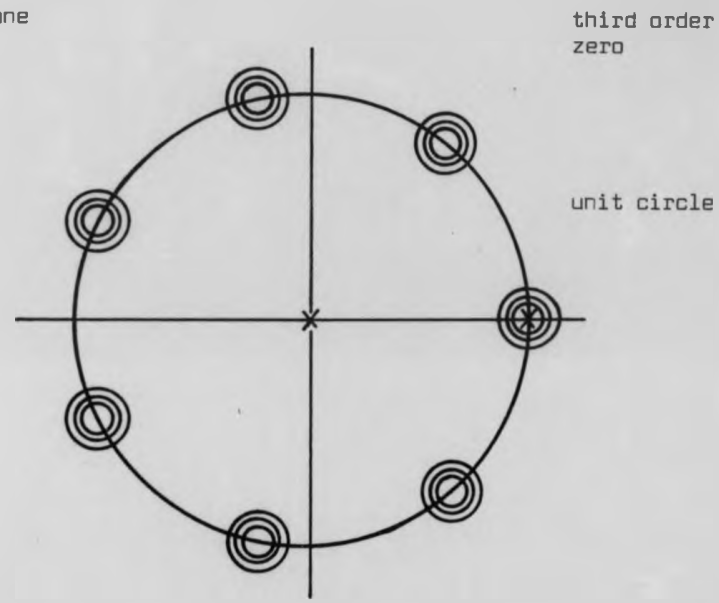

Figure 81 Pole - zero configuration of a low-pass digital filter having linear-phase characteristics.

O zero

X pole

Using Z-transform notation, the equivalent frequency domain of equation B2 becomes:

$$H(z) = \frac{Y(z)}{X(z)} = \frac{1 - 3z^{-7} + 3z^{-14} - z^{-21}}{1 - 3z^{-1} + 3z^{-2} - z^{-3}} \qquad \ldots\ldots B3$$

The coefficients were calculated from the general formula after selecting the number of poles and the cutoff frequency.

Annex C

This annex shows the program list for applying an adaptive transversal filter to the ECG. In its early investigation, using 32 filter order with 0.01 convergence factor, it also shows a subroutine to plot the input/output result.

```
      Dimension IDATA (2,3600),W(32)
      Common IDATA, ISAM
      DATA NSAM/3600/,NCOF/32/
      DATA W/32*.01/
      Type 10
      Format (' LMS Adaptive Transversal Filter'//' Enter U:'$)
      Accept 11,U
      Format (F10.8)
      IPOINT=NCOF+1
      Type 9
9     Format (' Use Data From File?'$)
      Accept 16, IReply
      If (IReply.NE. 'Y')Goto 8
      Open (Unit=3,Name = 'DY0:3Dat', Type = 'Unknown',
     @ CarriageControl = 'None', ERR=99, Form = 'Unformatted')
      Read(3) IDATA, ISAM
      Close(Unit=3)
      Goto 22
8     Type 14
14    Format ('Enter Sampling Period:'$)
      Accept 11, SAM
      ISAM=SAM*1000.0
C     Read Input Samples
      Call ADC(ISAM,IDATA,2,NSAM,IFLAG,0)
      IF(IFLAG.NE.1) Goto 2
      Type 20
```

```
20  Format ('ADC Error')
    Goto 1
2   Open (Unit=3,Name='DYO:3DAT'.TYPE='UNKNOWN',
  @ Err=99, CarriageControl = 'None', Form = 'Unformatted')
    Write (3) IDATA, ISAM
    Close (Unit=3)
22  Type 15
15  Format ('Plot Input Waveform?(Y/N)'$)
    Accept 16, IReply
16  Format (A1)
    if (Reply. EQ.'Y')Call Plot (1)
C   Form Output and Error
    DO 300 I=IPoint, NSAM
    Y = 0.0
    DO 200 J=1, NCOF
    Y = Y+W(J)*IDATA(1,I - J)
200 Continue
    E = IDATA(2, I -1)-Y
C   Updata Coefficients
    C=2*U*E
    DO100 J = 1,NCOF
    W(J)=W(J)+C*IDATA(1,I-J)
100 Continue
    IDATA(2,I-NCOF)=Y
    IDATA(1,I-NCOF)=E
300 Continue
    Type 17
17  Format ('Plot Noise Canceller Output?'$)
    Accept 16, Reply
    If (IREPLY. EQ'Y' IREPLY)
    Type 18
18  Format (' Plot Filter Output?'$)
    Accept 16, Reply
    If (IREPLY. EQ'Y') Call Plot 2
```

```
      Type 19
 19   Format (' Continue?'$)
      Accept 16, IREPLY
      If (IREPLY. EQ. 'Y') Goto 1
      Stop
 99   Stop 'File Error'
      End

      Subroutine Plot (I)
      Dimension IDATA (2,3600)
      Common IDATA, ISAM
 1    Type 10
 10   Format ('Enter Starting Coordinates"'$)
      Accept 11, IX, IY
 11   Format (214)
      Type 13
 13   Format ('Enter Amplitude Scale Factor"'$)
      Accept 14.IYS
 14   Format (15)
      Type 17
 17   Format ('Enter Time Scale (MS/MM):'$)
      Accept 18, TScale
 18   Format (F8,3)
      Type 15
 15   Format ('Enter Trace Duration (MS):'$)
      Accept 18, Time
      Call Move (IX,IDATA II,1)/IYS+IY)
      INC=ISAM/(100.*TScale)
      N=Time*1000 ./ISAM
      DO 100 J=1,N
      Call Draw (J*INC,IDATA (I,J).IYS+IY)
 100  Continue
      Call Move (IX.IY)
      Type 21
 21   Format ('Repeat?'$)
      Accept 22, IReply
 22   Format (A1)
      If (IReply,EQ,'Y' Goto 1)
      Return
      End
```

Annex D

Most of the tape recorders produce some noise within the recorded signal. Surface recording of the ECG were recorded on the low noise BASF tape using a Bell and Howell FM recorder having the following specifications:

Gain	Unit
Bandwidth	0.1 - 6 KHz
Signal to noise ratio	46dB $\frac{Rms}{Rms}$ with the noise canceller on
	40dB $\frac{Rms}{Rms}$ without the noise canceller
Total harmonic distortion	(1 - 5)%
Input level	1 volt r.m.s.. (2.5 p.p)
Input impedance	100k

Annex E

Method to test the Stationarity of the ECG

Any biomedical data can be characterised in terms of its statistical properties (Bendat, 1962, 1964). Stationarity means that the statistical properties computed over the ensemble of all the data must not vary with time. The statistical property of a signal can be evaluated by its mean and its variance, or by its power spectrum if it is in frequency domain.

The test of stationarity may be conducted by either of the following methods:

(a) The ensemble test, which can be conducted by taking the ensemble average of the data with respect to time. If the result of the ensemble average does not vary with the variation of time, the data is said to be stationary, otherwise, the data is non-stationary.

(b) A progressive mean test (Bendal & Peirsol, 1966), implemented in the following way;

(i) by taking a length of record sampled in accordance with the Nyquist criterion,

(ii) segmenting the record into N equal time intervals,

(iii) calculate the mean values of the individual segmented intervals,

(iv) calculate the mean square value of the whole record,

(v) choose an appropriate percentage level of significance, $\alpha = 0.05$.

(vi) by taking the mean square value as a line of reference on the plots of mean values against number of samples, the number of 'runs'

is determined. A 'run' may be defined as the number of times the data is partitioned by the mean square value line.

If the number of runs falls within the values cited in Table E1 for specified limits, then the data is said to be stationary.

The record was segmented into N = 10, 20 and 100 segments and the means were plotted with respect to the number of samples (figures E1, E2 and E3).

The test indicated that the data considered was stationary, with N = 10 and 20 and becoming non-stationary as N increases to 100.

Table E1

Percentage Points of Run Distribution

Values of $r_{n,\alpha}$ such that Prob $[r_n > r_{n,\alpha}] = \alpha$, where $n = N_1 = N_2 = N/2$

	α					
n = N/2	0.99	0.975	0.95	0.05	0.025	0.01
5	2	2	3	8	9	9
6	2	3	3	10	10	11
7	3	3	4	11	12	12
8	4	4	5	12	13	13
9	4	5	6	13	14	15
10	5	6	6	15	15	16
11	6	7	7	16	16	17
12	7	7	8	17	18	18
13	7	8	9	18	19	20
14	8	9	10	19	20	21
15	9	10	11	20	21	22
16	10	11	11	22	22	23
18	11	12	13	24	25	26
20	13	14	15	26	27	28
25	17	18	19	32	33	34
30	21	22	24	37	39	40
35	25	27	28	43	44	46
40	30	31	33	48	50	51
45	34	36	37	54	55	57
50	38	40	42	59	61	63
55	43	45	46	65	66	68
60	47	49	51	70	72	74
65	52	54	56	75	77	79
70	56	58	60	81	83	85
75	61	63	65	86	88	90
80	65	68	70	91	93	96
85	70	72	74	97	99	101
90	74	77	79	102	104	107
95	79	82	84	107	109	112
100	84	86	88	113	115	117

Table adapted from Bendal & Peirsol, 1966.

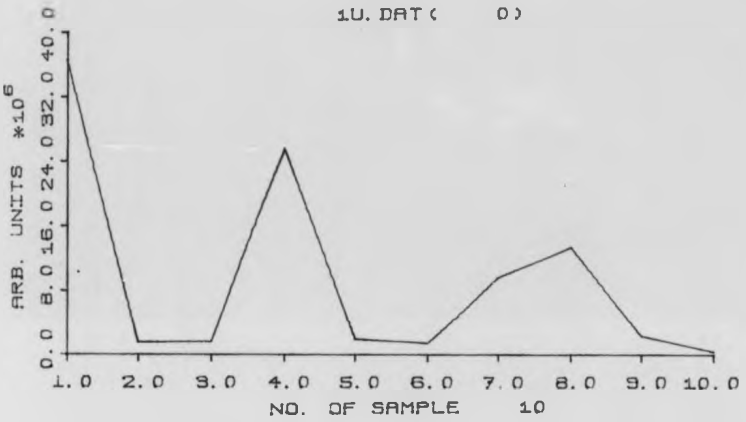

Figure E1 The plot of the mean with respect to number of samples.

Number of samples N = 10

Number of runs = 6

$n = \frac{N}{2} = 5$

α - between 0.95 and 0.025

the mean square value is 9.4×10^6, the data behave stationary.

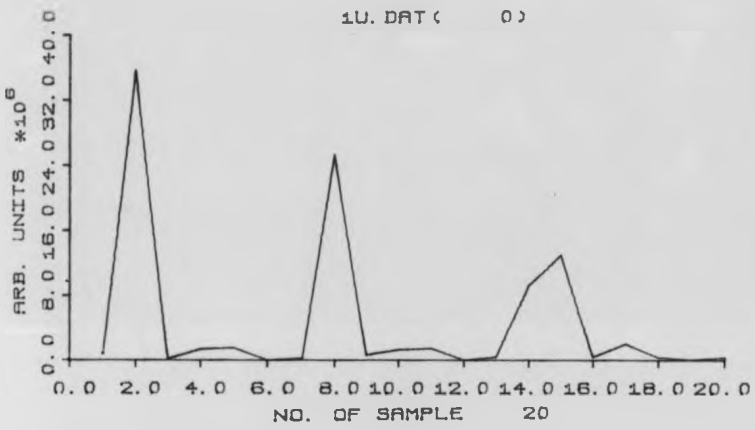

Figure E2 The plot of mean with respect to number of samples

Number of samples N = 20

Number of runs = 7

α - between 0.95 and 0.025

the mean square value is 4.72×10^6, the data behave stationary.

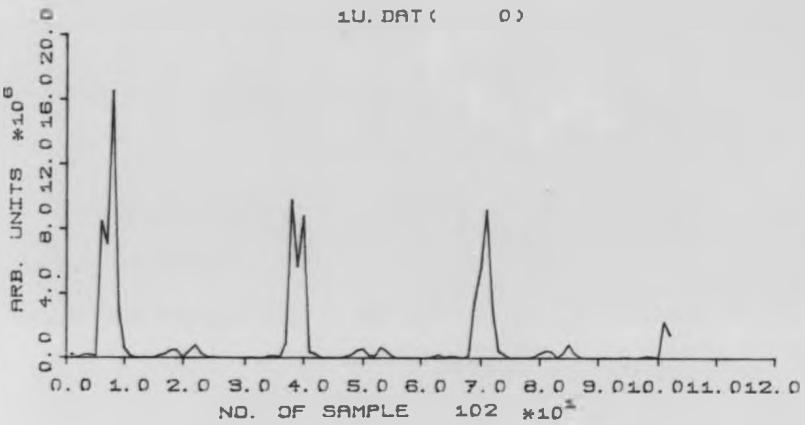

Figure E3 The plot of mean with respect to number of samples

Number of samples = 102

Number of runs = 8

n = 51

The data behave non-stationary.

Annex F

The Hardware and Software Aspects of Signal Processing

A DEC PDP 11/23 was already selected for the Device Application Group in the Physics Department for the reasons of compatibility with the existing departmental equipment, sharing of software and hardware experience both internally and externally.

The PDP 11/23 was obtained with the following configuration:

- LSI 11/23 processor with Memory Management Unit (MMU)
- 128 Kbytes DRAM
- Twin RX02 floppy disc drives
- 16-channel multiplexed analogue input to 12 bit ADC
- Digital I/O interface
- Quad serial line interface, and
- ROM bootstrap board
- Two RK05 hard disk drives were added later providing 5MB of storage

In addition the peripherals included an LA36 DecWriter, Watanabe digital plotter which was later replaced by a Gould colourwriter digital plotter and a Televideo 192C VDU, all serviced via serial lines.

The ADC has a range of -5 to +5 volts, while the tape recorder has a maximum output of approximately 1.4 volt rms, and additional

pre-amplification was used in order to provide a full use of the ADC resolution.

In order to process the data recorded using the PDP 11/23, it is necessary to sample and store the raw data, to do this a sampling rate of 1 and 2 msec was chosen. To avoid error in sampling due to aliasing, it is well known that signal components must not exist above half the sampling frequency, which is known as the Nyquist frequency.

Digital signal processing package

The software package was developed to perform routine spectral analyses such as power spectrum, correlation and coherence, adaptive filter such as adaptive noise cancellation, transversal filter and time-sequence adaptive filter. The sub-routines are based on programmes described by the digital processing committee (1978) and by Carter and Ferrie (1979), whilst the other programmes are developed by the author, and by Winski (1985).

An example of spectral analysis, parameters and commands required is described below.

For spectral analysis, each required the results of fast-fourrier transform (FFT) on the raw data. this could be done by the Command SXY, which will compute the spectra Gxx, Gyy and the cross spectrum Re[Gxy] and Im[Gxy], which is stored for use by subsequent commands: LPS, CCF, ACF, COH, which can be called after executing SXY in any order.

Parameters required

NWN — Length of segment of data, it could be given when calling SXY, or otherwise previous value is used, which must be >4 and <512, which should not exceed the input data record.

NFT — is computed to be the next power of 2 that is > NWN = 100, NFT will be made equal to 128. This is the FFT segment length, max length = 512

PoV — 'percentage overlap'. Data records larger than 512 cannot be processed as one record since max.FFT is 512. A percentage overlap of 0, 50 and 75 may be used as a argument when SXY is called, otherwise the previous value is used.

(SAM) — the sampling rate in μsec. It is only needed to determine the frequency range of the spectra.

Description of commands

S — Do initial computations to obtain spectra Gxx, Gyy, and Gxy for use by other command

Format — SXY V_1 V_2 (NWN) (PoV)

V_1 is the input 'X' vector

V_2 is the input 'Y' vector

these must be the same size or an error message appears,

NWN sets the segment size for FFT, it should be a power of 2, if it is not a power of 2, zero's are automatically added to make it so, which will degrade the accuracy of the spectral estimates, so it is best to use a power of 2 if possible.

PoV selects the percentage overlap if more than one segment is needed to process data,
set to 0, 50 or 75 only,

After executing the command SXY, the following command may be used as required.

(a) Log power spectrum (LPS)

Format LPS $V_1(V_2)$

The log of the power spectra Gxx (and Gyy) are computed from Gxx (and Gyy) and put into V_1 and V_2 if specified. If V_2 is omitted, only Gxx is stored in V_1.

The size of V_1 and V_2 is important, for an N-point FFT there are $\frac{N}{2} + 1$ values for the spectrum, the first being the dc component. The size of NFT determines the size of the power spectrum vector ie. $\frac{NFT}{2} + 1$.

(b) Autocorrelation function (ACF)

Format ACF $V_1(V_2)$

Computes the ACF of 'X' (and 'Y' if V_2 is specified) input data record from the inverse FFT of the power spectra Gxx and Gyy. Because the ACF is symmetric, only one half is provided. The size of V_1 (and V_2) must not exceed $\frac{NFT}{2} + 1$, it could be less if desired.

For large values of NFT, it is convenient to have V_1 and V_2 equal to a power of 2 for plotting and display. The autocorrelation of X is put into V_1 and the autocorrelation of Y is put into V_2.

(c) Crosscorrelation function (CCF)

Format CCF $V_1(V_2)$

From the cross-spectrum GXY, the crosscorrelation function is obtained from the inverse FFT and the result is put into V_1. Because the CCF is not generally symmetrical, V_1 must be equal to NFT in size. It may be smaller if only a part of the CCF is required. If V_2 is specified it contains the impulse response of the function.

(d) Coherence function (COH)

Format COH V_1 (V_2) (V_3) (V_4)

Several functions are provided by this command. The value of the magnitude square coherence (MSC);

$$\gamma^2 = \frac{Gxy.Gxy}{Gxx.Gxy}$$

is stored in V_1. This can take values in the range 0-1, V_1 must not exceed

$\frac{NFT}{2} + 1$,

if V_2 is provided, it will contain the log power cross-spectrum,

if V_3 is provided, it contains the phase cross-spectrum in degree,

if V_4 is specified, it contains the modulus of the transfer function $H_{\frac{Y}{X}}(f)$ in dB.

Example:

Having two vectors A and B of size 512 each and sampled at 1KHz, obtain the spectral function.

1KHz sampling means Nyquist frequency of 500Hz, so any data components above 500Hz will alias back into 0-500Hz band. Thus this is the frequency range.

To determine the resolution, the power spectrum will be stored in a vector of size 257 $\frac{512}{2} + 1$ and will represent 500Hz. As the first bin represents the dc. component:

NWN is 512 and so is NFT

$\therefore$ resolution = $\frac{500}{512} \simeq 1$Hz

To get log power spectrum:

SXY A B 512

LPS L_1 L_2 where L_1 and L_2 are of length 256

ACF A_1 A_2 gives auto-correlation function. A_1 and A_2 of length 256

CCF R_1 R_2 gives cross correlation function and impulse response, R_1 and R_2 length 256

For resolution less than 1Hz, it is required that the sampling frequency must be smaller, i.e. less than 500Hz, but this depends upon the bandwidth of the input signal.

Some of the Dispac Commands and parameters are listed below

H	:List help information
EX	:Execute the commands in the named command file
CR	:Create a command file
STP	:Stop the programme
VDU	:Send all output to VDU
PRI	:Send all output to printer
AP	:Allocate a parameter given name, type, location
SP	:Set the named parameter to the given value
LP	:List the values of all parameters
INC	:Increment named parameter by given constant
DEC	:Decrement named parameter by given constant
AL	:Allocate space for named array given dimensions and start
DE	:Deallocate storage for the named array
MAP	:List a map of storage allocation
L	:List the named array
SAM	:Sample ADC and store in memory
P	:Plot vector
D	:Display vector
XY	:Control the plotter directly
AX	:Plot axes using T/LIN/LOG, NDX, NDY,(Y-axis text),(Box)
G	:Drive the Gould colourwriter directly

```
SC          :Scale the vector by a constant
SH          :Shift the vector by a constant
AD          :Add the first vector to the second vector
SUB         :Subtract first vector from second vector
MUL         :Multiply first vector by second vector
DIV         :Divide first vector by second vector
C           :Clear the vector to zero
CPY         :Copy the first array to the second
W           :Write the array to disk 1
R           :Read array from disk file

SIN         :Generate sinewave for given period
S           :Simple statistics - min, max, mean, sum, standard dev,
             rms power
SNS         :Signal/noise power ratio given noisy signal and
             signal vectors
SXY         :Compute the spectra of X and Y
LPS         :Compute log power spectrum
ACF         :Compute autocorrelation function
CCF         :Compute cross correlation function
COH         :Compute coherence
AF          :Simple adaptive filter
TAF         :Time-sequenced adaptive filter
```

To perform the axes, the following command should be executed:

```
     T
AX - LIN  - NDX - NDY - 'Y axix test' - BOX
     LOG
```

T is the plot of the time against amplitude

LIN Linear plot for coherence

LOG Log plot for transfer function and log power spectrum

NDX, NDY are the number of divisions in the X and Y axes

An example of performing adaptive filtering

It is required that four arrays are allocated with the same size, i.e. 2048 bin, the following command should be executed:

```
AL   A    2048   $1
AL   B    2048   $21
AL   Y    2048   $41
AL   E    2048   $61
```

The above allocation is the name of the array A and B and the two required inputs to the adaptive filter. Y is the output of the adaptive filter while E is the error. They are all of size 2048 and they are all placed in a specific position in the storage, as it will be shown in the map.

It is also required to allocate the number of coefficient by AL W 64 $81, that means allocate an array called W of size 64 and standard from position 81.

To perform the adaptive filter it is required to set the a value to the

convergence factor μ , i.e. 0.001, and to set a delay of $\frac{M}{2} + 1$.

The command is:

AF A B Y E

The following map show the location of the arrays in the storage which consist of 256 blocks of 128 words.

Block	1	2	3	4	5	6	7	8	9	10	11	12	13	14	15	16	17	18	19	20
0	A	A	A	A	A	A	A	A	A	A	A	A	A	A	A	A				
20	B	B	B	B	B	B	B	B	B	B	B	B	B	B	B	B				
40	Y	Y	Y	Y	Y	Y	Y	Y	Y	Y	Y	Y	Y	Y	Y	Y				
60	E	E	E	E	E	E	E	E	E	E	E	E	E	E	E	E				
80	W	W																		
100																				
120																				
140																				
160																				
180																				
200																				
220																				
240																				

BRITISH LIBRARY

IMAGING SERVICES NORTH

Boston Spa, Wetherby
West Yorkshire, LS23 7BQ
www.bl.uk

PAGE/PAGES EXCLUDED UNDER INSTRUCTION FROM THE UNIVERSITY

REFERENCES

Abboud, S., & Sedeh, D. (1982) The waveforms' alignment procedures in the averaging process for external recording of the His Bundle Activity.
Computers and Biomedical Research, 15, 212-219.

Bendat, J.S. (1964) Mathematical Analysis of Average response values for nonstationary Data.
IEEE Tran. on Biomedical Engineering. pp72-81.

Bendat, J.S. (1962) Interpretation and Application of Statistical Analysis for Random Physical Phenomena.
IRE Transactions on Biomedical Electronics. pp31-44.

Berbari, E.J., Lassara, R., Scherlag, B.J. (1979) The Effect of Filtering the His-Purkinje system Electrocardiogram.
IEEE Trans. on Biomedical Engineering, Vol. BME-26 No.2. pp82-85.

Berbari, E.J., Collins, S.M., Saly, Y. & Arzbaecher, R. (1983) Orthogonal surface lead recordings of His-Purkinje activity.
IEEE trans. on Biomedical Engineering, 30, 160-167.

Berbari, E.J., Scherlag, B.J., El-Sherif, N., Befeler, B., Aranda, J.M. & Lazzara, R. (1976) The His-Purkinje Electrocardogram in man.
Circulation Vol. 54, No. 2, 219-224.

Berbari, E.J., Lazzara, R., Samet, P. & Scherlag, B.J. (1973)
Non-invasive technique for detectoin of electrical activity during the P-R segment.
Circulation 48, 1005-1013.

Berbari, E.J., Lazzara, R., El-Sherif, N. & Scherlag, B.J. (1973)
Signal averaging applications in cardiac electrophysiology.
Circulation 48, 396-402.

Bergveld, P. & Meijer, W.J.H. (1981) A new technique for the suppression of the MEGG.
IEEE Trans. on Biomedical Engineering, Vol. BME-28, No.4, 348-354.

Betts, R.P. & Brown, B.H. (1976) Method for recording electrocardiograms with dry electrodes applied to unprepared skin.
Medical & Biological Engineering. 313-315.

Bognor, E.E. & Constantinides, A.G. (1975) Introduction to digital filtering.
John Wiles & Sons.

Boyle, D., Carson, P. & Hamer, J. (1966) High frequency electrocardiography in ischaemic heart disease.
British Medical Journal, 28, 539-545.

Carter, G.C., Knapp C.J. & Nuttall, A.H. (1973) Estimation of the magnitude square coherence function via overlapped fast Fourier transform Processing.
IEEE Trans. on Audio and Electrocoustics. Vol. Au. 21, No. 4. 337-344.

Carlton, E.H. & Katz, S. (1980) Is Wiener Filtering an Effective method of Improving Evoked Potential Estimation.
IEEE Trans. on Biomedical Engineering Vol. BME-27, No.4, 187-192.

Chien, I.C., Tompkins, W.J. & Briller, S.A. (1980) Computer methods for analysing the high-frequency electrocardiogram.
Medical & Biological Engineering & Computing, 18, 303-312.

Clark, G.A., Parker, S.R. & Mitra, S.K. (1983) A Unified Approach to time and frequency Domain realisation of FIR. Adaptive Digital filters.
IEEE Trans. on Accoustics, speech and signal processing. Vol. Assp-31, No.5, 1073-1083.

Clark, G.A. (1976) Cancel 50Hz and other noise with adaptive filters.
Electronic Design, 20, 74-79.
Cowan, C.F.N. & Grant, P.M. (1985) Adaptive Filters.
Prentice-Hall Inc., Englewood Cliffs, New Jersey 07632.

Denes, P., Santorelli, P. Hauser, R.G. & Uretz, E.F. (1983) Quantitative analysis of the high frequency components of the terminal portion of the body surface QRS in normal subjects and in patients with ventricular tachycardia.
Circulation, 67, 1129-1138.

Dentino, M., McCool, J. & Widrow, B. (1978) Adaptive filtering in the frequency domain.
Proc. IEEE. Vol. 66, No.12, 1658-1659.

Denyer, P.B., Mavor, J. & Arthur, J.W. (1979) Miniature Programmable Transversal filtering using CCD/MOS Technology.
Proc. IEEE. Vol. 67, No.1, 42-49.

Djafari, A.M., Heron, F., Duperdu, R. & Perrin, J. (1981) Non-invasive recording of His-Purkinje system electrical activity by a digital system design.
J. Biomedical Engineering. 3, 147-152.

Ellis, R.C. (1976) Signal averaging and medical applications.
Medical Electronics & Data. Pittsburgh, PA 15216 7(2), 41-43.

Ferrara, E.R. & Widrow, B. (1981) Multichannel adaptive filtering for signal enhancement.
IEEE Trans. on Circuits and Systems. Vol. CAS-28, No.6, 606-610.

Ferrara, E.R. Jnr. (1977) The Time-sequency adaptive filter.
Ph.D. Dissertation.

Ferrara, E.J. & Widrow, B. (1982) Fetal Electrocardiogram Enhancement by Time-sequenced adaptive filtering.
IEEE Trans. on Biomedical Engineering. Vol. BME-29, No.6, 458-460

Ferrara, E.R. & Widrow, B. (1981) The Time-sequenced adaptive filter.
IEEE Trans. on Circuits and Systems. Vol. Cas-28, No.6, 679-683.

Flowers, N.C. Shvartsman, N., Kennelly, B.M. Sohi, G.S. & Horan, L.G. (1981) Surface recording of His-Purkinje activity on an every-beat basis without digital averaging.
Circulation, 63, 948-952.

Flowers, N.G., Horam, L.G., Thomas, J.R. & Tolleson, W.J. (1969) The anatomical basis for high-frequency components in the electrocardiogram.
Circulation, 33, 531-539.

Fraden, J. & Neuman, M.R. (1986) QRS wave detection.
Med. & Biol. Eng. & Comput. 1980. 19, 125-132.

French, A.S. (1980) Coherence Improvement in white noise Analysis by the use of a Repeated Random sequence generator.
IEEE Trans. on Biomedical Engineering, Vol. BME-27, No.1, 51-53.

Furno, G.S. & Tompkins, W.J. (1983) A learning filter for removing noise interference.
IEEE Trans. on Biomedical Engineering, Vol. BME-30, No.4, 234-235.

Furness, A. (1976) Progress in recording Electrical Events of the PR segment Part I; Cavity Recording Techniques.
Journal of Cardiovascular Technology. 13-25.

Furness, A. (1976) Progress in recording Electrical Events of the PR segment Part II: Surface Recording Techniques.
Journal of Cardiovascular Technology. 18,2, 14-21.

Furness, A., Sharratt, G.P. & Carson, P. (1975) The Feasibility of detecting His-bundle activity from the body surface.
Cardiovascular Research, 91, 390-396.

Geselowitz, D.B., Langner, P.H. & Mansure, F.T. (1962) Further studies of the first derivative of the electrocardiogram, including instruments available for clinical use.
American Heart Journal, 64, 805-814.

Glover, J.R. (1979) High order alhorithms for adaptive filters.
IEEE Trans. on communications, Vol. Com-27 No.1, 216-221.

Glover, J.R. (1977) Adaptive noise cancelling applied to sinusoidal interferences.
IEEE Trans. on Accoustics, speech and signal processing. Vol. Assp-25, No.6, 484-491.

Goovaerts, H.G., Ros, H.H., Van den Akker, T.J. & Schneider, H. (1976) A digitised QRS Detector based on the Principle of Contour Limiting.
IEEE Trans. on Biomedical Engineering. 154-160

Gordon, D.H. (1975) Triboelectric interference in ECG.
IEEE Trans. on Biomedical Engineering. 252-257.

Griffiths, L.J. (1967) Signal Extraction using Real-time adaptation of a Linear multichannel filter.
Ph.D Dissertation.

Gupta, M.M. & Prasad, K. (1980) Studies on the effects of Glucagon on Ouabain - induced cardiac disorders using the PISA method.
Advances in Myocardiology Vol.1. University Park Press, Baltimore. 313-319.

Hambley, A.R., Moruzzi, R.L. & Feldman, C.L. (1974) The Use of Intrinsic Components in an ECG filter.
IEEE Trans. on Biomedical Engineering, Vol. BME-21, No.6, 469-473.

Hamstra, G.H., Peper, A. & Grimbergen, C.A. (1984) Low-power, low-noise instrumentation amplifier for physiological signal. Med. & Biol. Eng & Comput. 22, 272-274.

Hoopen, M.T. & Reuver, H.A. (1972) Aspects of average response computation by aperiodic stimulation. Med & Biol. Eng. Vol.10, 621-630

Huhta, J.C. & Webster, J.C. (1973) 60Hz interference in Electrocardiography. IEEE Trans. on Biomedical Engineering Vol. BME-20, No.2, 91-101

Hunter, I.W. & Kearner, R.E. (1983) Two-sided linear filter identification. Med & Biol Eng & Comput, 21, 203-209.

Inamoto, Y., Sumimoto, K., Noto, H., Terai, T. & Kawashima, K. (1982) Real-time analysis of foetal heart rate patterns using a computer system Med & Biol Eng & Comput. 20, 223-230.

Johnson, T.L., Wright, S.C. & Segall, A. (1979) Filtering of Muscle artefact from the Electroencephalogram. IEEE Trans. on Biomedical Engineering, Vol. BME-26, No.10, 556-563.

Jones, P.L. (1973) Artefact and Safety in ECG monitoring.
Proc. Roy. soc. Med., 66, 55-59.

Jones, N.B. & Lago, P.J.A. (1982) Spectral analysis and the interference ECG.
IEEE Proc. Vol.129, Pt A, No.9, 673-678.Journee, H.L. & Manen, J. (1984) Automatic method to detect and determine the preferential frequency of EMG signal from patients with pathological tumours.
Med & Biol Eng. & Comput. , 322-325.

Kaunitz, J. & Widrow, B. (1973) Final report on noise subtracting filter study.
Naval Ship systems command, Washington DC. 1-170.

Keuntie, M.A., Van der Schee, E.J., Grashuis, J.L. & Smout, A.J.P.M. (1981) Adaptive filtering of canine electrogastrographic signal. Part I: System design.
Med & Biol. Eng & Comput. 19 ,759-764.

Keuntie, M.A., Van der Schee, E.J., Grashuis, J.L., & Smout, A.J.P.M. (1981) Adaptive filtering of canine electrogastrographic signal. Part 2: Filter performance.
Med & Biol. Eng & Comput. 19, 765-769.

Kim, Y. & Tomkins, W.J. (1981) Forward and inverse high frequency electrocardiography.
Med & Biol. Eng & Comput. 19, 11-22.

Knott, K.F. & Unsworth, L. (1874) Mains rejection tracking filter. Wirelss World, , 375-379.

Langner, P.H. & Lauer, J.A. (1966) The relative significance of high-frequency and low frequency notches in the electrocardiogram. American Heart Journal, 71, 34-42.

Langner, P.H., Geselowitz, D.B. & Briller, S.A. (1973) Wide band recording of the electrocardiogram and coronary heart disease. American Heart Journal, 86, 308-317.

Langner, P.H. (1952) The value of high fidelity electrocardiography using the cathode ray oscilloscope and an expanded time scale. Circulation, 5, 249-256.

Langner, P.H. (1953) Further studies in high fidelity electrocardiography: Myocardial infarction. Circulation, 8, 905-913.

Langner, P.H. & Geselowitz, D.B. (1960) Characteristics of the high frequency spectrum in normal electrocardiograms and in subjects following myocardial infarction. Circulation Research, 8, 577-589

Langner, P.H., Geselowitz, D.B. & Mansure, F.T. (1961) High-frequency components in the electrocardiograms of normal subjects and of patients with coronary heart disease.
American Heart Journal, 62, 747-755.

Langner, P.H. & Geselowitz, D.B. (1962) First derivatives of the ECG.
Circulation Research, 10, 220-226.

Lee, T.Y. (1974) An Amplitude-modulation model for the QRS complexes of Electrocardiograms.
IEEE Trans. on Biomedical Engineering, Vol, BME-21, No.5, 381-386.

Levkov, C., Michov, G., Ivanov, R. & Daskalow, I.K. (1984) Subtraction of 50Hz interference from the electrocardiogram.
Med & Biol. Eng. & Comput. 22, 371-373.

Levy, J.B. & Linkens, D.A. (1984) Spectral analysis of short-time biomedical data using adaptive filters.
IEEE Proc., Vol. 131, Pt. A. No.3, 164-169

Linkens, D.A. (1982) Short-time series spectral analysis of biomedical data.
IEEE Proc. Vol.129, Pt.A, No.9, 663-672.

Lynn, P.A. (1971) Recursive digital filters for Biological signals.
Med & Biol Eng. 9, 37-43.

Lynn, P.A. (1971) Recrsive digital filters with linear-phase characteristics.
The Computer Journal, Vol 15, No.4, 337-342.

Lynn, P.A. (1977) Online digital filters for biological signals: Some fast design for a small computer.
Med & Biol Eng & Comput. 15, 534-540

Masenter, W.K. (1979) Adaptive signal processing.
IEEE Conf. Pub. 180, 168-177.

McCool, J.M. & Widrow, B. (1976) Principles and applications of adaptive filters. A Tutorial Review.
IEEE Conf. Pub. 144, 84-89.

Mehra, R., Kelen, G.J. Zacler, R., Zephiran, D. Fried, P., Gomer, J.A. & El-Sherif, N. (1972) Non-invasive His bundle Electrogram. Value of three vector lead recordings.
American Journal of Cardiology, 49, 344-348.

Mintz, G.D. Frecker, R.C. & Joy, M.L.G. (1980) Specification and design of an evoked-response data-acquisition system. Med & Biol Eng. & Comput., 18, 167-168.

Miyano, H., Masunda, R. & Sadoyama, T. (1980) A note of the time constant in low-pass filtering of rectified surface EMG. IEEE Trans. on Biomedical Engineering. Vol BME-27, No.5, 274-278.

Morgan, D.R. & Craig, S.E. (1976) Real-time adaptive linear prediction using the least mean square gradient algorithm. IEEE Trans. on Acoustic, speech and signal processing, Vol. assp-24, No.6, 499-507.

Nandagopal, D., Mazumdat,J., Bogner, R.D. & Goldblatt, E. (1984) Spectral analysis of second heart sound in normal children by selective linear prediction coding. Med & Biol Eng. & Comput. , 229-239.

Nelson, C.V. & Geselowitz, D.B. (1976) The Theoretical basis of electrocardiography. Clarendon Press. Oxford.

Nuttall, A.H. & Carter, G.C. (1976) Bias of the Estimate of Magnitude-squared coherence. IEEE Trans. on Acoustics, speech and Signal processing, , 71-79.

Nuttall, A.H. & Carter, G.C. (1981) an approximation to the cumulative distribution function of the magnitude-square coherence estimate.
IEEE Trans. on Acoustics, speech and signal processing, Vol. assp-29, No.4, 582-583.

Ogue, J.C. saito, t. & Hoshiko, Y. (1983) A Fast Convergence frequency domain adaptive filter.
IEEE Trans. on Acoustics, speech and signal processing, Vol. assp-31, No.5, 320-335.

Oldenburg, J.T. & Macklin, M. (1977) Processing the abdominal fetal ECG.
IEEE Trans. on Biomedical Engineering, Vol. BME-24, No.6, 501-507.

Olivier, Y.de Vel. (1984) R-wave detection in the presence of muscle artifacts.
IEEE Trans. on Biomedical Engineering. Vol. BME-31 No.11, 715-717.

Pahlm, O., Sornmo, L. (1984) Software QRS detection in ambulatory monitoring.
Med & Biol Eng. & Comput. , 289-297.

Plonsey, R. (1971) The Biophysical Basis for Electrocardiography.
CRC Critical Reviews in Bioengineering, pp1-47.

Prasad, K. & Gupta, M.M. (1981) PISA: A non:invasive method in detection and quantifications of Acid-induced myocardial infarction in dogs.
Clin. Cardiol. 4, 180-187.

Prasad, K., Gupta, M.M. & Graham, B.L. (1978) A preliminary study in the detection of cardiac disorders via phase invariant. Signature algorithm of ECG.
Jap. Heart Journal, , 383-395.

Prasad, K. & Gupta, M.M. (1980) A new non-invasive method for early detection and quantification of heart disease.
Advances in Myocardiology, 1 University Park Press, Baltimore. Vol 1. pp287-312.

Rautaharju, P. (1965) The exercise electrocardiogram.
Am. Heart Journal. , 315-320.

Rhyne, V.T. (1969) A comparison of coherent averaging techniques for repetitive biological signals.
Med. Res. Eng. 8, 22-26.

Ribeiro, J.E., Caprihan, G., Gianellaneto, A., Wiederehecker, N.G. & Infastosi, A.F. (1980) Theoretical Analysis of Eeor during signal averaging for detection of His-bundle activity.
IEEE Trans. on Biomedical Engineering. Vol. BME-27, No.4, 473-476.

Richardson, J.M. Murthy, V.K. & Haywood, L.J. (1979) Effect of Random Frequency modulation on ECG power spectra.
IEEE Trans. on Biomedical Engineering, Vol. BME-26, No.2, 109-112.

Rompelmans, O. & Janssen, R.J. (1982) Use of phase spectral information assessment of frequency contents of ECG waveforms.
IEEE Proc. Vol.129, Pt.A, No.9, 679-683.

Rosen, K.M. (1973) Catheter recordings of His bundle electrograms.
Journal of American Heart Ass. XLII, 23-27.

Roth, P.R. (1971) How to use the spectrum and coherence function sound and vibration.
IEEE Spectrum, , 10-15. Hewlett-Packard Company, Paolo Alto, California.

Roth, P.R. (1971) Effective measurements using digital signal analysis.
IEEE Spectrum, , 62-71. Hewlett-Packard Company.

Roy, D. & Menad, P. (1978) High performance digitally programmable analogue transversal filters.
Electronics Letters, Vol.14, No.20, 671-672.

Roy, O.Z., Mortimer, A.J., Trollope, B.J. & Villeneuve, E.J. (1984) Effects of short duration transients on cardiac rhythm.
Med & Biol Eng. & Comput. 22, 225-228.

Sanderson, A.C. (1980) Adaptive filtering of neuronal spike train data.
IEEE on Biomedical Engineering. Vol. BME-27, No.5, 271-273.

Santopietro, R.P. (1974) measurement, analysis and reduction of noise in the high frequency electrocardiogram.
Ph.D Thesis.

Santopietro, R.P. (1977) The origin and characteristics of the primary signal, noise and interference sources in the high frequency electrocardiogram.
Proc. IEEE, Vol.65, No.5, 180-187.

Sapoznikov, D. & Weinman, J. (1975) Computer simulation of notches on HFECG and an interpretation of their origin.
Medical & Biological Engineering. 13, 825-830.

Sato, H. (1982) Functional characteristics of human muscle revealed by spectral analysis of the surface electrocardiogram.
Electromyogr. Clin. Neurophysiol. 22, 459-516.

Scherlag, B.J., Samet, P. & Helfant, H. (1972) His bundle electrocardiogram.
Circulation, XLVI, 601-613.

Schick, T.D. & Powers, S.R. (1978) Spectral analysis of the high-frequency electrocardiogram in contusive myocardial injury.
Annals of Biomedical Engineering. 6, 154-160.

Shensa, M. (1979) Performance of the adaptive noise canceller with a noisy reference non-Wiener solution.
Technical report 381, Naval Ocean systems centre, San diego, California 92152, 1-44.

Shensa, M. (1980) Non-Wiener solutions of the adaptive noise canceller with a noisy reference.
IEEE Trans. on Acoustics, speech and signal processing, Vol. Assp-28, No.4, 468-473.

Sheild, J.E.A & Kirk, D.L. (1981) The use of Digital filters in enhancing the foetal electrocardiogram.
J. Biomed. Eng. 3, 218-225.

Shvartsman, V., Barnes, G.R., Shvartsmany, L. & Flowers, N.C. (1982) Multichannel signal processing based on logic averaging.
IEEE Trans. on Biomedical Engineering, Vol. BME-29, No.7, 531-536.

Simson, M.B. (1981) Use of signals in the terminal QRS complex to identify patients with ventricular tachycardia after myocardial infarction.
Circulation, 64, 235-242.

Simson, M.B., Unterecker, W.J., Speilman, S.R., Horowitz, L.N., Marcus, N.H., Falone, R.A., Harken, A.H. & Josephson, M.E. (1983) Relation between late potentials on the body surface and directly recorded fragmented electrograms in patients with ventricular tachycardia.
Am. J. Cardiol. 51, 105-112.

Tam, H.W. & Webster, J.G. (1977) Minimising Electrode Motion Artifact by skin abrasion.
IEEE Trans. on Biomedical Engineering, Vol. BME-24, No.2, 134-139.

Tayler, D. & Vincent, R. (1983) Signal distortion in the Electrocardiogram due to inadequate phase response.
IEEE Trans. on Biomedical Engineering, Vol. BME-30, No.6, 352-356.

Taylor, T.P. & Macfarlane, P.W. (1974) Digital filtering of the ECG - a comparison of low-pass digital filters on a small computer.
Medical & Biological Engineering, ,493-502.

Thakor, N.V. & Webster, J.G. (1980) Ground-free ECG recording with two electrodes.
IEEE Trans. on Biomedical Engineering. Vol. BME-27, No.12, 699-704.

Thakor, N.V. (1978) Reliable R-wave detection from ambulatory subjects.
Dept. of Electrical and Computer Engineering, University of Wisconsin-Madison, Madison, Wisconsin 53706, 67-72.

Trimble, C.R. (1968) What is signal averaging?
Hewlett-Packard Journal. Vol.19, No.8, 2-16.

Vincent, R., Stroud, N.P., Jenner, R., English, M.J., Woollons, D.J. & Chamberlain, D.A. (1978) Non-invasive recording of electrical activity in the PR segment in man.
British Heart Journal, 40, 124-130.

Vincent, R., English, M.J., Mackintosh, A.F., Stroud, N., Chamberlain, D.A. & Woollons, D.J. (1980) A flexible signal averaging system for cardiac waveforms.
J. Biomed. Eng. 2, 15-24.

Webster, J.G. (1977) Interference and motion artifact in Biopotentials.
IEEE 1977 Region 6 conference Record. 53-64.

Weerd, J.P.C. & Kap, J.I. (1981) A Posterior Time-varying filtering of averaged evoked potentials.
Biol. cybern. 41, 223-234.

de Weerd, J.P.C. (1981) Facts and Fancies about Posterior Wiener Filtering.
IEEE Trans. on Biomedical Engineering. Vol. BME-28, No.3, 252-257.

de Weerd, J.P.C. (1981) Estimation of evoked potentials.

Weiss, P.L., Hurter, I.W. & Kearney, R.E. (1983) Technical note: Reduction of physiological signal contamination using linear filter identification.
Med & Biol. Eng & Comput. 21, 521-524.

Widrow, B. & McCool, J.M. (1976) A comparison of adaptive algorithms based on the methods of steepest descent and random search.
IEEE Trans. on antennae and propagation, Vol. Ap-24, No.5, 615-637.

Widrow, B. (1981) Adaptive filters. From aspects of network and systems theory.
Special Communication, 563-587.

Widrow, B., McCool, J.M., Larimore, M.G. & Johnson, C.R. (1976) Stationary and nonstationary learning characteristics of LMS adaptive filter.
Proc. IEEE, Vol.64, No.8, 1151-1162.

Widrow, B., Glover, J.R., McCool, J.M. Kaunitz, J., Williams, C.S., Hearn, R.H., Zeidler, J.R. & Goolin, R.C. (1975) Adaptive noise cancelling: Principles and applications.
Proc. IEEE, Vol.63, No.12, 1692-1716.

Widrow, B., Mantey, P.E., Griffiths, L.J. & Goode, B.B. (1967) Adaptive antenna systems.
Proc. IEEE, Vol.55, No.12, 2143-2159.

Widrow, B., McCool, J. & Ball, M. (1974) The complex LMS alGorithm.
The Institute of Electrical and Electronic Engineers, Inc. Printed in USA, Annals No.504PR016, 719-720.

Widrow, B. (1966) Adaptive filters 1: Fundamental.
Technical Report No.6764-6, Stanford University, Centre for Systems Research, 1-58.

White, M.H., Mack, I.A., Borsuk, G.M., Lampe D.R. & Kub, F. (1978) CCD analog adaptive signal processing .
Pre-publication, San Diego CCd, 1-14.

Winski, R. (1985) Adaptive techniques for signal anhancement in the Human Electroencephalogram.
Ph.D Thesis. University of Keele.

Winter, D.A. Analysis and reduction of noise in Exercise Electrocardiogram.
Ph.D Thesis. Dalhousie University, Halifax, Nova Scotia.

Winter, D.A., Rautaharju, P.M. & Wolfe, H.K. (1966) Measurement and characteristics of overall noise content in exercise electrocardiograms.
Dalhousie University, Halifax, Nova Scotia, Canada, , 324-331.

Winter, D.A. & Trenholm, B.G. (1969) Reliable triggering for exercise electrocardiogram.
IEEE Trans. on Biomedical Engineering, Vol. BME-16, No.1, 75-79.

Wolthuis, R.A. Hopkirky, A., Keiser, N. & Fischer, J.R. (1979) T-waves in the Exercise ECG: Their location and occurence.
IEEE Trans. on Biomedical Engineering, Vol. BME-26, No.11, 639-643.

Woody, C.D. (1967) Characterisation of an adaptive filter for the analysis of variable latency neuroelectric signals.
Med. & Biol. Engineering, 5, 539-553.

Woolans, D.J., English, M.J., Carroll, D. & Vincent, R. (1982) Signal processing for recovery of cardiac conducting system activity.
IEEE Proc. Vol.129, Pt.A, No.9, 684-692.!np

Wu, Y.S. & Horvath, S. (1980) Non-stationary acoustic noise cancellers using an adaptive recursive filter.
Paper presented at the IEEE L'Aquila workshop on digital signal processing, L'Aquila, Italy, 1-25.

Yelderman, M., Widrow, B., Cloffi, J.M., Hesler, E. & Leddy, J.A. (1983) ECG enhancement by adaptive cancellation of Electrosurgical Interference.
IEEE Trans. on Biomedical Engineering, Vol, BME-30, No.7, 392-398.